Cell-Encapsulating Microbeads for Therapeutic Vascularization of Ischemic Tissues

by

Nicole E. Friend

A dissertation submitted in partial fulfillment
of the requirements for the degree of
Doctor of Philosophy
(Biomedical Engineering)
in the University of Michigan
2023

Doctoral Committee:

Professor Andrew J. Putnam, Co-Chair
Professor Jan P. Stegemann, Co-Chair
Assistant Professor Sasha Cai Lesher-Pérez
Professor Lonnie D. Shea

Nicole E. Friend

nicfri@umich.edu

ORCID iD: 0000-0001-5090-6538

Dedication

To my family, who have provided me with endless love and support in everything I do.

To Dustin and Madison, who inspire me every day to be the best version of myself.

Acknowledgements

I would like to thank my dissertation advisors, Dr. Andrew Putnam and Dr. Jan Stegemann, for the support and guidance you have offered me throughout the past six years of my graduate studies. You both have helped me become a better scientist and mentor to others. Thank you for helping me see the positives of science when I am being overly critical and for helping me develop the skills necessary to be a successful researcher. Furthermore, thank you for making the effort to get to know me as a person and encouraging me to pursue my passions in every aspect of life. I would also like to thank my committee members, Dr. Sasha Cai Lesher-Pérez and Dr. Lonnie Shea, for providing me with scientific guidance. Your thoughtful insights helped improve and advance my work. Additionally, I would like to thank Dr. Aileen Huang-Saad for the tremendous emotional support you have provided me as well as helping foster my passion for teaching and engineering education research.

Next, I would like to thank the current and past members of my research groups. One of the best things about being co-advised is getting to be a part of two really great labs who have made graduate school so much more enjoyable. Working with you all has truly been a blessing and I have greatly appreciated all of your help along the way. A special shoutout goes to Dr. Nick Schott and Dr. Emily Margolis, for being the best lab mates anyone could ask for. You both have supported me scientifically as well as emotionally throughout this journey and my graduate school experience wouldn't have been nearly as fulfilling without you two. You both inspire me to never give up and to always pursue my passions in science. Also, Atticus and Irene, being a mentor to

you both the past few years has been one of my favorite things about graduate school. I have loved every second of watching you develop as researchers, and I cannot wait to see all of the awesome things you both do.

Last, but certainly not least, I would like to thank my friends and family for the endless emotional support and encouragement you have given me throughout my educational (and life)

journey. Stephanie, Cassie, Nick, Emily, and Evan, thank you for being the very best friends anyone could ever ask for. You make life more enjoyable every day and I am so thankful to have your support and friendship. A special thank you goes to Evan, who has been by my side every step of graduate school. I am so thankful we both chose Michigan and I truly cherish you every day. Thank you for being one of the reasons graduate school was so enjoyable, even in the tough times. A huge thank you goes to my wonderful family. You all have been a tremendous source of strength and encouragement throughout the past six years. I am thankful every second of every day for your endless love and support. To Dustin and Madison, everything I do, I do for you, and I hope I have made you as proud as you both have made me.

Table of Contents

List of Figures

List of Appendices

List of Abbreviations

(Symbols, Numerical Order, Alphabetical Order)

°C	Degrees Celsius
3D	Three-dimensional
α-SMA	Alpha-smooth muscle actin
ANOVA	Analysis of variance
Anti-Anti	Antibiotic antimycotic
BM	Basement membrane
BMMNC	Bone marrow mononuclear stem cells
BSA	Bovine serum albumin
CLI	Critical limb ischemia
CHD	Coronary heart disease
CVD	Cardiovascular disease
D10	DMEM + 10% FBS
DAPI	4',6- diamidino-2-phenylindole
DexVS	Dextran vinyl sulfone
DMEM	Dulbecco's modified eagle medium
DMSO	Dimethyl sulfoxide
DSU	Disc spinning unit

dVPMS	Double VPMS: Ac-GCRD<u>VPMS</u>MRGGG<u>VPMS</u>MRGGDRCG-NH$_2$
EC	Endothelial cells
ECFC	Endothelial colony forming cells
ECM	Extracellular matrix
EGF	Epidermal growth factor
EGM2	Endothelial growth medium – 2
EPC	Endothelial progenitor cell
FB	Fibroblast
FBS	Fetal bovine serum
FDA	Food and Drug Administration
FGF	Fibroblast growth factor
FPA	Fibrinopeptides A
FPB	Fibrinopeptides B
G'	Shear modulus
GelMA	Gelatin methacrylate
GF	Growth factor
HAMA	Hyaluronic acid methacrylate
HGF	Hepatocyte growth factor
HIF	Hypoxia-inducible factor
HLI	Hindlimb ischemia
HMVEC	Human microvascular endothelial cells
HUVEC	Human umbilical vein endothelial cells
IF	Immunofluorescent

IPA	Isopropyl alcohol
IPN	Interpenetrating network
iPSC	Induced pluripotent stem cells
LDPI	Laser doppler perfusion imaging
LDL-C	Low-density lipoprotein cholesterol
NHDF	Normal human dermal fibroblast
NHLF	Normal human lung fibroblast
MI	Myocardial infarction
MMP	Matrix metalloproteinase
MSC	Mesenchymal stem/stromal cell
MTA	Michael type addition
NG2	Neuron-glial antigen 2
NIH	National Institutes of Health
OEC	Outgrowth endothelial cells
PAD	Peripheral artery disease
PBMNC	Peripheral blood mononuclear cells
PBS	Phosphate buffered saline
PC	Pre-culture
PCL	Polycaprolactone
PDGF	Platelet-derived growth factor
PDMS	Polydimethylsiloxane
PEG	Poly(ethylene glycol)
PEGDA	Poly(ethylene glycol)-diacrylate

PEGMAL	Poly(ethylene glycol)-maleimide
PEGNB	Poly(ethylene glycol)-norbornene
PEGVS	Poly(ethylene glycol)-vinyl sulfone
PLGA	Poly-lactic-glycolic acid
PLLA	Poly-L-lactic acid
RGD	Arginine-Glycine-Aspartic Acid peptide sequence
RM	Regenerative medicine
RT	Room temperature
SC	Stromal cells
SCID	Severe combined immunodeficiency disease
SF-EGM2	Serum free EGM2
SMC	Smooth muscle cells
sVPMS	Single VPMS: Ac-GCRD<u>VPMS</u>MRGGDRCG-NH2
TBS	Tris buffered saline
TCP	Tissue culture plastic
TE	Tissue engineering
UEA	Ulex europaeus agglutinin I
VEGF	Vascular endothelial growth factor
VSMC	Vascular smooth muscle cells
Z-fix	Zinc-buffered formalin fixative

Abstract

Restoring blood flow to ischemic regions following tissue damage remains a significant challenge in treating a variety of diseases and injuries. Efforts to revascularize ischemic tissues utilizing growth factor (GF) delivery have had minimal clinical success. Cell-based approaches have been explored as an alternative to GF delivery but have been plagued by low cell retention at the target site and reduced cell viability due to the harsh ischemic environment. Prevascularization of tissue constructs may promote more rapid inosculation with host vasculature, potentially enhancing tissue survival and improving therapeutic efficacy; however, implantation of these constructs often requires invasive surgery. This dissertation focuses on the development of injectable, vascularizing tissue modules using both natural and synthetic matrices to address the overarching hypothesis that prevascularized microbeads can jump-start inosculation with host vasculature upon implantation to rapidly revascularize ischemic tissues.

Fibrin-based microbeads, containing endothelial (EC) and stromal cells (SC), were pre-cultured in suspension to allow for the formation of primitive microvascular networks within the microbead matrix. *In vitro*, vessel-like structures sprouted from microbeads to vascularize the surrounding hydrogel. Microbeads pre-cultured for 3 days were implanted into dorsal subcutaneous pockets and within intramuscular pockets in a mouse model of hindlimb ischemia (HLI). In both models, vessels originating from microbeads formed functional connections to host vasculature within 3 days and exhibited extensive, mature microvascular networks after 7 days. The total number of human-derived vessels decreased over time as networks were remodeled and an increase in mature, pericyte-supported vascular structures was observed. In the HLI model,

animals treated with microbeads showed increased macroscopic reperfusion of ischemic foot pads 14 days after surgery and improved limb salvage compared to cellular controls.

Despite these promising findings, cell-laden fibrin-based microbeads tended to aggregate with extended pre-culture, limiting injectability of prevascularized modules. Degradable, cell-adhesive poly(ethylene glycol)-norbornene (PEGNB) was investigated as an alternative material platform to support the formation of injectable, non-aggregating, prevascularized microbeads. Bulk PEGNB hydrogel formulations that supported vessel morphogenesis were first identified. Enhanced cell-mediated remodeling of PEGNB hydrogels, achieved either by reduced crosslinking or increased degradability, led to more rapid vessel formation and higher degrees of cell-mediated stiffening. EC and SC were then encapsulated in PEGNB microbeads using microfluidic flow-focusing biofabrication. These cell-laden PEGNB microbeads nucleated the formation of robust, well-distributed microvascular networks *in vitro*. However, while extended pre-culture of PEGNB microbeads enabled vessel morphogenesis within the beads without aggregation, increased pre-culture time led to decreased angiogenic sprouting. *In vivo* data revealed human-derived capillary-like structures as well as some evidence of lumen formation within PEGNB microbeads implanted in subcutaneous pockets, though in most cases these structures failed to extensively vascularize the surrounding implant region.

This dissertation developed vascularizing microbeads using two different material platforms. Fibrin-based microbeads catalyzed the formation of functional microvascular networks *in vivo*, successfully restoring perfusion to ischemic tissues; however, their tendency to aggregate limited their injectability and ability to be cultured in suspension as discrete units. PEGNB-based microbeads overcame this issue, initiating the formation of well-distributed microvascular networks *in vitro* and permitting extended pre-culture without microbead aggregation; however,

strategies to encourage sprouting from prevascularized PEGNB microbeads need to be explored to more fully realize the potential of this approach. Overall, these findings demonstrate the potential of modular, prevascularized microbeads as a minimally invasive therapeutic for restoring blood flow to ischemic tissues.

Chapter 1 – Introduction

1.1 Clinical Motivation: Cardiovascular Disease

Cardiovascular disease (CVD) is the leading cause of death worldwide with disease management resulting in a high economic burden globally (Fig. 1.1) [1]. In a variety of CVD conditions, atherosclerotic plaque buildup in the arteries leads to reduced blood flow to tissues, such as the brain, heart, and lower extremities in incidence of stroke, coronary heart disease (CHD), and peripheral artery disease (PAD), respectively (Fig. 1.2). This lack of blood flow often results in cell death and tissue necrosis that result in loss of tissue function. In severe cases, this tissue necrosis can progress to myocardial infarction (MI) in individuals with CHD [2] or critical limb ischemia (CLI) in individuals with PAD [3, 4].
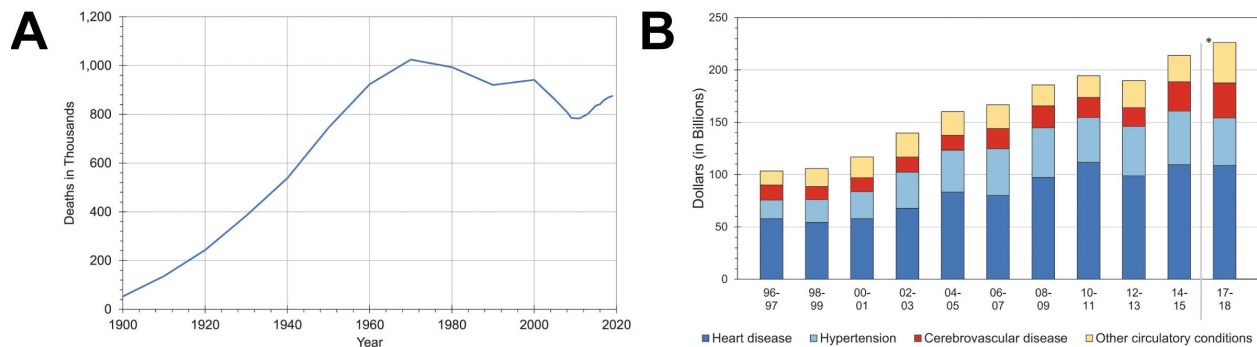
Figure 1.1: Cardiovascular disease data in the United States. *(A) Total deaths and (B) cost resulting from CVD over time. Images reproduced from [1], Copyright 2022, American Heart Association.*

In the United States alone, approximately 6.5 million adults over the age of forty have PAD [1], with an estimated 2 million individuals having CLI [3]. Patients with CLI experience a reduced quality of life as they suffer from ischemic rest pain, non-healing ulcers, and/or symptomatic gangrene which often result in a dependency on caregivers for support, the need for permanent

local wound treatment, and the chronic use of pain-relieving medications [3, 5]. In the absence of

revascularization, an estimated 30-50% of CLI patients will require above the ankle amputations

within one year of diagnosis [4]. Furthermore, common comorbidities, such as diabetes, are

associated with higher amputation rates, and amputation is associated with elevated mortality rates

[3].

Atherosclerotic Plaque Buildup

Progression to MI or PAD

Myocardial
Infarction (MI)

Peripheral Artery
Disease (PAD)

Common Surgical Interventions

Stenting

Bypass

Lifestyle Changes
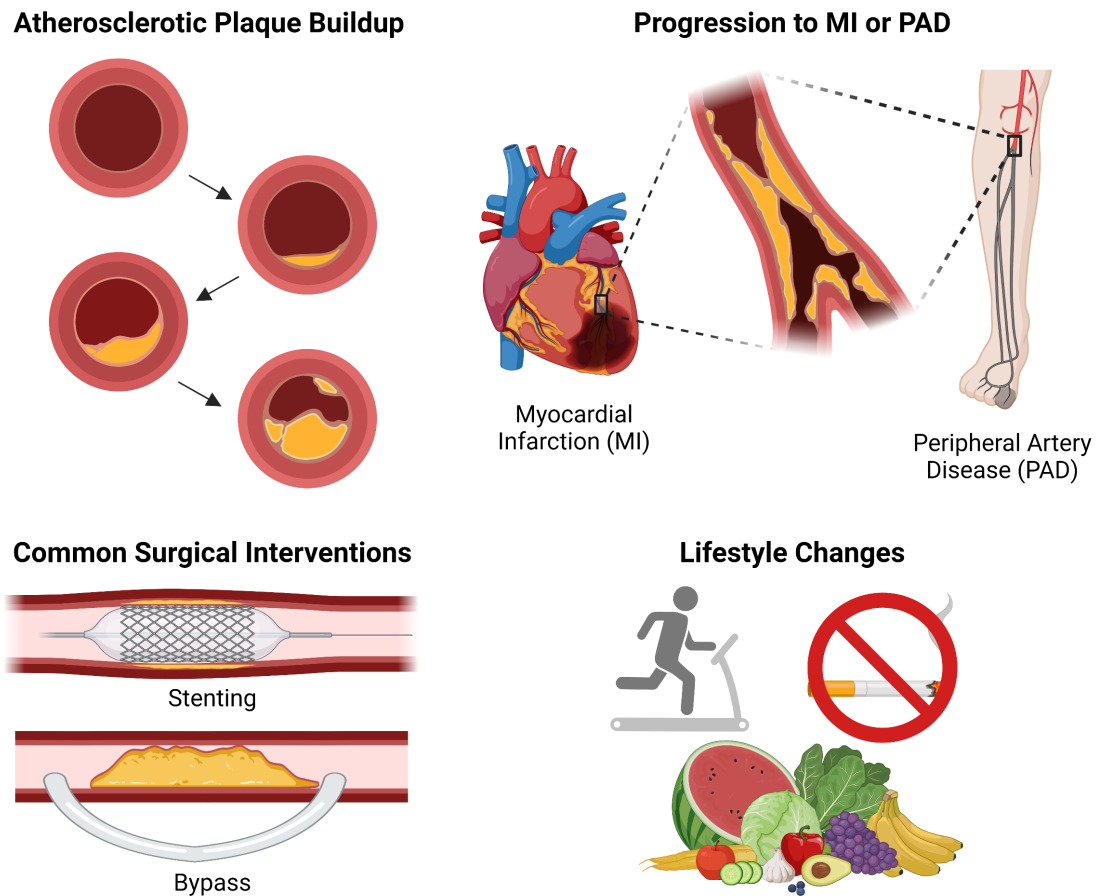
Figure 1.2: Disease progression and treatments of cardiovascular disease. *Atherosclerotic plaque buildup in arteries results in a reduction of blood flow, ultimately leading to myocardial infarction or peripheral artery disease. Common surgical interventions include inserting a stent via balloon catheter to open the occlusion or placing a bypass graft to circumvent the blockage and restore blood flow. Additionally, lifestyle changes are recommended, and often required, to delay disease progression. Created with Biorender.com.*

1.2 Current Treatments of Critical Limb Ischemia

CLI treatment is highly variable, depending on a variety of patient-specific factors, with the overall goal of pain relief, wound healing, improved function, amputation prevention, and reduced mortality [6]. The majority of CLI patients require revascularization interventions to improve distal perfusion in order to salvage the ischemic limb. These surgical interventions typically include stenting or bypassing the obstructive plaque using various techniques (Fig. 1.2) [4, 7]; however, less than 45% of patients are eligible for these procedures due to high incidence of comorbidities, such as coronary artery disease, neurological disorders, cerebrovascular disease, and diabetes, or surgical related issues, such as difficult access due to narrow vessels [8]. Patients are also considered "no option patients" if occlusions are present in smaller arteries [5].

Pharmacological treatments are recommended to reduce pain and slow disease progression, especially for patients who are ineligible for revascularization surgeries. Elevated levels of total cholesterol, low-density lipoprotein cholesterol (LDL-C), triglycerides, and lipoprotein(s) are risk factors for development and progression of PAD. Therefore, it is recommended that patients take statins to lower cholesterol levels [6]. Prostanoids can act as vasodilators and have anti-inflammatory properties, which can prevent the formation of blood clots [9]. Furthermore, phosphodiesterase inhibitors can act to reduce blood viscosity and Naftidrofuryl can inhibit blood vessel blockage by reducing aggregation of erythrocytes and platelets [9]. To manage pain, patients can use nonsteroidal anti-inflammatory drugs; however, opioids are often required to manage severe pain and, in some cases, pain may be neuropathic, requiring an alternative therapeutic approach [6]. In addition to pharmacological interventions, lifestyle changes are recommended, and often required, to manage disease development. These changes involve quitting smoking, changing diet, and exercising, if possible [6, 10].

1.3 Regenerative Medicine Strategies for Revascularization

Though surgical and pharmacological interventions exist for the management of CLI, many of these strategies are not completely effective in reducing limb-specific events [8]. Therefore, people have turned toward regenerative medicine strategies for promoting revascularization of the ischemic tissue. These strategies often involve one or more aspects of the tissue engineering triad: cells, signals, and scaffolds (Fig. 1.3). Proangiogenic growth factors (GFs) have been investigated for revascularization in CLI patients for nearly 30 years, dating back to the first study to deliver vascular endothelial growth factor (VEGF) to rabbits with hindlimb ischemia (HLI) in 1994 [9]. Since, research has focused on the delivery of a variety of GFs to encourage the formation of new blood vessels in the ischemic limb, including hepatocyte growth factor (HGF), fibroblast growth factor (FGF), platelet-derived growth factor (PDGF), and epidermal growth factor (EGF) [10].

Regenerative Medicine Strategies for Treating CLI

Cell Delivery
MSC, iPSC, EPC, BMMNC, PBMNC

Cells

TE Triad

Signals   **Scaffolds**

Proangiogenic Factors
VEGF, HGF, FGF, PDGF, EGF

Biomaterials
Alginate, chitosan, collagen, HA, gelatin, dextran, fibrin, PLGA, PEG, PLGA
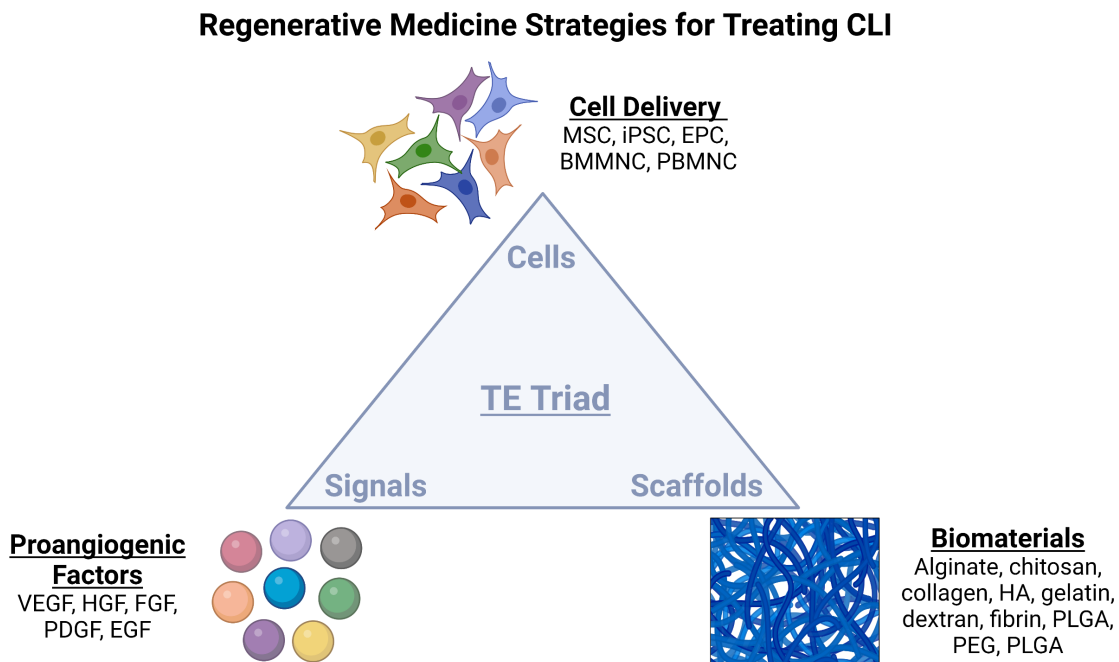
Figure 1.3: Regenerative medicine strategies for treating critical limb ischemia. *Strategies often involve one or more aspects of the tissue engineering (TE) triad: cells, signals, and scaffolds. Created with Biorender.com.*

Despite the promise of proangiogenic GF and recombinant protein delivery to stimulate vascularization in preclinical animal modes, clinical efficacy is often limited by short half-life and inadequate retention of factors at the site of ischemia [5, 11, 12]. Concerns regarding GF over expression, such as VEGF over expression leading to cancer-like leaky capillaries, adverse health effects, and a lack of knowledge of the appropriate route and dosage have limited the clinical potential of these therapies [5, 10]. Furthermore, the delivery of only a single GF may not fully recapitulate the complex GF cascade required for angiogenesis [9]. For these reasons, there are no FDA-approved treatments for CLI based on GF delivery [5]. Recent work is focusing on the use of exosomes to increase the complexity of delivered factors as well as microRNA therapy to circumvent the issue of GF half-life; however, there are concerns regarding inadequate *in vivo* transfection efficacy and persistent overexpression of GFs that could lead to tumor-related abbreviations [5, 8].

Cell-based therapies have been explored to overcome some of the shortfalls of GF delivery, with an emphasis on stem cells due to their regenerative potential and ability to be harvested from various sources in the body (bone marrow, adipose tissue), providing an autologous cell source. Mesenchymal stromal/stem cells (MSC), induced pluripotent stem cells (iPSC), endothelial progenitor cells (EPC), bone marrow mononuclear stem cells (BMMNC), and peripheral blood mononuclear cells (PBMNC) have all been investigated as cell-based therapies for CLI treatment [6, 8-10, 13], many of which have shown promise in preclinical trials [5]. Cells can act as a continuous reservoir for GFs and other cytokines, which is regulated in response to the pathologic environment [5]. MSC are the most commonly used cells for treating CVD due to their reported ability to promote angiogenesis through recruitment of endothelial cells (EC), release of soluble angiogenic factors, and immunomodulation via cytokine secretion [8]. EC have also been

administered, either alone or in combination with other support cells, into the ischemic hindlimb in preclinical animal studies with the goal of providing an exogenous cell source that can form vasculature at the site of implantation [5]. Like GF delivery, there are still questions surrounding the appropriate administration (intravenous versus intramuscular) and dosage of cell-based therapies [8]. While these stem cell-based therapies have demonstrated some clinical efficacy in patients with severed stages of PAD [8], there still remains challenges associated with cell survival and retention/engraftment at the site of ischemia [5, 9].

Lastly, research efforts have been made to develop biomaterials that can be used either as standalone therapeutics or in combination with the other aforementioned regenerative medicine strategies to improve their efficacy. Chitosan, gelatin, fibrin, alginate, hyaluronic acid, and other natural materials as well as poly(ethylene glycol) (PEG), poly(Latic-co-glycolic acid) (PLGA), and other synthetic materials have all been used in CLI studies [14]. Decellularized extracellular matrix (ECM) derived from porcine muscle has also shown promising results as a standalone treatment for CLI [15]. To improve cell survival or GF delivery, biomaterial scaffolds have been used as delivery platforms to provide anchorage for cells and support controlled release of pro-regenerative factors at the site of ischemia [13]. Previous studies have demonstrated the promise of biomaterial platforms to effectively delivery cells to the site of tissue injury or damage, but further work is still needed to identify effective biomaterial approaches to obtain therapeutic angiogenesis [5].

1.4 Hypothesis

The overarching goal of this dissertation is to develop cell-laden biomaterial platforms that support the therapeutic vascularization of ischemic tissues. This project combines the benefits of

multiple biomaterial and vascularization approaches to develop injectable, vascularizing microbeads from both natural and synthetic materials that support vessel morphogenesis *in vitro* and *in vivo*. To accomplish this, different fabrication techniques were developed to fabricate fibrin and PEG matrices with EC and stromal cells (SC) distributed within the modular microbeads. These modular biomaterial platforms were then utilized to address the overarching hypothesis that prevascularized microbeads can jump-start inosculation with host vasculature upon implantation, rapidly vascularizing ischemic tissues.

1.5 Specific Aims

The following specific aims were developed to evaluate this hypothesis:

Aim 1: Evaluate the vascularization capability of established fibrin-based microbeads *in vivo* in a subcutaneous implant and hindlimb ischemia model. Fibrin-based microbeads containing EC and SC were fabricated via bulk emulsification and pre-cultured prior to being embedded in a larger tissue mimic for culture *in vitro* or implanted *in vivo* in immunocompromised mice in both a subcutaneous implant and hindlimb ischemia (HLI) model. The goal of this aim was to assess how prevascularization of cell-laden fibrin microbeads influenced vascularization potential *in vitro* and if pre-cultured microbeads could form functional microvasculature networks *in vivo*. Furthermore, the HLI model was used to probe if pre-cultured microbeads could enhance the perfusion of ischemic tissues and increase limb salvage.

Aim 2: Develop PEG-based microbeads that facilitate the formation of well-distributed microvascular networks within a tissue mimic *in vitro*. Cell-encapsulating, PEG-based microbeads were formed via microfluidic droplet generation. The first goal of this aim was to identify degradable, cell-adhesive bulk PEG-norbornene (PEGNB) hydrogel formulations that

facilitated robust vessel morphogenesis. The second goal of this aim was to formulate PEGNB microbeads that support the encapsulation of viable cells that, when embedded in a larger tissue mimic *in vitro*, facilitate the formation of robust, well-distributed microvascular networks.

Aim 3: Assess the prevascularization potential and subsequent performance of PEG-based microbeads *in vitro* and *in vivo*. PEG microbeads were cultured in suspension for up to 7 days to assess vessel morphogenesis within the microbeads. Prevascularized microbeads were embedded in a larger tissue mimic *in vitro* to evaluate angiogenic sprouting. Microbeads were implanted within subcutaneous pockets on the dorsal flanks of immunocompromised mice for 7 days to evaluate microvascular network formation *in vivo*. The goal of this aim was to determine how prevascularization of PEG-based microbeads influences angiogenic sprouting *in vitro* and *in vivo*.

1.6 Overview of Dissertation

Chapter 1 highlights cardiovascular disease, specifically critical limb ischemia, and the limitations of current therapeutic interventions as a motivation for this dissertation. Chapter 2 discusses different cell-based and biomaterial approaches to engineering vascularized tissues as well as prevascularization strategies and modular approaches.

In Chapter 3, fibrin-based microbeads were prevascularized to form primitive vascular networks within the modular structures prior to being implanted into subcutaneous pockets on the dorsal flanks of immunocompromised mice. The purpose of these studies was to examine the effect of pre-culture duration on vessel development *in vitro* and *in vivo*. After 3 days *in vivo,* lumenized vessels originating from pre-cultured microbeads contained host erythrocytes while day 0 microbeads showed minimal evidence of functional connection to host vasculature. Overall, pre-cultured microbeads showed vascularization potential comparable to bulk cellular hydrogel

controls in this animal model, which motivated the need to assess their therapeutic potential in a model of ischemia. This chapter addresses the first half of Aim 1 and has recently been published in *Scientific Reports* [16].

In Chapter 4, fibrin-based microbeads were pre-cultured for 3 days before being implanted into intramuscular pockets in immunocompromised mice in a model of HLI. The purpose of this study was to investigate if pre-cultured microbeads could more rapidly vascularize ischemic tissues. By 14 days post-surgery, animals treated with pre-cultured microbeads showed increased macroscopic reperfusion of ischemic foot pads and improved limb salvage compared to the cellular controls. Pre-cultured microbeads implants contained extensive, perfused microvascular networks after 7 days *in vivo*. Despite these promising findings, fibrin-based microbeads tended to aggregate with extended pre-culture which limited the injectability of prevascularized modules and motivated the need to develop non-aggregating microbeads. This chapter addresses the second half of Aim 1 and has recently been published in *Journal of Biomaterials Research Part A* [17].

In Chapter 5, EC and SC were co-encapsulated in degradable, cell-adhesive PEGNB hydrogels in which stiffness and degradability were tuned to assess their independent and synergistic effects on vessel network formation and cell-mediated matrix remodeling longitudinally. The purpose of this study was to identify PEGNB matrices that supported vessel morphogenesis, with the goal of applying these materials to a microbead format. These results indicated that enhanced cell-mediated remodeling of PEG hydrogels, achieved either by reduced crosslinking or increased degradability, led to more rapid vessel formation and higher degrees of cell-mediated stiffening. Bulk PEGNB formulations that supported vascularization were then used to fabricate vascularizing microbeads. This chapter addresses the first half of Aim 2 and has recently been published in *Biomaterials* [18].

In Chapter 6, PEGNB-based microbeads containing EC and SC were developed using microfluidic droplet generation. Microbeads containing both cell types distributed throughout the PEG matrix supported extended pre-culture without microbead aggregation, resulting in discrete, prevascularized modules. Microbeads pre-cultured for 1 day formed robust, well-distributed microvascular networks *in vitro*. Despite the presence of preformed vessel-like structures within microbeads, vessel sprouting diminished with extended pre-culture time. *In vivo* data revealed human-derived capillary-like structures as well as some evidence of lumen formation within implants containing microbeads; however, in most cases these structures failed to robustly vascularize the surrounding implant region. This chapter addresses the second half of Aim 2 and Aim 3 and is in preparation for submission as a peer-reviewed journal article.

Finally, Chapter 7 summarizes the key findings and overall contributions of this dissertation to the field of tissue engineering and regenerative medicine. Future directions to improve and implement this work for various applications are also discussed. Overall, this dissertation presents the development and application of cell-encapsulating, vascularizing microbeads, which are a promising biomaterial and cell-based platform for the therapeutic vascularization of ischemic tissues as well as an attractive approach to formulating complex engineered tissues.

1.7 References

[1]   C. W. Tsao *et al.*, "Heart Disease and Stroke Statistics-2022 Update: A Report From the American Heart Association," *Circulation,* vol. 145, no. 8, pp. e153-e639, Feb 22 2022, doi: 10.1161/CIR.0000000000001052.

[2]   T. J. Cahill, R. P. Choudhury, and P. R. Riley, "Heart regeneration and repair after myocardial infarction: translational opportunities for novel therapeutics," *Nat Rev Drug Discov,* vol. 16, no. 10, pp. 699-717, Oct 2017, doi: 10.1038/nrd.2017.106.

[3]   S. Duff, M. S. Mafilios, P. Bhounsule, and J. T. Hasegawa, "The burden of critical limb ischemia: a review of recent literature," *Vasc Health Risk Manag,* vol. 15, pp. 187-208, 2019, doi: 10.2147/VHRM.S209241.

[4]   S. R. Levin, N. Arinze, and J. J. Siracuse, "Lower extremity critical limb ischemia: A review of clinical features and management," *Trends Cardiovasc Med,* vol. 30, no. 3, pp. 125-130, Apr 2020, doi: 10.1016/j.tcm.2019.04.002.

[5]   G. Marsico, S. Martin-Saldana, and A. Pandit, "Therapeutic Biomaterial Approaches to Alleviate Chronic Limb Threatening Ischemia," *Adv Sci (Weinh),* vol. 8, no. 7, p. 2003119, Apr 2021, doi: 10.1002/advs.202003119.

[6]   L. Uccioli, M. Meloni, V. Izzo, L. Giurato, S. Merolla, and R. Gandini, "Critical limb ischemia: current challenges and future prospects," *Vasc Health Risk Manag,* vol. 14, pp. 63-74, 2018, doi: 10.2147/VHRM.S125065.

[7]   E. J. Armstrong *et al.*, "Multidisciplinary Care for Critical Limb Ischemia: Current Gaps and Opportunities for Improvement," *J Endovasc Ther,* vol. 26, no. 2, pp. 199-212, Apr 2019, doi: 10.1177/1526602819826593.

[8]   L. Beltran-Camacho, M. Rojas-Torres, and M. C. Duran-Ruiz, "Current Status of Angiogenic Cell Therapy and Related Strategies Applied in Critical Limb Ischemia," *Int J Mol Sci,* vol. 22, no. 5, Feb 26 2021, doi: 10.3390/ijms22052335.

[9]   M. Hassanshahi *et al.*, "Critical limb ischemia: Current and novel therapeutic strategies," *Journal of Cellular Physiology,* vol. 234, no. 9, pp. 14445-14459, 2019, doi: 10.1002/jcp.28141.

[10]   Y. Pan *et al.*, "Advances for the treatment of lower extremity arterial disease associated with diabetes mellitus," *Front Mol Biosci,* vol. 9, p. 929718, 2022, doi: 10.3389/fmolb.2022.929718.

[11]   X. Li, K. Tamama, X. Xie, and J. Guan, "Improving Cell Engraftment in Cardiac Stem Cell Therapy," *Stem Cells Int,* vol. 2016, p. 7168797, 2016, doi: 10.1155/2016/7168797.

[12]   F. A. Auger, L. Gibot, and D. Lacroix, "The pivotal role of vascularization in tissue engineering," *Annu Rev Biomed Eng,* vol. 15, pp. 177-200, 2013, doi: 10.1146/annurev-bioeng-071812-152428.

[13]   M. Qadura, D. C. Terenzi, S. Verma, M. Al-Omran, and D. A. Hess, "Concise Review: Cell Therapy for Critical Limb Ischemia: An Integrated Review of Preclinical and Clinical Studies," *Stem Cells,* vol. 36, no. 2, pp. 161-171, Feb 2018, doi: 10.1002/stem.2751.

[14]   Z. Xing, C. Zhao, S. Wu, C. Zhang, H. Liu, and Y. Fan, "Hydrogel-based therapeutic angiogenesis: An alternative treatment strategy for critical limb ischemia," *Biomaterials,* vol. 274, p. 120872, Jul 2021, doi: 10.1016/j.biomaterials.2021.120872.

[15]   J. L. Ungerleider *et al.*, "Extracellular Matrix Hydrogel Promotes Tissue Remodeling, Arteriogenesis, and Perfusion in a Rat Hindlimb Ischemia Model," *JACC Basic Transl Sci,* vol. 1, no. 1-2, pp. 32-44, Jan-Feb 2016, doi: 10.1016/j.jacbts.2016.01.009.

[16]   N. E. Friend *et al.*, "Injectable pre-cultured tissue modules catalyze the formation of extensive functional microvasculature in vivo," *Sci Rep,* vol. 10, no. 1, p. 15562, Sep 23 2020, doi: 10.1038/s41598-020-72576-5.

[17]   N. E. Friend, J. A. Beamish, E. A. Margolis, N. G. Schott, J. P. Stegemann, and A. J. Putnam, "Pre-cultured, cell-encapsulating fibrin microbeads for the vascularization of ischemic tissues," *J Biomed Mater Res A,* Jun 16 2023, doi: 10.1002/jbm.a.37580.

[18]   N. E. Friend, A. J. McCoy, J. P. Stegemann, and A. J. Putnam, "A combination of matrix stiffness and degradability dictate microvascular network assembly and remodeling in cell-laden poly(ethylene glycol) hydrogels," *Biomaterials,* vol. 295, p. 122050, Apr 2023, doi: 10.1016/j.biomaterials.2023.122050.

Chapter 2 – Cell-based Approaches to Vascularization

2.1 Physiological Formation of Microvascular Networks

Microvasculature is formed via two distinct processes: vasculogenesis, the *de novo* formation of blood vessels from individual cells, and angiogenesis, the formation of new vessels from preexisting blood vessels (Fig. 2.1). During embryonic development, blood vessel formation occurs through vasculogenesis, which establishes a primitive vascular plexus. These vessel networks continue to expand through angiogenesis [1]. Vascular development is a dynamic process involving interactions between endothelial cells (EC) and supporting pericytes to form functional and mature microvascular networks. In cases of tissue injury and repair, revascularization through angiogenesis is modulated by oxygen tension in the local microenvironment. When exposed to low oxygen conditions, cells in the surrounding tissue experience an increase in hypoxia-inducible factor (HIF)-1α, which leads to downstream transcriptional cascades resulting in an up-regulation of vascular protein secretion, such as vascular endothelial growth factor (VEGF). Gradients of VEGF and other angiogenic factors spatially and temporally control the invasion of sprouting vessels into the ischemic tissue to restore blood supply [2-4].
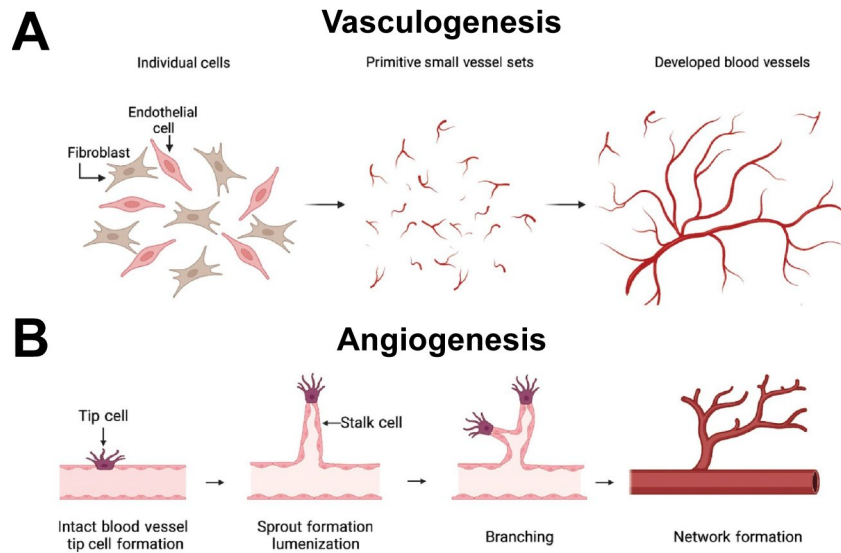
Figure 2.1: Processes of microvasculature formation. *Microvasculature is either formed via (A) vasculogenesis, the de novo formation of blood vessels from individual cells or (B) angiogenesis, the formation of new vessels from preexisting blood vessels. Images modified from [5], Copyright 2023, Elsevier, Ltd.*

Sprouting angiogenesis involves the proliferation and migration of EC to form neovessels, which either regress or proceed to maturity through interactions with pericytes [4]. Though the identity of pericytes is not well-defined, these cells are generally described as peri-endothelial stromal cells (SC) that play a role in vascular development and homeostasis [6]. Pericytes also aid in vessel maturation through extracellular matrix (ECM) deposition to establish the vascular basement membrane (BM), which provides mechanical stability and serves as a scaffold for signaling proteins [7]. The formation of a BM is orchestrated by both EC and pericytes; however, pericytes serve as the primary contributor as they deposit many critical ECM components, including collagen IV, fibronectin, laminins, and nidogens [8].

2.2 Cell Types for Engineering Microvasculature

A variety of EC types have been explored as potential cell sources for engineering vascularized tissues. Human umbilical vein endothelial cells (HUVEC) remain the most commonly utilized cell type for models of angiogenesis and vasculogenesis [9], in part because other populations of EC do not generate microvasculature of similar quantities or qualities [10-12]. Endothelial progenitor cells (EPC) are circulating progenitor cells found in the peripheral blood that differentiate toward an EC phenotype and give rise to microvascular networks [13]. Endothelial colony-forming cells (ECFC) [14] and outgrowth endothelial cells (OEC) [15] have been explored as autologous EC sources with promising clinical potential; however, one major limitation is the ability to generate enough cells for a therapeutic does due to their low frequency in peripheral and cord blood [16]. Furthermore, studies have found that type 1 diabetic patients have significantly lower levels of EPC compared to both type 2 diabetic patients and non-diabetic controls [17]. Induced pluripotent stem cell-derived EC (iPSC-EC) have also been explored as an alternative autologous EC source with varying degrees of success. Macklin et al. found that iPSC-EC and HUVEC spheroids both supported the formation of a similar number of vessel sprouts *in vitro* [18], but Bezenah et al. found that iPSC-EC did not produce as robust of microvascular networks compared to HUVEC *in vitro* [10] or *in vivo* [11].

While some studies focus only on EC monocultures for the generation of vascularized constructs to prevent increased regulatory barriers that may arise from using multiple cell types [5], SC are often necessary for network maturation and long-term stability [17, 19]. SC regulate capillary permeability, sprouting angiogenesis, and vascular lumen formation either by direct association with blood vessels or through the secretion of specific stromal-derived matricellular factors [20]. Multiple SC types have also been explored as supportive pericyte-like cells, including

mesenchymal stem/stromal cells (MSC), fibroblast (FB), and vascular smooth muscle cells (VSMC). Studies have shown that stromal cell identity modulates vascular morphogenesis *in vitro* and *in vivo*. Margolis et al. found lung FB supported the most robust microvascular network formation with functional perfusion using a microvasculature-on-a-chip platform [21]. Grainger et al. found that stromal cell identity (bone marrow-derived MSC, adipose-derived MSC, or lung FB) influenced engineered vessel functionality *in vivo* as MSC-supported microvasculature had reduced permeability compared to FB-supported vessels [22].

2.3 Biomaterials to Support Vascular Tissue Engineering

Biomaterials can serve as supportive matrices for cells cultured on or within hydrogel constructs. A wide range of biomaterials have been explored to support the formation of microvascular networks both *in vitro* and *in vivo*. These materials provide instructional biophysical cues to encapsulated cells in the form of stiffness, porosity, adhesivity, degradability, geometry, and topography, all of which influence cell fate and have the potential to enhance the vascularization capacity of cell delivery platforms [23, 24].

2.3.1 Natural Materials

Various natural materials have been explored as hydrogel-based platforms for *in vitro* and *in vivo* vascularization. Alginate, an algae-derived polysaccharide, has been implemented in tissue engineering strategies as a result of its biocompatibility, biodegradability, non-antigenicity and chelating ability [25]. When modified with adhesive ligands, such as arginine-glycine-aspartic acid (RGD), alginate can support cell culture and vessel morphogenesis [26-28]. Other materials, such as collagen and its hydrolytic product, gelatin, naturally possess peptide sequences that are

recognized by cell receptors allowing direct cell-ECM interaction and adhesion [29]. Collagen hydrogels have a fibrillar architecture, whose characteristics can be controlled by crosslinking temperature and pH [30], which can subsequently influence vascular network formation [31].

Fibrin is of particular interest given its role in the early stages of wound healing and established FDA approval for use as a surgical glue (e.g., Baxter's Tisseel and Artiss) [32]. Fibrin hydrogels are formed when thrombin is mixed with soluble fibrinogen. First, thrombin initiates fibrin assembly by the cleavage of fibrinopeptides A (FPA) and B (FPB) on the N-termini of the Aα and Bβ chains of fibrinogen, resulting in the formation of fibrin monomers [33, 34]. Cleavage of FPA and FPB exposes binding sites in the central domain of fibrinogen molecules that are complementary to binding sites on the end of adjacent molecules, resulting in protofibrils comprised of half-stagger fibrin monomers [35]. As protofibrils grow, they aggregate to form longer fibers that eventually branch to form the three-dimensional (3D) fibrin network [34]. Factor XIIIa, generated from its precursor, factor XIII by thrombin in the presence of calcium ions, results in the formation of covalent bonds further stabilizing the clot *in vivo* [34, 35]. Fibrin clots are broken down when circulating plasminogen binds to fibrin followed activation to its active protease, plasmin, by tissue-type plasminogen activator (tPa) [33, 34].

Fibrin is a viscoelastic polymer with a fibrillar architecture. Studies have shown that some growth factors and proteins, such as fibroblast growth factor (FGF), VEGF, heparin, and fibronectin, naturally bind to fibrin [34]. This fibronectin binding and presentation of adhesive domains, such as RGD, allows cells to bind directly to the fibrin matrix [32]. Various studies have investigated the use of fibrin as a vascularization platform, evaluating how different material properties regulate vessel morphogenesis. Kniazeva et al. found that increasing the density of fibrin has an inhibitory effect on vessel assembly *in vitro* and *in vivo* [36]. Sacchi et al. developed fibrin

hydrogels with slower degradation rates for sustained delivery of VEGF [37]. Other studies have focused on how cells interact with the fibrin matrix during vascularization, with specific studies highlighting the different modes of degradation employed by different SC types [38, 39].

2.3.2 Synthetic Materials

Although natural have been extensively studied for vascularization applications, these materials are often derived from animal sources and can exhibit batch-to-batch variability which pose potential barriers to translation. Synthetic materials utilize chemical synthesis to generate synthetic polymers capable of forming 3D networks, largely mitigating batch-to-batch variability and promoting highly reproducible scaffold properties. Synthetic polymers allow better control over their chemistry and the material properties of the subsequent hydrogels [30]. Though a variety of synthetic scaffolds have been used to generate large-scale tissue engineering vascular grafts [5], the focus of this dissertation is on small-scale microvascular networks.

While modified polycaprolactone (PCL) [40-42] and poly-lactic-glycolic acid (PLGA) [43, 44] scaffolds have showed some promise as vascularization platforms, materials such as these often have to be combined with other materials for effective vessel morphogenesis [30]. Poly(ethylene glycol), or PEG, has emerged as a promising material for tissue engineering applications due to its ability to be functionalized with a variety of end groups, affording relatively easy customization of hydrogel properties [45, 46]. PEG hydrogels can be crosslinked by a multitude of chemical reactions (Michael type addition (MTA), photopolymerization, etc.) which can change the crosslinking kinetics of the reaction [47]. Due to their fully synthetic nature, PEG hydrogels must also be modified with adhesive ligands and degradable moieties to be suitable platforms for cell culture. Previous studies have evaluated the effect of altering PEG macromer type, polymer wt. % [48-57], adhesive and crosslinking peptide identity and concentrations [57-

63], and crosslinking ratios [59, 64] on vessel morphogenesis in PEG-based hydrogels. These studies have elucidated the importance of key matrix physiochemical characteristics. Vessel morphogenesis has been shown to more readily occur in hydrogels with softer initial stiffness, increased degradability, and greater cell adhesion motifs.

2.3.3 Hybrid Materials and Interpenetrating Networks

An additional tissue engineering approach for generating vascularized matrices is the implementation of hybrid/composite materials or interpenetrating networks (IPNs) with the goal of harnessing the attractive properties of multiple natural and/or synthetic materials in one hydrogel system. Modifying natural materials with synthetic side/end groups allows for greater control over material crosslinking mechanisms and often lends greater mechanical strength and long-term stability. Methacrylated gelatin (GelMA) [65] and hyaluronic acid (HAMA) [66] as well as dextran vinyl sulfone (DexVS) [67] have demonstrated vascularization potential. A similar approach of conjugating natural materials to PEG molecules, PEGylation, has been used to generate vascularized PEG-collagen [68] and PEG-fibrinogen [69-71] composite hydrogels with the biological properties defined by the protein and microarchitectures by the synthetic polymer.

Composite materials can also be a combination of two natural materials, such as collagen-fibrin [72, 73], collagen-glycosaminoglycan [74], and alginate-gelatin [75], all of which have demonstrated vascularization potential. Lastly, two materials can be combined into IPNs, defined as a class of polymer composites composed of two crosslinked networks that are topologically entangled and yet cannot be separated without disrupting existing chemical bonds [76]. IPNs typically exist to improve the mechanical properties and long-term stability of materials like fibrin [77] and prevent compaction in materials like collagen [78].

2.4 Prevascularization Strategies

Cell-based approaches to treat ischemic tissues have been plagued by low cell retention at the target site and reduced cell viability due to the harsh ischemic environment [79, 80]. To improve cell engraftment, researchers have explored the delivery of cells within hydrogels (some of which were described previously); however, even when cell engraftment is improved, implanted cells can experience apoptosis as diffusion of the necessary nutrients is limited within implanted constructs. Though diffusion may not be limited by tissue thickness during *in vitro* culture [81], necrosis may occur at the core of larger tissue constructs once implanted *in vivo* as diffusion of nutrients to the center will rely solely on timely inosculation with host vasculature [82].

Prevascularization is a promising method for promoting the rapid inosculation of engineered vasculature with that of the host. Prevascularization strategies focus on developing a microvascular network *in vitro* in tissue constructs prior to transplantation in an attempt to expedite the process of functional inosculation and quickly provide tissue scaffolds with the necessary nutrients to survive *in vivo*. One approach to generating prevascularized constructs is the generation of scaffold-free cell sheets. EC and/or SC containing sheets are cultured to confluence, allowing cells to deposit their own ECM, before being stack on top of one another to create a multilayered tissue construct [83, 84]. Cell sheet approaches may also include the culture of cells on top of hydrogel matrices to form prevascularized sheets [85, 86].

Whole hydrogel constructs have been prevascularized *in vitro* using some of the cell-based approaches previously discussed. Prevascularized hydrogels have demonstrated accelerated formation of functional anastomosis with host vasculature for HUVEC and lung FB containing fibrin [87] and PLLA/PLGA scaffolds (Fig. 2.2) [43]. Endothelialized, patterned scaffolds have rescued perfusion in a model of hindlimb ischemia (HLI) [88]. Other studies have vascularized

tissue constructs *in vivo* by implanting a hydrogel into one animal, allowing time for the hydrogel to become vascularized, either by co-implanted cells or by the host's own vasculature, before removing the hydrogel and transferring it to a secondary animal [44, 89].
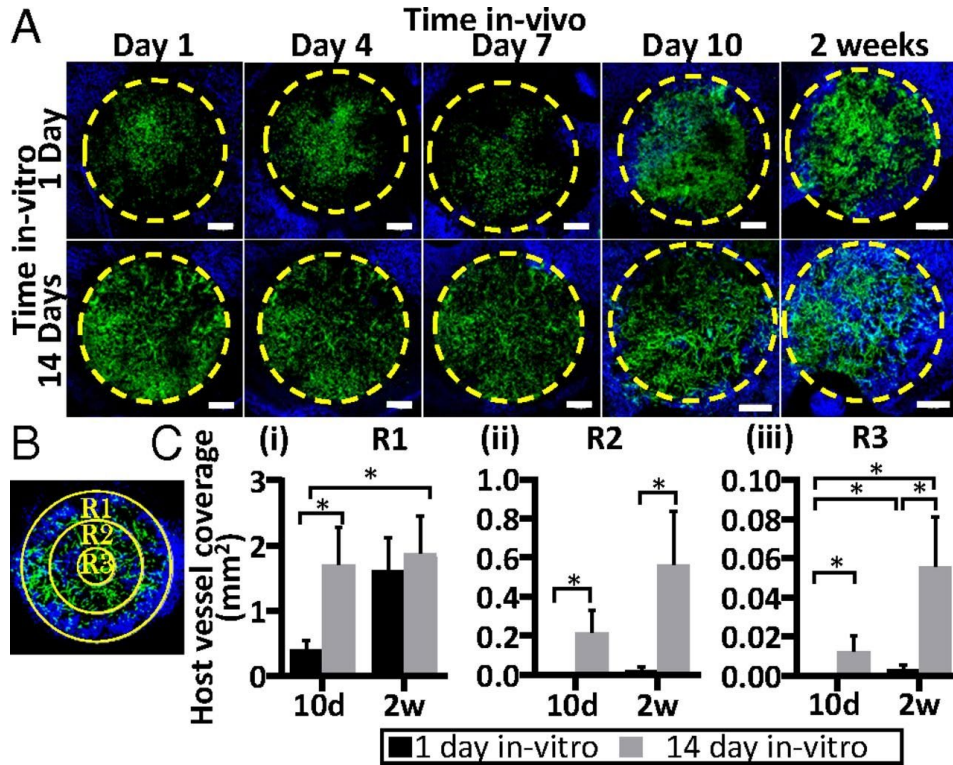
Figure 2.2: Prevascularized scaffolds demonstrate greater host vessel invasion compared to non-prevascularized scaffolds. *(A) Implanted grafts had been cultured for 1 day (upper) or 14 days (lower) before implantation. Graft perimeter (6 mm) is marked by a yellow dashed line, implanted GFP-labelled EC are in green, and host vessels are in blue. (B) Three different regions of the graft: R1 represents the outermost ring in the graft perimeter (6 mm), R2 represents the middle ring, and R3 is the center of each graft. (C) Host vessel coverage (mm^2) analysis in R1, R2, and R3 (C, i–iii, respectively). Data are presented as means $\pm$ SEM. $n \geq 4$ (*$p < 0.05$) (Scale bar = 1mm.). Images from [43], Copyright 2019, National Academy of Science.*

Furthermore, prevascularization approaches have also been shown to support the formation of new tissue, such as muscle [90] and bone [91, 92], upon implantation. Despite the promise of prevascularizing cell sheets, matrices, or entire tissue constructs, these approaches are limited to invasive surgical procedures for the implantation of materials. As patients with vascular diseases, such as CLI, often have comorbidities (e.g., diabetes) that render them ineligible for invasive

surgical procedures [93], alternative prevascularization approaches must be explored to improve the therapeutic efficacy of cell-based therapies for treating ischemic tissues.

2.5 Modular Approaches to Vascularization

Although prevascularization strategies may expedite functional inosculation of implanted microvasculature within engineered tissue constructs, without immediate perfusion (only possible with invasive surgical implantation and anastomosis) the center of larger tissue constructs greater than 400 µm in diameter, commonly discussed as the estimated diffusion limitation in many tissues [94, 95], is susceptible to necrosis without timely supply of oxygen and nutrients. Modular tissue constructs may overcome some of the limitations of large-scale, whole construct prevascularization as they can be fabricated with small diameters to circumvent this potential diffusion restriction. Furthermore, microtissues can provide encapsulated cells with a hydrogel matrix that facilitates prevascularization while maintaining injectability, allowing them to be delivered in a minimally invasive manner (Fig. 2.3).

Cell aggregates, or spheroids, have emerged as a scaffold-free method for prevascularization. HUVEC monoculture spheroids have formed functional microvascular networks *in vivo* [96-98]. Various SC types, such as bone marrow-derived MSC [91], adipose-derived MSC [99-101], smooth muscle cells (SMC) [102], dermal FB [100], and dental pulp stem cells [103], have been incorporated into co-culture spheroids to fabricate prevascularized tissue modules for tissue-specific applications. HUVEC have also been coated on myofibroblast spheroids for muscle regeneration approaches [104]. The use of cell spheroids offers injectability; however, spheroids can be subject to similar obstacles as other direct cell delivery treatments discussed previously. EC have also been coated on the surface of modular hydrogels for cell

delivery applications [105, 106]. Cell-laden modular hydrogels in which EC were coated on the outer surface have shown enhanced engraftment and vascularization when delivered *in vivo* [107, 108].
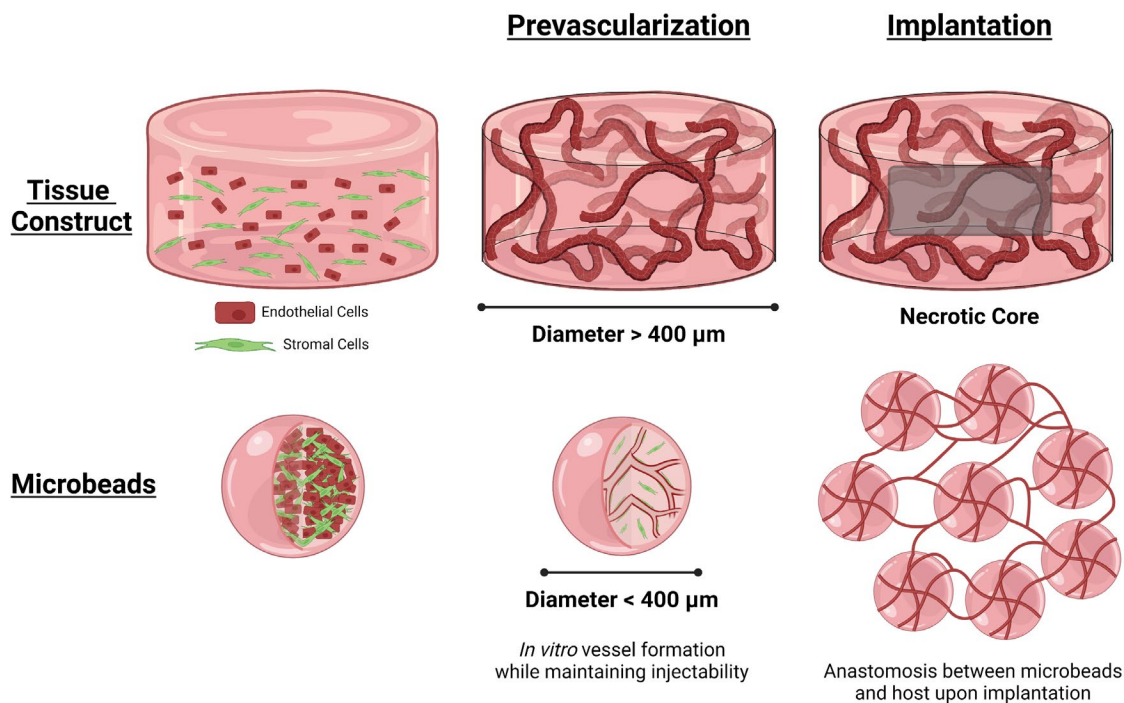
Figure 2.3: Comparison of bulk scaffold and microbead prevascularization. *Without timely inosculation to host vasculature, prevascularized bulk tissue constructs are susceptible to developing a necrotic core. Microbeads have the potential to overcome this challenge due to small diameters that reduce diffusion limitations. Created with Biorender.com.*

Encapsulating cells within modular hydrogels can provide the added benefit of instructive cues, structure, and protection provided by the matrix during injection, which may be especially advantageous for improving cell viability and engraftment when implanted into ischemic environments. OEC have been encapsulated in alginate microgels with the addition of VEGF and hepatocyte growth factor (HGF) which resulted in perfusion recovery in a HLI model [28]. Similarly, HUVEC encapsulated in collagen microgels with DNA programmed with VEGF aptamers showed vessel assembly in wound healing and liver regeneration models [109]. HUVEC or OEC have been co-encapsulated with MSC in RGD-oxiHM-alginate [26, 27] and GelMA [65]

microgels, both of which supported prevascularization as evidenced by EC assembly within the microgels. Furthermore, prevascularized microgels supported vessel formation *in vivo* in a chick embryo and subcutaneous implant model [26, 27]. To date, these are the few studies that focus on the prevascularization of modular tissue constructs via encapsulation of cells in a micron-sized hydrogel matrix, none of which have tested vascularization potential in ischemic tissues.
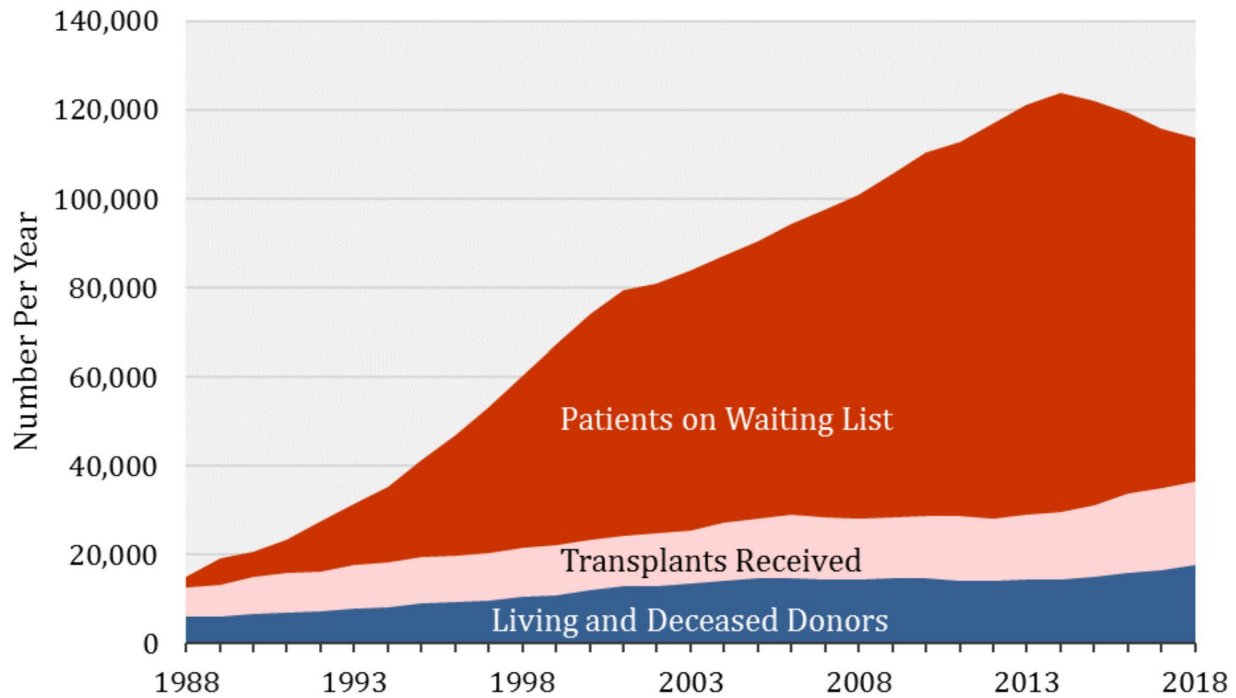
Figure 2.4: Transplant statistics in the United States. *The number of patients on the transplant waiting list far outweighs the number of donors and transplants received each year. Image reproduced from [110], Copyright 2020, Gallup, Inc.*

Further, strategies employed to bioengineer large functional tissues to overcome the challenge of organ shortages (Fig. 2.4) are limited by their lack of adequate vascularization throughout the tissue constructs [12, 82, 111]. Though research has made great strides toward fabricating large-scale vessels, there are still many challenges associated with forming functional capillary beds within tissue engineered constructs [12]. Prevascularized microbeads can offer a method of incorporating nodes of microvasculature throughout larger constructs that allow for the rapid formation of a robust, spatially distributed microvascular network. These microbeads could

24

be incorporated into various tissue engineering strategies, such as creating vascularized bone [91] or implanting pancreatic islet or beta cells within a functional vascular network to improve survival and long-term function [112].

2.6 References

[1]   M. A. Traore and S. C. George, "Tissue Engineering the Vascular Tree," *Tissue Eng Part B Rev,* vol. 23, no. 6, pp. 505-514, Dec 2017, doi: 10.1089/ten.teb.2017.0010.

[2]   A. J. Melchiorri, B. N. Nguyen, and J. P. Fisher, "Mesenchymal stem cells: roles and relationships in vascularization," *Tissue Eng Part B Rev,* vol. 20, no. 3, pp. 218-28, Jun 2014, doi: 10.1089/ten.TEB.2013.0541.

[3]   E. A. Phelps and A. J. Garcia, "Update on therapeutic vascularization strategies," *Regen Med,* vol. 4, no. 1, pp. 65-80, Jan 2009, doi: 10.2217/17460751.4.1.65.

[4]   M. S. Wietecha, W. L. Cerny, and L. A. DiPietro, "Mechanisms of vessel regression: toward an understanding of the resolution of angiogenesis," *Curr Top Microbiol Immunol,* vol. 367, pp. 3-32, 2013, doi: 10.1007/82_2012_287.

[5]   E. A. Margolis, N. E. Friend, M. W. Rolle, E. Alsberg, and A. J. Putnam, "Manufacturing the multiscale vascular hierarchy: progress toward solving the grand challenge of tissue engineering," *Trends Biotechnol,* May 9 2023, doi: 10.1016/j.tibtech.2023.04.003.

[6]   A. Armulik, G. Genove, and C. Betsholtz, "Pericytes: developmental, physiological, and pathological perspectives, problems, and promises," *Dev Cell,* vol. 21, no. 2, pp. 193-215, Aug 16 2011, doi: 10.1016/j.devcel.2011.07.001.

[7]   L. B. Payne *et al.*, "The pericyte microenvironment during vascular development," *Microcirculation,* vol. 26, no. 8, p. e12554, Nov 2019, doi: 10.1111/micc.12554.

[8]   A. N. Stratman, K. M. Malotte, R. D. Mahan, M. J. Davis, and G. E. Davis, "Pericyte recruitment during vasculogenic tube assembly stimulates endothelial basement membrane matrix formation," *Blood,* vol. 114, no. 24, pp. 5091-101, Dec 3 2009, doi: 10.1182/blood-2009-05-222364.

[9]   K. T. Morin and R. T. Tranquillo, "In vitro models of angiogenesis and vasculogenesis in fibrin gel," *Exp Cell Res,* vol. 319, no. 16, pp. 2409-17, Oct 1 2013, doi: 10.1016/j.yexcr.2013.06.006.

[10]   J. R. Bezenah, Y. P. Kong, and A. J. Putnam, "Evaluating the potential of endothelial cells derived from human induced pluripotent stem cells to form microvascular networks in 3D cultures," *Sci Rep,* vol. 8, no. 1, p. 2671, Feb 8 2018, doi: 10.1038/s41598-018-20966-1.

[11]   J. R. Bezenah, A. Y. Rioja, B. Juliar, N. Friend, and A. J. Putnam, "Assessing the ability of human endothelial cells derived from induced-pluripotent stem cells to form functional microvasculature in vivo," *Biotechnol Bioeng,* vol. 116, no. 2, pp. 415-426, Feb 2019, doi: 10.1002/bit.26860.

[12]   P. Chandra and A. Atala, "Engineering blood vessels and vascularized tissues: technology trends and potential clinical applications," *Clin Sci (Lond),* vol. 133, no. 9, pp. 1115-1135, May 15 2019, doi: 10.1042/CS20180155.

[13]   E. B. Peters, "Endothelial Progenitor Cells for the Vascularization of Engineered Tissues," *Tissue Eng Part B Rev,* vol. 24, no. 1, pp. 1-24, Feb 2018, doi: 10.1089/ten.TEB.2017.0127.

[14]   J. M. Melero-Martin, "Human Endothelial Colony-Forming Cells," *Cold Spring Harb Perspect Med,* vol. 12, no. 12, Dec 1 2022, doi: 10.1101/cshperspect.a041154.

[15]   S. Fuchs, E. Dohle, M. Kolbe, and C. J. Kirkpatrick, "Outgrowth endothelial cells: sources, characteristics and potential applications in tissue engineering and regenerative medicine," *Adv Biochem Eng Biotechnol,* vol. 123, pp. 201-17, 2010, doi: 10.1007/10_2009_65.

[16]   C. Keighron, C. J. Lyons, M. Creane, T. O'Brien, and A. Liew, "Recent Advances in Endothelial Progenitor Cells Toward Their Use in Clinical Translation," *Front Med (Lausanne),* vol. 5, p. 354, 2018, doi: 10.3389/fmed.2018.00354.

[17]   G. Yang, B. Mahadik, J. Y. Choi, and J. P. Fisher, "Vascularization in tissue engineering: fundamentals and state-of-art," *Prog Biomed Eng (Bristol),* vol. 2, no. 1, Jan 2020, doi: 10.1088/2516-1091/ab5637.

[18]   B. L. Macklin *et al.*, "Intrinsic epigenetic control of angiogenesis in induced pluripotent stem cell-derived endothelium regulates vascular regeneration," *NPJ Regen Med,* vol. 7, no. 1, p. 28, May 12 2022, doi: 10.1038/s41536-022-00223-w.

[19]   H. G. Song *et al.*, "Transient Support from Fibroblasts is Sufficient to Drive Functional Vascularization in Engineered Tissues," *Adv Funct Mater,* vol. 30, no. 48, Nov 25 2020, doi: 10.1002/adfm.202003777.

[20]   M. B. Curtis, N. Kelly, C. C. W. Hughes, and S. C. George, "Organotypic stromal cells impact endothelial cell transcriptome in 3D microvessel networks," *Sci Rep,* vol. 12, no. 1, p. 20434, Nov 28 2022, doi: 10.1038/s41598-022-24013-y.

[21]   E. A. Margolis *et al.*, "Stromal cell identity modulates vascular morphogenesis in a microvasculature-on-a-chip platform," *Lab Chip,* vol. 21, no. 6, pp. 1150-1163, Mar 21 2021, doi: 10.1039/d0lc01092h.

[22]   S. J. Grainger, B. Carrion, J. Ceccarelli, and A. J. Putnam, "Stromal cell identity influences the in vivo functionality of engineered capillary networks formed by co-delivery of endothelial cells and stromal cells," *Tissue Eng Part A,* vol. 19, no. 9-10, pp. 1209-22, May 2013, doi: 10.1089/ten.TEA.2012.0281.

[23]   S. V. Lopes, M. N. Collins, R. L. Reis, J. M. Oliveira, and J. Silva-Correia, "Vascularization Approaches in Tissue Engineering: Recent Developments on Evaluation Tests and Modulation," *ACS Appl Bio Mater,* vol. 4, no. 4, pp. 2941-2956, Apr 19 2021, doi: 10.1021/acsabm.1c00051.

[24]   C. A. Dessalles, C. Leclech, A. Castagnino, and A. I. Barakat, "Integration of substrate- and flow-derived stresses in endothelial cell mechanobiology," *Commun Biol,* vol. 4, no. 1, p. 764, Jun 21 2021, doi: 10.1038/s42003-021-02285-w.

[25]   J. Sun and H. Tan, "Alginate-Based Biomaterials for Regenerative Medicine Applications," *Materials (Basel),* vol. 6, no. 4, pp. 1285-1309, Mar 26 2013, doi: 10.3390/ma6041285.

[26]   A. L. Torres, S. J. Bidarra, M. T. Pinto, P. C. Aguiar, E. A. Silva, and C. C. Barrias, "Guiding morphogenesis in cell-instructive microgels for therapeutic angiogenesis," *Biomaterials,* vol. 154, pp. 34-47, Feb 2018, doi: 10.1016/j.biomaterials.2017.10.051.

[27]   A. L. Torres *et al.*, "Microvascular engineering: Dynamic changes in microgel-entrapped vascular cells correlates with higher vasculogenic/angiogenic potential," *Biomaterials,* vol. 228, p. 119554, Jan 2020, doi: 10.1016/j.biomaterials.2019.119554.

[28]   P. H. Kim *et al.*, "Injectable multifunctional microgel encapsulating outgrowth endothelial cells and growth factors for enhanced neovascularization," *J Control Release,* vol. 187, pp. 1-13, Aug 10 2014, doi: 10.1016/j.jconrel.2014.05.010.

[29]   R. Parenteau-Bareil, Gauvin, R., and Berthod, F. , "Collagen-Based Biomaterials for Tissue Engineering Applications," *Materials (Basel),* vol. 3, no. 3, pp. 1863-1887, 2010, doi: 10.3390/ma3031863.

[30]   S. Bist, A. Banerjee, I. P. Patra, S. R. Jayaprakash, R. Sureka, and S. Pradhan, "Hydrogel-Based Tissue-Mimics for Vascular Regeneration and Tumor Angiogenesis," Springer Nature Singapore, 2023, pp. 143-180.

[31]   M. G. McCoy, B. R. Seo, S. Choi, and C. Fischbach, "Collagen I hydrogel microstructure and composition conjointly regulate vascular network formation," *Acta Biomaterialia,* vol. 44, pp. 200-208, 2016, doi: 10.1016/j.actbio.2016.08.028.

[32]   J. Ceccarelli and A. J. Putnam, "Sculpting the blank slate: how fibrin's support of vascularization can inspire biomaterial design," *Acta Biomater,* vol. 10, no. 4, pp. 1515-23, Apr 2014, doi: 10.1016/j.actbio.2013.07.043.

[33]   M. W. Mosesson, "Fibrinogen and fibrin structure and functions," *J Thromb Haemost,* vol. 3, no. 8, pp. 1894-904, Aug 2005, doi: 10.1111/j.1538-7836.2005.01365.x.

[34] J. W. Weisel, "Fibrinogen and fibrin," *Adv Protein Chem,* vol. 70, pp. 247-99, 2005, doi: 10.1016/S0065-3233(05)70008-5.

[35] P. A. Janmey, J. P. Winer, and J. W. Weisel, "Fibrin gels and their clinical and bioengineering applications," *Journal of The Royal Society Interface,* vol. 6, no. 30, pp. 1-10, 2009, doi: 10.1098/rsif.2008.0327.

[36] E. Kniazeva, S. Kachgal, and A. J. Putnam, "Effects of extracellular matrix density and mesenchymal stem cells on neovascularization in vivo," *Tissue Eng Part A,* vol. 17, no. 7-8, pp. 905-14, Apr 2011, doi: 10.1089/ten.TEA.2010.0275.

[37] V. Sacchi *et al.*, "Long-lasting fibrin matrices ensure stable and functional angiogenesis by highly tunable, sustained delivery of recombinant VEGF164," *Proc Natl Acad Sci U S A,* vol. 111, no. 19, pp. 6952-7, May 13 2014, doi: 10.1073/pnas.1404605111.

[38] C. M. Ghajar *et al.*, "Mesenchymal cells stimulate capillary morphogenesis via distinct proteolytic mechanisms," *Exp Cell Res,* vol. 316, no. 5, pp. 813-25, Mar 10 2010, doi: 10.1016/j.yexcr.2010.01.013.

[39] S. Kachgal and A. J. Putnam, "Mesenchymal stem cells from adipose and bone marrow promote angiogenesis via distinct cytokine and protease expression mechanisms," *Angiogenesis,* vol. 14, no. 1, pp. 47-59, Mar 2011, doi: 10.1007/s10456-010-9194-9.

[40] S. Singh, B. M. Wu, and J. C. Dunn, "Accelerating vascularization in polycaprolactone scaffolds by endothelial progenitor cells," *Tissue Eng Part A,* vol. 17, no. 13-14, pp. 1819-30, Jul 2011, doi: 10.1089/ten.TEA.2010.0708.

[41] K. Xu *et al.*, "Enhanced vascularization of PCL porous scaffolds through VEGF-Fc modification," *J Mater Chem B,* vol. 6, no. 27, pp. 4474-4485, Jul 21 2018, doi: 10.1039/c8tb00624e.

[42] S. Gniesmer *et al.*, "In vivo analysis of vascularization and biocompatibility of electrospun polycaprolactone fibre mats in the rat femur chamber," *J Tissue Eng Regen Med,* vol. 13, no. 7, pp. 1190-1202, Jul 2019, doi: 10.1002/term.2868.

[43] S. Ben-Shaul, S. Landau, U. Merdler, and S. Levenberg, "Mature vessel networks in engineered tissue promote graft-host anastomosis and prevent graft thrombosis," *Proc Natl Acad Sci U S A,* vol. 116, no. 8, pp. 2955-2960, Feb 19 2019, doi: 10.1073/pnas.1814238116.

[44] M. W. Laschke *et al.*, "Improvement of vascularization of PLGA scaffolds by inosculation of in situ-preformed functional blood vessels with the host microvasculature," *Ann Surg,* vol. 248, no. 6, pp. 939-48, Dec 2008, doi: 10.1097/SLA.0b013e31818fa52f.

[45] J. Zhu, "Bioactive modification of poly(ethylene glycol) hydrogels for tissue engineering," *Biomaterials,* vol. 31, no. 17, pp. 4639-56, Jun 2010, doi: 10.1016/j.biomaterials.2010.02.044.

[46]   X. Li, Q. Sun, Q. Li, N. Kawazoe, and G. Chen, "Functional Hydrogels With Tunable Structures and Properties for Tissue Engineering Applications," *Front Chem,* vol. 6, p. 499, 2018, doi: 10.3389/fchem.2018.00499.

[47]   J. Kim, Y. P. Kong, S. M. Niedzielski, R. K. Singh, A. J. Putnam, and A. Shikanov, "Characterization of the crosslinking kinetics of multi-arm poly(ethylene glycol) hydrogels formed via Michael-type addition," *Soft Matter,* vol. 12, no. 7, pp. 2076-85, Feb 21 2016, doi: 10.1039/c5sm02668g.

[48]   B. A. Juliar, J. A. Beamish, M. E. Busch, D. S. Cleveland, L. Nimmagadda, and A. J. Putnam, "Cell-mediated matrix stiffening accompanies capillary morphogenesis in ultra-soft amorphous hydrogels," *Biomaterials,* vol. 230, p. 119634, Feb 2020, doi: 10.1016/j.biomaterials.2019.119634.

[49]   J. A. Beamish, B. A. Juliar, D. S. Cleveland, M. E. Busch, L. Nimmagadda, and A. J. Putnam, "Deciphering the relative roles of matrix metalloproteinase- and plasmin-mediated matrix degradation during capillary morphogenesis using engineered hydrogels," *J Biomed Mater Res B Appl Biomater,* vol. 107, no. 8, pp. 2507-2516, Nov 2019, doi: 10.1002/jbm.b.34341.

[50]   Y. J. He *et al.*, "Immobilized RGD concentration and proteolytic degradation synergistically enhance vascular sprouting within hydrogel scaffolds of varying modulus," *J Biomater Sci Polym Ed,* vol. 31, no. 3, pp. 324-349, Feb 2020, doi: 10.1080/09205063.2019.1692640.

[51]   Y. J. He *et al.*, "Cell-Laden Gradient Hydrogel Scaffolds for Neovascularization of Engineered Tissues," *Adv Healthc Mater,* vol. 10, no. 7, p. e2001706, Apr 2021, doi: 10.1002/adhm.202001706.

[52]   Y. J. He *et al.*, "Protease-Sensitive Hydrogel Biomaterials with Tunable Modulus and Adhesion Ligand Gradients for 3D Vascular Sprouting," *Biomacromolecules,* vol. 19, no. 11, pp. 4168-4181, Nov 12 2018, doi: 10.1021/acs.biomac.8b00519.

[53]   S. Mahadevaiah, K. G. Robinson, P. M. Kharkar, K. L. Kiick, and R. E. Akins, "Decreasing matrix modulus of PEG hydrogels induces a vascular phenotype in human cord blood stem cells," *Biomaterials,* vol. 62, pp. 24-34, Sep 2015, doi: 10.1016/j.biomaterials.2015.05.021.

[54]   J. J. Moon *et al.*, "Biomimetic hydrogels with pro-angiogenic properties," *Biomaterials,* vol. 31, no. 14, pp. 3840-7, May 2010, doi: 10.1016/j.biomaterials.2010.01.104.

[55]   E. H. Nguyen, M. R. Zanotelli, M. P. Schwartz, and W. L. Murphy, "Differential effects of cell adhesion, modulus and VEGFR-2 inhibition on capillary network formation in synthetic hydrogel arrays," *Biomaterials,* vol. 35, no. 7, pp. 2149-61, Feb 2014, doi: 10.1016/j.biomaterials.2013.11.054.

[56]   R. M. Schweller and J. L. West, "Encoding Hydrogel Mechanics via Network Cross-Linking Structure," *ACS Biomater Sci Eng,* vol. 1, no. 5, pp. 335-344, May 11 2015, doi: 10.1021/acsbiomaterials.5b00064.

[57]   M. Vigen, J. Ceccarelli, and A. J. Putnam, "Protease-sensitive PEG hydrogels regulate vascularization in vitro and in vivo," *Macromol Biosci,* vol. 14, no. 10, pp. 1368-79, Oct 2014, doi: 10.1002/mabi.201400161.

[58]   M. Brown and D. G. Lowe, "Automatic Panoramic Image Stitching using Invariant Features," *International Journal of Computer Vision,* vol. 74, no. 1, pp. 59-73, 2007/08/01 2007, doi: 10.1007/s11263-006-0002-3.

[59]   N. E. Friend, A. J. McCoy, J. P. Stegemann, and A. J. Putnam, "A combination of matrix stiffness and degradability dictate microvascular network assembly and remodeling in cell-laden poly(ethylene glycol) hydrogels," *Biomaterials,* vol. 295, p. 122050, Apr 2023, doi: 10.1016/j.biomaterials.2023.122050.

[60]   J. S. Miller, C. J. Shen, W. R. Legant, J. D. Baranski, B. L. Blakely, and C. S. Chen, "Bioactive hydrogels made from step-growth derived PEG-peptide macromers," *Biomaterials,* vol. 31, no. 13, pp. 3736-43, May 2010, doi: 10.1016/j.biomaterials.2010.01.058.

[61]   R. M. Schweller, Z. J. Wu, B. Klitzman, and J. L. West, "Stiffness of Protease Sensitive and Cell Adhesive PEG Hydrogels Promotes Neovascularization In Vivo," *Ann Biomed Eng,* vol. 45, no. 6, pp. 1387-1398, Jun 2017, doi: 10.1007/s10439-017-1822-8.

[62]   S. Sokic, M. C. Christenson, J. C. Larson, A. A. Appel, E. M. Brey, and G. Papavasiliou, "Evaluation of MMP substrate concentration and specificity for neovascularization of hydrogel scaffolds," *Biomater Sci,* vol. 2, no. 10, pp. 1343-1354, Oct 1 2014, doi: 10.1039/C4BM00088A.

[63]   S. Sokic and G. Papavasiliou, "Controlled proteolytic cleavage site presentation in biomimetic PEGDA hydrogels enhances neovascularization in vitro," *Tissue Eng Part A,* vol. 18, no. 23-24, pp. 2477-86, Dec 2012, doi: 10.1089/ten.TEA.2012.0173.

[64]   M. R. Zanotelli *et al.*, "Stable engineered vascular networks from human induced pluripotent stem cell-derived endothelial cells cultured in synthetic hydrogels," *Acta Biomater,* vol. 35, pp. 32-41, Apr 15 2016, doi: 10.1016/j.actbio.2016.03.001.

[65]   C. M. Franca *et al.*, "High-Throughput Bioprinting of Geometrically-Controlled Pre-Vascularized Injectable Microgels for Accelerated Tissue Regeneration," *Adv Healthc Mater,* p. e2202840, May 23 2023, doi: 10.1002/adhm.202202840.

[66]   D. Lu *et al.*, "Macroporous methacrylated hyaluronic acid hydrogel with different pore sizes forin vitroandin vivoevaluation of vascularization," *Biomed Mater,* vol. 17, no. 2, Jan 25 2022, doi: 10.1088/1748-605X/ac494b.

[67]   W. Y. Wang *et al.*, "Direct comparison of angiogenesis in natural and synthetic biomaterials reveals that matrix porosity regulates endothelial cell invasion speed and sprout diameter," *Acta Biomater,* vol. 135, pp. 260-273, Nov 2021, doi: 10.1016/j.actbio.2021.08.038.

[68]   R. K. Singh, D. Seliktar, and A. J. Putnam, "Capillary morphogenesis in PEG-collagen hydrogels," *Biomaterials,* vol. 34, no. 37, pp. 9331-40, Dec 2013, doi: 10.1016/j.biomaterials.2013.08.016.

[69]   W. J. Seeto, Y. Tian, S. Pradhan, P. Kerscher, and E. A. Lipke, "Rapid Production of Cell-Laden Microspheres Using a Flexible Microfluidic Encapsulation Platform," *Small,* vol. 15, no. 47, p. e1902058, Nov 2019, doi: 10.1002/smll.201902058.

[70]   W. J. Seeto, Y. Tian, R. L. Winter, F. J. Caldwell, A. A. Wooldridge, and E. A. Lipke, "Encapsulation of Equine Endothelial Colony Forming Cells in Highly Uniform, Injectable Hydrogel Microspheres for Local Cell Delivery," *Tissue Eng Part C Methods,* vol. 23, no. 11, pp. 815-825, Nov 2017, doi: 10.1089/ten.TEC.2017.0233.

[71]   R. L. Winter *et al.*, "Cell engraftment, vascularization, and inflammation after treatment of equine distal limb wounds with endothelial colony forming cells encapsulated within hydrogel microspheres," *BMC Vet Res,* vol. 16, no. 1, p. 43, Feb 4 2020, doi: 10.1186/s12917-020-2269-y.

[72]   R. R. Rao *et al.*, "Effects of hydroxyapatite on endothelial network formation in collagen/fibrin composite hydrogels in vitro and in vivo," *Acta Biomater,* vol. 10, no. 7, pp. 3091-7, Jul 2014, doi: 10.1016/j.actbio.2014.03.010.

[73]   R. R. Rao, A. W. Peterson, J. Ceccarelli, A. J. Putnam, and J. P. Stegemann, "Matrix composition regulates three-dimensional network formation by endothelial cells and mesenchymal stem cells in collagen/fibrin materials," *Angiogenesis,* vol. 15, no. 2, pp. 253-64, Jun 2012, doi: 10.1007/s10456-012-9257-1.

[74]   R. do Amaral, B. Cavanagh, F. J. O'Brien, and C. J. Kearney, "Platelet-derived growth factor stabilises vascularisation in collagen-glycosaminoglycan scaffolds in vitro," *J Tissue Eng Regen Med,* vol. 13, no. 2, pp. 261-273, Feb 2019, doi: 10.1002/term.2789.

[75]   S. Nemati *et al.*, "Alginate-gelatin encapsulation of human endothelial cells promoted angiogenesis in in vivo and in vitro milieu," *Biotechnol Bioeng,* vol. 114, no. 12, pp. 2920-2930, Dec 2017, doi: 10.1002/bit.26395.

[76]   C. O. Crosby, B. Stern, N. Kalkunte, S. Pedahzur, S. Ramesh, and J. Zoldan, "Interpenetrating polymer network hydrogels as bioactive scaffolds for tissue engineering," *Rev Chem Eng,* vol. 38, no. 3, pp. 347-361, Apr 26 2022, doi: 10.1515/revce-2020-0039.

[77]   F. Lee and M. Kurisawa, "Formation and stability of interpenetrating polymer network hydrogels consisting of fibrin and hyaluronic acid for tissue engineering," *Acta Biomater,* vol. 9, no. 2, pp. 5143-52, Feb 2013, doi: 10.1016/j.actbio.2012.08.036.

[78] C. O. Crosby *et al.*, "Phototunable interpenetrating polymer network hydrogels to stimulate the vasculogenesis of stem cell-derived endothelial progenitors," *Acta Biomater,* vol. 122, pp. 133-144, Mar 1 2021, doi: 10.1016/j.actbio.2020.12.041.

[79] M. Hassanshahi *et al.*, "Critical limb ischemia: Current and novel therapeutic strategies," *Journal of Cellular Physiology,* vol. 234, no. 9, pp. 14445-14459, 2019, doi: 10.1002/jcp.28141.

[80] G. Marsico, S. Martin-Saldana, and A. Pandit, "Therapeutic Biomaterial Approaches to Alleviate Chronic Limb Threatening Ischemia," *Adv Sci (Weinh),* vol. 8, no. 7, p. 2003119, Apr 2021, doi: 10.1002/advs.202003119.

[81] C. K. Griffith *et al.*, "Diffusion limits of an in vitro thick prevascularized tissue," *Tissue Eng,* vol. 11, no. 1-2, pp. 257-66, Jan-Feb 2005, doi: 10.1089/ten.2005.11.257.

[82] F. A. Auger, L. Gibot, and D. Lacroix, "The pivotal role of vascularization in tissue engineering," *Annu Rev Biomed Eng,* vol. 15, pp. 177-200, 2013, doi: 10.1146/annurev-bioeng-071812-152428.

[83] N. Asakawa *et al.*, "Pre-vascularization of in vitro three-dimensional tissues created by cell sheet engineering," *Biomaterials,* vol. 31, no. 14, pp. 3903-9, May 2010, doi: 10.1016/j.biomaterials.2010.01.105.

[84] L. Chen *et al.*, "Pre-vascularization Enhances Therapeutic Effects of Human Mesenchymal Stem Cell Sheets in Full Thickness Skin Wound Repair," *Theranostics,* vol. 7, no. 1, pp. 117-131, 2017, doi: 10.7150/thno.17031.

[85] L. Zhang, Z. Qian, M. Tahtinen, S. Qi, and F. Zhao, "Prevascularization of natural nanofibrous extracellular matrix for engineering completely biological three-dimensional prevascularized tissues for diverse applications," *J Tissue Eng Regen Med,* vol. 12, no. 3, pp. e1325-e1336, Mar 2018, doi: 10.1002/term.2512.

[86] S. Y. Song *et al.*, "Prevascularized, multiple-layered cell sheets of direct cardiac reprogrammed cells for cardiac repair," *Biomater Sci,* vol. 8, no. 16, pp. 4508-4520, Aug 21 2020, doi: 10.1039/d0bm00701c.

[87] X. Chen *et al.*, "Prevascularization of a fibrin-based tissue construct accelerates the formation of functional anastomosis with host vasculature," *Tissue Eng Part A,* vol. 15, no. 6, pp. 1363-71, Jun 2009, doi: 10.1089/ten.tea.2008.0314.

[88] T. Mirabella *et al.*, "3D-printed vascular networks direct therapeutic angiogenesis in ischaemia," *Nat Biomed Eng,* vol. 1, 2017, doi: 10.1038/s41551-017-0083.

[89] K. T. Kang, P. Allen, and J. Bischoff, "Bioengineered human vascular networks transplanted into secondary mice reconnect with the host vasculature and re-establish perfusion," *Blood,* vol. 118, no. 25, pp. 6718-21, Dec 15 2011, doi: 10.1182/blood-2011-08-375188.

[90] L. Perry, U. Merdler, M. Elishaev, and S. Levenberg, "Enhanced Host Neovascularization of Prevascularized Engineered Muscle Following Transplantation into Immunocompetent versus Immunocompromised Mice," *Cells,* vol. 8, no. 12, Nov 20 2019, doi: 10.3390/cells8121472.

[91] B. M. Roux *et al.*, "Preformed Vascular Networks Survive and Enhance Vascularization in Critical Sized Cranial Defects," *Tissue Eng Part A,* vol. 24, no. 21-22, pp. 1603-1615, Nov 2018, doi: 10.1089/ten.TEA.2017.0493.

[92] C. Zhang *et al.*, "Novel hiPSC-based tri-culture for pre-vascularization of calcium phosphate scaffold to enhance bone and vessel formation," *Mater Sci Eng C Mater Biol Appl,* vol. 79, pp. 296-304, Oct 1 2017, doi: 10.1016/j.msec.2017.05.035.

[93] L. Beltran-Camacho, M. Rojas-Torres, and M. C. Duran-Ruiz, "Current Status of Angiogenic Cell Therapy and Related Strategies Applied in Critical Limb Ischemia," *Int J Mol Sci,* vol. 22, no. 5, Feb 26 2021, doi: 10.3390/ijms22052335.

[94] R. K. Jain, P. Au, J. Tam, D. G. Duda, and D. Fukumura, "Engineering vascularized tissue," *Nature Biotechnology,* vol. 23, no. 7, pp. 821-823, 2005, doi: 10.1038/nbt0705-821.

[95] T. L. Place, F. E. Domann, and A. J. Case, "Limitations of oxygen delivery to cells in culture: An underappreciated problem in basic and translational research," *Free Radic Biol Med,* vol. 113, pp. 311-322, Dec 2017, doi: 10.1016/j.freeradbiomed.2017.10.003.

[96] S. H. Bhang *et al.*, "Three-dimensional cell grafting enhances the angiogenic efficacy of human umbilical vein endothelial cells," *Tissue Eng Part A,* vol. 18, no. 3-4, pp. 310-9, Feb 2012, doi: 10.1089/ten.TEA.2011.0193.

[97] A. Alajati *et al.*, "Spheroid-based engineering of a human vasculature in mice," *Nat Methods,* vol. 5, no. 5, pp. 439-45, May 2008, doi: 10.1038/nmeth.1198.

[98] A. M. Laib, A. Bartol, A. Alajati, T. Korff, H. Weber, and H. G. Augustin, "Spheroid-based human endothelial cell microvessel formation in vivo," *Nat Protoc,* vol. 4, no. 8, pp. 1202-15, 2009, doi: 10.1038/nprot.2009.96.

[99] A. A. Gorkun *et al.*, "Angiogenic potential of spheroids from umbilical cord and adipose-derived multipotent mesenchymal stromal cells within fibrin gel," *Biomed Mater,* vol. 13, no. 4, p. 044108, May 22 2018, doi: 10.1088/1748-605X/aac22d.

[100] L. De Moor *et al.*, "High-throughput fabrication of vascularized spheroids for bioprinting," *Biofabrication,* vol. 10, no. 3, p. 035009, Jun 12 2018, doi: 10.1088/1758-5090/aac7e6.

[101] L. Benmeridja *et al.*, "High-throughput fabrication of vascularized adipose microtissues for 3D bioprinting," *J Tissue Eng Regen Med,* vol. 14, no. 6, pp. 840-854, Jun 2020, doi: 10.1002/term.3051.

[102] T. Korff, S. Kimmina, G. Martiny-Baron, and H. G. Augustin, "Blood vessel maturation in a 3-dimensional spheroidal coculture model: direct contact with smooth muscle cells

regulates endothelial cell quiescence and abrogates VEGF responsiveness," *FASEB J,* vol. 15, no. 2, pp. 447-57, Feb 2001, doi: 10.1096/fj.00-0139com.

[103] W. L. Dissanayaka, L. Zhu, K. M. Hargreaves, L. Jin, and C. Zhang, "Scaffold-free Prevascularized Microtissue Spheroids for Pulp Regeneration," *J Dent Res,* vol. 93, no. 12, pp. 1296-303, Dec 2014, doi: 10.1177/0022034514550040.

[104] J. M. Kelm *et al.*, "Design of custom-shaped vascularized tissues using microtissue spheroids as minimal building units," *Tissue Eng,* vol. 12, no. 8, pp. 2151-60, Aug 2006, doi: 10.1089/ten.2006.12.2151.

[105] G. Ramirez-Calderon, H. H. Susapto, and C. A. E. Hauser, "Delivery of Endothelial Cell-Laden Microgel Elicits Angiogenesis in Self-Assembling Ultrashort Peptide Hydrogels In Vitro," *ACS Appl Mater Interfaces,* vol. 13, no. 25, pp. 29281-29292, Jun 30 2021, doi: 10.1021/acsami.1c03787.

[106] M. Sofman, A. Brown, L. G. Griffith, and P. T. Hammond, "A modular polymer microbead angiogenesis scaffold to characterize the effects of adhesion ligand density on angiogenic sprouting," *Biomaterials,* vol. 264, p. 120231, Jan 2021, doi: 10.1016/j.biomaterials.2020.120231.

[107] M. J. Butler and M. V. Sefton, "Cotransplantation of adipose-derived mesenchymal stromal cells and endothelial cells in a modular construct drives vascularization in SCID/bg mice," *Tissue Eng Part A,* vol. 18, no. 15-16, pp. 1628-41, Aug 2012, doi: 10.1089/ten.TEA.2011.0467.

[108] A. P. McGuigan and M. V. Sefton, "Vascularized organoid engineered by modular assembly enables blood perfusion," *Proc Natl Acad Sci U S A,* vol. 103, no. 31, pp. 11461-6, Aug 1 2006, doi: 10.1073/pnas.0602740103.

[109] H. Zhao, Wang, Z., Jiang, S., Wang, J., Hu, Z., Lobie, P. E., Ma, S. , "Microfluidic Synthesis of Injectable Angiogenic Microgels," *Cell Reports Physical Science,* vol. 1, no. 5, p. 100047, 20 May 2020 2020, doi: 10.1016/j.xcrp.2020.100047.

[110] H. R. U.S. Department of Health and Human Services, and Services Administration, "National survey of organ donation attitudes and practices, 2019: report of findings, 2019," 2020. [Online]. Available: https://www.organdonor.gov/awareness/materials/psas.html

[111] M. W. Laschke and M. D. Menger, "Prevascularization in tissue engineering: Current concepts and future directions," *Biotechnol Adv,* vol. 34, no. 2, pp. 112-21, Mar-Apr 2016, doi: 10.1016/j.biotechadv.2015.12.004.

[112] J. D. Weaver *et al.*, "Vasculogenic hydrogel enhances islet survival, engraftment, and function in leading extrahepatic sites," *Sci Adv,* vol. 3, no. 6, p. e1700184, Jun 2017, doi: 10.1126/sciadv.1700184.

Chapter 3 – Injectable Pre-cultured Fibrin Tissue Modules Catalyze the Formation of Extensive Functional Microvasculature *in Vivo*

3.1 Introduction

Cardiovascular diseases (CVDs) are the most deadly and costly problems facing our healthcare system today, and their prevalence is increasing at an alarming rate. Atherosclerosis, characterized by the presence of fatty plaques, inflammation, and aberrant extracellular matrix (ECM) in arterial walls, is one form of CVD that is often asymptomatic and can lead to complete vessel occlusion and ischemia downstream of the lesions. Atherosclerosis in the coronary arteries is the leading cause of heart attacks, or myocardial infarction, but can also affect the peripheral vasculature with severe consequences. Approximately 18 million Americans suffer from peripheral arterial disease (PAD), and 2 million of these patients develop critical limb ischemia (CLI) – the end stage of lower limb PAD [1-4]. While invasive procedures (i.e., bypass surgery, stenting) can restore blood flow in atherosclerotic arteries, patients with co-morbidities may not be suitable candidates for such invasive surgeries. Hence, there is an urgent clinical need for new approaches to revascularize ischemic tissues without the need for open surgery.

Pro-angiogenic growth factors have been extensively studied in both pre-clinical models and clinical trials to promote the creation of new functional microvasculature and restore perfusion to ischemic tissues [5-7]. However, these therapies are limited in part by protein instability, the inability of single factors to faithfully recapitulate vascular development, and the inability to deliver multiple factors with precise spatiotemporal control [8]. As a consequence, clinical trials of therapeutic angiogenesis have been disappointing [9, 10]. Cell-based approaches have also generated a great deal of enthusiasm, especially with the emergence of induced pluripotent stem cells and the ability to differentiate them into endothelial cells [11, 12]. However, most cell-based approaches to-date have relied on delivery of cells alone, either intravenously or directly into a harsh ischemic microenvironment [13], or embedded in a hydrogel biomaterial that gels *in situ* around the cells. In such cases, the delivered cells are expected to either promote host vessel invasion into the ischemic region or directly participate in vascular assembly.

An alternative strategy involves the creation of tissue constructs with vascular networks pre-formed *in vitro* that can be subsequently implanted into ischemic regions or used in the context of engineered tissues. Inosculation between host vessels and the vessels within prevascularized tissues has been demonstrated [14, 15], leading to improved viability and function of parenchymal cells after transplantation [16, 17]. Similarly, *in vivo* prevascularization has also been achieved via the surgical implantation of avascular scaffolds close to an artery and/or vein, subsequent host vessel invasion within the implant over the time course of weeks, followed by surgically moving the now-vascularized tissue to the ischemic region where the implant and the host vessels are connected surgically via microsurgical anastomoses [18, 19]. However, the invasiveness of possibly multiple surgical procedures makes such an approach undesirable and perhaps even infeasible for patients with CLI and other ischemic conditions.

36

Modular microtissues that can be delivered in a minimally invasive manner and subsequently self-assemble into macroscale vascularized networks *in situ* represent a new approach to recreate microvasculature in ischemic tissues that leverages the potential benefits of both prevascularized tissues and injectable delivery. The small sizes of modular microtissues (100-300 μm in diameter) ensure cells encapsulated within them are better sustained by nutrient and oxygen diffusion alone [20-24]. While a wide range of biomaterials have been fabricated into modular formats, here we fabricated tissue modules using fibrin, a naturally occurring biopolymer that promotes wound healing and neovascularization [25] and is FDA cleared for some applications in humans [26], such as a surgical sealant (e.g. Baxter's TISSEEL and ARTISS). In prior work, we have shown that co-encapsulation of endothelial cells with stromal fibroblasts in modular microtissues (microbeads) fabricated from fibrin undergo a morphogenetic program akin to vasculogenesis inside the microbeads and sprout outside the microbeads via angiogenesis when embedded in larger hydrogels that mimic surrounding tissue. Nascent endothelial sprouts also inosculate with sprouts from neighboring microbeads in 3D tissue models. Further, these microbeads have displayed high cell viability even after injection through a needle, demonstrating applicability for minimally invasive applications [27]. The purpose of this pilot study was to determine if microbeads can be pre-cultured for a period of time *in vitro*, subsequently delivered *in vivo* in a minimally invasive manner, and form functional connections with host microvasculature. Our findings demonstrate microbead fabrication and pre-culture do not have deleterious effects on vascularization potential *in vivo*. While vascularization potential of these microbeads was similar to that of cells uniformly distributed throughout bulk hydrogels, our findings demonstrate that pre-cultured microbeads delivered via injection are capable of forming functional microvasculature extensively distributed across tissue volumes. Our results also suggest

37

cellular microbeads may have advantageous properties compared to cells delivered via bulk hydrogels, including implant volume preservation, enhanced vascular network distribution, and accelerated maturation, which may aid in improved revascularization of ischemic tissues.

3.2 Materials and Methods

3.2.1 Cell culture

Human umbilical vein endothelial cells (HUVEC) were either purchased from a commercial source (Lonza, Inc., Walkersville, MD) or isolated from umbilical cords from the University of Michigan Mott Children's Hospital as previously described [28]. [Umbilical cords were obtained by a process considered exempt by the University of Michigan's Institutional Review Board (notice of determination dated August 21, 2014) because the tissue is normally discarded, and no identifying information is provided to the researchers who receive the cords.] These two different HUVEC sources were evaluated *in vitro* to demonstrate the robustness of the system, regardless of endothelial source, as shown in the past [29]. HUVEC isolated from fresh cords were used for *in vitro* studies and the commercial HUVEC were used for the *in vivo* studies. This was due to limited availability of fresh cords for HUVEC isolation. Purchasing HUVEC from a commercial source ensured all experimental condition contained HUVEC from a single source to prevent variability in *in vivo* data due to cell sourcing. Regardless of source, HUVEC were grown in endothelial growth media (EGM2; Lonza), and used from passages 4-7. Normal human lung fibroblasts (NHLF) were also purchased (Lonza), cultured in Media 199 (M199, Life Technologies, Grand Island, NY) with 10% fetal bovine serum (FBS), and used from passages 9-14 for *in vitro* and *in vivo* experiments.

3.2.2 Fibrin microbead production

Fibrin microbeads were made in a water-in-oil emulsification process, as previously described [27]. Prior to starting the emulsification process, 75 mL of 100 cSt polydimethylsiloxane (PDMS) oil (Clearco Products Co. Inc., Bensalem, PA) was placed into a 100 mL beaker and left on ice. Cells were pelleted in a 1:1 HUVEC:NHLF ratio in a conical tube at the initial cell density of 2×10^6 total cells/mL (*in vitro* studies) or 5×10^6 total cells/mL (*in vivo* studies). Lower cell concentrations were used for the *in vitro* studies to facilitate quantification of vessel-like structures. Each batch of microbeads (3 mL total volume) was made by mixing 765 µL serum-free endothelial growth media (SF-EGM2), 300 µL fetal bovine serum (FBS, 10% final), 60 µL of 50U/mL thrombin (1U/mL final), and 1875 µL of fibrinogen stock solution (2.5 mg/ml final clottable protein) with the HUVEC-NHLF pellet. The cell and protein mixture was then added to the PDMS bath, which was kept on ice at 0 °C. Bovine fibrinogen (FGN, Sigma-Aldrich, St. Louis, MO) stock solution was made by mixing protein with SF-EGM2 at 37 °C. The cell-fibrin solution was mixed at 600 RPM for 5 min at 0 °C to allow for emulsion, and then mixed for 25 min at 37 °C to allow for gelation. The microbeads and PDMS solution were collected and separated with the addition of phosphate buffer saline (PBS) with 100 ppm of L101 surfactant (BASF, Florham Park, NJ) for inversion mixing, followed by 4-5 centrifugation steps (200g for 5min/each). After each centrifugation step, PDMS was removed from the fibrin microbeads. The microbeads were then re-suspended with EGM2 and placed in vented 15 mL conical tubes with filters (CELLTREAT Scientific Products, Shirley, MA) prior to starting any experimental procedures. Medium was changed the day after microbead fabrication then every other day after.

3.2.3 Embedding of microbeads in fibrin hydrogels

Fibrin microbeads were embedded in fibrin hydrogels immediately, 1, 3, 5, or 7 days after their fabrication process. One tenth of a 3 mL microbead stock was utilized to make 3 fibrin hydrogels, with ~100 µL of microbeads per hydrogel. Constructs were made by mixing the microbead pellet thoroughly with 382.5 µL of SF-EGM2, 150 µL of FBS (10% final), 30 µL of 50 U/mL thrombin (1 U/mL final), and 937.5 µL of fibrinogen stock solution (2.5 mg/mL final clottable protein). 500 µL of the microbead-protein mixture was added per well of a standard 24-well culture plate, and left at room temperature for 5 min before being placed in the incubator for 25 min at 37 °C. EGM2 (1 mL/well) was added to each hydrogel after the complete gelation process. Medium was replaced the next day then every other day after for the duration of the culture. In some experiments, microbeads were labeled with FITC-fibrinogen prior to embedding as previously shown [27].

3.2.4 Endothelial cell staining, imaging, and quantification

Prior to staining, microbeads alone or embedded in fibrin hydrogels were fixed in zinc-buffered formalin (Z-Fix, Anatech, Battle Creek, MI). After 10 min, the fixative was removed and the samples were washed 2x with PBS. The endothelial cell specific lectin Ulex Europaeus Agglutinin I (UEA-I; Vector Laboratories, Burlingame, CA) was utilized to stain the HUVEC. A staining solution consisting of 1% BSA, 20 µg/mL rhodamine-labeled UEA-I, and 10 nM DAPI in PBS was incubated with microbead samples and left for 45 min at room temperature. Samples were then washed with PBS 2-4x prior to imaging. Hydrogels were taken out of the wells of a 24-well plate, placed on a microscope slide (Superfrost Plus Microscope Slides, Fisher Scientific, Pittsburgh, PA), and then overlaid with a microscope cover glass (Vista Vision Cover Glass, VWR International, LLC, Radnor, PA). The scan slide tool in the Olympus software (IX2-BSW, version

01.07; Olympus, Center Valley, PA) and an optical microscope (Olympus IX81; Olympus) was used to take single plain fluorescent images of endothelial networks formed by fibrin microbeads embedded in fibrin hydrogels. To evaluate microbead characteristics, both after continuous suspension culture and culture in a larger fibrin hydrogel, z-stacks of areas of interest were acquired and flattened to produce maximum intensity projection images. ImageJ (National Institutes of Health, Bethesda, MD) was utilized to merge fluorescent and bright-field images. Prior to quantification, all endothelial images were cropped and processed using the Kirsch filter to detect edges of endothelial sprouts. The processing and imaging settings were kept constant for all conditions. The Angiogenesis Tube Formation module in Metamorph Premier imaging software (https://www.moleculardevices.com/products/cellular-imaging-systems/acquisition-and-analysis-software/metamorph-microscopy, version 7.8.6.0, Molecular Devices, Sunnyvale, CA) was then used to quantify the area of each fibrin hydrogel occupied by endothelial tubules as a metric of microvascular network coverage. At least 12 individual hydrogels per pre-culture condition were quantified to assess differences between experimental groups.

3.2.5 Sample preparations for subcutaneous injection

Subcutaneous implants consisted of 2×10^6 cells (HUVEC:NHLF in a nominal 1:1 ratio) in 500 µL of a fibrin precursor solution for all 3 experimental groups containing cells. To ensure the same numbers of cells were injected into each mouse across different microbead preparations, a method was developed to quantify the number of cells within a given volume of microbeads after fabrication (as opposed to relying only on the theoretical starting cell concentration, as is more typical), and the volume of cell-laden beads injected into each mouse was adjusted in order to ensure consistent delivery of 2×10^6 cells per implant. Briefly, microbead pellets from each batch were re-suspended in 1 mL of EGM2 and transferred into vented 15 mL conical tubes with filters

(CELLTREAT) and either processed immediately or cultured for 1 day. The total volume of microbeads and media was noted, and then 100 μL was transferred to a 96-well plate. An equal volume (100 μL) of a solution containing the fibrinolytic enzyme nattokinase (NSK-SD; Japan Bio Science Laboratory Co., Ltd) at a concentration of 50 FU/mL (fibrin degradation units) in D-PBS (calcium- and magnesium-free) containing 1 mM EDTA [30] was then added on top and mixed. The plate was incubated at 37 °C for 30 min to allow the microbeads to degrade. Following fibrinolysis, cells were counted using a hemocytometer, and the microbead volume preparations adjusted to yield 2.4 x 10^6 total cells, assuming half HUVEC and half NHLF. Samples for all 4 experimental groups (control microbeads, pre-cultured microbeads, acellular microbeads, or cellular hydrogels) were then centrifuged at 200g for 1-5 min to form cell or microbead pellets, supernatant removed, and the pellets resuspended in 600 μL of fibrin hydrogel precursor solution comprising 270 μL of SF-EGM2, 60 μL of FBS (10% final), 12 μL of thrombin (1 U/mL final), and 258 μL of fibrinogen stock solution (2.5 mg/mL final clottable protein). Each solution was rapidly mixed, transferred into a 1-mL syringe fitted with a BD PrecisionGlide 20G needle, and 500 μL of the 600 μL solution was subsequently injected into the animal to deliver 2 x 10^6 total cells per implant.

3.2.6 Subcutaneous injections

All animal procedures were compliant with the NIH Guide for Care and Use of Laboratory Animals and approved by the University of Michigan's Institutional Animal Care and Use Committee (IACUC). Male C.B-17 SCID mice, 6 to 8 weeks of age, (Taconic Labs, Hudson, NY) were acclimated for ≥72 h prior to surgery. An anesthetic/analgesic drug mixture of ketamine (80-120 mg/kg), xylazine (5-10 mg/kg), and buprenorphine (0.05-0.01 mg/kg) was administered to each animal via intraperitoneal injection. Ophthalmic ointment (Puralube Vet Ointment; Dechra,

Overland Park, KS) was added to the eyes of each mouse. Dorsal lumbar flanks were shaved and depilatory agent (Nair; Fisher Scientific, Pittsburg, PA) was applied to remove remaining hair. The injection sites were sterilized by wiping the flanks 3x with alternating ethanol and Betadine (Thermo Fisher Scientific, Fremont, CA). A sterile surgical field was created to place the syringes, needles, and forceps on prior to injection. The samples were prepared, mixed, and injected subcutaneously on the dorsal flanks of the mouse with sterile gloves. The needle was left in the injection site for 30 s to allow for initial gelation of the solution prior to removal. Mice were allowed to recover from the anesthesia before being placed in their normal housing. The following four experimental groups were evaluated: (1) Acellular microbeads, (2) cellular hydrogels, (3) D0 microbeads (no pre-culture), and (4) D3 microbeads (pre-cultured for 3 days post-fabrication). Microbeads in all conditions were delivered in 500 μL of acellular fibrin precursor solution which gelled *in situ*. Bilateral implants were injected per animal, one on each flank in a randomized fashion. A total of 20 mice (n = 5 implants/condition, 2 implants/mouse) were used for this study. A second dose of buprenorphine (0.05-0.01 mg/kg) was administered to each animal 12 h after subcutaneous injections. Animals were monitored every day post-surgery.

3.2.7 Implant retrieval and post-processing

After 3 or 7 days, animals were euthanized. Implants were located, removed with scissors and forceps, placed immediately in 20 mL glass scintillation vials with Z-fix, and subsequently fixed for 24 h at 4°C. In some cases, implants could not be reliably located in the subcutaneous space after time 3 or 7 days, presumably due to rapid fibrinolysis, and therefore not all formulations resulted in implants that could be retrieved for sample processing. Implants that could not be reliably retrieved were not included in analyses. After fixation, implants were washed with PBS 3-4x (5 min/wash), submerged in 70% ethanol, and stored at 4°C until further processing. Samples

were then placed in pink cassettes (Unisette Tissue Cassettes, Simport, Canada), embedded in paraffin in a KD-BMII tissue embedding center (IHC World, Ellicott City, MD), and sectioned through their entire volume with a Thermo Scientific HM 325 rotary microtome (6 μm sections) for further analysis.

3.2.8 Hematoxylin and eosin (H&E) staining

Sections were stained with Mayer's hematoxylin (Electron Microscopy Sciences, Hatfield, PA) and eosin Y (Sigma-Aldrich). Slides were dewaxed with xylene twice (5 min/wash), and then transferred to 100%, 95%, 70% ethanol, and deionized water baths (3 min/wash, two baths per ethanol concentration). Slides were submerged in hematoxylin bath for 15 min, and then rinsed with tap water for an additional 15 min. Slides were then placed in 95% ethanol for 30 s, followed by their immersion in eosin for 1 minute. Slides were subsequently transferred into 95% ethanol bath for 1 minute, and 2 separate 100% ethanol baths (1 minute/bath). Samples were cleared by submerging them into 2 xylene baths (3 min/wash). Toluene mounting solution was added to each slide prior to placing the coverslips. Slides were left to dry overnight prior to imaging.

3.2.9 Human CD31 (hCD31) and alpha-smooth muscle actin (α-SMA) staining

The largest cross-sectional area of each implant (approximating the center of the implant region) within the explanted tissue sections was first identified with H&E staining. The subsequent serial section of each implant was then deparaffinized with xylene and rehydrated through a series of graded ethanol washes and ending with water. Slides were placed in antigen retrieval solution (Dako: Agilent, Santa Clara, CA) and placed in steamer (95 - 99°C) for 35 min. The antigen retrieval solution with the samples was then removed and slides equilibrated to room temperature. Slides were rinsed 3x with tris-buffered saline (TBS-T), 2 min/wash. The area around the tissue

was marked with an ImmEdge pen (Vector Laboratories). The Dako EnVision System-HRP (DAB) kit (Dako) was utilized for hCD31 and α-SMA staining. Slides were rinsed with TBS-T (3 times, 2 min/wash) before any solution from the Dako kit was added to the samples. First, peroxidase blocking solution was added to each tissue for 5 min. For hCD31 labeling, a mouse anti-human CD31 monclonal antibody (Dako, 1:50 dilution in TBS-T) was used as the primary antibody, incubated at 4 °C for 16 h. For α-SMA labeling, a mouse anti-alpha smooth muscle actin monoclonal antibody (1A4 (asm-1)) (Invitrogen: Thermo Fisher Scientific) was used as the primary antibody, incubated at room temperature for 2 h. The HRP-labeled polymer solution was added to each sample and left for 30 min. Samples were then kept with DAB+ substrate-chromogen buffer solution for 5 min. At least one sample from each experimental condition was subjected to the entire staining protocol without primary antibody as a negative control to confirm the specificity of the staining. Most samples were counter-stained with hematoxylin and/or eosin. Slides were then washed with 95% ethanol, 100% ethanol, and xylene. Toluene mounting medium was added prior to covering the samples with coverslips.

3.2.10 Vessel quantification

Bright-field images (4x and 20x) of each complete implant stained for H&E, hCD31, and α-SMA were taken with an inverted Nikon microscope (Nikon Instruments Inc., Melville, NJ). Auto stitch software, developed by Brown and Lowe [31], was utilized to create complete images of each implant from the 4x images taken. The total cross-sectional area (mm^2) of each implant was quantified using ImageJ after first defining the perimeter of the implant using H&E staining. For hCD31+ vessel quantification, five 20x hCD31-stained images from each implant were quantified to determine the average vessel density (# of vessels/mm^2). The cross-sectional area (mm^2) was then multiplied by the average vascular density (# of vessels/mm^2) to determine the

total number of hCD31+ vessels found within each implant at days 3 and 7. For α-SMA+ vessel quantification, 20x images were taken of the entire implant and all images were quantified to determine the total number of vessels in the implant region. Vessels were defined by the presence of a lumen surrounded by a complete brown rim of positive hCD31 or α-SMA staining, depending on the quantification. If host erythrocytes were present in the lumens, vessels were considered perfused.

3.2.11 Measurement of implant volumes

The volumes of model implants fabricated in a manner identical to real implants were evaluated via ultrasound. Instead of injecting constructs into mice, the same volume (500 µL) delivered *in vivo* was pipetted into the transparent caps of 5 mL Eppendorf Tubes that had been placed in wells of 6-well plates. Samples were then placed in the incubator for 25 to 30 min at 37°C to allow complete gelation. To prevent samples from drying, 6 mL of EGM2 was added to each construct, and constructs were then flipped upside-down and left in the incubator overnight. High frequency ultrasound imaging was employed using the Vevo 770 (VisualSonics Inc., Toronto, Canada) with the same parameters described previously [32] to image cellular implants and quantify their volumes. The implant volumes were normalized to the volume of the pre-cultured condition, which was found to be close to 500 µL, the expected initial implant volume. Implant volumes for each test condition were averaged over three implants.

3.2.12 Statistical analysis

Statistical analyses for multiple comparisons for *in vitro* experiments were performed using one-way ANOVA followed by Tukey's *post hoc* test and *in vivo* experiments were performed using Brown-Forsythe and Welch ANOVA followed by Dunnett's *post hoc* test using GraphPad

Prism version 8.4.2 for Windows, GraphPad Software, San Diego, California USA, www.graphpad.com. Data are reported as mean ± standard deviation (SD). Values of $p < 0.05$ were considered statistically significant.

3.3 Results

3.3.1 Microbeads support vascular morphogenesis

Fibrin microbeads containing a nominal 1:1 ratio of HUVEC and NHLF were made via an emulsification process, and either embedded within acellular fibrin hydrogels right away or after a period of pre-culture for up to 7 days (Fig. 3.1a). We selected a 1:1 ratio based on previous studies from our group and others [33-35]. HUVEC within the microbeads formed sprouts both within and outside the beads when embedded in acellular hydrogels immediately after fabrication, as previously reported [27]. Images from UEA-I stained cultures show HUVEC remained in the microbeads when cultured in suspension and sprouted from the beads to invade their surroundings once embedded within a larger fibrin hydrogel (Fig. 3.1b). Phase contrast images demonstrated that cells within microbeads pre-cultured in suspension for up to 7 days coalesced during the pre-culture period (Fig. 3.1c) and initiated cell-cell contacts in that context. Primitive microvascular networks formed within these microbead suspensions after 7 days (Fig. 3.1d). Subsequent embedding of these D7 microbeads in fibrin hydrogels (Fig. 3.1e) followed by an additional 7 or 14 days of culture yielded extensive vessel-like networks and functional connections between endothelial sprouts (red) coming from neighboring microbeads (FITC-labeled, green) as evidenced by observation of 3D image data sets and the presence of overlapping vessel-like structures in image projections. The additional 7 days of culture enabled maturation of the vessel-like networks and more extensive interconnectedness. Blue nuclei not contained within red HUVEC reveal the

NHLF, demonstrating their presence throughout the model tissue (Fig. 3.1e). We have previously shown that NHLF adopt a mural cell-like localization around the vessel-like structures, and express a subset of pericyte markers [36-38].
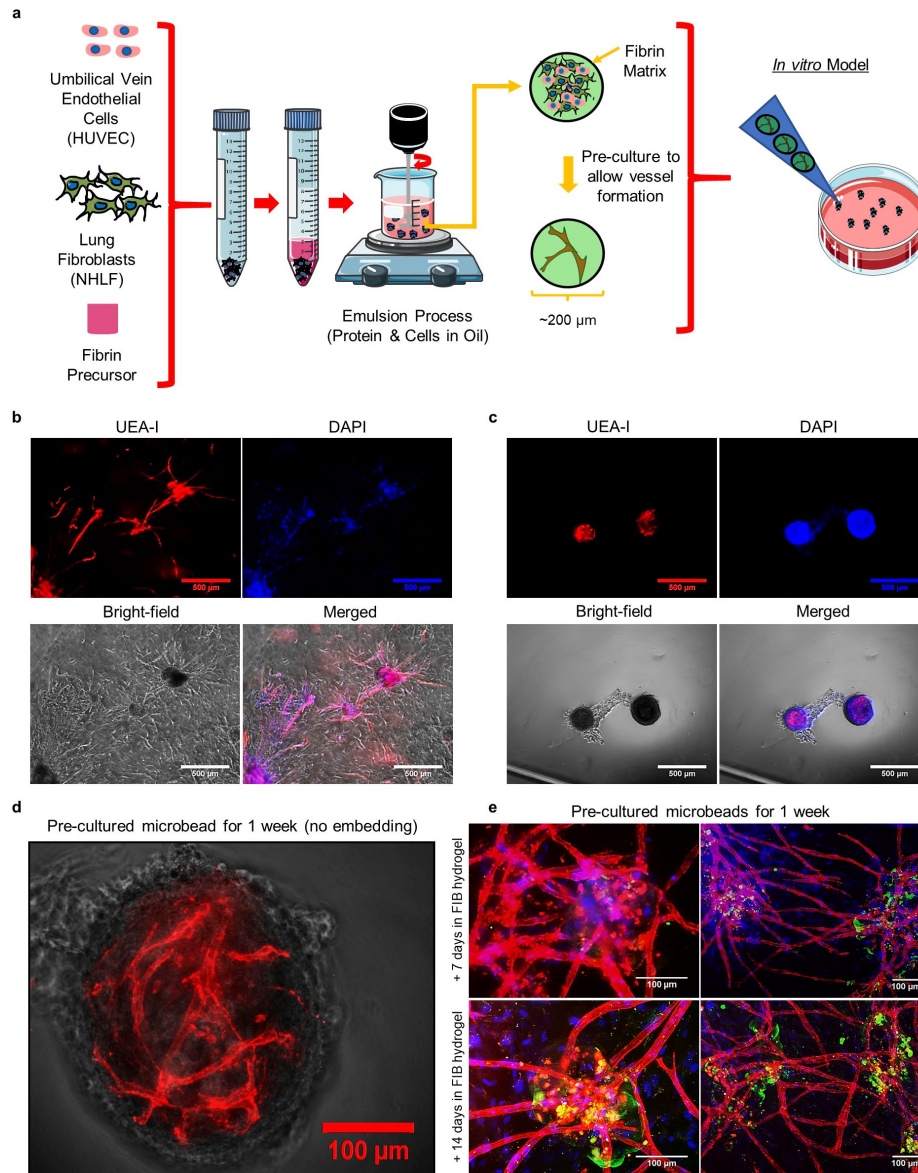
Figure 3.1: Fibrin microbeads support vascular morphogenesis.*Fibrin microbeads containing human umbilical vein endothelial cells (HUVEC) and normal human lung fibroblasts (NHLF) were made via an emulsification process. **(b.)** Cell-containing microbeads embedded in fibrin gels immediately after fabrication catalyzed morphogenesis from the beads into the surrounding microenvironment at day 7. **(c.)** Those cultured in suspension for 7 days supported both inter-bead and intra-bead morphogenesis. **(d.)** A higher magnification image of a cell-laden microbead pre-cultured for 7 days in suspension shows intra-bead vascular morphogenesis. **(e.)** Subsequent embedding of these pre-cultured microbeads in fibrin gels for an additional 7 (top row) or 14 days (bottom row) led to the formation of extensive interconnected inter-*

bead vascular networks initiated from the pre-cultured microbeads. Endothelial sprouts (red) were stained with UEA-I, nuclei (blue) were stained with DAPI, and microbeads (green) were labeled with FITC-fibrinogen (scale bar = 500 μm in panels b and c, and 100 μm in panels d and e). Portions of this figure were created using images modified from Servier Medical Art. (Servier, http://smart.servier.com, licensed under a Creative Commons Attribution 3.0 Unported License).

3.3.2 Pre-culture time affects extent of vascular morphogenesis in vitro

We next assessed if pre-culturing microbeads prior to embedding them caused any differences in the overall extent of the vessel-like networks formed *in vitro*. Microbeads containing HUVEC and NHLF were embedded in fibrin hydrogels after 1 (Fig. 3.2a), 3 (Fig. 3.2b), 5 (Fig. 3.2c), and 7 (Fig. 3.2d) days of suspension pre-culture, and subsequently cultured for an additional 7 days within the hydrogels. Each tissue construct was imaged in its entirety, and the fractional area occupied by endothelial tube-like structures was quantified. Extended periods of pre-culture beyond 3 days prior to embedding resulted in reduced coverage of the tubular structures within the fibrin hydrogel, indicative of a less extensive vessel-like network (Fig. 3.2e). Microbeads pre-cultured for 3 days produced significantly more extensive vascular networks compared to microbeads pre-cultured for 7 days ($p < 0.05$), and we therefore selected this pre-culture condition for subsequent *in vivo* studies.
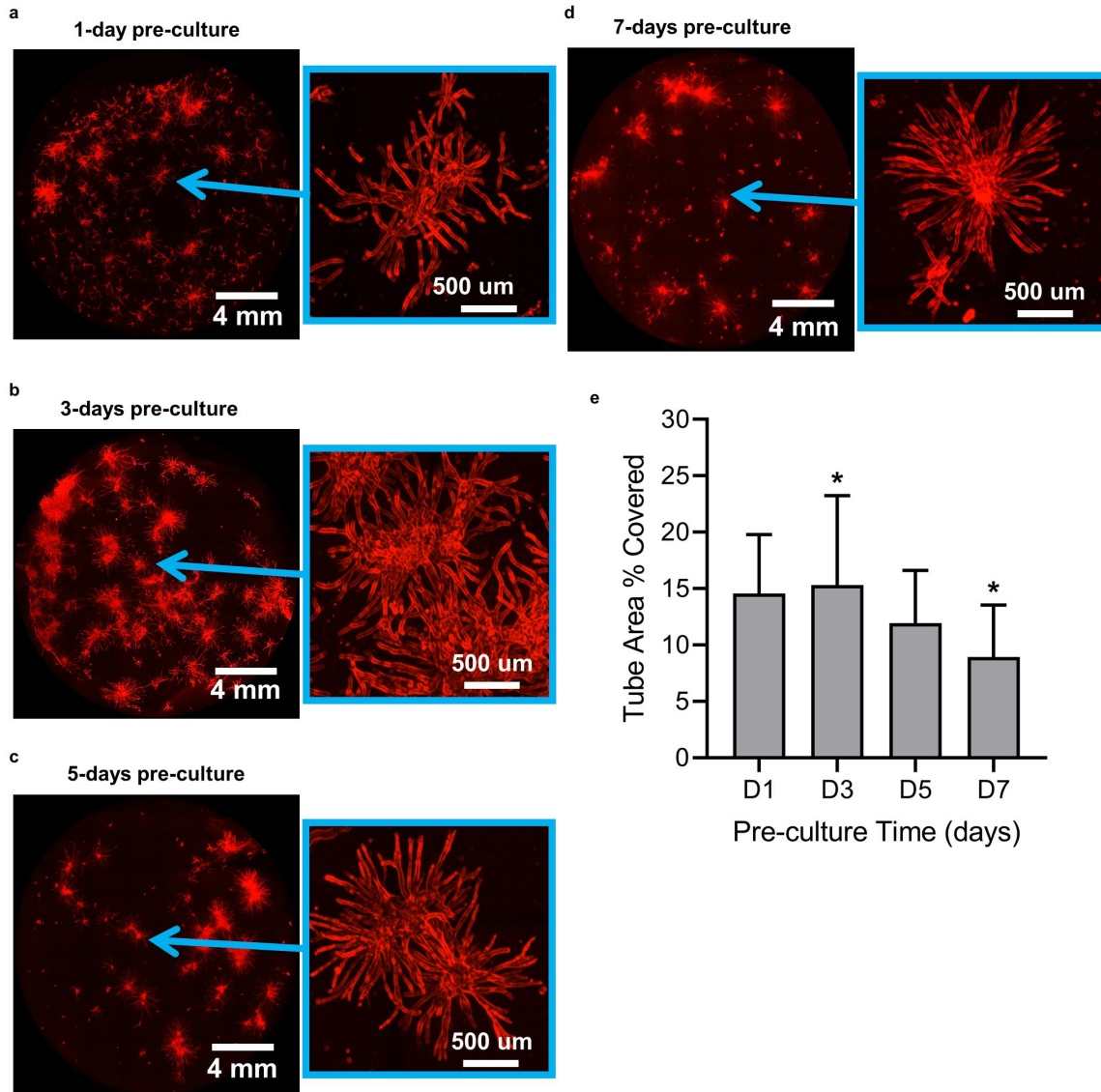
Figure 3.2: Pre-culture time affects vascular distribution in vitro. Microbeads were pre-cultured in suspension for (a.) 1 day, (b.) 3 days, (c.) 5 days, or (d.) 7 days, and subsequently embedded in fibrin hydrogels for an additional 7 days. Endothelial sprouts (red) were stained with UEA-I. Images on the right for each pair show regions of the hydrogel that were magnified and adjusted with a Kirsch filter to facilitate edge detection and quantification. (e.) Quantification of the fractional area of each fibrin construct occupied by tubular structures as a metric of distribution showed that 3 days of pre-culture time led to the most extensive vascular networks. The symbol (*) on the graph indicates values were statistically different ($p \leq 0.05$). Error bars indicate $\pm$ SD.

3.3.3 *Cellular microbeads direct vascular morphogenesis in vivo*

Pre-cultured microbeads were then evaluated for their ability to form functional microvasculature *in vivo*. Microbeads containing HUVEC and NHLF pre-cultured in suspension

50

for 3 days (D3 microbeads) were injected in an acellular fibrin precursor solution into subcutaneous pockets on the dorsal surface of SCID mice (Fig. 3.3a). Their ability to form functional microvasculature was compared to D0 microbeads (encapsulating HUVEC and NHLF without pre-culture), acellular microbeads, or cellular hydrogels (HUVEC and NHLF delivered in a fibrin precursor solution, which gels *in situ*). All implants containing human cells showed evidence of vascular morphogenesis after implantation for 3 and 7 days (Fig. 3.3b). HUVEC were identified in explanted tissue constructs via immunohistochemical (IHC) staining of human CD31 (Fig. 3.3c, brown). Host erythrocytes within the lumens of these hCD31+ neovessels confirmed the formation of functional anastomoses with host vasculature. Murine vessels (white arrows, negative for hCD31) were sometimes visible in sections counter-stained with hematoxylin. We also occasionally observed structures that simultaneously consisted of both human endothelial cells (in brown) and murine endothelial cells (not stained) in the same structure, suggestive of chimeric vessels (Fig. 3.3c, right panel, dashed rectangle). Representative images of hCD31+ sections of the four experimental groups at both days 3 and 7 and two different magnifications are shown (Fig. 3.3d). Quantification of the vessel and perfused vessel densities was achieved by counting the number of hCD31+ and erythrocyte-perfused hCD31+ structures with lumens, respectively. No significant differences in the average numbers of total hCD31+ vessels or perfused hCD31+ vessels per mm^2 were observed across any of the implants containing cells at day 3 (Fig. 3.3e, f) and day 7 (Fig. 3.3g, h).
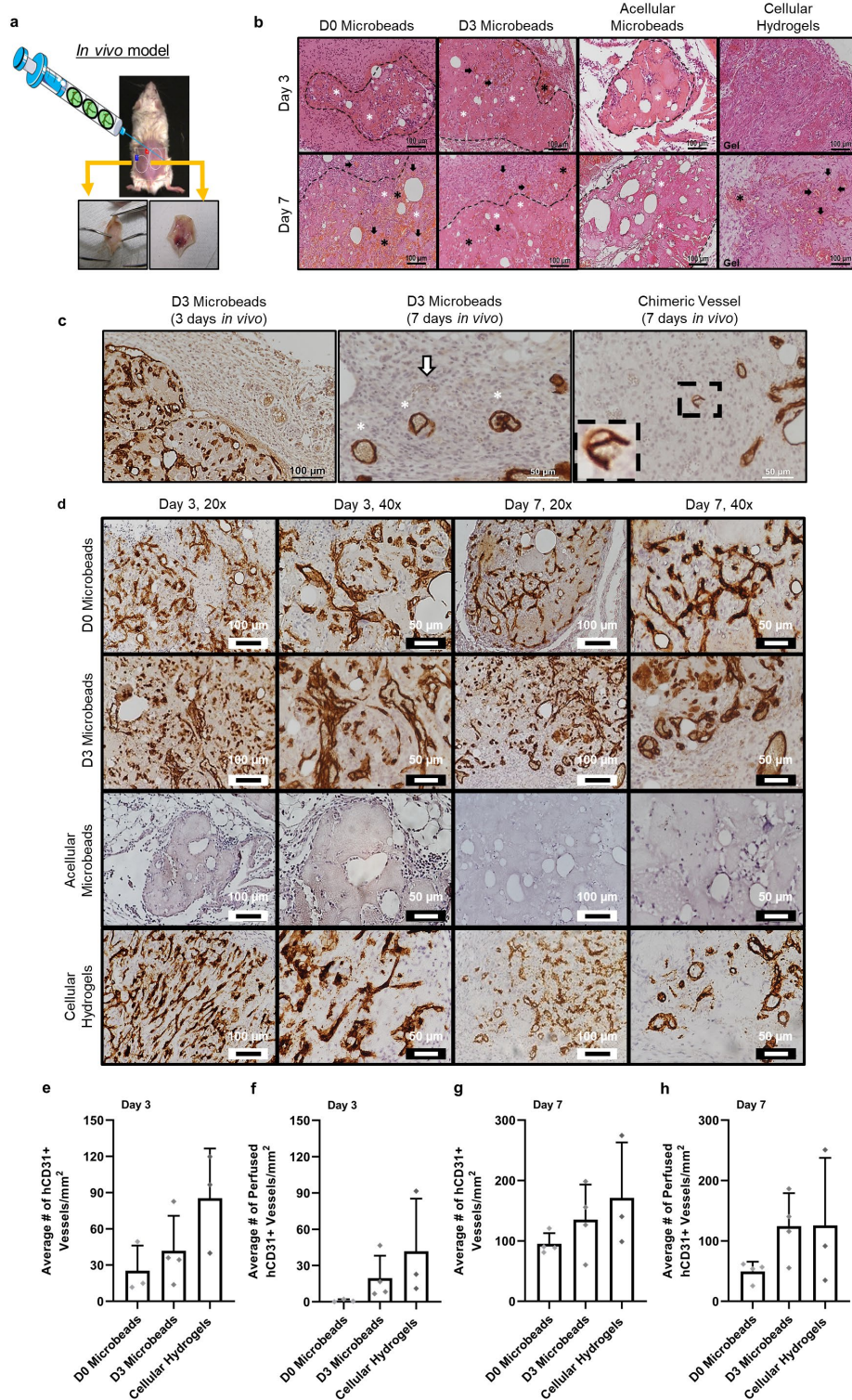
Figure 3.3: Cell-laden fibrin microbeads catalyze the formation of functional microvasculature in vivo. *Implants were injected into the subcutaneous space on the dorsal surface of SCID mice. (b.) Implants were retrieved, fixed, processed, embedded, and then stained with hematoxylin and eosin. Representative images of H&E-stained sections show vessel formation and cell infiltration in D0 microbeads (first column), D3 microbeads (second column), acellular microbeads (third column), and cellular hydrogels*

(fourth column) for 3 days (top row) and 7 days (bottom row). Dashed circles highlight the clusters of microbeads located within the implant. Arrows indicate representative vessels, black asterisks indicate representative regions where host erythrocytes are clearly present, and white asterisks indicate representative individual microbeads. (c.) Implants were also IHC-stained for hCD31 (dark brown) to confirm the human origin of the neovessels. Implants containing D3 microbeads evaluated in vivo for 3 (left image) and 7 (middle and right image) days showed evidence of inosculation with host vessels. The white arrow in the day 7 micrograph (middle image) identifies a perfused mouse vessel (hCD31-), while white asterisks highlight hCD31+ vessels with red blood cells. The dashed black rectangle suggests a chimeric vessel formed by both mouse and human cells (right image). The magnified inset demonstrates the presence of host erythrocytes within the vessel. (d.) Vessel structures containing human endothelial cells (hCD31+) were identified in all implants except for those containing acellular microbeads. Shown are representative 20x and 40x images implants stained for hCD31 after 3 and 7 days in vivo. Quantification of both total and perfused human EC-derived vessel density for each condition after (e., f.) 3 days and (g., h.) 7 days was performed. No significant differences were observed in vessel and perfused vessel density between any of the experimental groups containing human endothelial cells after 3 or 7 days in vivo. Individual data points on graphs represent a single implant quantified per condition. Error bars indicate ± SD. Portions of this figure were created using images modified from Servier Medical Art. (Servier, http://smart.servier.com, licensed under a Creative Commons Attribution 3.0 Unported License).

3.3.4 Cellular microbeads form extensive functional vascular networks in vivo

Implants containing cellular microbeads appeared larger in volume upon extraction from the mice. To evaluate this observation, implants were histologically sectioned through their entire volume, each section (6 µm) was stained for H&E, and then the section with the maximum area (approximating the center of the implant region) was identified by quantifying stitched images of the entire implant region (Fig. 3.4a). Using this approach, the implant area (in mm^2) and the total number of vessels in the maximum implant area were quantified in tissues explanted after 3 and 7 days *in vivo* (Fig. 3.4b-i). While trends in the data suggest implants containing cellular microbeads had larger average cross-sectional areas than both acellular microbeads and cellular hydrogels on day 3 and 7, these differences were not statistically significant (Fig. 3.4b, c). With the exception of D0 microbeads, the average implant cross-sectional area of all conditions decreased from day 3 to day 7 *in vivo*.

We then multiplied these implant areas by the average vessel density to calculate the total numbers of vessels within the implant groups and found all cellular implants contained comparable total numbers of hCD31+ vessels after 3 days *in vivo* (Fig. 3.4d, e). D0 microbeads still showed

53

minimal evidence of vessel perfusion on day 3 even when considering total vessel coverage throughout the entire implant (Fig. 4e, f). For all conditions, the total numbers of hCD31+ vessels and hCD31+ perfused vessels increased from day 3 to day 7 (Fig. 3.4g, h); however, this increase was notably smaller in cellular hydrogels, which only showed a 1.2-fold increase in total number of vessels from day 3 to day 7 *in vivo* compared to a 3.31-fold and 2.44-fold increase in D0 and D3 microbeads, respectively. Implants containing D0 and D3 microbeads also exhibited greater increases in the total numbers of perfused vessels (233.9-fold and 5.1-fold, respectively) from day 3 to day 7 than cellular hydrogels (only 1.8-fold). Furthermore, of the total number of hCD31+ vessels formed by day 7 (Fig. 3.4i), 91.8% of vessels in D3 microbead implants were perfused, compared to only 54.8% and 64% in D0 microbeads and cellular hydrogels, respectively.
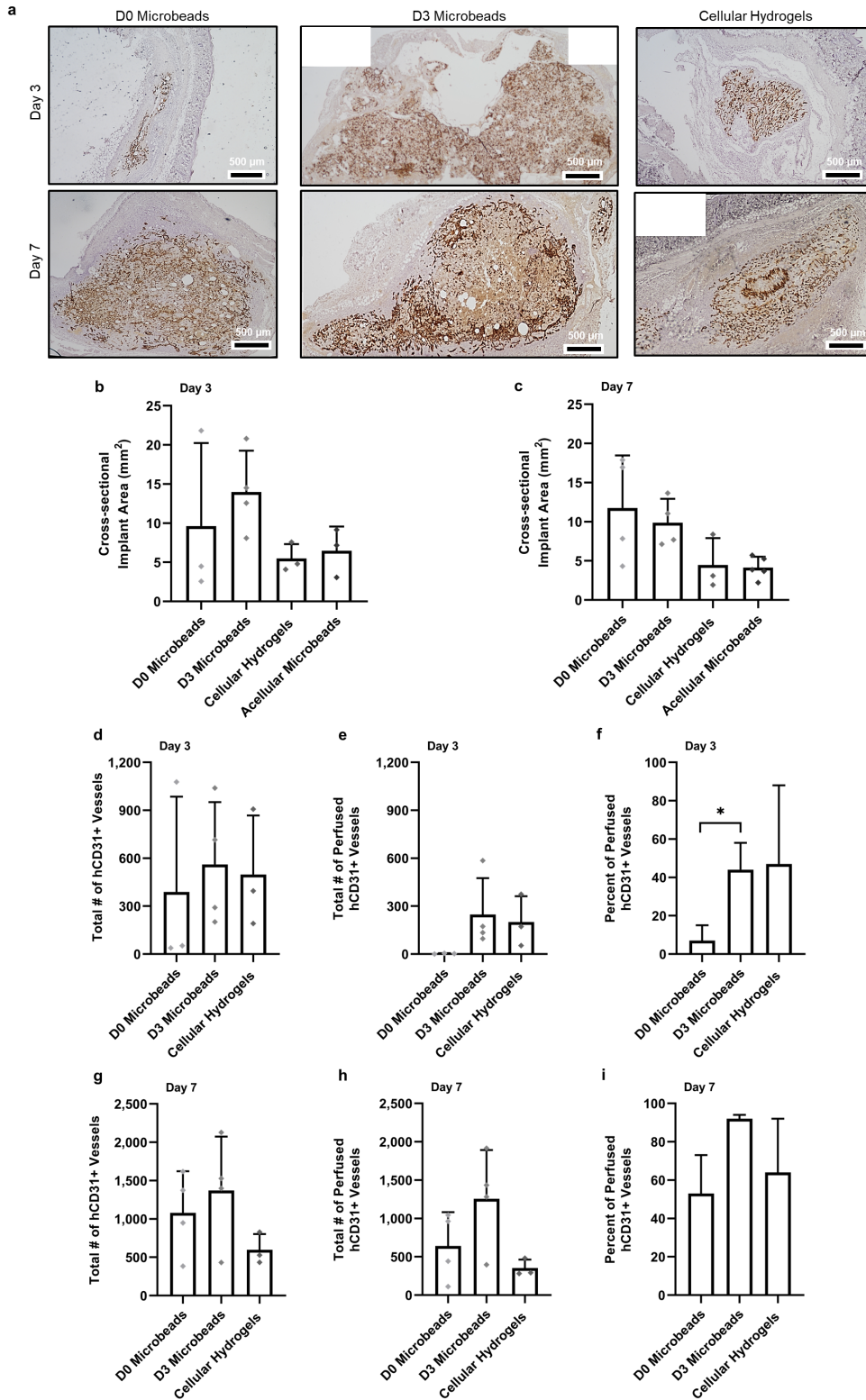
Figure 3.4: Cellular microbeads form extensive microvasculature in vivo. *(a.) Representative images of the cross-sectional areas of hCD31-stained tissues are shown for all 3 of the cell-containing experimental groups. D0 microbeads (left column), D3 microbeads (middle column), and cellular hydrogels (right*

column) were implanted for 3 (top row) and 7 days (bottom row) prior to their excision (black scale bar = 500 µm). Implant sizes were quantified by measuring the cross-sectional area of the implant region using H&E staining after (b.) 3 and (c.) 7 days in vivo. No significant differences in implant area were found between any of the experimental groups after 3 or 7 days. The total number of hCD31+ (d., g.) vessels and (e., h.) perfused vessel in the entire implant region was quantified after 3 and 7 days in vivo. No significant differences were observed between any of the cell-laden experimental groups after either time point. Percent of perfused hCD31+ vessels in the implant region after (f.) 3 and (i.) 7 days. After 3 days in vivo, D3 microbeads had a significantly greater percent of perfused vessel compared to D0 microbeads. After an additional 4 days in vivo, no significant differences were observed between any of the cellular conditions. Statistically significant differences (p ≤ 0.05) are indicated by matched symbols. Individual data points on graphs represent a single implant quantified per condition. Error bars indicate ± SD.

3.3.5 Cellular implants attain α-SMA expression in vivo

IHC staining of smooth muscle alpha-actin (α-SMA), a pericyte marker, was also performed to determine the extent of vessel maturation across the different experimental groups. At the day 3 time point, α-SMA expression (brown stain with black arrows) was sparse in all four experimental groups, even when images were magnified to better visualize stained structures (Fig. 3.5a). Most positive α-SMA staining observed within the implant region at this early time point was diffuse and not necessarily localized subjacent to vessel structures. Positive α-SMA staining around vasculature was readily observed in the host tissue localized outside of the implant region, displayed at the top left corner of the cellular hydrogel image in Fig. 3.5a (magnified in Fig. 3.5b). After an additional 4 days *in vivo*, cellular conditions all displayed stronger α-SMA staining compared to the day 3 time point (Fig. 3.5c). Implants containing acellular microbeads exhibited minimal α-SMA+ staining within the implant region (Fig. 3.5c). Quantification of vessels stained positive for α-SMA showed the extent of vessel maturation differed significantly only between cellular conditions and acellular microbeads (Fig. 3.5d-f). Specifically, D3 microbead and cellular hydrogel groups both had a significantly higher total numbers of α-SMA+ vessels than acellular microbeads (p = 0.04 for both conditions) (Fig. 3.5d). Quantification of the total number of perfused α-SMA+ vessels revealed the D3 microbead group had the highest numbers of these mature vessels, although the only significant difference was observed compared to the acellular

microbead group (p = 0.05) (Fig. 3.5e). D0 and D3 microbead conditions also had a significantly

higher percent of α-SMA+ vessels perfused compared to acellular microbeads after 7 days *in vivo*

(Fig. 3.5f).
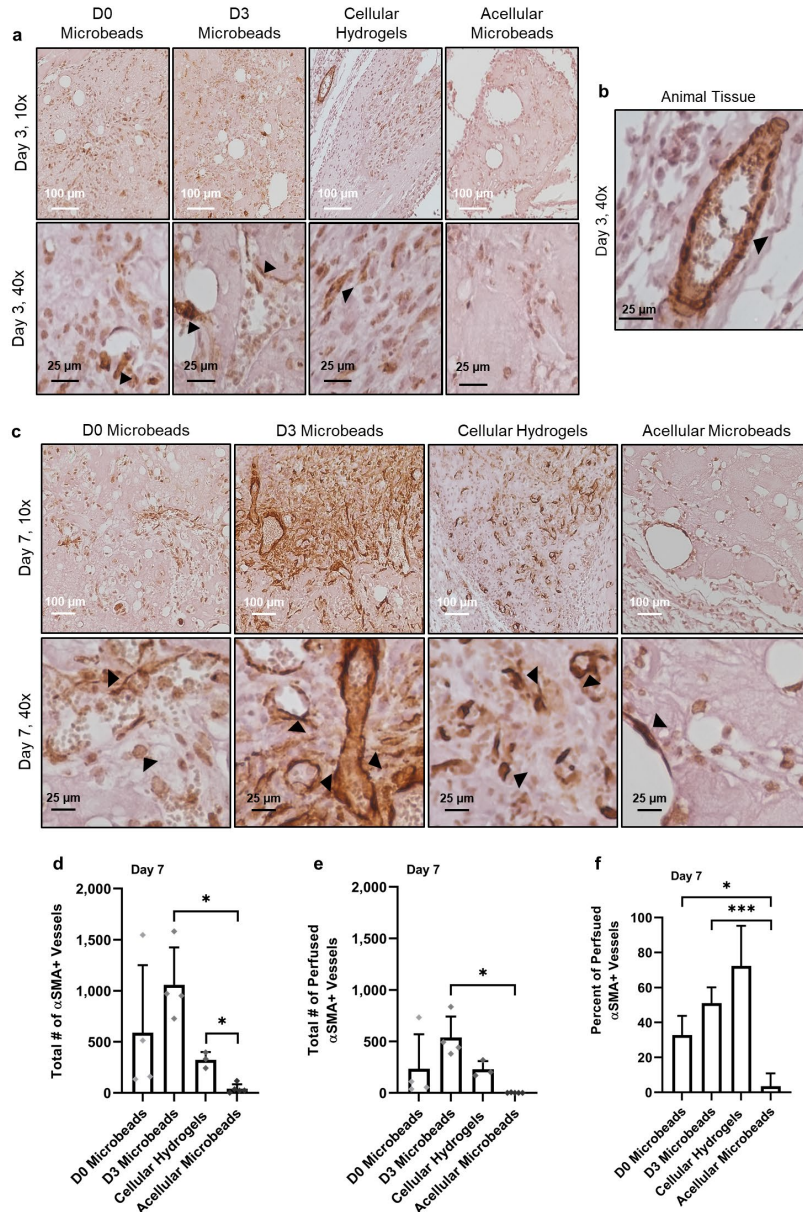
***Figure 3.5: Implants containing cell-laden microbeads contained α-SMA supported vessels.** (a.) D0 microbeads (first column), D3 microbeads (second column), cellular hydrogels (third column), and acellular microbeads (fourth column) that were injected and kept in vivo for 3 days displayed minimal evidence of α-SMA+ staining. Images acquired via 10x (top row) and 40x (bottom row) objectives highlight α-SMA staining in brown (black arrows). (b.) Vessels within the surrounding host tissue were positive for α-SMA as shown by 40x image from animal tissue near 3-day cellular hydrogel implant. (c.) After 7 days, expression of α-SMA positive structures was higher in all conditions. White scale bar = 100 µm, and black*

scale bar = 25 μm. Quantification of total number of (d.) α-SMA+ and (e.) perfused α-SMA+ vessels in the implant region after 7 days in vivo. D3 microbeads had significantly higher α-SMA+ vessel and perfused vessel densities, and total number of perfused α-SMA+ vessels than acellular microbeads. D3 microbeads and cellular hydrogels both had a higher total number of α-SMA+ vessels than acellular microbeads. (f.) Percent of perfused α-SMA+ vessels in the implant region after 7 days. Both D0 and D3 microbeads had a significantly greater percent of perfused vessel compared to acellular microbeads. Statistically significant differences (p ≤ 0.05) are indicated by matched symbols. Individual data points on graphs represent a single implant quantified per condition. Error bars indicate ± SD.

3.3.6 Volume preservation of cellular microbeads may influence maximum implant area and vascular network distribution

The observed differences in implant morphologies suggested the cellular microbead formulations may yield larger implants in part because of their ability to better preserve implant volume over time. While the cellular hydrogel group exhibited higher hCD31+ vessel densities, the total numbers of hCD31+ vessels across the implants trended highest in the cellular microbead groups after 7 days *in vivo*, suggesting microbead formulations may be particularly useful in creating a more distributed vascular network throughout the entirety of an implant. To assess this directly, implant volumes were measured in model constructs *in vitro* the day after fabrication via 3D high-resolution ultrasound imaging (Fig. 3.6a). Fibrin-based constructs containing D3 microbeads did not significantly change volume within 24 h. By contrast, the volumes of constructs containing D0 microbeads or uniformly distributed cells ("cellular hydrogels") significantly compacted, attaining volumes that were 17% and 47% less, respectively, than those containing D3 microbeads after only 24 h of incubation *in vitro*. All measured volumes were statistically different from one another (p ≤ 0.05, Fig. 6b). Further, we investigated if differences observed between microbead conditions could be attributed to cell invasion from microbeads into the surround fibrin hydrogel, leading to matrix remodeling and implant compaction. Phase contrast images qualitatively showed fewer cells migrated out of D3 microbeads than D0 microbeads in the surrounding fibrin matrix, especially at early time points (Fig. 3.6c). This observation is clearer

when microbeads are left in the fibrin hydrogels for 3 days rather than 7 days since there is less time for cells to remodel the matrix. Collectively, these data reveal that constructs containing cellular microbeads exhibited less compaction, potentially due to delayed cell invasion and matrix remodeling, relative to cellular hydrogels, which may influence maximum implant area and vascular network distribution observed *in vivo*.
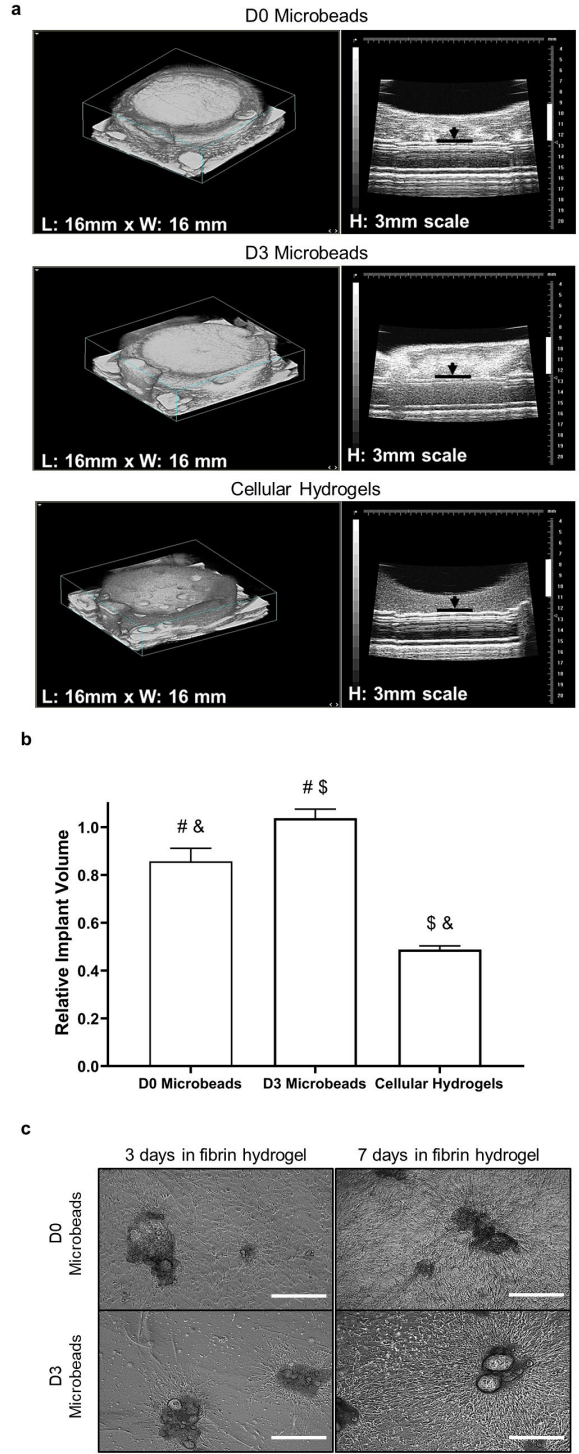
Figure 3.6: Constructs with D3 microbeads do not compact after 1 day of in vitro culture. *(a.) 3D ultrasound images of model fibrin implants containing D0 microbeads (top row), D3 microbeads (middle row), or uniformly suspended cells (cellular hydrogels, bottom row). Black lines and arrows in the images on the right-hand side show the bottom of the implant; white vertical lines are 3 mm scale bars. (b.) Relative implant volumes were quantified and normalized to the model implants containing D3 microbeads, whose volumes were constant after 24 h of in vitro culture. Statistically significant differences (p ≤ 0.05) are*

indicated by matched symbols. Constructs containing D3 microbeads were of significantly larger volume than those containing D0 microbeads or the cellular hydrogels. (c.) Cells deployed more slowly from D3 microbeads when embedded in fibrin hydrogels. Bright-field images of D0 (top row) and D3 (bottom row) microbeads embedded in fibrin hydrogels for 3 (left column) and 7 days (right column). Scale bar = 500 μm. Error bars indicate ± SD.

3.4 Discussion

Creating functional microvasculature remains a major challenge to engineering functional tissue replacements and restoring function in many ischemic pathologies. In this proof-of-concept study, we examined an approach to engineer microvasculature *in vivo* based on sub-millimeter vascularized tissue modules (microbeads) that can be injected via syringe in a minimally invasive manner. Similar approaches based on cell spheroids [39-47], microgels containing cells [48-50], and modular microtissues with an exterior coating of endothelial cells [23] have all shown microvascular potential *in vitro* and *in vivo*. Inspired by these and other previous studies, our approach here preserves many of the attractive features of macroscale prevascularized tissue constructs [14-17], including the flexibility to be fabricated with a range of materials and cell types [27, 29, 37] and the ability to support the complex morphogenetic programs necessary to recreate microvasculature that can inosculate with host vasculature following delivery *in situ.* While other studies have investigated the use of scaffold-free multicellular aggregates for vascularization applications [39-47], the use of ECM proteins for cell encapsulation provides an immediate 3D matrix conducive to remodeling during vascular assembly, which may be beneficial for more rapidly producing robust vascular networks throughout microbeads prior to implantation *in vivo*. Fibrin was chosen as the material for our microbeads for applications in tissue vascularization because it improves cell survival during injection [25], promotes wound healing and endothelial

morphogenesis [27, 28], and is cleared by the FDA for use as a surgical sealant in humans [26]. Additionally, fibrin's microstructure and polymerization rate can be readily modified [26].

Consistent with our prior study [27], we first demonstrated here that HUVEC co-encapsulated with NHLF in fibrin microbeads were capable of sprouting into a surrounding fibrin matrix and forming interconnected networks of vessel-like structures. We then assessed the value added by pre-culture prior to either embedding the microbeads in a model tissue *in vitro* or injecting them *in vivo*. Cells encapsulated in microbeads held in static suspension culture without embedding in an additional matrix for up to 7 days were able to form primitive vessel-like structures within each bead. Once embedded, endothelial sprouts from adjacent pre-cultured microbeads appeared to form connections with each other within the surrounding fibrin matrix. The distribution of the microvasculature nucleated by the microbeads embedded in larger model tissues (quantified by the area fraction occupied by endothelial tubules) was significantly improved when microbeads were pre-cultured for 3 days prior to embedding. Longer pre-culture times led to less extensive and more heterogeneous networks, perhaps due to microbead aggregation during pre-culture, which may have resulted in less uniform distribution of microbeads in the matrix. The observed formation of vessel-like structures within and between microbeads is consistent with other studies using endothelial and stromal supportive cells encapsulated in microgels of varying matrices [48-50]. Other studies have found longer pre-culture times (up to 14 days) beneficial, especially when compared to non-pre-cultured controls [48, 49]; however, optimal pre-culture time is influenced by cell type, cell density, and material properties of the microgels.

The *in vivo* vascularization potential of these microbeads pre-cultured for 3 days (D3 microbeads) was then compared to D0 microbeads (containing HUVEC and NHLF but no period of pre-culture), acellular microbeads, and cellular hydrogels (HUVEC and NHLF delivered in a

fibrin precursor solution, which gels *in situ*). All four experimental groups were delivered as injectable formulations, with microbeads being delivered within an acellular fibrin precursor solution, into subcutaneous pockets on the dorsal surface of SCID mice. Pre-culturing microbeads for 3 days prior to delivery did not significantly accelerate the formation of anastomoses with host vessels in this particular animal model, as all three groups containing cells showed evidence of hCD31+ vessel formation by day 3. Further, at this time point D3 microbeads and cellular hydrogels also showed evidence of functional perfusion (i.e., the presence of erythrocytes). D0 microbeads showed little evidence of perfusion by day 3, perhaps indicating that the fabrication process of the microbeads may result in the encapsulated cells needing additional time to equilibrate to the new matrix prior to vessel morphogenesis, causing a delay in their ability to anastomose with host vasculature. After 7 days *in vivo*, all cellular implants contained perfused hCD31+ vessels. All three cellular conditions showed an increase in total number of vessels and perfused vessels from day 3 to day 7 *in vivo*, however, increases observed in cellular hydrogels were much lower than those of cellular microbeads. Though cellular hydrogels had greater average hCD31+ vessel densities, the total number of hCD31+ vessels throughout the entire implant region trended higher in D0 and D3 microbead conditions after 7 days, likely due to the larger sizes of cellular microbead implants. The total number of perfused hCD31+ vessels also trended higher for the D3 microbead group than D0 microbeads and cellular hydrogels. Interestingly, in a similar study utilizing pre-cultured multicellular alginate microgels implanted in a fibrin plug, non-pre-cultured (D1) microgels failed to assemble into vascular networks in the subcutaneous space after 7 days. Pre-cultured (D14) microgels showed some evidence of vessel perfusion after 7 days, but required an additional 7 days *in vivo* to show significant evidence of vessel perfusion throughout the implant [49].

Further, tissue sections were also stained for α-SMA to characterize pericyte coverage and vessel maturity within the implants. Mature vessels were only found in the surrounding mouse tissue on day 3, but by day 7 all cellular implants exhibited higher levels of α-SMA expression. Acellular microbeads had minimal α-SMA expression throughout the implant even at the day 7 time point indicating minimal infiltration of host vasculature. All cellular conditions had comparable α-SMA+ vessel densities and total number of α-SMA+ vessels after 7 days *in vivo*, but only D3 microbeads had a significantly higher average α-SMA+ vessel and perfused vessel density compared to acellular microbeads. D3 microbeads were also the only group to have a significantly higher total number of perfused α-SMA+ vessels compared to acellular microbeads. This could be a result of pro-angiogenic growth factor sequestration to the fibrin matrix of microbeads during pre-culture. These growth factors could aid in the recruitment of mature host vessels into the implant region upon delivery of pre-cultured microbeads *in vivo*, leading to greater expression of α-SMA throughout the implant. Further experiments are needed to more definitively determine if the α-SMA+ mural cells observed around the vessels were due to host vasculature infiltration or differentiation of the NHLF into bona fide pericytes, although previous evidence from our group suggests NHLF only express a subset of pericyte markers, at least in our *in vitro* models [36].

The larger size of implants containing cellular microbeads translated to trends of higher numbers of total vessels across the entire implant volume, likely resulting in a more extensive vascular distribution. As observed differences in implant area were not statistically significantly, possibly due to the inherent variability in sample collection and histological processing, we used ultrasound to quantify the volumes of model implants cultured *in vitro*. A phenomenon similar to the compaction observed *in vivo* was also observed in these *in vitro* constructs. Constructs

containing D3 microbeads did not compact, while those with D0 microbeads compacted approximately 20%. By contrast, the cellular hydrogel constructs, in which the cells were initially dispersed uniformly, compacted ~50% in just 24 h. Furthermore, constructs containing D3 microbeads contained higher density features (presumably the cell-laden beads) based on the higher attenuation displayed in the ultrasound images relative to the other constructs. Cells encapsulated in the D3 microbeads also took longer to infiltrate the surrounding fibrin hydrogel than the ones residing in the D0 microbeads, perhaps due to increased local ECM density [51]. The volume preservation of constructs containing cellular microbeads, combined with the delayed deployment of cells from these beads, may underscore the utility of cellular microbead formulations to create more distributed microvascular networks.

In summary, this study demonstrated that fibrin microbeads containing cellular building blocks of microvasculature readily vascularize a fibrin construct in subcutaneous tissue and support a high degree of vascularity comparable to cellular hydrogels. This finding demonstrates that the fabrication and subsequent pre-culture of cellular microbeads do not have deleterious effects on the ability of these microbeads to form functional vasculature upon implantation *in vivo*. While other studies have investigated the use of cells spheroids and microgels for vascularization applications, few have utilized ECM protein-based microbeads for the encapsulation of multiple cell types to create discrete units for vascularization. Though differences observed between experimental groups were often not significant, the data suggest that cellular microbeads may have advantageous properties over cells uniformly distributed throughout bulk hydrogels, such as implant volume preservation and enhanced vascular network distribution. Pre-culturing microbeads may accelerate vessel inosculation with host vasculature and maturation characterized by an increase in the total numbers of pericyte-invested perfused microvessels. However, while

the subcutaneous model is straightforward and commonly used to evaluate vascularization strategies *in vivo*, it does not mimic the harsh ischemic conditions typical of many clinical conditions. This proof-of-concept study therefore lays the groundwork for higher-powered animal studies in more physiologically-relevant models of ischemia, where cell survival may be more challenging due to the lack of oxygen and nutrients. Whereas encapsulated cells might not survive long enough to form vessels *de novo*, primitive microvasculature deployed from injectable pre-cultured microbeads may better withstand harsh ischemic environments and nucleate a distributed vascular network that can rapidly inosculate with host vessels to support parenchymal cells for regenerative applications.

3.5 Supplementary Data
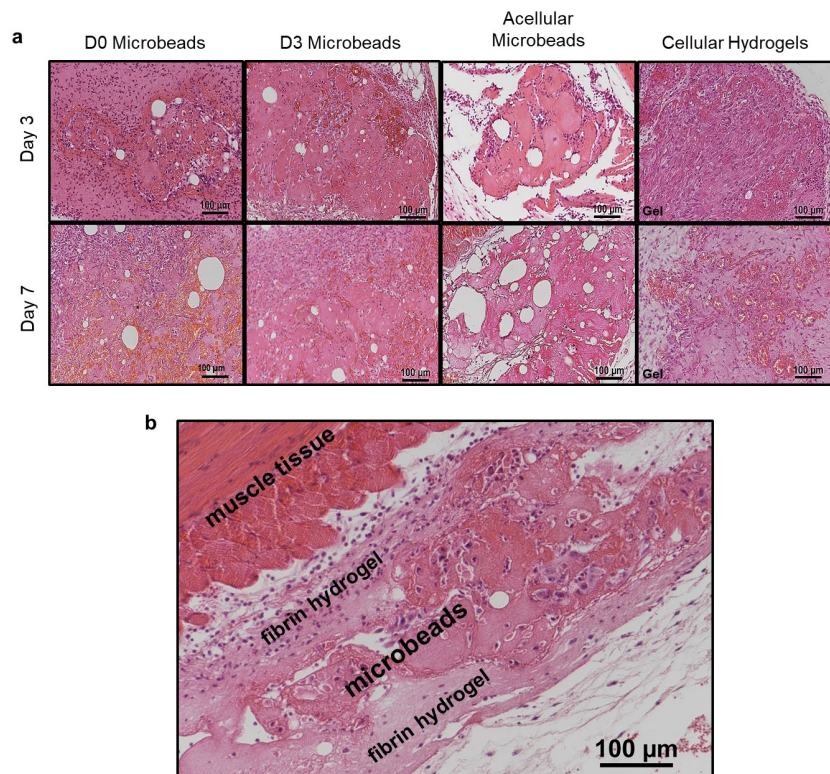
Figure 3.7: Representative images of H&E-stained sections. *(a.) Unlabeled version of Figure 3b to allow visualization of histological features in the absence of highlight labels. (b.) Representative image at higher magnification showing the histological appearance of different tissue and material types.*

3.6 References

[1]   N. Falluji and D. Mukherjee, "Critical and acute limb ischemia: an overview," *Angiology,* vol. 65, no. 2, pp. 137-46, Feb 2014, doi: 10.1177/0003319712470966.

[2]   J. Sanguily, Martinsen, B., Igyarto, Z. & Pham, M, "Reducing Amputation Rates in Critical Limb Ischemia Patients Via a Limb Salvage Program: A Retrospective Analysis.," *Vasc. Dis. Manag. ,* vol. 13, pp. E112–E119, 2016.

[3]   M. Yost, *Critical Limb Ischemia Volume I: United States Epidemiology*. The SAGE Group, 2010.

[4]   Z. Raval and D. W. Losordo, "Cell therapy of peripheral arterial disease: from experimental findings to clinical trials," *Circ Res,* vol. 112, no. 9, pp. 1288-302, Apr 26 2013, doi: 10.1161/CIRCRESAHA.113.300565.

[5]   N. Ferrara and K. Alitalo, "Clinical applications of angiogenic growth factors and their inhibitors," *Nat Med,* vol. 5, no. 12, pp. 1359-64, Dec 1999, doi: 10.1038/70928.

[6]   A. Rivard and J. M. Isner, "Angiogenesis and vasculogenesis in treatment of cardiovascular disease," *Mol Med,* vol. 4, no. 7, pp. 429-40, Jul 1998. [Online]. Available: https://www.ncbi.nlm.nih.gov/pubmed/9713822.

[7]   M. Simons and J. A. Ware, "Therapeutic angiogenesis in cardiovascular disease," *Nat Rev Drug Discov,* vol. 2, no. 11, pp. 863-71, Nov 2003, doi: 10.1038/nrd1226.

[8]   G. D. Yancopoulos, S. Davis, N. W. Gale, J. S. Rudge, S. J. Wiegand, and J. Holash, "Vascular-specific growth factors and blood vessel formation," *Nature,* vol. 407, no. 6801, pp. 242-8, Sep 14 2000, doi: 10.1038/35025215.

[9]   D. W. Losordo and S. Dimmeler, "Therapeutic angiogenesis and vasculogenesis for ischemic disease: part II: cell-based therapies," *Circulation,* vol. 109, no. 22, pp. 2692-7, Jun 8 2004, doi: 10.1161/01.CIR.0000128596.49339.05.

[10]   D. W. Losordo and S. Dimmeler, "Therapeutic angiogenesis and vasculogenesis for ischemic disease. Part I: angiogenic cytokines," *Circulation,* vol. 109, no. 21, pp. 2487-91, Jun 1 2004, doi: 10.1161/01.CIR.0000128595.79378.FA.

[11]   J. P. Cooke and D. W. Losordo, "Modulating the vascular response to limb ischemia: angiogenic and cell therapies," *Circ Res,* vol. 116, no. 9, pp. 1561-78, Apr 24 2015, doi: 10.1161/CIRCRESAHA.115.303565.

[12]   A. J. Rufaihah *et al.*, "Endothelial cells derived from human iPSCS increase capillary density and improve perfusion in a mouse model of peripheral arterial disease," *Arterioscler Thromb Vasc Biol,* vol. 31, no. 11, pp. e72-9, Nov 2011, doi: 10.1161/ATVBAHA.111.230938.

[13]   R. Gupta and D. W. Losordo, "Cell therapy for critical limb ischemia: moving forward one step at a time," *Circ Cardiovasc Interv,* vol. 4, no. 1, pp. 2-5, Feb 1 2011, doi: 10.1161/CIRCINTERVENTIONS.110.960716.

[14]   X. Chen *et al.*, "Prevascularization of a fibrin-based tissue construct accelerates the formation of functional anastomosis with host vasculature," *Tissue Eng Part A,* vol. 15, no. 6, pp. 1363-71, Jun 2009, doi: 10.1089/ten.tea.2008.0314.

[15]   L. Perry, U. Merdler, M. Elishaev, and S. Levenberg, "Enhanced Host Neovascularization of Prevascularized Engineered Muscle Following Transplantation into Immunocompetent versus Immunocompromised Mice," *Cells,* vol. 8, no. 12, Nov 20 2019, doi: 10.3390/cells8121472.

[16]   S. Levenberg *et al.*, "Engineering vascularized skeletal muscle tissue," *Nat Biotechnol,* vol. 23, no. 7, pp. 879-84, Jul 2005, doi: 10.1038/nbt1109.

[17]   K. R. Stevens *et al.*, "Physiological function and transplantation of scaffold-free and vascularized human cardiac muscle tissue," *Proc Natl Acad Sci U S A,* vol. 106, no. 39, pp. 16568-73, Sep 29 2009, doi: 10.1073/pnas.0908381106.

[18]   K. T. Kang, P. Allen, and J. Bischoff, "Bioengineered human vascular networks transplanted into secondary mice reconnect with the host vasculature and re-establish perfusion," *Blood,* vol. 118, no. 25, pp. 6718-21, Dec 15 2011, doi: 10.1182/blood-2011-08-375188.

[19]   M. M. Stevens, R. P. Marini, D. Schaefer, J. Aronson, R. Langer, and V. P. Shastri, "In vivo engineering of organs: the bone bioreactor," *Proc Natl Acad Sci U S A,* vol. 102, no. 32, pp. 11450-5, Aug 9 2005, doi: 10.1073/pnas.0504705102.

[20]   D. M. Dean and J. R. Morgan, "Cytoskeletal-mediated tension modulates the directed self-assembly of microtissues," *Tissue Eng Part A,* vol. 14, no. 12, pp. 1989-97, Dec 2008, doi: 10.1089/ten.tea.2007.0320.

[21]   D. M. Dean, A. P. Rago, and J. R. Morgan, "Fibroblast elongation and dendritic extensions in constrained versus unconstrained microtissues," *Cell Motil Cytoskeleton,* vol. 66, no. 3, pp. 129-41, Mar 2009, doi: 10.1002/cm.20335.

[22]   J. M. Kelm *et al.*, "Design of custom-shaped vascularized tissues using microtissue spheroids as minimal building units," *Tissue Eng,* vol. 12, no. 8, pp. 2151-60, Aug 2006, doi: 10.1089/ten.2006.12.2151.

[23]   A. P. McGuigan and M. V. Sefton, "Vascularized organoid engineered by modular assembly enables blood perfusion," *Proc Natl Acad Sci U S A,* vol. 103, no. 31, pp. 11461-6, Aug 1 2006, doi: 10.1073/pnas.0602740103.

[24]   J. Youssef, A. K. Nurse, L. B. Freund, and J. R. Morgan, "Quantification of the forces driving self-assembly of three-dimensional microtissues," *Proc Natl Acad Sci U S A,* vol. 108, no. 17, pp. 6993-8, Apr 26 2011, doi: 10.1073/pnas.1102559108.

[25] K. L. Christman, A. J. Vardanian, Q. Fang, R. E. Sievers, H. H. Fok, and R. J. Lee, "Injectable fibrin scaffold improves cell transplant survival, reduces infarct expansion, and induces neovasculature formation in ischemic myocardium," *J Am Coll Cardiol,* vol. 44, no. 3, pp. 654-60, Aug 4 2004, doi: 10.1016/j.jacc.2004.04.040.

[26] J. Ceccarelli and A. J. Putnam, "Sculpting the blank slate: how fibrin's support of vascularization can inspire biomaterial design," *Acta Biomater,* vol. 10, no. 4, pp. 1515-23, Apr 2014, doi: 10.1016/j.actbio.2013.07.043.

[27] A. Y. Rioja, R. Tiruvannamalai Annamalai, S. Paris, A. J. Putnam, and J. P. Stegemann, "Endothelial sprouting and network formation in collagen- and fibrin-based modular microbeads," *Acta Biomater,* vol. 29, pp. 33-41, Jan 2016, doi: 10.1016/j.actbio.2015.10.022.

[28] C. M. Ghajar, K. S. Blevins, C. C. Hughes, S. C. George, and A. J. Putnam, "Mesenchymal stem cells enhance angiogenesis in mechanically viable prevascularized tissues via early matrix metalloproteinase upregulation," *Tissue Eng,* vol. 12, no. 10, pp. 2875-88, Oct 2006, doi: 10.1089/ten.2006.12.2875.

[29] A. Y. Rioja, E. L. H. Daley, J. C. Habif, A. J. Putnam, and J. P. Stegemann, "Distributed vasculogenesis from modular agarose-hydroxyapatite-fibrinogen microbeads," *Acta Biomater,* vol. 55, pp. 144-152, Jun 2017, doi: 10.1016/j.actbio.2017.03.050.

[30] B. Carrion, I. A. Janson, Y. P. Kong, and A. J. Putnam, "A safe and efficient method to retrieve mesenchymal stem cells from three-dimensional fibrin gels," *Tissue Eng Part C Methods,* vol. 20, no. 3, pp. 252-63, Mar 2014, doi: 10.1089/ten.TEC.2013.0051.

[31] M. Brown and D. G. Lowe, "Automatic Panoramic Image Stitching using Invariant Features," *International Journal of Computer Vision,* vol. 74, no. 1, pp. 59-73, 2007/08/01 2007, doi: 10.1007/s11263-006-0002-3.

[32] M. S. Gudur, R. R. Rao, A. W. Peterson, D. J. Caldwell, J. P. Stegemann, and C. X. Deng, "Noninvasive quantification of in vitro osteoblastic differentiation in 3D engineered tissue constructs using spectral ultrasound imaging," *PLoS One,* vol. 9, no. 1, p. e85749, 2014, doi: 10.1371/journal.pone.0085749.

[33] J. M. Melero-Martin *et al.*, "Engineering robust and functional vascular networks in vivo with human adult and cord blood-derived progenitor cells," *Circ Res,* vol. 103, no. 2, pp. 194-202, Jul 18 2008, doi: 10.1161/CIRCRESAHA.108.178590.

[34] S. J. Grainger, B. Carrion, J. Ceccarelli, and A. J. Putnam, "Stromal cell identity influences the in vivo functionality of engineered capillary networks formed by co-delivery of endothelial cells and stromal cells," *Tissue Eng Part A,* vol. 19, no. 9-10, pp. 1209-22, May 2013, doi: 10.1089/ten.TEA.2012.0281.

[35] R. R. Rao, A. W. Peterson, J. Ceccarelli, A. J. Putnam, and J. P. Stegemann, "Matrix composition regulates three-dimensional network formation by endothelial cells and

mesenchymal stem cells in collagen/fibrin materials," *Angiogenesis,* vol. 15, no. 2, pp. 253-64, Jun 2012, doi: 10.1007/s10456-012-9257-1.

[36]   C. M. Ghajar *et al.*, "Mesenchymal cells stimulate capillary morphogenesis via distinct proteolytic mechanisms," *Exp Cell Res,* vol. 316, no. 5, pp. 813-25, Mar 10 2010, doi: 10.1016/j.yexcr.2010.01.013.

[37]   A. W. Peterson, D. J. Caldwell, A. Y. Rioja, R. R. Rao, A. J. Putnam, and J. P. Stegemann, "Vasculogenesis and Angiogenesis in Modular Collagen-Fibrin Microtissues," *Biomater Sci,* vol. 2, no. 10, pp. 1497-1508, Oct 1 2014, doi: 10.1039/C4BM00141A.

[38]   R. Tiruvannamalai Annamalai, A. Y. Rioja, A. J. Putnam, and J. P. Stegemann, "Vascular Network Formation by Human Microvascular Endothelial Cells in Modular Fibrin Microtissues," *ACS Biomater Sci Eng,* vol. 2, no. 11, pp. 1914-1925, Nov 14 2016, doi: 10.1021/acsbiomaterials.6b00274.

[39]   A. Alajati *et al.*, "Spheroid-based engineering of a human vasculature in mice," *Nat Methods,* vol. 5, no. 5, pp. 439-45, May 2008, doi: 10.1038/nmeth.1198.

[40]   A. M. Laib, A. Bartol, A. Alajati, T. Korff, H. Weber, and H. G. Augustin, "Spheroid-based human endothelial cell microvessel formation in vivo," *Nat Protoc,* vol. 4, no. 8, pp. 1202-15, 2009, doi: 10.1038/nprot.2009.96.

[41]   T. Korff, S. Kimmina, G. Martiny-Baron, and H. G. Augustin, "Blood vessel maturation in a 3-dimensional spheroidal coculture model: direct contact with smooth muscle cells regulates endothelial cell quiescence and abrogates VEGF responsiveness," *FASEB J,* vol. 15, no. 2, pp. 447-57, Feb 2001, doi: 10.1096/fj.00-0139com.

[42]   L. De Moor *et al.*, "High-throughput fabrication of vascularized spheroids for bioprinting," *Biofabrication,* vol. 10, no. 3, p. 035009, Jun 12 2018, doi: 10.1088/1758-5090/aac7e6.

[43]   C. E. Vorwald, S. Joshee, and J. K. Leach, "Spatial localization of endothelial cells in heterotypic spheroids influences Notch signaling," *J Mol Med (Berl),* vol. 98, no. 3, pp. 425-435, Mar 2020, doi: 10.1007/s00109-020-01883-1.

[44]   K. C. Murphy, J. Whitehead, D. Zhou, S. S. Ho, and J. K. Leach, "Engineering fibrin hydrogels to promote the wound healing potential of mesenchymal stem cell spheroids," *Acta Biomater,* vol. 64, pp. 176-186, Dec 2017, doi: 10.1016/j.actbio.2017.10.007.

[45]   S. H. Bhang *et al.*, "Three-dimensional cell grafting enhances the angiogenic efficacy of human umbilical vein endothelial cells," *Tissue Eng Part A,* vol. 18, no. 3-4, pp. 310-9, Feb 2012, doi: 10.1089/ten.TEA.2011.0193.

[46]   B. M. Roux *et al.*, "Preformed Vascular Networks Survive and Enhance Vascularization in Critical Sized Cranial Defects," *Tissue Eng Part A,* vol. 24, no. 21-22, pp. 1603-1615, Nov 2018, doi: 10.1089/ten.TEA.2017.0493.

[47]   A. A. Gorkun *et al.*, "Angiogenic potential of spheroids from umbilical cord and adipose-derived multipotent mesenchymal stromal cells within fibrin gel," *Biomed Mater,* vol. 13, no. 4, p. 044108, May 22 2018, doi: 10.1088/1748-605X/aac22d.

[48]   A. L. Torres, S. J. Bidarra, M. T. Pinto, P. C. Aguiar, E. A. Silva, and C. C. Barrias, "Guiding morphogenesis in cell-instructive microgels for therapeutic angiogenesis," *Biomaterials,* vol. 154, pp. 34-47, Feb 2018, doi: 10.1016/j.biomaterials.2017.10.051.

[49]   A. L. Torres *et al.*, "Microvascular engineering: Dynamic changes in microgel-entrapped vascular cells correlates with higher vasculogenic/angiogenic potential," *Biomaterials,* vol. 228, p. 119554, Jan 2020, doi: 10.1016/j.biomaterials.2019.119554.

[50]   P. Du, A. D. S. Da Costa, C. Savitri, S. S. Ha, P. Y. Wang, and K. Park, "An injectable, self-assembled multicellular microsphere with the incorporation of fibroblast-derived extracellular matrix for therapeutic angiogenesis," *Mater Sci Eng C Mater Biol Appl,* vol. 113, p. 110961, Aug 2020, doi: 10.1016/j.msec.2020.110961.

[51]   C. M. Ghajar *et al.*, "The effect of matrix density on the regulation of 3-D capillary morphogenesis," *Biophys J,* vol. 94, no. 5, pp. 1930-41, Mar 1 2008, doi: 10.1529/biophysj.107.120774.

Chapter 4 – Pre-cultured, Cell-encapsulating Fibrin Microbeads for the Vascularization of Ischemic Tissues

*Chapter 4 was previously published as: N. E. Friend, J. A. Beamish, E. A. Margolis, N. G. Schott, J. P. Stegemann, and A. J. Putnam, "Pre-cultured, cell-encapsulating fibrin microbeads for the vascularization of ischemic tissues," *J Biomed Mater Res A*, 1-13 (2023), doi: 10.1002/jbm.a.37580.

4.1 Introduction

Cardiovascular disease (CVD) is the leading cause of death worldwide and medical costs associated with disease management result in a high economic burden globally [1]. In CVD conditions, such as coronary heart disease (CHD) and peripheral artery disease (PAD), buildup of atherosclerotic plaque in blood vessels causes a reduction of blood flow to tissues, often resulting in loss of tissue function or necrosis. Cell death and tissue necrosis can progress to heart failure in cases of CHD [2] or critical limb ischemia (CLI) in severe cases of PAD [3, 4]. CLI affects approximately 2 million individuals in the United States alone [3], with an estimated 30%-50% of patients requiring amputation within the first year without revascularization efforts [4]. Further, less than 45% of CLI patients are eligible for common revascularization strategies due to associated comorbidities, such as coronary artery disease, neurological disorders, cerebrovascular disease, and diabetes [3, 5]. The complications of CVD, as well as many other pathological conditions resulting in ischemic tissues, has led to an increased demand for effective strategies for

tissue repair and replacement; however, efforts to repair ischemic tissues utilizing drug therapies or direct cell delivery have been met with minimal clinical success [2, 5-7].

Delivery of pro-angiogenic factors to stimulate therapeutic vascularization is often limited by short half-life, inadequate retention of factors at the site of ischemia, and the inability to fully recapitulate the complex spatiotemporal ques required for vascular development [8, 9]. Cell-based approaches to treat ischemic tissues have the potential to overcome limitations associated with pro-angiogenic factors but have been plagued by low cell retention at the target site and reduced cell viability post-transplantation due to the harsh ischemic environment [7, 10]. To improve cell engraftment, the delivery of cells within hydrogels has been explored; however, even when cell engraftment is improved, the implanted cells can experience apoptosis as diffusion of the necessary nutrients is limited within implanted constructs. Though diffusion may not be limited by tissue thickness during *in vitro* culture [11], necrosis may occur at the core of larger tissue constructs once implanted *in vivo* as diffusion of nutrients to the center will be insufficient to support cell survival and function without timely inosculation with host vasculature [9].

Prevascularization is the formation of vascular networks *in vitro* before transplantation of tissue constructs *in vivo*. It is a promising method for promoting rapid inosculation of engineered vasculature with host blood supply*,* with the goal of providing timely perfusion of nutrients [12]. Many approaches to generate prevascularized constructs have been described [13, 14], including the generation of vascularized matrices [12, 15, 16] and the application of cell sheets [17, 18]. Despite the promise of prevascularizing cell sheets or entire tissue constructs [19, 20], these approaches require invasive surgical procedures to implant the constructs, which could be impracticable for patients with CLI.

Injection of populations of cell-encapsulating, modular microbeads can provide the benefits of prevascularization while maintaining the ability to be delivered in a minimally invasive manner. This approach has the goal of rapidly revascularizing ischemic tissues through the *in situ* formation of a microvascular network, as vessels from neighboring beads inosculate with each other and the host blood supply. We have previously demonstrated that endothelial and stromal cells can be co-encapsulated within fibrin microbeads with high cell viability and support the formation of vessel-like structures that sprout to vascularize larger fibrin matrices [21]. Furthermore, using a murine subcutaneous model, we showed that microbeads pre-cultured *in vitro* can initiate the formation of extensive, functional microvascular networks upon implantation *in vivo* [22]. Building upon our previous work, this study assesses the ability of populations of pre-cultured microbeads to form functional microvascular networks and restore tissue perfusion in a mouse model of critical limb ischemia.

4.2 Materials and Methods

4.2.1 Cell culture

Human umbilical vein endothelial cells (HUVEC; Lonza, Inc., Walkersville, MD) were cultured in fully supplemented endothelial growth media (EGM2; Lonza) and used from passages 4-7. Human bone marrow-derived mesenchymal stem cells (MSC; RoosterBio Inc., Frederick, MD) were cultured in RoosterNourish-MSC media (RoosterBio Inc.) and used from passages 6-8. All cells were cultured at 37 °C and 5% CO_2 with media replacement every 48 h.

4.2.2 Fibrin microbead production

Fibrin microbeads were fabricated using a water-in-oil emulsification process, as previously described (Fig. 1A) [21, 22]. Prior to starting the emulsification process, 75 mL of 100 cSt polydimethylsiloxane (PDMS) oil (Clearco Products Co. Inc., Bensalem, PA) was placed into a sterile 100 mL beaker and stored on ice. Either 6×10^6 (*in vitro)* or 20×10^6 (*in vivo*) total cells were pelleted in a 1:1 HUVEC:MSC ratio in a conical tube. To prepare 3 mL of fibrin microbead precursor solution, the following components were added and mixed thoroughly: 765 µL serum-free endothelial growth medium (SF-EGM2), 300 µL fetal bovine serum (FBS, 10% final), 60 µL of 50U/mL stock thrombin (1U/mL final), and 1875 µL of fibrinogen stock solution (2.5 mg/mL final clottable protein). Sterile bovine fibrinogen (Sigma-Aldrich, St. Louis, MO) stock solution was prepared by mixing fibrinogen with SF-EGM2 at 37 °C until fully dissolved and then filtering the solution. The HUVEC-MSC cell pellet was resuspended in the precursor solution and added to the PDMS bath. The solution was mixed at 600 RPM for 5 min on ice to allow for emulsion, then mixed for 25 min at 37 °C to allow for gelation. The mixture of microbeads in PDMS was transferred to 50 mL conical tubes and 5 mL of 0.1% L101 surfactant (BASF, Florham Park, NJ) in phosphate buffer saline (PBS) was added to each tube for inversion mixing, followed by 4-5 centrifugation steps (200g for 5 min/each). After each centrifugation step, PDMS was removed from the fibrin microbeads. The microbeads were then re-suspended with 25 mL of EGM2 and placed in vented 50 mL conical tubes with filters (CELLTREAT Scientific Products, Shirley, MA) prior to starting any experimental procedures. Media was changed the day after fabrication, and microbeads were cultured in suspension for 3 days (D3 PC microbeads) before implantation.

4.2.3 In vitro vasculogenesis

Fibrin microbeads were embedded in bulk fibrin hydrogels immediately, 1, 3, or 5 days after fabrication. One tenth of a 3 mL microbead stock was utilized to make three fibrin hydrogels, with ~ 100 μL of microbeads per hydrogel. Constructs were made by mixing the microbead pellet thoroughly with SF-EGM2, FBS (10% final), thrombin (1 U/mL final), and fibrinogen stock solution (2.5 mg/mL final clottable protein). Then, 500 μL of the microbead-protein mixture was added per well of a standard 24-well culture plate and incubated at room temperature for 5 min before being placed in the incubator for 25 min at 37 °C. EGM2 (1 mL/well) was added to each hydrogel after the complete gelation process. Cellular bulk fibrin hydrogels containing 3 x 10^6 cells/mL in a 1:1 HUVEC:MSC ratio were also fabricated. Media was changed the day after, then every other day for 7 days.

4.2.4 In vitro sample staining and fluorescent imaging

Hydrogels were fixed in zinc-buffered formalin (Z-Fix; Anatech, Battle Creek, MI) for 10 min, rinsed, and stained overnight with Ulex europaeus agglutinin I (UEA, 1:200; Vector Laboratories, Newark, CA), 4',6-diamidino-2-phenylindol (DAPI, 1 μg/mL; Thermo Fisher Scientific, Waltham, MA), and AlexaFluor 488 phalloidin (1:200; Thermo Fisher Scientific) which label endothelial cells, cell nuclei, and F-actin, respectively. Samples were rinsed overnight with PBS prior to imaging. Images were acquired using an Olympus IX81 microscope equipped with a disk-scanning unit (DSU; Olympus America, Center Valley, PA) and Metamorph Premier software (Molecular Devices, Sunnyvale, CA). The scan slide tool in the Olympus software (IX2-BSW, version 01.07; Olympus) was used to take single plain fluorescent images of endothelial networks formed throughout the bulk fibrin hydrogels. Single plane 10x magnification phase images were acquired of microbeads in suspension. Confocal z-stacks (225 μm total depth, 75

μm/slice, 4 slices/stack) imaged at 4x magnification were acquired at specific regions of interest of the hydrogels using the DSU. Z-series stacks were then collapsed into maximum intensity projections using ImageJ [23].

4.2.5 Sample preparation for intramuscular implants

Intramuscular implants consisted of 3 x 10^6 cells (HUVEC:MSC in a nominal 1:1 ratio) in either 150 µL of fibrin precursor solution or 250 µL total volume of microbeads in a fibrin precursor solution, for experimental groups containing cells. To ensure the same number of cells was implanted into each mouse across different microbead preparations, the number of cells within a given volume of microbeads was quantified immediately after fabrication and the volume of cell-encapsulating microbeads implanted into each mouse was adjusted in order to ensure delivery of the same number of cells per implant. Briefly, microbead pellets from each batch were resuspended in 1 mL of EGM2 and then 100 µL was transferred to a 96-well plate. An equal volume (100 µL) of a solution containing the fibrinolytic enzyme nattokinase (NSK-SD; Japan Bio Science Laboratory Co., Ltd) at a concentration of 50 FU/mL (fibrin degradation units) in D-PBS (calcium- and magnesium-free) containing 1 mM EDTA [24] was then added and mixed. The plate was incubated at 37 °C for 30 min to allow microbead degradation. Following fibrinolysis, 200 µL of PBS was added to dilute the solution and cells were counted using a hemocytometer. Before preparing implants, the microbead volume preparations were adjusted to yield 3 x 10^6 total cells, assuming half HUVEC and half MSC. Samples for cellular experimental groups (D3 PC microbeads or cellular bulk hydrogels) were then centrifuged at 200g for 5 min to form microbead or cell pellets, supernatant removed, and the pellets resuspended in fibrin hydrogel precursor solution comprising of SF-EGM2, FBS (10% final), thrombin (1 U/mL final), and fibrinogen stock solution (2.5 mg/mL final clottable protein). Each solution was rapidly mixed and subsequently

injected into an intramuscular pocket adjacent to the site of artery ligation. The following four experimental groups were evaluated: (1) D3 PC microbeads, (2) cellular bulk hydrogels, (3) acellular bulk hydrogels, and (4) saline (sham). Microbeads were delivered in an acellular fibrin precursor solution which gelled *in situ*. Prior to surgery, implants and timepoints for each animal were predetermined. Control hydrogels, which contained microbeads or cells used for surgery were fabricated as described above and cultured in fully supplemented EGM2 for 7 days *in vitro* to confirm microvasculature network formation.

4.2.6 Murine hindlimb ischemia model

All animal procedures were compliant with the NIH Guide for Care and Use of Laboratory Animals and approved by the University of Michigan's Institutional Animal Care and Use Committee (IACUC). Male C.B-17 SCID mice (Taconic Labs, Hudson, NY), 6 to 8 weeks of age, were acclimated for ≥ 72 h prior to surgery. Animals were anesthetized with vaporized isoflurane (1%-5%) and prophylactic analgesia, carprofen (5 mg/kg), was administered to each animal via intraperitoneal injection. Body temperature was maintained on a heating pad throughout the entirety of the surgical procedure. Ophthalmic ointment (Puralube Vet Ointment; Dechra, Overland Park, KS) was added to the eyes of each mouse with a cotton swab. The ventral surface of the animal limb (from the mid abdomen to the bilateral feet) was shaved and depilatory agent (Nair; Thermo Fisher Scientific) was applied to remove remaining fur. The shaved area was sterilized by alternating Betadine (Thermo Fisher Scientific) and alcohol rinses, each repeated three times. A sterile surgical field was created using a sterile fenestrated drape, sterile tools were placed on the sterile field, and sterile gloves were donned prior to beginning the surgical procedure. The left hindlimb was visualized using a stereomicroscope. An incision (~1.5 cm) in the skin was made from the popliteal fossa to the inguinal ligament and held open with retractors. The

subcutaneous tissue above the femoral neurovascular bundle was dissected and the overlaying fascia was dissected to further expose the bundle. Using fine tipped forceps, the artery was carefully separated from the vein and nerve. The femoral artery was ligated below the superficial epigastric/proximal caudal branch and just above the popliteal/saphenous bifurcation (Fig. 4.2B) using 5-0 silk sutures (Oasis, Mettawa, IL) and was dissected between the two ligation sites. An intramuscular pocket was created directly adjacent to the ligation site using two forceps, and the full implant volume was injected directly into the pocket using a P-1000 pipettor and allowed to polymerize for 3 min (Fig. 4.2C). The forceps and retractors were removed, and the skin incision was closed using 5-0 nylon sutures (Oasis). Mice were allowed to recover from the anesthesia before being placed in their normal housing. An additional dose of carprofen was administered to each animal 24 h after surgery, then daily as needed if animals had abnormal appearance. A total of 38 animals were used for the completion of this study, with a minimum of 3 mice/group evaluated for statistical analyses at both day 7 and 14 timepoints. The number of mice per group varied (saline N = 5, acellular fibrin N = 9, cellular fibrin N = 14, D3 PC microbeads N = 10) as a consequence of strict euthanasia criteria intended to minimize animal suffering in our approved IACUC protocol. Mice were prematurely euthanized before the predetermined experimental timepoint if autoamputation of more than two toes occurred and were not included in endpoint analysis.

4.2.7 Laser Doppler perfusion imaging

Laser Doppler perfusion imaging (LDPI) was performed immediately after, and 1, 3, 5, 7, 10, and 14 days after surgery on both the ischemic and contralateral hindlimb using a PeriScan PIM 3 System (PeriMed Inc., Las Vegas, NV). Briefly, mice were anesthetized using vaporized isoflurane and body temperature was maintained on a heating pad throughout LDPI measurements.

Mice were placed in a prone position and LDPI measurements were taken of both foot pads. PeriMed software was used to calculate the mean perfusion for each foot pad. Results are expressed as relative LDPI signal compared to the contralateral (unligated control) hindlimb to account for variation in ambient light, temperature, and arterial pressure between animals and timepoints. If mice were prematurely euthanized due to autoamputation, the LDPI data for all measurements prior to euthanasia were included.

4.2.8 Distribution of hindlimb ischemia severity

Color images of both hindlimbs were acquired after 1, 7, and 14 days after surgery with mice in both the prone and supine position to longitudinally assess hindlimb ischemia severity over time. Hindlimbs were described as (1) normal if the ischemic limb was comparable to the control limb, (2) discolored if the limb appeared purple, (3) necrotic if there was evidence of toe or foot necrosis, or (4) autoamputation, which resulted in euthanasia if more than two toes.

4.2.9 Implant retrieval and post-processing

After 7 or 14 days, animals were euthanized via isoflurane overdose followed by secondary pneumothorax. Implants and the surrounding muscle tissue were excised with scissors and forceps, placed immediately in 20 mL glass scintillation vials with Z-Fix and subsequently fixed for 24 h at 4°C. After fixation, implants were washed three times with PBS (5 min/wash), submerged in 70% ethanol, and stored at 4°C until further processing. Samples were then placed in tissue cassettes (Unisette Tissue Cassettes, Simport, Canada), embedded in paraffin in a KD-BMII tissue embedding center (IHC World, Ellicott City, MD), and sectioned through their entire volume with a Thermo Scientific HM 325 rotary microtome (5 μm sections) for further analysis.

4.2.10 Hematoxylin and eosin (H&E) staining

Sections were stained with Mayer's hematoxylin (Electron Microscopy Sciences, Hatfield, PA) and eosin Y (Sigma-Aldrich). Slides were deparaffinized with xylene twice (5 min/wash) and then transferred to 100%, 95%, 70% ethanol, and deionized water baths (3 min/wash, two baths per ethanol concentration). Slides were submerged in a hematoxylin bath for 15 min, and then rinsed with tap water for an additional 15 min. Slides were then placed in 95% ethanol for 30 s, followed by submersion in eosin Y for 1 min. Slides were subsequently transferred into a 95% ethanol bath for 1 min, and two separate 100% ethanol baths (1 min/bath) and two separate xylene baths (3 min/wash) to dehydrate the samples. Toluene mounting solution (Permount; Electron Microscopy Sciences) was added to each slide prior to covering samples with coverslips. Slides dried overnight prior to imaging.

4.2.11 Human CD31 (hCD31) and alpha-smooth muscle actin (α-SMA) staining

The center of each implant was determined by the largest cross-sectional area of H&E-stained explanted tissue sections. The subsequent serial section of each implant was then deparaffinized with xylene and rehydrated through a series of graded ethanol washes, ending with water. Slides were placed in 1x antigen retrieval solution (Agilent Dako, Santa Clara, CA) and placed in a steamer (95-99°C) for 35 min. The antigen retrieval solution and slides were removed and equilibrated to room temperature. Slides were rinsed 3x with 0.1% Tween-20 in tris-buffered saline (TBS-T) for 2 min. The area around the tissue was marked with an ImmEdge Hydrophobic Barrier PAP pen (Vector Laboratories). The Dako EnVision System-HRP kit (Agilent Dako) was utilized for hCD31 and α-SMA staining. First, tissues were incubated with peroxidase blocking solution for 5 min at room temperature. For human CD31 (hCD31) labeling, a mouse anti-human CD31 monoclonal antibody (Agilent Dako) diluted 1:50 in TBS-T was used as the primary

antibody, incubated at 4 °C overnight. For alpha-smooth muscle actin (α-SMA) labeling, a mouse anti-alpha smooth muscle actin monoclonal antibody (1A4 [asm-1]) (Thermo Fisher Scientific) diluted 1:200 in TBS-T was used as the primary antibody, incubated at room temperature for 2 h. The HRP-conjugated secondary antibody solution was added to each sample and incubated at room temperature for 30 min. Samples were then incubated with DAB+ substrate-chromogen solution for 5 min at room temperature. Samples were counter-stained with hematoxylin for 15 min, washed in tap water for 15 min, then dehydrated with 95% ethanol, 100% ethanol, and xylene washes as described above. Toluene mounting solution was added prior to covering the samples with coverslips. Slides dried overnight prior to imaging.

4.2.12 In vivo vessel quantification

Bright-field images (4x, 10x, and 20x) of each implant stained for H&E, hCD31, and α-SMA were taken using an Olympus IX81 microscope with a DP2-Twain color camera (Olympus) and the CellSens Imagining Software (Olympus). The total cross-sectional area (mm^2) of each implant was quantified for 4x images using ImageJ after first defining the perimeter of the implant identified by H&E staining. For hCD31+ vessel quantification, a minimum of two 20x hCD31-stained images from each implant were quantified to determine the average vessel density (# of vessels/mm^2). Vessels were defined by the presence of a hollow lumen surrounded by a complete brown rim of positive hCD31. If host erythrocytes were present in the lumens, vessels were considered perfused. Quantification of vessels derived from the implanted human cells was conducted by two independent evaluators via a one-side blinded study for hCD31. The cross-sectional area (mm^2) was then multiplied by the average vascular density (# of vessels/mm^2) to determine the total number of hCD31+ vessels found within each implant at days 7 and 14.

Acellular bulk hydrogel controls were not analyzed or shown because they did not contain any human-derived vessels.

4.2.13 Statistics

Statistical analysis was performed using Prism (GraphPAD, La Jolla, CA). Data are represented as mean ± standard deviation (SD) of at least three independent experimental replicates. Data were analyzed using two-way ANOVA with Sidak post-hoc testing. Values of $p < 0.05$ were considered statistically significant.

4.3 Results

4.3.1 Assessment of microvascular network formation catalyzed by fibrin microbeads in vitro

Fibrin microbeads containing HUVEC and MSC were fabricated using a bulk emulsification process and were pre-cultured in suspension (Fig. 4.1A) prior to being embedded in a larger fibrin matrix to assess vessel morphogenesis *in vitro*. Microbead diameters immediately post-fabrication were previously characterized, ranging from 50 to 300 μm with an average of 140 μm [21, 22]. Over the course of extended pre-culture, microbeads tended to aggregate into larger tissue structures (Fig. 4.1B-D). In line with previous work from our group [22, 25], microbeads pre-cultured for 1, 3, or 5 days supported vessel morphogenesis to a similar degree after 7 days (Fig. 4.1E-G). Prior work found evidence that extended culture could reduce the vascularization capacity of pre-cultured microbeads [22]. Further, as aggregation could reduce microbead distribution and injectability, D3 PC microbeads were selected for the remainder of the study. Importantly, D3 PC microbeads facilitated MSC and vessel invasion into the surround matrix (Fig.

4.1H). HUVEC and MSC in bulk fibrin hydrogels resulted in a dispersed, distributed microvascular network (Fig. 4.1I).
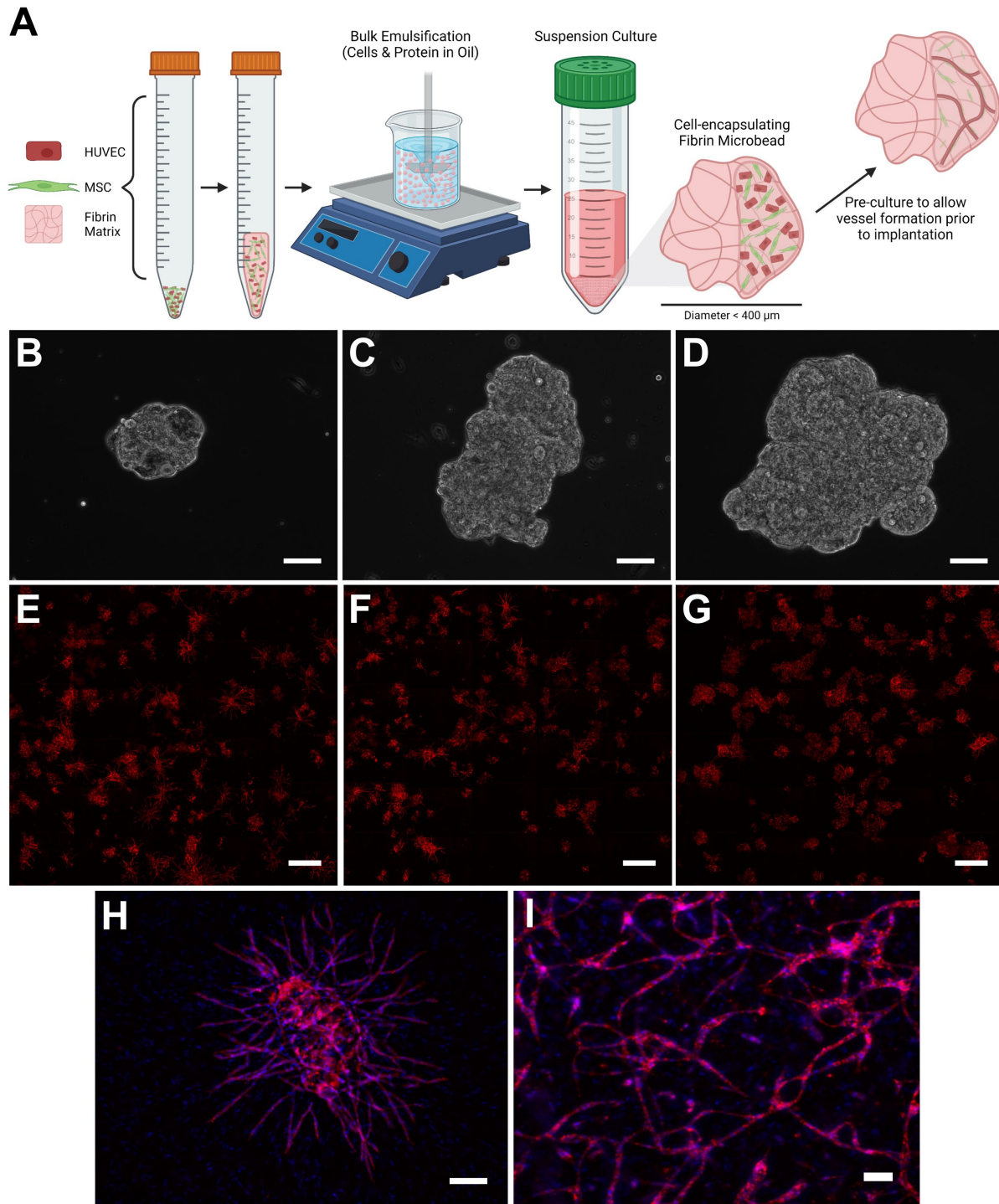
Figure 4.1: Pre-cultured microbeads vascularize larger tissue mimics in vitro. *(A) Fibrin microbeads, containing HUVEC and MSC, were fabricated using a bulk emulsification process and cultured in suspension before embedding in a larger fibrin matrix in vitro or implanted in a model of hindlimb ischemia*

in vivo. Schematic created with BioRender.com. Microbeads were pre-cultured in suspension culture for (B) 1, (C) 3, or (D) 5 days (scale bar = 100 μm). Then, (E) D1, (F) D3, and (G) D5 PC microbeads were embedded and cultured in a larger matrix for 7 days (scale bar = 1000 μm). (H) Vessels and stromal cells from D3 PC microbeads invade surrounding matrix (scale bar = 200 μm). (I) HUVEC+MSC vascularize bulk fibrin hydrogels after 7 days (scale bar = 100 μm). Samples stained with UEA (endothelial cells; red) and DAPI (nuclei; blue).

4.3.2 Evaluation of pre-cultured microbeads to alleviate ischemia and improve limb salvage

Fibrin microbeads were implanted in a murine model of hindlimb ischemia (Fig. 4.2A). The femoral artery of SCID mice was separated from the nerve and vein, ligated (Fig. 4.2B), and dissected before implants were embedded in an intramuscular pocket directly adjacent to the severed artery (Fig. 4.2C). An intramuscular pocket was utilized to ensure precise and uniform implant location between animals relative to the ischemic area. D3 PC microbeads in an acellular fibrin gel were compared to cellular bulk hydrogels (HUVEC and MSC in a fibrin gel), acellular bulk hydrogels, and saline (sham).
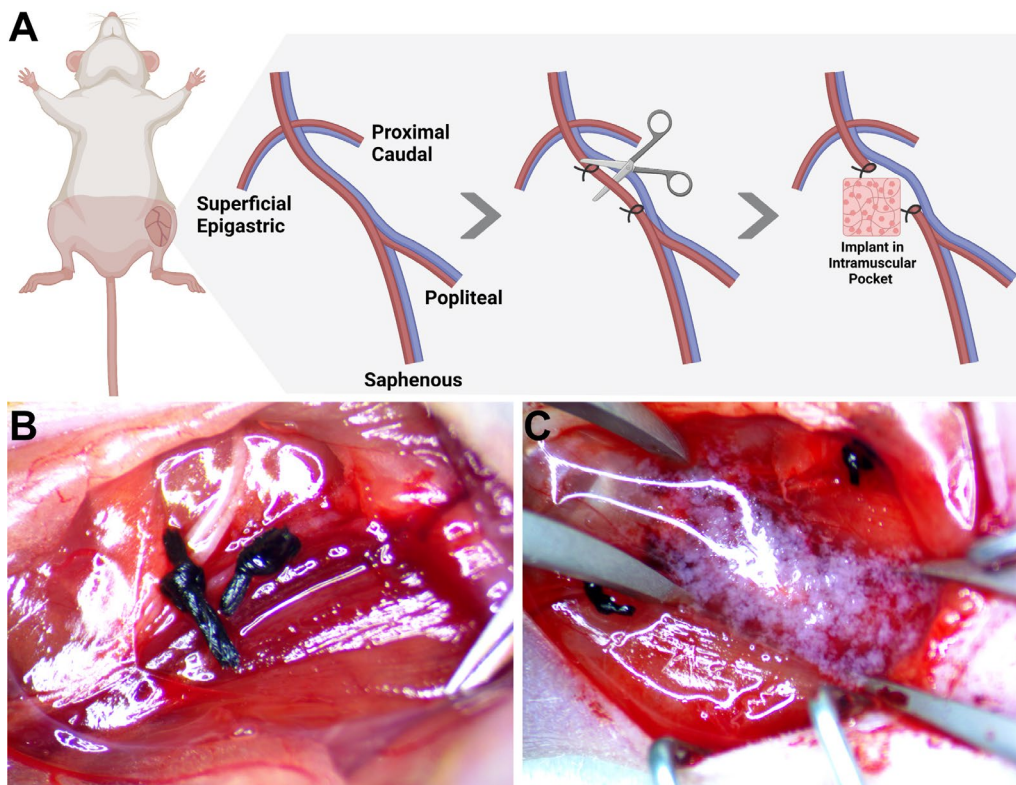
Figure 4.2: Cell-encapsulating fibrin microbeads were implanted in a murine model of hindlimb ischemia. *(A) Hindlimb ischemia was induced via the ligation and dissection of the femoral artery.*

Schematic created with BioRender.com. (B) Ligation site, below the superficial epigastric/proximal caudal branch and just above the popliteal/saphenous, prior to excision of artery. (C) Microbeads in an acellular fibrin precursor were implanted in an intramuscular muscular pocket adjacent to the ligation site. Immediately after surgery (day 0), relative LDPI signal confirmed a marked decrease in perfusion ($\leq 5\%$) of the ischemic compared to the contralateral (unligated control) foot pad across all experimental groups (Fig. 4.3A, B, D). Interestingly, animals receiving acellular gel implants had significantly greater perfusion compared to D3 PC microbeads at day 5 and cellular gels at days 7 and 10; however, perfusion in the acellular fibrin gel group plateaued around 40% compared to the control foot pad after day 10. Animals containing cellular bulk hydrogels consistently had the lowest relative LDPI signal throughout the entirety of the 14-day study, only reaching an average 31% perfusion. By day 14, animals containing D3 PC microbeads had significantly greater relatively LDPI signal than both acellular and cellular bulk hydrogels, reaching perfusion levels that were 65% of contralateral control limbs.

Descriptors of hindlimb ischemia severity were assigned to animals to characterize the ischemic hindlimb on days 1, 7, and 14 (Fig. 4.3C). Due to the severity of the induced ischemia, all experimental groups experienced autoamputation in some animals by the day after surgery. By day 7, 60% of animals that received saline experienced autoamputation, compared to 36% and 40% of animals in the cellular bulk fibrin and D3 PC microbeads groups, respectively. Animals containing cellular bulk fibrin and D3 PC microbeads showed similar degrees of foot necrosis, 29% and 30%, respectively. Due to a high rate of autoamputation in the sham (saline) controls, this experimental group was not continued beyond the day 7 timepoint for humane reasons. Unexpectedly, only 11% of animals that received acellular fibrin showed evidence of autoamputation and the remaining animals in this group had either mild ischemia in the form of limb discoloration or normal-appearing limbs. By day 14, all animals that received acellular fibrin had normal hindlimb appearance, despite having less than 50% perfusion. Conversely, the rate of autoamputation in animals that received cellular bulk fibrin increased to 60%, comparable to saline controls at day 7. Animals that received D3 PC microbeads exhibited autoamputation of only 25% autoamputation by day 14. While 50% of the remaining animals had limb necrosis, it had not progressed to autoamputation as in the cellular bulk gel group. Taken together, these data demonstrate cell-encapsulating pre-cultured microbeads restore macroscopic perfusion of the

ischemic hindlimb to the highest degree of the groups evaluated. The pre-cultured microbeads also

support increased limb salvage of necrotic tissue compared to cells delivered in bulk fibrin.
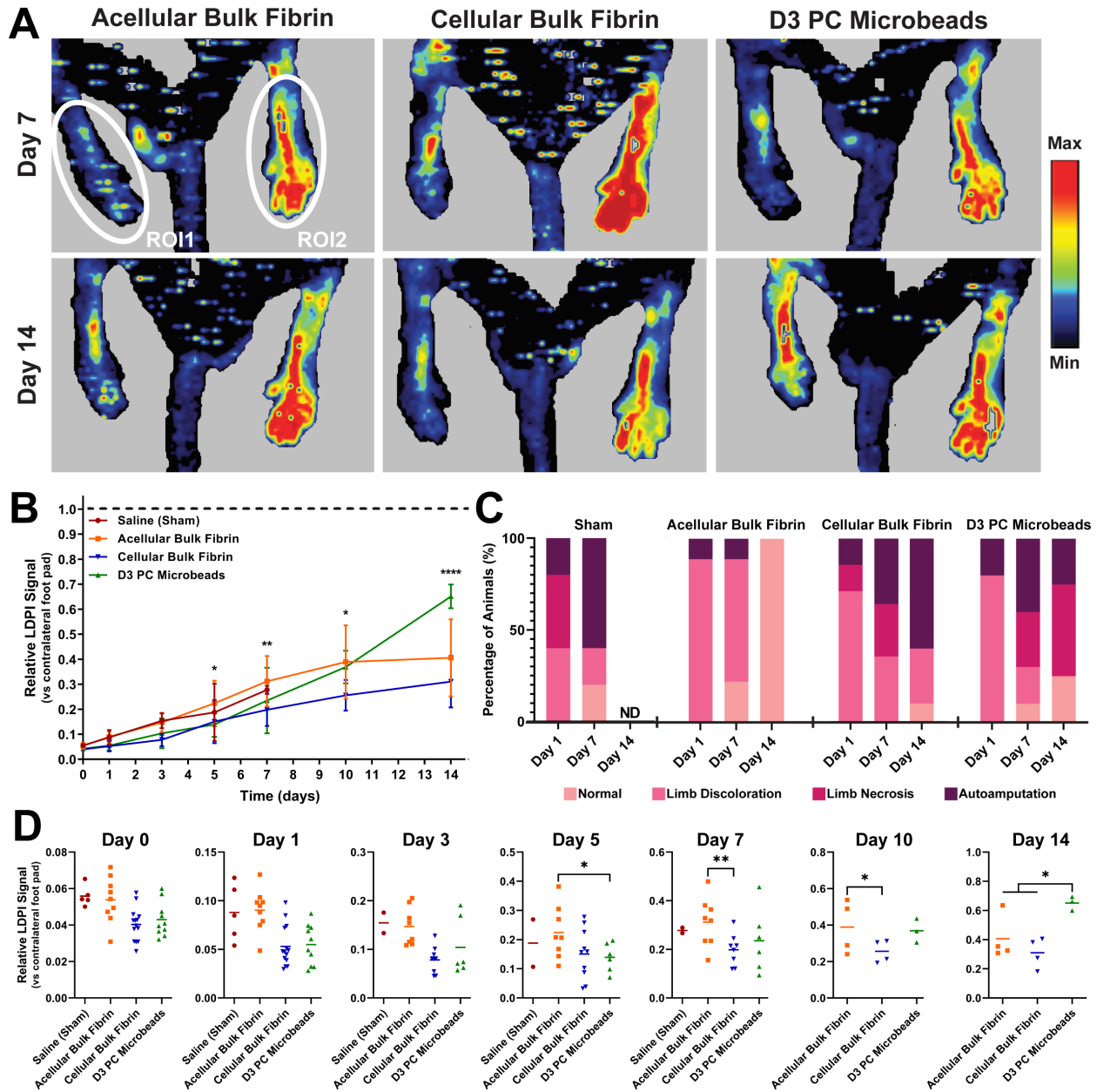
Figure 4.3: Pre-cultured microbeads improved macroscopic perfusion and rescued ischemic hindlimb.
(A) Representative LDPI illustrate reduced perfusion in ischemic (left) compared to contralateral (control, right) foot pad on days 7 and 14. Example region of interest (ROI) used to calculate mean LDPI signal indicated by white circles. (B) Relative LDPI signal of ischemic versus contralateral foot pad over 14 days. Day 5: * p < 0.05 acellular bulk fibrin compared to D3 PC microbeads; Day 7: ** p < 0.01 acellular compared to cellular bulk fibrin; Day 10: * p < 0.05 acellular compared to cellular bulk fibrin; Day 14: **** p < 0.0001 D3 PC microbeads compared to both acellular and cellular bulk fibrin; N ≥ 3. (C) Distribution of hindlimb ischemia severity on days 7 and 14; N ≥4 with the exception of sham N = 2 after

4.3.3 Analysis of microvasculature networks formed by endothelial cells delivered to the ischemia environment by pre-cultured microbeads

Implants were collected after 7 and 14 days for histological analysis. Hematoxylin and eosin (H&E) staining was used to identify implants and assess implant morphology (Fig. 4.4A, dashed lines). After implants were sectioned in their entirety and stained with H&E, the section with the maximum area (approximating the center of the implant) was identified and cross-sectional area was quantified by stitched images of the entire implant region for implants containing human cells. Acellular bulk fibrin implants were heavily remodeled and degraded by host cells as evidenced by the presence of densely packed nuclei (purple) and reduced implant area over time. In most cases, acellular fibrin implants were completely degraded, and therefore cross-sectional area was not quantified. Cellular bulk gels and D3 PC microbeads had comparable cross-sectional areas on both day 7 and 14 (Fig. 4.4B). Average implant area for both cellular conditions was reduced by 33% from day 7 to 14 as the implants were remodeled *in vivo*, though this result did not reach statistical significance.
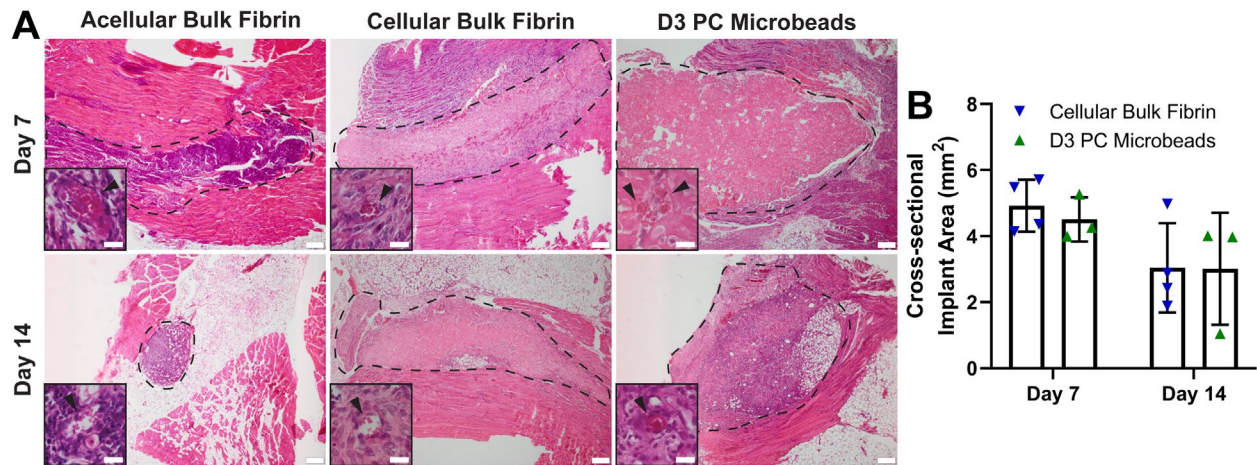
Figure 4.4: Cellular implants were more slowly remodeled by host cells compared to acellular fibrin controls. *(A) Hematoxylin (purple) and eosin (pink) staining of explanted tissue on days 7 and 14 (implant outlined in dashed lines, scale bar = 200 μm). Insets identify vessels perfused with host erythrocytes (black arrows, scale bar = 20 μm). (B) Quantification of implant area on days 7 and 14; N = 3-4.*

Cellular implants were stained for human CD31 (hCD31) and counterstained with hematoxylin to visualize implanted endothelial cells and host erythrocytes, respectively. Both cellular bulk fibrin and D3 PC microbead implants contained hCD31+ positive vessels on days 7 and 14 (Fig. 4.5A, dark brown stain). Blinded quantification of hCD31+ structures revealed that D3 PC microbeads and cellular bulk fibrin groups had comparable numbers of total vessels in the implant region after 7 days *in vivo* (Fig. 4.5B). Total hCD31+ structures were comparable between both groups at day 14 as well; however, the numbers of human cell-derived vessels were significantly decreased over time, a 67% and 52% decrease in D3 PC microbeads and cellular bulk fibrin, respectively, as the microvascular network was remodeled. Perfused hCD31+ vessels, defined as positively stained vessels with host erythrocytes present in the lumens, were also quantified. Similar to trends observed in total vessel number, D3 PC microbeads and cellular bulk fibrin supported similar degrees of microvasculature network perfusion on day 7, which also decreased by day 14 (Fig. 4.5C). D3 PC microbead implants had 43% and 28% of hCD31+ vessels

perfused on days 7 and 14, respectively, whereas 48% and 38% of hCD31+ vessels in cellular

fibrin were perfused on days 7 and 14, respectively.
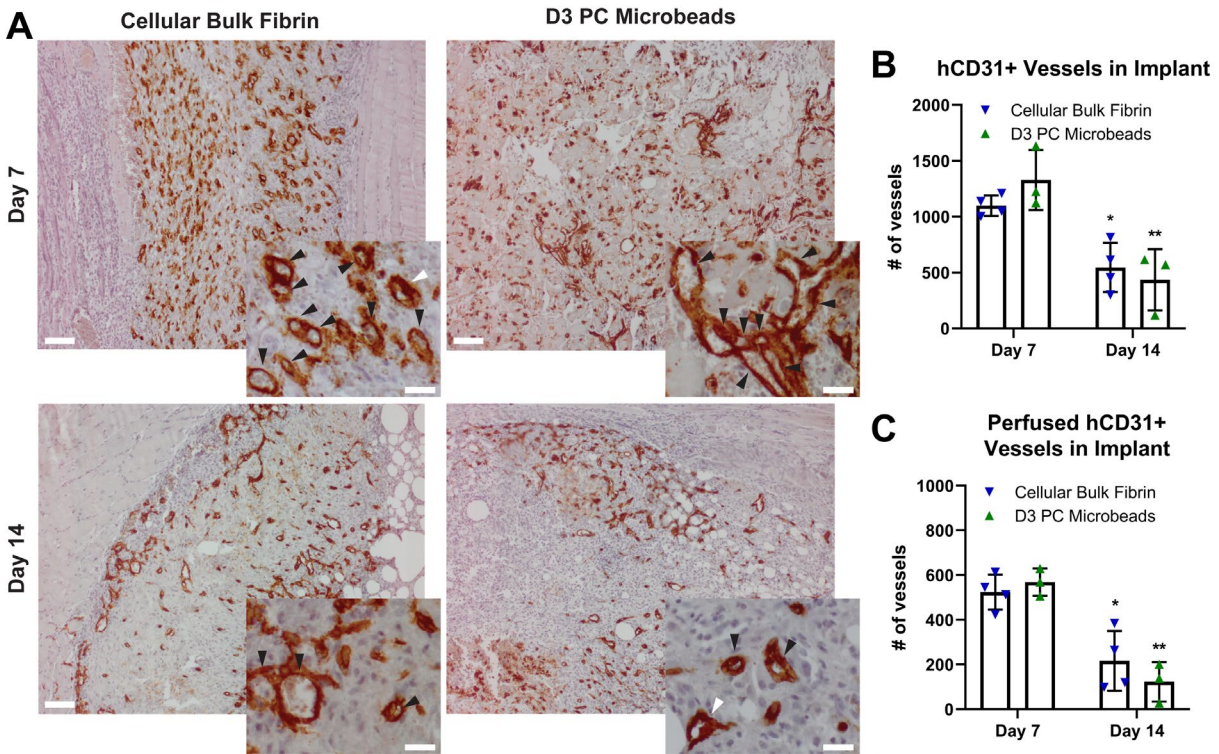
Figure 4.5: Implanted endothelial cells formed perfused hCD31+ microvascular networks. *(A) Cellular implants were IHC-stained for hCD31 (dark brown) on days 7 and 14 to identify human-derived vessels (scale bar = 100 μm). Insets identify hCD31+ vessels with lumens (white arrows), containing host erythrocytes (black arrows, scale bar = 50 μm). Quantification of (B) total and (C) perfused hCD31+ vessels on days 7 and 14. * p < 0.05 compared to day 7; ** p < 0.01 compared to day 7; N = 3-4.*

Cellular implants were also stained for alpha-smooth muscle actin (αSMA), a pericyte

marker, and counterstained with hematoxylin to identify mature, perfused microvascular structures

(Fig. 4.6). Qualitative analysis revealed that on day 7, both cellular conditions had sparse staining

of αSMA within the implant regions, with minimal evidence of αSMA+ microvasculature on the

periphery of implants. After 14 days, a greater fraction of αSMA+ microvascular structures were

identified within the implant regions, suggesting maturation of the human-derived vessels or

recruitment of mature host vessels into the implant area. This protein was still mainly localized to

the periphery of the implants, and a subset of the αSMA+ vessels contained host erythrocytes within their lumens.
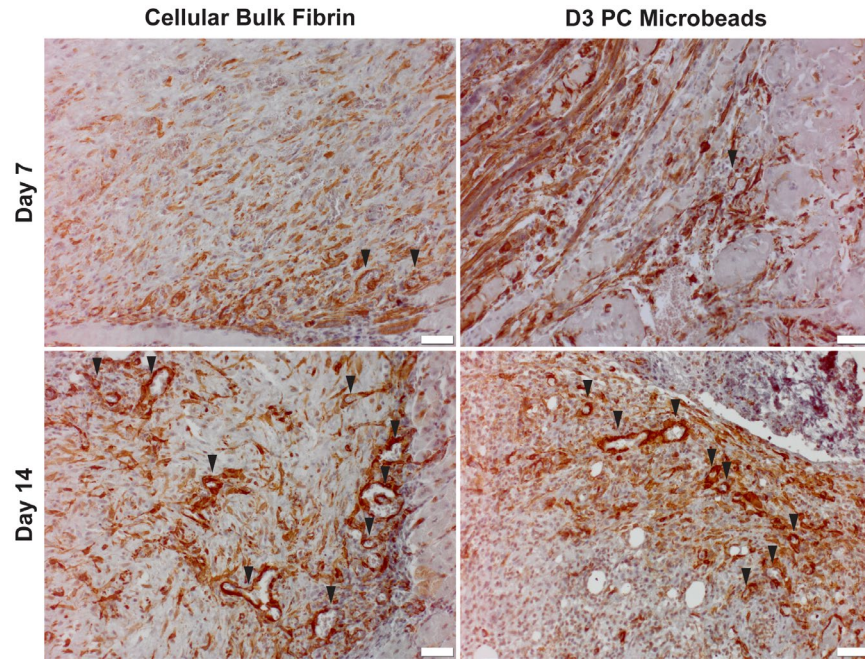
Figure 4.6: Cellular implants contained mature, α-SMA+ microvascular structures. *Cellular implants were IHC-stained for αSMA (dark brown) on days 7 and 14 to identify mature vessels (black arrows) within implants (scale bar = 50 μm).*

4.4 Discussion

Modular tissue constructs are a promising platform for a variety of tissue engineering applications, including as a potential therapy for revascularization of ischemic tissues. Building on prior work from our group, which demonstrated the vascularization potential of pre-cultured microbeads in a subcutaneous model *in vivo* [22], the goal of this study was to test the therapeutic benefit of these cell-laden microbeads in a more challenging and clinically-relevant model of ischemia. Fibrin microbeads, containing HUVEC and MSC, were first pre-cultured in suspension for 3 days to facilitate primitive vessel morphogenesis within the microbeads. HUVEC were used as the endothelial cell type due to their proven ability to create robust microvascular networks

reliably and reproducibly *in vitro* and *in vivo*, and for consistency with previous work [26, 27]. Consistent with our earlier findings, vessel structures and stromal cells emerged from pre-cultured microbeads to catalyze the formation of microvascular networks in a surrounding fibrin matrix *in vitro*. Though extended suspension culture resulted in a degree of microbead aggregation, D3 PC microbeads maintained relatively small diameters necessary to preserve injectability. When delivered into the ischemic hindlimbs of SCID mice following femoral artery ligation, D3 PC microbeads induced a 12-fold increase in perfusion from day 0 to 14. By comparison, control animals that received either acellular fibrin gels or constructs containing cells within bulk fibrin gels exhibited more modest increases in relative perfusion (6-fold and 4.4-fold, respectively) from the baseline post-surgical levels. Further, while other experimental groups plateaued in perfusion after 10 days, relative perfusion assessed by LDPI continued to increase in the D3 PC microbead condition throughout the 14-day duration of our experiments. Future work could include longer experimental timepoints to more fully evaluate the potential of pre-cultured microbeads to enhance downstream macroscopic perfusion.

Modular approaches to creating prevascularized tissues potentially offer a variety of advantages over approaches in which cells capable of forming microvasculature are encapsulated within macroscopic scaffolds or bulk hydrogels. One such advantage is their small size (50-350 μm diameter [21, 25]), which may improve diffusion of oxygen and nutrients and enable the benefits of injectability combined with the ability to be prevascularized. Scaffold-free cell spheroid approaches to vascularization offer these benefits as well and have been widely reported [28-35]. Modular-based approaches in which endothelial cells were coated on the outer surface of cell-laden hydrogel rods have also been shown to enhance engraftment and vascularization when delivered *in vivo* [36, 37]. However, encapsulating endothelial cells in a hydrogel matrix affords

the opportunity to provide tissue-specific instructive cues, structure, and protection provided by the extracellular matrix, which may be especially important when injected into harsh ischemic environments. Consistent with this idea, recent work has shown that endothelial colony forming cells encapsulated within PEG-fibrinogen materials via a droplet microfluidic biofabrication enhanced wound healing in a large animal model [38]. In work most similar to ours, co-encapsulation of outgrowth EC and MSC within alginate microgels has been used to create vascularized microtissue modules [39]. Following a 14-day period of maturation *in vitro*, these alginate-based vascularized microtissues supported improved cell engraftment and survival compared to those encapsulated for only 1 day before implantation [40]. In our study here, we extended these types of approaches using fibrin as the cell-encapsulating material, and also evaluated them in the ischemic hindlimb model that has been widely used to evaluate therapeutic angiogenesis strategies [41].

After 14 days, animals that received implants containing D3 PC microbeads had significantly greater perfusion compared to all other experimental groups tested, restoring perfusion from very low levels (< 5%) to levels that were 65% of the values measured in contralateral (unligated control) limbs. While other studies evaluating human cell-based therapies in the ischemic limbs of immunocompromised mice have reported similar results in overall perfusion levels over time, our surgical model reliably induced acute ischemia in C.B-17 SCID mice, with perfusion levels in the ischemic limb as low as just 4%-5% of the contralateral limb as assessed at the foot pads immediately post-surgery. By contrast, relative ischemia was reduced to a minimum of ~10% compared to the control limb post-surgery in other studies, with a more modest increase of 30%-50% perfusion from day 0 to the experimental endpoint observed [42-44]. Studies that reported up to 80% relative perfusion following therapy had very mild levels of

ischemia to start, with relative perfusion decreased only to 50% post-surgery [45]. While these are potentially insightful comparisons, variation in surgical procedure [46, 47] as well as the strain/background of mice used [48, 49] can influence both response to surgery and natural revascularization potential. We also investigated cellular implants in a small cohort of NOD SCID mice (Fig. 4.7) and found that while a comparable reduction in perfusion was observed immediately post-surgery, mice did not experience foot necrosis or autoamputation, further supporting previously published literature that the strain of mice influences response to ischemia [48, 49].

Due to the severity of induced ischemia, a subset of animals in all experimental groups exhibited some level of autoamputation by day 1. Surprisingly, there were fewer instances of tissue necrosis or autoamputation in the acellular fibrin gel conditions over the entire 14-day study, relative to other experimental groups. This observation could be attributed to significantly higher, though still relatively low, perfusion at earlier timepoints than in other conditions. Though only achieving up to 41% perfusion in the ischemic foot pad, animals receiving acellular fibrin exhibited the lowest levels of ischemic severity and necrosis and therefore the highest degree of limb salvage. This unexpected result could be attributed to several factors. First, fibrin alone is known to possess intrinsic regenerative properties, due in part to its growth-factor binding characteristics [50]. Second, the presence of fibrin may influence the innate immune system of the mice to mitigate necrosis. The C.B-17 strain of immunocompromised mice in this study lack both T and B cells, but they retain macrophages, neutrophils, and natural killer (NK) cells, all of which can play roles in revascularization [51]. NK cells have been shown to influence vascularization of ischemic tissues [52]. Neutrophils and macrophages can be recruited to the site of ischemia and assist in angiogenesis [53-55]. The presence of these cells could explain the magnitude of cellular invasion

and tissue remodeling observed in H&E-stained tissue sections of acellular implants, which was not observed in cellular conditions. While investigating the role these innate immune cells plays in revascularization is outside the scope of this study, it could be an insightful avenue to investigate in future work.

Animals receiving cellular bulk hydrogels exhibited the overall lowest degrees of reperfusion throughout the entirety of the study. This correlated with the greatest percentage of animals exhibiting autoamputation by day 14. Conversely, animals receiving D3 PC microbeads displayed lower rates of autoamputation and a greater percentage of limb necrosis, indicating that vascularization nucleated by microbeads may increase limb salvage over time by preventing tissue necrosis from advancing to autoamputation. This finding would correlate with the marked, yet delayed, increase in perfusion from day 10 to 14 and significantly greater perfusion observed in microbeads at day 14 compared to cellular bulk fibrin gels.

Implanted cells delivered in both cellular bulk fibrin gels and D3 PC microbeads formed human-derived (hCD31+) microvessels after 7 days *in vivo*, almost half of which were perfused with host erythrocytes. The total number of vessels significantly decreased from day 7 to 14 for both cellular conditions, likely a result of network remodeling and vascular pruning over time [56]. Despite the total number of hCD31+ vessels, both empty and perfused, being relatively comparable at days 7 and 14, the reduction in vessel number between experimental timepoints was greater in D3 PC microbeads. This could indicate that the microvascular network of pre-formed vessels in D3 PC microbead implants had begun being remodeled more quickly than those formed *in situ* in cellular fibrin implants. Human-derived vasculature was only observed in the implant region and did not appear to invade the surrounding muscle tissue. This may be due to microenvironmental differences, such as stiffness, between the implanted fibrin and surrounding muscle. Despite this,

the presence of host erythrocytes in the lumens of the engineered microvasculature is indicative of inosculation with the host blood supply and evidence of integration between the implanted cells and the host. Implants containing human cells were also stained for αSMA to characterize pericyte coverage and vessel maturation. While αSMA+ vascular structures were relatively sparse for both conditions on day 7, there was an observed presence of αSMA+ vessels, though mostly near the periphery of implants, at day 14. Additional experiments would be required to determine if this positive staining is a result of mature host vessel infiltration or implanted human MSC differentiation toward a pericyte-like phenotype.

Though we did not find histological evidence that pre-cultured microbeads jumpstarted inosculation with host blood supply at the explored experimental timepoints, it is feasible that this could have occurred at an earlier timepoint. Chen et al. noted multicellular lumens in prevascularized tissue implants as early as 3 days and perfusion was observed by day 5, suggesting inosculation between days 4 and 5 [12]. Mirabella et al. also observed perfusion of patterned endothelialized channels by day 5 [45]. While this study focused on long-term therapeutic effect of pre-cultured microbeads, future efforts should be made to include shorter timepoints for histological analysis which could shed light on if prevascularized microbeads accelerate inosculation earlier than 7 days post-implantation.

4.5 Conclusions

There is a critical need to develop effective methods for enhancing the efficacy of vascularization therapies for treating ischemic diseases. This study demonstrates the therapeutic potential of modular, pre-cultured, cellular microbeads in a clinically relevant model of ischemia. Pre-cultured microbeads applied to ischemic muscle following femoral artery ligation promoted

the restoration of downstream macroscopic perfusion to the ischemic foot pads, reducing the rate of autoamputation and improving limb salvage. Endothelial cells co-delivered with supportive mesenchymal stromal cells in these fibrin microbeads catalyzed the formation of a functional microvascular network, despite the harsh ischemic environment. Given the flexibility of these modular microtissues, our findings suggest that these cell-encapsulating microbeads can be customized for specific applications, manipulated *in vitro*, and delivered either alone or with additional parenchymal cells to revascularize and restore function in a wide range of regenerative applications.

4.6 Supplementary Data

A

B
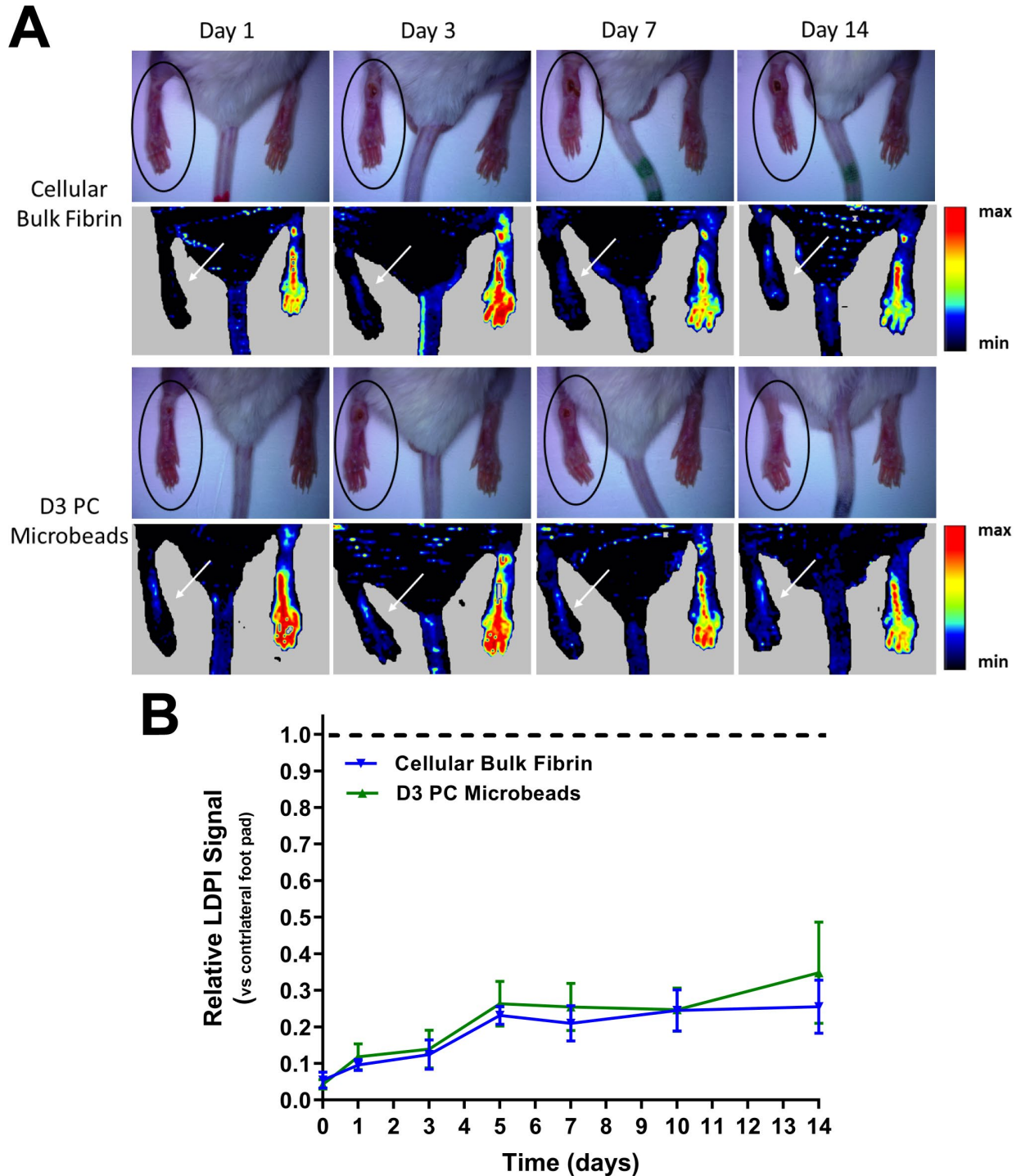
Figure 4.7: Cellular therapies for hindlimb ischemia in NOD SCID mice. *(A) Representative LDPI illustrate reduced perfusion in ischemic (left) compared to contralateral (control, right) foot pad on days 1, 3, 7 and 14. Ischemic foot pad identified by circles and arrows. (B) Relative LDPI signal of ischemic versus contralateral foot pad over 14 days; N = 6 cellular bulk fibrin, N = 4 D3 PC Microbeads.*

4.7 References

[1]   C. W. Tsao *et al.*, "Heart Disease and Stroke Statistics-2022 Update: A Report From the American Heart Association," *Circulation,* vol. 145, no. 8, pp. e153-e639, Feb 22 2022, doi: 10.1161/CIR.0000000000001052.

[2]   T. J. Cahill, R. P. Choudhury, and P. R. Riley, "Heart regeneration and repair after myocardial infarction: translational opportunities for novel therapeutics," *Nat Rev Drug Discov,* vol. 16, no. 10, pp. 699-717, Oct 2017, doi: 10.1038/nrd.2017.106.

[3]   S. Duff, M. S. Mafilios, P. Bhounsule, and J. T. Hasegawa, "The burden of critical limb ischemia: a review of recent literature," *Vasc Health Risk Manag,* vol. 15, pp. 187-208, 2019, doi: 10.2147/VHRM.S209241.

[4]   S. R. Levin, N. Arinze, and J. J. Siracuse, "Lower extremity critical limb ischemia: A review of clinical features and management," *Trends Cardiovasc Med,* vol. 30, no. 3, pp. 125-130, Apr 2020, doi: 10.1016/j.tcm.2019.04.002.

[5]   L. Beltran-Camacho, M. Rojas-Torres, and M. C. Duran-Ruiz, "Current Status of Angiogenic Cell Therapy and Related Strategies Applied in Critical Limb Ischemia," *Int J Mol Sci,* vol. 22, no. 5, Feb 26 2021, doi: 10.3390/ijms22052335.

[6]   L. Uccioli, M. Meloni, V. Izzo, L. Giurato, S. Merolla, and R. Gandini, "Critical limb ischemia: current challenges and future prospects," *Vasc Health Risk Manag,* vol. 14, pp. 63-74, 2018, doi: 10.2147/VHRM.S125065.

[7]   M. Qadura, D. C. Terenzi, S. Verma, M. Al-Omran, and D. A. Hess, "Concise Review: Cell Therapy for Critical Limb Ischemia: An Integrated Review of Preclinical and Clinical Studies," *Stem Cells,* vol. 36, no. 2, pp. 161-171, Feb 2018, doi: 10.1002/stem.2751.

[8]   X. Li, K. Tamama, X. Xie, and J. Guan, "Improving Cell Engraftment in Cardiac Stem Cell Therapy," *Stem Cells Int,* vol. 2016, p. 7168797, 2016, doi: 10.1155/2016/7168797.

[9]   F. A. Auger, L. Gibot, and D. Lacroix, "The pivotal role of vascularization in tissue engineering," *Annu Rev Biomed Eng,* vol. 15, pp. 177-200, 2013, doi: 10.1146/annurev-bioeng-071812-152428.

[10]   S. Golpanian, A. Wolf, K. E. Hatzistergos, and J. M. Hare, "Rebuilding the Damaged Heart: Mesenchymal Stem Cells, Cell-Based Therapy, and Engineered Heart Tissue," *Physiol Rev,* vol. 96, no. 3, pp. 1127-68, Jul 2016, doi: 10.1152/physrev.00019.2015.

[11]   C. K. Griffith *et al.*, "Diffusion limits of an in vitro thick prevascularized tissue," *Tissue Eng,* vol. 11, no. 1-2, pp. 257-66, Jan-Feb 2005, doi: 10.1089/ten.2005.11.257.

[12]   X. Chen *et al.*, "Prevascularization of a fibrin-based tissue construct accelerates the formation of functional anastomosis with host vasculature," *Tissue Eng Part A,* vol. 15, no. 6, pp. 1363-71, Jun 2009, doi: 10.1089/ten.tea.2008.0314.

[13]   M. W. Laschke and M. D. Menger, "Prevascularization in tissue engineering: Current concepts and future directions," *Biotechnol Adv,* vol. 34, no. 2, pp. 112-21, Mar-Apr 2016, doi: 10.1016/j.biotechadv.2015.12.004.

[14]   D. Sharma, D. Ross, G. Wang, W. Jia, S. J. Kirkpatrick, and F. Zhao, "Upgrading prevascularization in tissue engineering: A review of strategies for promoting highly organized microvascular network formation," *Acta Biomater,* vol. 95, pp. 112-130, Sep 1 2019, doi: 10.1016/j.actbio.2019.03.016.

[15]   S. Ben-Shaul, S. Landau, U. Merdler, and S. Levenberg, "Mature vessel networks in engineered tissue promote graft-host anastomosis and prevent graft thrombosis," *Proc Natl Acad Sci U S A,* vol. 116, no. 8, pp. 2955-2960, Feb 19 2019, doi: 10.1073/pnas.1814238116.

[16]   K. T. Kang, P. Allen, and J. Bischoff, "Bioengineered human vascular networks transplanted into secondary mice reconnect with the host vasculature and re-establish perfusion," *Blood,* vol. 118, no. 25, pp. 6718-21, Dec 15 2011, doi: 10.1182/blood-2011-08-375188.

[17]   L. Zhang, Z. Qian, M. Tahtinen, S. Qi, and F. Zhao, "Prevascularization of natural nanofibrous extracellular matrix for engineering completely biological three-dimensional prevascularized tissues for diverse applications," *J Tissue Eng Regen Med,* vol. 12, no. 3, pp. e1325-e1336, Mar 2018, doi: 10.1002/term.2512.

[18]   S. Y. Song *et al.*, "Prevascularized, multiple-layered cell sheets of direct cardiac reprogrammed cells for cardiac repair," *Biomater Sci,* vol. 8, no. 16, pp. 4508-4520, Aug 21 2020, doi: 10.1039/d0bm00701c.

[19]   L. Perry, U. Merdler, M. Elishaev, and S. Levenberg, "Enhanced Host Neovascularization of Prevascularized Engineered Muscle Following Transplantation into Immunocompetent versus Immunocompromised Mice," *Cells,* vol. 8, no. 12, Nov 20 2019, doi: 10.3390/cells8121472.

[20]   A. A. Szklanny *et al.*, "3D Bioprinting of Engineered Tissue Flaps with Hierarchical Vessel Networks (VesselNet) for Direct Host-To-Implant Perfusion," *Adv Mater,* vol. 33, no. 42, p. e2102661, Oct 2021, doi: 10.1002/adma.202102661.

[21]   A. Y. Rioja, R. Tiruvannamalai Annamalai, S. Paris, A. J. Putnam, and J. P. Stegemann, "Endothelial sprouting and network formation in collagen- and fibrin-based modular microbeads," *Acta Biomater,* vol. 29, pp. 33-41, Jan 2016, doi: 10.1016/j.actbio.2015.10.022.

[22]   N. E. Friend *et al.*, "Injectable pre-cultured tissue modules catalyze the formation of extensive functional microvasculature in vivo," *Sci Rep,* vol. 10, no. 1, p. 15562, Sep 23 2020, doi: 10.1038/s41598-020-72576-5.

[23]   J. Schindelin *et al.*, "Fiji: an open-source platform for biological-image analysis," *Nat Methods,* vol. 9, no. 7, pp. 676-82, Jun 28 2012, doi: 10.1038/nmeth.2019.

[24]   B. Carrion, I. A. Janson, Y. P. Kong, and A. J. Putnam, "A safe and efficient method to retrieve mesenchymal stem cells from three-dimensional fibrin gels," *Tissue Eng Part C Methods,* vol. 20, no. 3, pp. 252-63, Mar 2014, doi: 10.1089/ten.TEC.2013.0051.

[25]   N. G. Schott, H. Vu, and J. P. Stegemann, "Multimodular vascularized bone construct comprised of vasculogenic and osteogenic microtissues," *Biotechnol Bioeng,* vol. 119, no. 11, pp. 3284-3296, Nov 2022, doi: 10.1002/bit.28201.

[26]   J. R. Bezenah, A. Y. Rioja, B. Juliar, N. Friend, and A. J. Putnam, "Assessing the ability of human endothelial cells derived from induced-pluripotent stem cells to form functional microvasculature in vivo," *Biotechnol Bioeng,* vol. 116, no. 2, pp. 415-426, Feb 2019, doi: 10.1002/bit.26860.

[27]   J. R. Bezenah, Y. P. Kong, and A. J. Putnam, "Evaluating the potential of endothelial cells derived from human induced pluripotent stem cells to form microvascular networks in 3D cultures," *Sci Rep,* vol. 8, no. 1, p. 2671, Feb 8 2018, doi: 10.1038/s41598-018-20966-1.

[28]   S. H. Bhang *et al.*, "Three-dimensional cell grafting enhances the angiogenic efficacy of human umbilical vein endothelial cells," *Tissue Eng Part A,* vol. 18, no. 3-4, pp. 310-9, Feb 2012, doi: 10.1089/ten.TEA.2011.0193.

[29]   B. M. Roux *et al.*, "Preformed Vascular Networks Survive and Enhance Vascularization in Critical Sized Cranial Defects," *Tissue Eng Part A,* vol. 24, no. 21-22, pp. 1603-1615, Nov 2018, doi: 10.1089/ten.TEA.2017.0493.

[30]   A. A. Gorkun *et al.*, "Angiogenic potential of spheroids from umbilical cord and adipose-derived multipotent mesenchymal stromal cells within fibrin gel," *Biomed Mater,* vol. 13, no. 4, p. 044108, May 22 2018, doi: 10.1088/1748-605X/aac22d.

[31]   A. Alajati *et al.*, "Spheroid-based engineering of a human vasculature in mice," *Nat Methods,* vol. 5, no. 5, pp. 439-45, May 2008, doi: 10.1038/nmeth.1198.

[32]   A. M. Laib, A. Bartol, A. Alajati, T. Korff, H. Weber, and H. G. Augustin, "Spheroid-based human endothelial cell microvessel formation in vivo," *Nat Protoc,* vol. 4, no. 8, pp. 1202-15, 2009, doi: 10.1038/nprot.2009.96.

[33]   T. Korff, S. Kimmina, G. Martiny-Baron, and H. G. Augustin, "Blood vessel maturation in a 3-dimensional spheroidal coculture model: direct contact with smooth muscle cells regulates endothelial cell quiescence and abrogates VEGF responsiveness," *FASEB J,* vol. 15, no. 2, pp. 447-57, Feb 2001, doi: 10.1096/fj.00-0139com.

[34]   L. De Moor *et al.*, "High-throughput fabrication of vascularized spheroids for bioprinting," *Biofabrication,* vol. 10, no. 3, p. 035009, Jun 12 2018, doi: 10.1088/1758-5090/aac7e6.

[35]   J. M. Kelm *et al.*, "Design of custom-shaped vascularized tissues using microtissue spheroids as minimal building units," *Tissue Eng,* vol. 12, no. 8, pp. 2151-60, Aug 2006, doi: 10.1089/ten.2006.12.2151.

[36]   M. J. Butler and M. V. Sefton, "Cotransplantation of adipose-derived mesenchymal stromal cells and endothelial cells in a modular construct drives vascularization in SCID/bg mice," *Tissue Eng Part A,* vol. 18, no. 15-16, pp. 1628-41, Aug 2012, doi: 10.1089/ten.TEA.2011.0467.

[37]   A. P. McGuigan and M. V. Sefton, "Vascularized organoid engineered by modular assembly enables blood perfusion," *Proc Natl Acad Sci U S A,* vol. 103, no. 31, pp. 11461-6, Aug 1 2006, doi: 10.1073/pnas.0602740103.

[38]   R. L. Winter *et al.*, "Cell engraftment, vascularization, and inflammation after treatment of equine distal limb wounds with endothelial colony forming cells encapsulated within hydrogel microspheres," *BMC Vet Res,* vol. 16, no. 1, p. 43, Feb 4 2020, doi: 10.1186/s12917-020-2269-y.

[39]   A. L. Torres, S. J. Bidarra, M. T. Pinto, P. C. Aguiar, E. A. Silva, and C. C. Barrias, "Guiding morphogenesis in cell-instructive microgels for therapeutic angiogenesis," *Biomaterials,* vol. 154, pp. 34-47, Feb 2018, doi: 10.1016/j.biomaterials.2017.10.051.

[40]   A. L. Torres *et al.*, "Microvascular engineering: Dynamic changes in microgel-entrapped vascular cells correlates with higher vasculogenic/angiogenic potential," *Biomaterials,* vol. 228, p. 119554, Jan 2020, doi: 10.1016/j.biomaterials.2019.119554.

[41]   J. P. Cooke and D. W. Losordo, "Modulating the vascular response to limb ischemia: angiogenic and cell therapies," *Circ Res,* vol. 116, no. 9, pp. 1561-78, Apr 24 2015, doi: 10.1161/CIRCRESAHA.115.303565.

[42]   K. T. Kang, R. Z. Lin, D. Kuppermann, J. M. Melero-Martin, and J. Bischoff, "Endothelial colony forming cells and mesenchymal progenitor cells form blood vessels and increase blood flow in ischemic muscle," *Sci Rep,* vol. 7, no. 1, p. 770, Apr 10 2017, doi: 10.1038/s41598-017-00809-1.

[43]   Z. E. Clayton *et al.*, "A comparison of the pro-angiogenic potential of human induced pluripotent stem cell derived endothelial cells and induced endothelial cells in a murine model of peripheral arterial disease," *Int J Cardiol,* vol. 234, pp. 81-89, May 1 2017, doi: 10.1016/j.ijcard.2017.01.125.

[44]   X. Gao *et al.*, "Human-Induced Pluripotent Stem-Cell-Derived Smooth Muscle Cells Increase Angiogenesis to Treat Hindlimb Ischemia," *Cells,* vol. 10, no. 4, Apr 2 2021, doi: 10.3390/cells10040792.

[45]   T. Mirabella *et al.*, "3D-printed vascular networks direct therapeutic angiogenesis in ischaemia," *Nat Biomed Eng,* vol. 1, 2017, doi: 10.1038/s41551-017-0083.

[46]   A. A. Hellingman *et al.*, "Variations in surgical procedures for hind limb ischaemia mouse models result in differences in collateral formation," *Eur J Vasc Endovasc Surg,* vol. 40, no. 6, pp. 796-803, Dec 2010, doi: 10.1016/j.ejvs.2010.07.009.

[47] Z. Aref, M. R. de Vries, and P. H. A. Quax, "Variations in Surgical Procedures for Inducing Hind Limb Ischemia in Mice and the Impact of These Variations on Neovascularization Assessment," *Int J Mol Sci,* vol. 20, no. 15, Jul 29 2019, doi: 10.3390/ijms20153704.

[48] P. K. Shireman and M. P. Quinones, "Differential necrosis despite similar perfusion in mouse strains after ischemia," *J Surg Res,* vol. 129, no. 2, pp. 242-50, Dec 2005, doi: 10.1016/j.jss.2005.06.013.

[49] D. Thomas *et al.*, "Variability in Endogenous Perfusion Recovery of Immunocompromised Mouse Models of Limb Ischemia," *Tissue Eng Part C Methods,* vol. 22, no. 4, pp. 370-81, Apr 2016, doi: 10.1089/ten.TEC.2015.0441.

[50] M. W. Mosesson, "Fibrinogen and fibrin structure and functions," *J Thromb Haemost,* vol. 3, no. 8, pp. 1894-904, Aug 2005, doi: 10.1111/j.1538-7836.2005.01365.x.

[51] J. Chen *et al.*, "The development and improvement of immunodeficient mice and humanized immune system mouse models," *Front Immunol,* vol. 13, p. 1007579, 2022, doi: 10.3389/fimmu.2022.1007579.

[52] V. van Weel *et al.*, "Natural killer cells and CD4+ T-cells modulate collateral artery development," *Arterioscler Thromb Vasc Biol,* vol. 27, no. 11, pp. 2310-8, Nov 2007, doi: 10.1161/ATVBAHA.107.151407.

[53] J. Zarubova, M. M. Hasani-Sadrabadi, R. Ardehali, and S. Li, "Immunoengineering strategies to enhance vascularization and tissue regeneration," *Adv Drug Deliv Rev,* vol. 184, p. 114233, May 2022, doi: 10.1016/j.addr.2022.114233.

[54] R. Z. Lin *et al.*, "Host non-inflammatory neutrophils mediate the engraftment of bioengineered vascular networks," *Nat Biomed Eng,* vol. 1, 2017, doi: 10.1038/s41551-017-0081.

[55] J. M. Melero-Martin, M. E. De Obaldia, P. Allen, A. C. Dudley, M. Klagsbrun, and J. Bischoff, "Host myeloid cells are necessary for creating bioengineered human vascular networks in vivo," *Tissue Eng Part A,* vol. 16, no. 8, pp. 2457-66, Aug 2010, doi: 10.1089/ten.TEA.2010.0024.

[56] M. S. Wietecha, W. L. Cerny, and L. A. DiPietro, "Mechanisms of vessel regression: toward an understanding of the resolution of angiogenesis," *Curr Top Microbiol Immunol,* vol. 367, pp. 3-32, 2013, doi: 10.1007/82_2012_287.

Chapter 5 – A Combination of Matrix Stiffness and Degradability Dictate Microvascular Network Assembly and Remodeling in Cell-laden Poly(ethylene glycol) Hydrogels

5.1 Introduction

Vascularizing large constructs remains a challenging hurdle in tissue engineering [1]. Without a functional vascular network, tissue constructs are limited to sizes sustained by passive nutrient diffusion and/or require rapid vascularization upon transplantation *in vivo*. The presence of functional microvascular networks within engineered tissues is important to facilitate transport of oxygen and nutrients, thereby mitigating cell death for constructs larger than 200 μm in thickness, the estimated diffusion limitation in many tissues [2]. Strategies to prevascularize tissues, involving the *in vitro* formation of microvascular networks that can inosculate with the host's blood vessels upon implantation, seek to overcome this limitation [3-5]. However, the success of prevascularization approaches may depend in part on the maturation state of the vessel network being implanted [6, 7]. A better understanding of how the physicochemical properties of the microenvironment influence the formation and maturation of microvascular networks would inform strategies to vascularize engineered tissues.

Synthetic materials, especially poly(ethylene glycol) (PEG) hydrogels, have shown promise for tissue regeneration applications and as platforms to better understand how the physicochemical properties of the microenvironment influence cells in 3D, in part because of their tunability [8, 9]. Previous studies involving vessel morphogenesis in PEG hydrogels have examined the effects of altering PEG macromer type, polymer wt. %, adhesive and crosslinking peptide identity and concentrations, and crosslinking ratios [10-13], though relatively little has been done to evaluate changes in network maturation and matrix remodeling over time. Having previously demonstrated the ability of RGD-functionalized, matrix metalloproteinase- (MMP-) susceptible PEG-vinyl sulfone (PEGVS) hydrogels to support the assembly of microvascular networks [14-16], here we have focused on photocrosslinkable PEG-norbornene (PEGNB) because it facilitates more rapid, homogeneous polymerization under physiological conditions conducive to cell encapsulation [17-19]. Further, previous studies have demonstrated vascularization in 8-arm PEGNB [12, 20-23].

Two known properties that influence vascularization are the stiffness and degradability of the surrounding microenvironment. Some studies suggest softer, less crosslinked hydrogels support more robust vascularization [14, 16, 24], whereas others suggest stiffer materials do [25]. Such discrepancies may be due to differences in the nano- and microscale architecture of different hydrogel biomaterials. While a large number of studies focused on the potential correlation between initial material properties and cellular phenotypes, consideration of the temporal evolution of mechanical properties is also important; we have previously shown that cells can stiffen the matrix to varying degrees dependent on initial material stiffness during neovascularization [16]. Moreover, hydrogel degradability can influence the degree to which cells spread, proliferate, and remodel their environment [10, 26], and prior studies have shown that

105

increased degradability enhances vascularization [27]. The identity of degradable crosslinking peptides (i.e., the protease susceptibility) has also been shown to impact the degree of vascularization [15, 27].

Here, we examined the impact of matrix stiffness and degradability on vessel network formation in degradable 4-arm PEGNB hydrogels. We interrogated vasculogenesis using a co-culture of human umbilical vein endothelial cells (HUVEC) and normal human lung fibroblasts (NHLF), previously used by our group and others [3, 28]. PEGNB hydrogels were crosslinked with MMP-1 and MMP-2 sensitive peptides containing either a single VPMS (sVPMS) or double VPMS (dVPMS) degradable sequence [10], and the extent of crosslinking (and consequently the initial stiffness) was altered by varying the ratio of norbornenes to thiols on the crosslinking peptides. Utilizing these hydrogels, we analyzed vessel network formation and cell-mediated matrix remodeling over time. We found more degradable hydrogels supported increased rates of vessel network formation and cell-mediated stiffening of the hydrogels. After 14 days of culture, vessel network formation equalized across both stiffness and degradability, with evidence of remodeling and maturation through the deposition of basement membrane proteins. The inclusion of stromal cells was essential for both vascular network formation and cell-mediated stiffening of the gels. These findings may facilitate the use of these materials to control the formation of prevascularized tissues *in vitro* or direct the *in situ* formation of microvascular networks upon delivery *in vivo*.

5.2 Materials and Methods

5.2.1 Cell culture

Human umbilical vein endothelial cells (HUVEC) were isolated from umbilical cords from the University of Michigan Mott Children's Hospital as previously described [29]. Umbilical cords were obtained by a process considered exempt by the University of Michigan's Institutional Review Board (notice of determination dated August 21, 2014) because the tissue is normally discarded, and no identifying information is provided to the researchers who receive the cords. HUVEC were cultured in fully supplemented EGM2 (Lonza, Inc., Walkersville, MD). HUVECs were used from passages 4-7. Normal human lung fibroblasts (NHLF; Lonza) were cultured in Dulbecco's modified eagle medium (DMEM; Gibco, Waltham, MA) supplemented with 10% fetal bovine serum (FBS; Gibco) NHLF were used from passage 10-15. All cells were cultured at 37 °C and 5% CO_2 with media replacement every two days.

5.2.2 PEGNB hydrogel formation

Cell-adhesive, degradable poly(ethylene glycol)-norbornene (PEGNB) hydrogels were formed via thiol-ene photopolymerization [17]. 4-arm PEGNB (20 kDa; Creative PEGWorks, Durham, NC) and lithium phenyl-2,4,6-trimethylbenzoylphosphinate ("LAP"; Sigma-Aldrich, St. Louis, MO) were purchased from commercial sources that provide the percent substitution of norbornene by NMR and purity by HPLC, respectively. The thiol containing adhesive peptide Ac-CGRGDS-NH₂ ("RGD"; AAPPTEC, Louisville, KY) and dithiol containing matrix metalloproteinase- (MMP-) sensitive crosslinking peptides Ac-GCRDVPMS↓MRGGDRCG-NH₂ ("sVPMS", cleavage site indicated by ↓; AAPPTEC) and Ac-GCRDVPMS↓MRGGGVPMS↓MRGGDRCG-NH₂ ("dVPMS", cleavage sites indicated by ↓;

AAPPTEC), which contain an N-terminal acetylation and a C-terminal amidation, were dissolved in 25 mM acetic acid, filtered through 0.22 μm filters (Sigma-Aldrich), lyophilized for 48 h, and stored in a desiccator at -20 °C. The thiol content (purity) of each batch of peptide aliquots was determined using Ellman's reagent (Thermo Fisher, Waltham, MA). PEGNB and LAP were suspended in phosphate-buffered saline (PBS, 7.4 pH, 1X; Gibco) and sterile filtered through 0.22 μm filters to create fresh stocks at desired concentrations for each experiment. Peptides were also resuspended in PBS to reach desired concentrations.

Using a one-pot synthesis, 3 wt. % PEGNB (w/v), 1 mM LAP, 1 mM RGD, crosslinking peptides at various concentrations, and PBS were combined to make hydrogel precursor solutions. Crosslinking ratio was controlled through the addition of 2.25 mM, 2.00 mM, 1.75 mM, or 1.50 mM of crosslinking peptide to nominally (theoretically) achieve 90%, 80%, 70%, or 60% (0.9, 0.8, 0.7, or 0.6 thiols per norbornene) crosslinking of available norbornene arms, after accounting for RGD concentration, respectively. The solution was gently vortexed, and then 50 μL was pipetted into a 1 mL syringe (Fisher, Waltham, MA) with the needle end cut off to cast each individual gel. Syringes with hydrogels were placed 1 inch under a 6-Watt LED 365 nm Gooseneck Illuminator (AmScope, Feasterville, PA) and irritated with UV light set to max intensity for 90 s, corresponding to approximately 50 mW/cm^2. Polymerized hydrogels were ejected into 2 mL of EGM2 in 24-well plates, which was changed after day 1 then replaced every 2 days. Acellular hydrogels were cultured in medium under conditions similar to cellular hydrogels to determine the influence of exogenous medium on hydrogel degradation.

5.2.3 Mechanical characterization of PEGNB hydrogels

Hydrogel shear storage moduli (G') were measured for all conditions on day 1 (to allow for overnight swelling) to confirm hydrogels had consistent initial mechanical properties.

Depending on the experiment, measurements were also taken on day 3, 5, 7, and 14. Hydrogels were centered between the Peltier plate and an 8-mm measurement head of an AR-G2 rheometer (TA Instruments, New Castle, DE). The Peltier plate and measurement head were covered with P800 sandpaper to reduce slippage. Shear storage modulus was averaged over a 1-min time sweep measured at 37 °C, 5% strain amplitude, 1 rad/s frequency and either 0.05 N normal force or a minimum gap height of 1000 μm, if hydrogels were too soft to reach the target normal force. For degradation experiments, hydrogels were swollen overnight in EGM2. The medium was replaced with 0.5 U/mL collagenase Type I from *Clostridium histolyticum* (Gibco) in PBS supplemented with 0.4 mM $CaCl_2$ and 0.1 mM $MgCl_2$. During collagenase digestion, well plates were incubated on a rocker plate at 37 °C. Shear storage moduli were measured at 0, 1, 2, 4, and 24 h.

5.2.4 Vasculogenesis assays

HUVEC and NHLF were co-encapsulated in hydrogels to imitate a 3D model of vasculogenesis, as previously described [15, 16]. Briefly, hydrogels were formulated as described above and the precursor solution was used to resuspend a cell pellet to achieve a final cell density of 4×10^6 total cells/mL in a 1:1 ratio (2×10^6 HUVEC/mL and 2×10^6 NHLF/mL). For monoculture experiments, either 2×10^6 HUVEC/mL or NHLF/mL were used. After UV exposure, hydrogels were ejected into 24-well plates containing 2 mL of EGM2, which was changed after day 1 and then every other day.

5.2.5 Fluorescent imaging and quantification methods

On days 3, 5, 7, or 14, hydrogels were fixed with zinc formalin (Z-Fix; Anatech, Battle Creek, MI) for 10 min, then washed three times with PBS for five min. Prior to staining, hydrogels were cut in half along the diameter of the gel by first pressing through the center of the gel with a

razor blade then running a scalpel along the blade to make a clean cut, yielding two semicircle halves. Hydrogels were stained overnight with rhodamine-conjugated lectin from *Ulex europaeus* agglutinin I (UEA, 1:200; Vector Labs, Newark, CA), 4', 6-diamidino-2-phenylindol (DAPI, 1 µg/mL; Thermo Fisher), and AlexaFluor 488 phalloidin (1:200; Thermo Fisher) which label endothelial cells, cell nuclei, and F-actin, respectively. Samples were rinsed overnight with PBS prior to imaging. Hydrogels were imaged on the flat cut side near the center of the gel to ensure images were representative of the cellular behavior within the bulk of the hydrogels. Images were acquired using an Olympus IX81 microscope equipped with a disk scanning unit (DSU; Olympus America, Center Valley, PA) and Metamorph Premier software (Molecular Devices, Sunnyvale, CA). For all analyses, confocal z-stacks were acquired using the DSU. Z-series stacks were then collapsed into maximum intensity projections using Fiji [30] before analyses. Quantification of vessel densities were performed on 300 µm stacks (30 µm/slice, 11 slices/stack) imaged at 4X magnification. Total vessel length was quantified using the Angiogenesis Tube Formation module in Metamorph and reported as vessel density length per volume of the region of interest (2.16 x 1.65 x 0.3 mm).

5.2.6 Immunofluorescent staining and imaging

For immunofluorescent staining of basement membrane proteins, gels were fixed with Z-Fix at day 7 or 14 as described above. A stock solution of 10X Tris buffered saline (TBS) was prepared with 44 g NaCl (Thermo Fisher), 15.75 g Tris (Bio-Rad, Hercules, CA), and 500 mL ddH$_2$O and adjusted to pH 7.4. Samples were permeabilized with 0.5% v/v Triton X-100 (Thermo Fisher) in 1X TBS for one hour, rinsed four times for 5 min with 0.1% v/v Tween-20 (Thermo Fisher) in 1X TBS (TBS-T), and blocked overnight at 4 °C in antibody diluting (AbDil) solution consisting of 2% w/v bovine serum albumin (BSA; Sigma-Aldrich) in TBS-T. Gels were incubated

with primary antibodies for collagen IV (1:500, mouse IgG$_1$; Thermo Fisher) or laminin beta-1 (1:500, rabbit IgG; Thermo Fisher) diluted in AbDil solution overnight at 4 °C. Gels were washed three times for 5 min and rinsed overnight at 4 °C with TBS-T. Gels were stained with appropriate secondary antibodies, AlexaFluor 488 goat anti-mouse (1:200, IgG$_{H+L}$; Thermo Fisher) or AlexaFluor 488 goat anti-rabbit (1:200, IgG$_{H+L}$; Thermo Fisher), diluted in TBS-T and UEA and DAPI, as described above, overnight at 4 °C. Gels were rinsed overnight at 4 °C with TBS-T prior to imaging. Representative images were acquired at 10X magnification using the DSU and presented as maximum intensity projections of 30 µm stacks (3 µm/slice, 11 slices/stack).

5.2.7 Statistics

Statistical analysis was performed using Prism (GraphPAD, La Jolla, CA). Data are represented as mean ± standard deviation (SD) of at least three independent experimental replicates. Data were analyzed using one- or two-way ANOVA with Sidak post-hoc testing with pre-specified comparisons between conditions on a given day and between days for a given condition. A value of $p < 0.05$ was considered significant.

5.3 Results

5.3.1 Hydrogels were designed to independently control the initial mechanical properties and the degradability

Hydrogels containing integrin ligand adhesion peptides and protease-sensitive peptide crosslinkers were formed via thiol-ene photopolymerization (Fig. 5.1A). Crosslinking ratios (% of available norbornene arms crosslinked) were varied to control the initial mechanical properties of the hydrogels. The identity of the crosslinking peptides, sVPMS or dVPMS, controlled hydrogel

proteolytic susceptibility. To confirm differences in mechanical properties were a result of crosslinking ratio and not peptide identity, the shear storage modulus (G') of hydrogels swollen in medium was measured. Hydrogels formed with either peptide had similar initial stiffness after overnight swelling (day 1) for matched crosslinking ratios (Fig. 5.1B). Hydrogels formed with 70-90% crosslinking ratios had similar shear storage moduli while 60% crosslinked hydrogels were significantly softer (approximately 0.5-fold decrease) than all other crosslinking ratios. Incubation of acellular hydrogels for 7 days in medium led to a significant decrease in hydrogel stiffness for all groups, with the exception of 90% sVPMS gels. Both sVPMS and dVPMS acellular gels showed similar reductions in stiffness when incubated in exogenous medium. In the presence of collagenase, hydrogels crosslinked with dVPMS were more rapidly degraded by after 2 h (G' = 111.2 Pa compared to 179.6 Pa for sVPMS). After 24 h of collagenase incubation, dVPMS and sVPMS had shear storage moduli of 45.43 Pa and 121.8 Pa, respectively (Fig. 5.1C). Taken together, these data showed that acellular hydrogels formulated with either peptide displayed comparable initial mechanical properties; however, hydrogels crosslinked with dVPMS degraded more rapidly by design when exposed to exogenous collagenase, a surrogate for expected cell-mediated MMP-degradation, confirming that these hydrogel formulations provide a suitable platform to separately probe the influences of initial stiffness and degradability on vascular network formation *in vitro*.
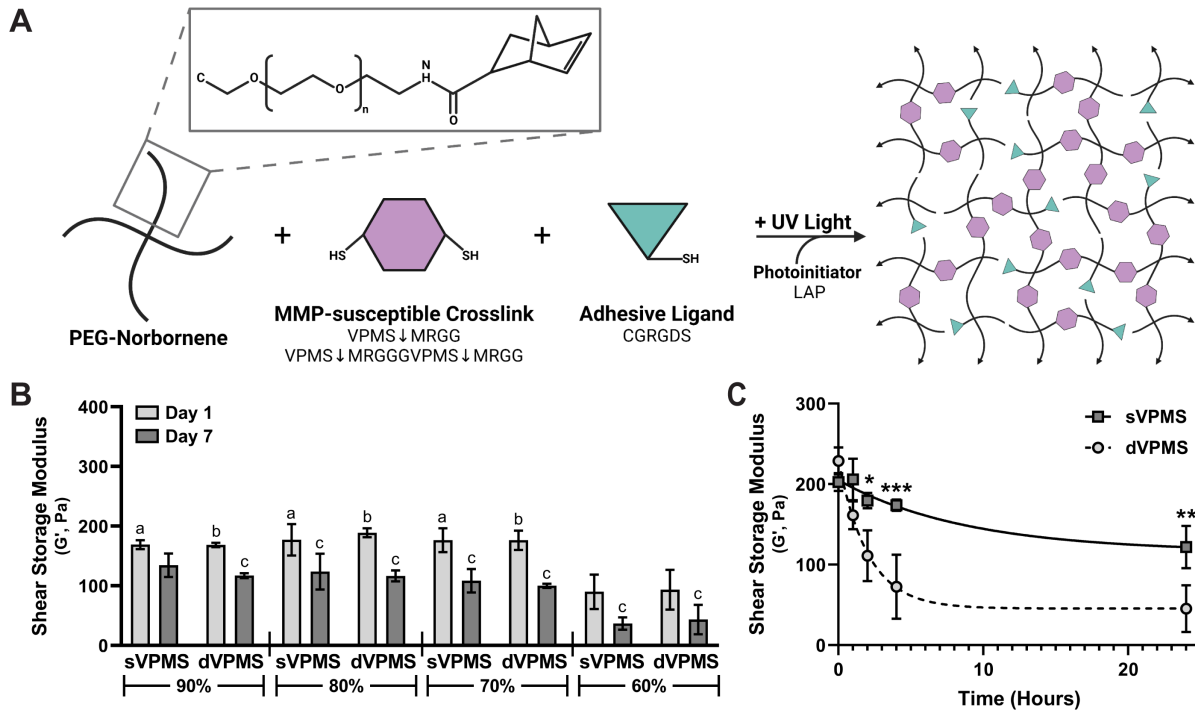
Figure 5.1: Hydrogels were designed to tune both the initial mechanical properties by altering the crosslinking ratio and proteolytic susceptibility via crosslinking peptide identity. *(A) Schematic of PEGNB hydrogel fabrication. Created with BioRender.com. (B) The shear storage modulus (G') of acellular hydrogels was measured after overnight swelling in medium (day 1) and 7 days of culture. a: $p < 0.05$ compared to 60% sVPMS at day 1; b: $p < 0.01$ compared to 60% dVPMS at day 1; c: $p < 0.05$ compared to day 1 of matched peptide, N = 3. (C) Pre-swollen 90% crosslinked hydrogels were incubated with collagenase (0.5 U/mL) for up to 24 h and characterized by shear rheology after 0, 1, 2, 4, and 24 h. *: $p < 0.05$; **: $p < 0.01$; ***: $p < 0.001$, N = 3.*

5.3.2 Enhanced hydrogel degradability supports greater vascular network assembly independent of initial hydrogel stiffness

HUVEC and NHLF were co-encapsulated in the hydrogel formulations described above to investigate how initial mechanical properties and rate of degradation influence vessel network formation. All hydrogel formulations supported the formation of vessel-like structures by day 7 (Fig. 5.2A and B, Fig. 5.6A) that persisted through 14 days of culture (Fig. 5.6B). In hydrogels crosslinked with sVPMS, softer 60% crosslinked gels facilitated significantly greater vessel network formation than other crosslinking ratios after 7 days of culture. Conversely, hydrogels crosslinked with dVPMS showed no significant differences among any of the crosslinking ratios

despite 60% crosslinked gels having lower initial stiffness. Hydrogels crosslinked with dVPMS supported greater vessel densities than sVPMS hydrogels at higher crosslinking ratios (90% 1.5-fold greater and 80% 1.3-fold greater). In fact, 70-90% crosslinked dVPMS gels supported similar vessel densities to 60% sVPMS gels after 7 days. Despite increased vessel network formation in hydrogels of lower bulk stiffness or higher degradability at day 7, all conditions had similar vessel density as microvascular networks were remodeled and matured over 14 days.

Consistent with previous work from our group [16], vessel network assembly was accompanied by hydrogel stiffening over time in all experimental conditions. dVPMS hydrogels stiffened at faster rates, with all dVPMS formulations significantly stiffer than the sVPMS hydrogels on day 7 (Fig. 5.2C-F). From day 1 to day 7, we observed a 3.7-, 3.9-, 5.2-, and 12.1-fold increase in stiffness in 90%, 80%, 70%, and 60% crosslinked dVPMS gels, respectively, compared to sVPMS gels which had a 2.2-, 2.2-, 2.8-, and 5.1-fold increase in stiffness in 90%, 80%, 70%, and 60%, respectively. In sVPMS hydrogels, only the less crosslinked 70% and 60% gels stiffened significantly after 7 days, while all conditions stiffened significantly from day 7 to day 14 as microvascular networks were matured (Fig. 5.6C). Conversely, for dVPMS, all conditions stiffened significantly after 7 days, while a subset of gels (80% and 70%) further stiffened significantly from day 7 to day 14 (Fig. 5.6D). Similar to trends observed in vessel density, all conditions attained similar shear storage moduli after 14 days of culture. This bulk gel stiffening may result from the deposition of new matrix as vascular networks are remodeled and matured over time. Consistent with this possibility, immunostaining for basement membrane components collagen IV (COL IV) and laminin beta-1 (LAM B1) revealed both were present and localized to UEA-positive vessel-like structures in day 7 (Fig. 5.3, Fig. 5.7) and day 14 cultures (Fig. 5.8).
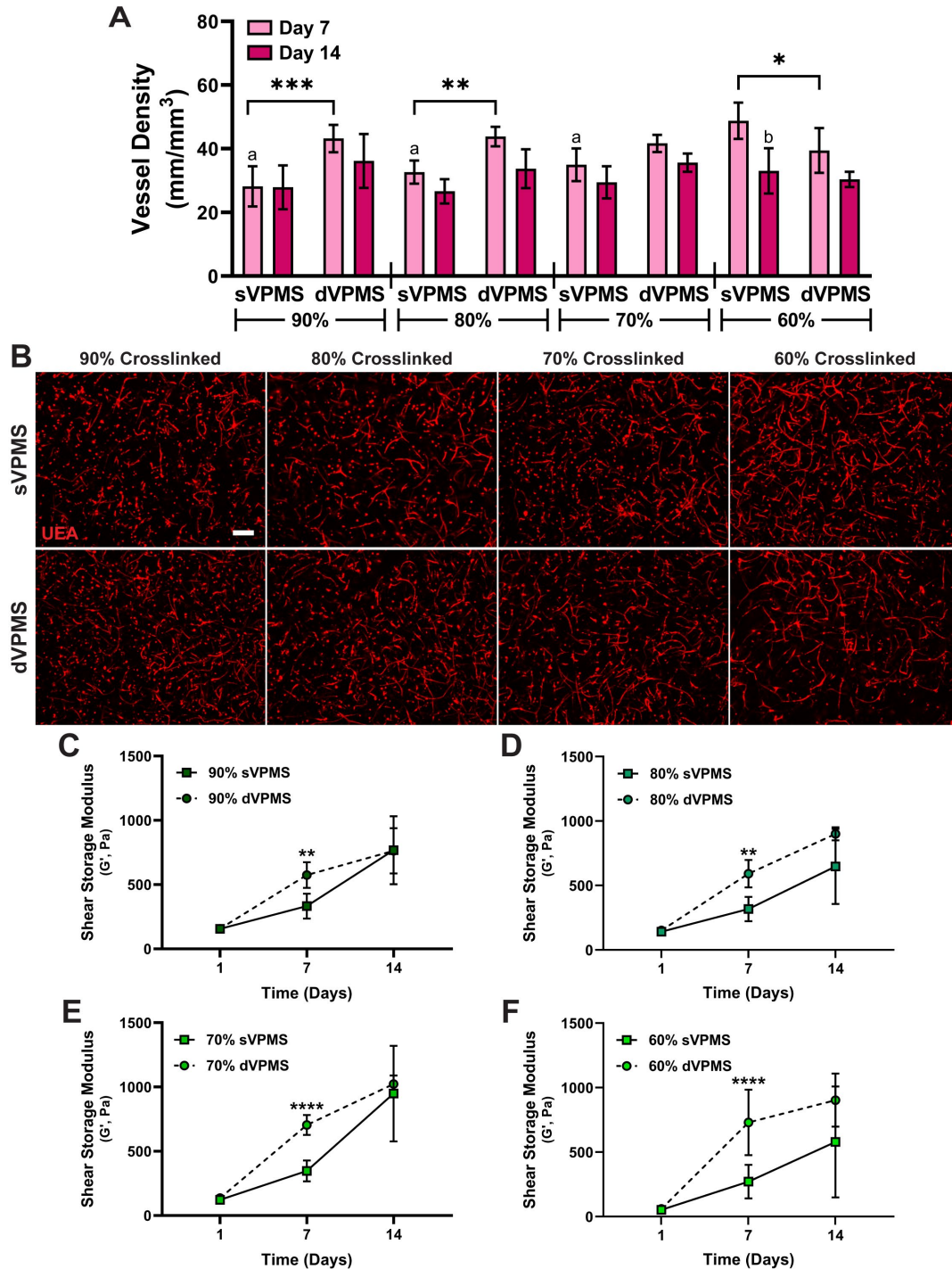
Figure 5.2: Vascular network assembly depends on initial hydrogel mechanical properties and degradability. *(A) Vessel density was quantified in cellular hydrogels of varying crosslinking densities and degradable crosslinking peptides cultured for 7 and 14 days. a: p < 0.01 compared to 60% sVPMS at day 7; b: p < 0.0001 compared to day 7 of matched peptide, *: p < 0.05; **: p < 0.01; ***: p < 0.001, N = 3-6. (B) Representative max intensity projections (Z = 300 μm) of vessel-like structures in hydrogels containing HUVEC-NHLF co-cultures after 7 days are shown stained with the endothelial-selective lectin from Ulex europaeus (UEA, red; scale bar = 200 μm). The shear storage modulus (G') of cellular hydrogels*
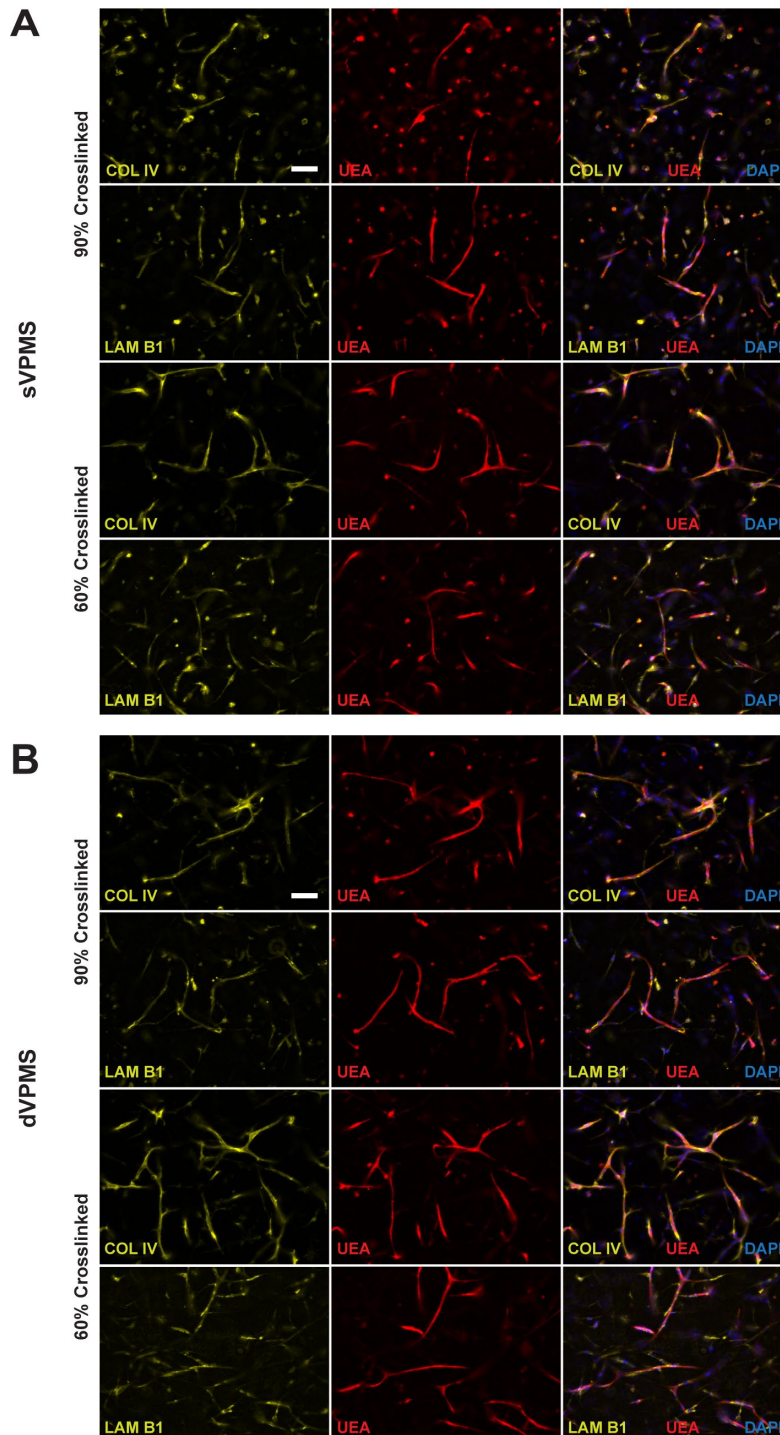
Figure 5.3: Fluorescent staining for basement membrane proteins confirms vascular network remodeling and maturation over time. *Representative max intensity projections (Z = 30 μm) of collagen IV and laminin beta-1 localized to UEA-positive vessel-like structures in the highest and lowest crosslinking ratio gels crosslinked with either (A) sVPMS or (B) dVPMS after 7 days of culture (scale bar = 100 μm).*

116

To further investigate if the increased rate of hydrogel stiffening in gels crosslinked with dVPMS correlated with a greater degree of vascularization at earlier timepoints, hydrogels were cultured for shorter durations (3 and 5 days), the shear storage moduli of constructs were determined, and microvascular structures were imaged (Fig. 5.4). As early as 3 days of culture, 80% and 60% dVPMS gels were significantly stiffer than matched sVPMS gels (Fig. 5.4B and C). After 5 days of culture, 70% and 60% dVPMS gels were significantly stiffer than matched sVPMS gels (Fig. 5.4C and D). In sVPMS crosslinked matrices, all crosslinking ratios showed significant stiffening after 5 days, with the initially softer 60% gels reaching similar stiffness as other ratios by day 5 of culture (Fig. 5.6E). A similar trend was observed for dVPMS gels; however, softer 60% gels increased in stiffness from day 1 to day 3, and even surpassed 90% and 80% gels by day 5 (Fig. 5.6F).

Fluorescent staining for UEA-positive vessel-like structures formed after 3 days of culture revealed that only 60% crosslinked sVPMS gels showed evidence of primitive network structures, whereas dVPMS crosslinked gels showed microvascular network assembly in all conditions (Fig. 5.4E). After 5 days of culture, higher crosslinking ratio sVPMS gels started, though very minimally, to have evidence of primitive vessel formation while 60% gels were still more vascularized, whereas again, dVPMS crosslinked gels continued to show vessel morphogenesis in all conditions (Fig. 5.4F).
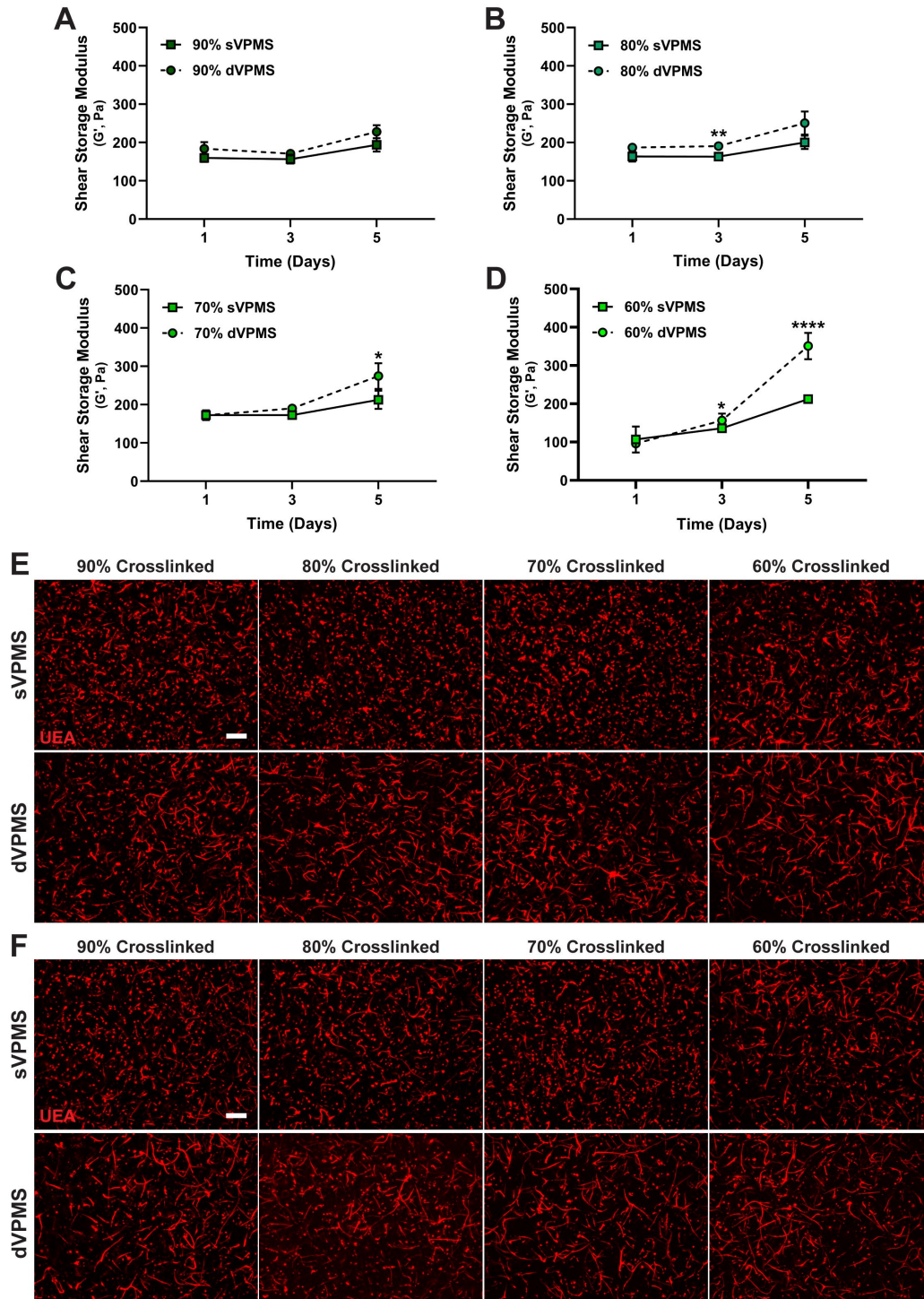
Figure 5.4: Enhanced hydrogel degradability facilitates vessel morphogenesis as early as 3 days of culture, regardless of crosslinking ratio and initial stiffness. The shear storage modulus (G') of cellular hydrogels were measured after overnight swelling in medium (day 1) and 3 and 5 days of culture for (A) 90%, (B) 80%, (C) 70% and (D) 60% crosslinked hydrogels. *: p < 0.05; **: p < 0.01; ****: p < 0.0001, N = 3. Representative max intensity projections (Z = 300 μm) of vessel-like structures in hydrogels containing HUVEC-NHLF co-cultures after (E) 3 and (F) 5 days of culture are shown stained with UEA (red; scale bar = 200 μm).

5.3.3 Matrix stiffening in degradable hydrogels is a direct result of vessel network formation in co-cultured endothelial cells and fibroblasts

In the absence of NHLF as a supportive stromal cell, hydrogels containing HUVEC monocultures softened from day 1 to day 7 of culture for all experimental conditions (Fig. 5.5A). Similar to acellular controls, there was no significant difference in stiffness between matched sVPMS and dVPMS conditions at day 7, indicating peptide degradability appears to have little effect on gel softening by HUVEC alone. Further, there was no evidence of vessel morphogenesis occurring within any of the tested conditions by day 7 (Fig. 5.5B, Fig. 5.9A).

In contrast to HUVEC monocultures, NHLF cultured in hydrogels without the inclusion of endothelial cells exhibited significant differences between gels crosslinked with sVPMS and dVPMS (Fig. 5.5C). In sVPMS crosslinked gels, the shear storage moduli were statistically unchanged after 7 days of culture. Conversely, dVPMS crosslinked gels increased in stiffness from day 1 to day 7 across all crosslinking formulations. As a result, the majority of dVPMS conditions (80%, 70%, and 60%) were significantly stiffer at day 7 than matched sVPMS conditions. Fluorescent imaging of F-actin-stained hydrogels revealed NHLF cultured in 60% sVPMS hydrogels appeared slightly more spread than other crosslinking ratios, while in dVPMS crosslinked hydrogels NHLF were vastly more spread than those in sVPMS crosslinked gels for all crosslinking ratios (Fig. 5.5D, Fig. 5.9B).
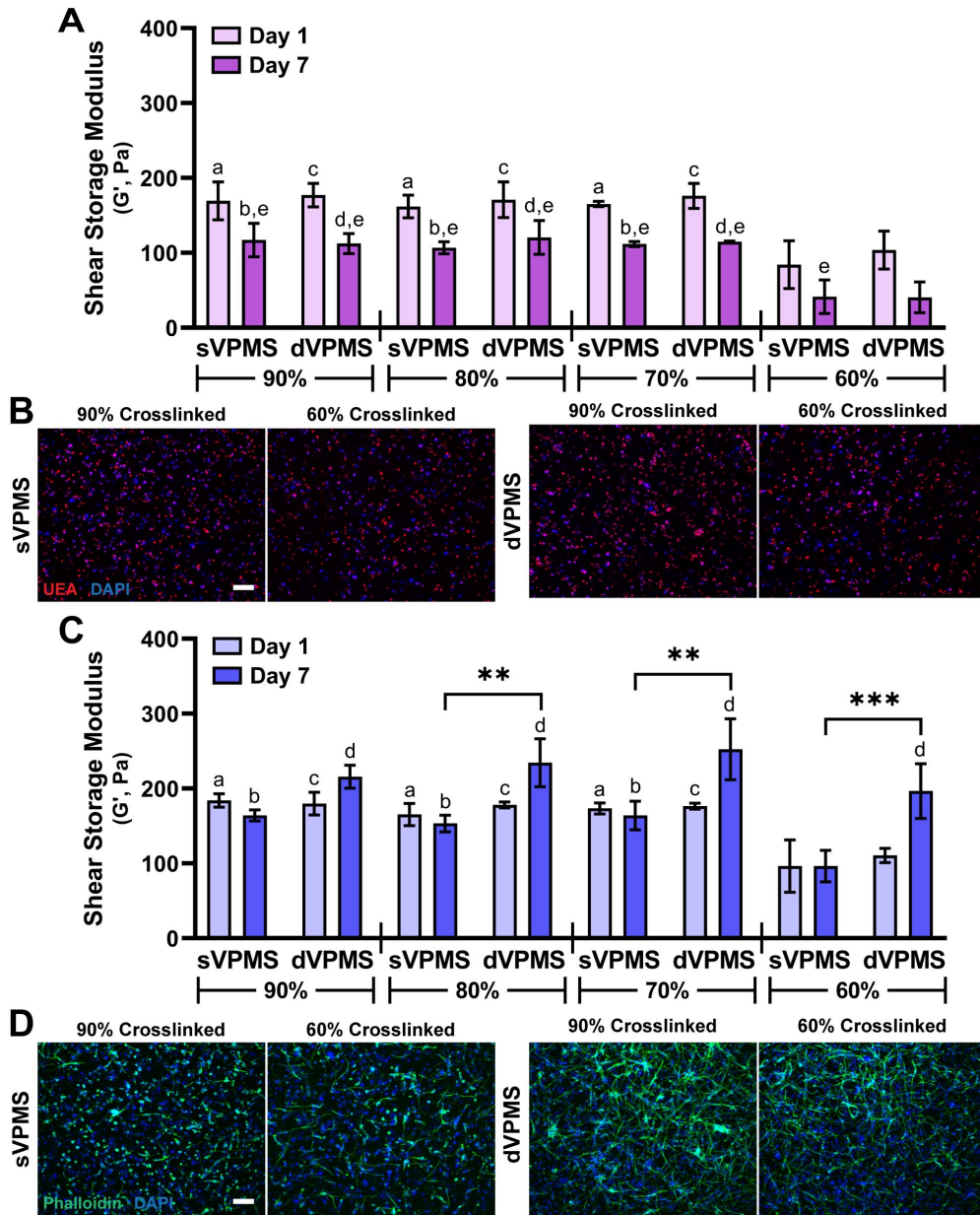
Figure 5.5: Stromal cell support is necessary for vessel morphogenesis. *(A) The shear storage modulus (G') of HUVEC monoculture hydrogels were measured after overnight swelling in medium (day 1) and 7 days of culture. a: p < 0.05 compared to 60% sVPMS at day 1; b: p < 0.01 compared to 60% sVPMS at day 7; c: p < 0.05 compared to 60% dVPMS at day 1; d: p < 0.01 compared to 60% dVPMS at day 7; e: p < 0.05 compared to day 1 of matched peptide; N = 3. (B) Representative max intensity projections (Z = 300 µm) images of highest and lowest crosslinking ratio hydrogels containing HUVEC monocultures after 7 days are shown stained with UEA (red) and DAPI (blue; scale bar = 200 µm). (C) The shear storage modulus (G') of NHLF monoculture hydrogels were measured after overnight swelling in medium (day 1) and 7 days of culture. a: p < 0.05 compared to 60% sVPMS at day 1; b: p < 0.05 compared to 60% sVPMS at day 7; c: p < 0.001 compared to 60% dVPMS at day 1; d: p < 0.01 compared to day 1 of matched peptide; **: p < 0.01; ***: p < 0.001, N = 3. (D) Representative max intensity projections (Z = 300 µm) images of highest and lowest crosslinking ratio hydrogels containing NHLF monocultures after 7 days are shown stained with phalloidin (green) and DAPI (blue; scale bar = 200 µm).*

5.4 Discussion

In this study, we utilized a 3D model of vasculogenesis in which endothelial cells and fibroblasts were co-encapsulated in cell-adhesive, degradable 4-arm PEGNB hydrogels designed to examine how the physicochemical properties of the microenvironment influence vascularization. Prior studies by our group [14-16] and others [12, 13, 23, 31-35] have shown that increasing the initial stiffness of PEG-based hydrogels results in decreased vascularization. However, many of these studies used a form of difunctional acrylate-based PEG hydrogels [11, 13, 15, 24, 27, 31-34, 36-38], which typically form crosslinked polymeric networks via chain growth photopolymerization and may exhibit spatial heterogeneities in material properties [17, 39], or PEG-vinyl sulfones, which react slowly with thiols via Michael-type addition reactions [19] and often involve buffers to increase reaction kinetics in more alkaline pH [17]. By contrast, step-growth thiol-norbornene photo-click hydrogels yield more homogeneous polymeric structures [39] and form more rapidly under physiological conditions without the need for additional buffer making them more cytocompatible [17, 18]. A handful of prior studies have used PEGNB-based hydrogels to study vascularization [12, 20-23], but to our knowledge these studies have exclusively utilized 8-arm, 20 kDa PEGNB, which have different structural and mechanical properties than our hydrogel platform [40]. Here, we controlled initial stiffness of 4-arm PEGNB hydrogels by varying the crosslinking ratio of thiols to norbornenes at a constant wt. % PEG rather than the more prevalent approach of changing the polymer density. This allowed us to formulate both soft and ultra-soft matrices conducive to vessel formation across all conditions tested. Further, we controlled the rate of degradation via the incorporation of an additional, identical protease-cleavage site to more directly compare the effects of enhanced degradability. We examined how initial stiffness and degradability independently and synergistically influenced the rate of vessel

network formation and cell-mediated matrix remodeling (i.e., stiffening) over time, including both early and later stage timepoints.

Decreasing the crosslinking ratio to 60% yielded hydrogels that were significantly softer than all other crosslinking ratios. Hydrogels formulated with either sVPMS or dVPMS displayed comparable initial stiffnesses at matched crosslinking ratios; as expected, dVPMS gels degraded more rapidly upon exposure to collagenase, confirming rate of degradation could be changed without changing other material properties. While incorporating an additional protease-sensitive cleavage site within dVPMS increases the molecular weight of the crosslinking peptide compared to its smaller sVPMS counterpart, the length of the crosslinking peptide is negligible compared to the length of the arms of the PEGNB molecules. Studies using single-site and tri-site degradable peptides have similarly demonstrated increased degradability without altering hydrogel swelling ratio, mesh size, or compressive modulus over a range of different wt. % PEG-diacrylate hydrogels [27, 34], supporting the addition of repeated protease-sensitive cleavage sites to enhance degradability without changing the hydrogel network structure. While increasing the crosslinking ratio or degradability of PEG-based hydrogels could influence diffusion, previous studies have reported that the diffusion of small, medium, and large molecules over time into PEG hydrogels of roughly 700 and 6,000 Pa was relatively similar, despite having significantly different mesh sizes [41]. As all our hydrogels are much softer overall and stiffen to similar degrees across conditions over time, we do not expect there expect diffusion of soluble cues to significantly influence our findings.

All hydrogel formulations supported vessel network formation after 7 days of culture, which persisted through 14 days of culture. Vessel morphogenesis varied as a function of both mechanical properties and degradability. Those gels that were initially softer (lower G') supported

vascularization to a greater extent in sVPMS hydrogels after 7 days of culture. Previous studies similarly reported that decreasing the wt. % PEG utilized in hydrogel formulations, thus producing softer microenvironments, resulted in increased vessel morphogenesis in self-assembled networks [12, 16] and increased sprouting from cell spheroids [13, 31, 32]. Others found that stiffer matrices resulted in decreased cell proliferation [35] and viability [23]. In our study, decreasing bulk stiffness by decreasing the crosslinking ratio of the network likely reduces the local polymer density cells need to remodel in order to spread, migrate, and assemble into vascular networks [12, 42]. In dVPMS hydrogels with enhanced protease susceptibility, there were no significant differences in vessel network formation across all crosslinking ratios despite 60% crosslinked gels being markedly softer, suggesting initial stiffness has little effect on vessel assembly when degradability of the microenvironment is increased, at least in these soft hydrogels (50-185 Pa). At higher crosslinking ratios, and thus increased stiffness, dVPMS gels supported greater vessel densities than matched sVPMS conditions. Regardless of whether the observed increase in day 7 vessel density resulted from initial matrix stiffness or proteolytic susceptibility, all conditions had similar vessel densities after 14 days of culture as a results of microvascular network remodeling and maturation, as evident by the presence of basement membrane proteins, collagen IV and laminin beta-1, that were localized to UEA-positive vessel structures. A previous study using a model akin to angiogenic sprouting reported that more degradable hydrogels supported greater sprouting than their less degradable counterparts, but those differences persisted for up to three weeks in culture [34].

Although a variety of studies have investigated the influence of initial stiffness on vascularization in synthetic matrices, comparatively little is known regarding how the microenvironment is remodeled over time. We longitudinally analyzed matrix stiffness and

observed bulk stiffening that accompanied vessel network assembly in all conditions. Hydrogels crosslinked with dVPMS significantly stiffened from day 1 to day 7, but significant stiffening was delayed in more tightly crosslinked, less degradable 90% and 80% sVPMS hydrogels. These findings are consistent with previous work from our group which showed stiffening coincided with vessel morphogenesis in soft (59 Pa), but not in intermediate (114 Pa) or stiff (209 Pa) sVPMS crosslinked PEGVS hydrogels by 7 days of culture [16]. Despite dVPMS peptides permitting more rapid enzymatic hydrogel degradation than sVPMS peptides, dVPMS hydrogels actually stiffened at a faster rate in response to vascular self-assembly, as evidenced by all dVPMS formulations being significantly stiffer than the sVPMS hydrogels on day 7. This is likely a result of cell-mediated contractile forces, which permit accelerated vascular self-assembly and mechanical remodeling in the more rapidly degraded hydrogels [16], and the production of new ECM during the aforementioned deposition of basement membrane proteins [11, 37, 38]. Interestingly, all experimental conditions attained similar stiffnesses after 14 days of culture regardless of initial stiffness or degradability, similar to trends observed in vessel density.

The observed cell-mediated bulk stiffening occurred coincident with vascular network assembly in co-cultures of endothelial cells and fibroblasts, but not in monocultures. HUVEC monocultures softened from day 1 to day 7 for all experimental conditions regardless of stiffness and degradability. The decrease in shear storage moduli of these HUVEC-only hydrogels closely mirrors the changes observed in acellular hydrogels incubated in cell culture medium after 7 days, suggesting matrix softening may not be due to endothelial cell degradation of the surrounding microenvironment but rather exogenous MMPs present in the fetal bovine serum of the culture medium [43, 44]. While others have shown microvascular assembly in endothelial cell only cultures under differing conditions (cell type, cell densities, material properties, growth factors,

etc.) [12, 20, 21], HUVEC monocultures showed no evidence of cell spreading or self-assembly in the absence of supportive NHLF for any experimental conditions. Conversely, NHLF monocultures were more responsive to changes in matrix properties. NHLF cultured in all dVPMS gels were qualitatively more spread than those cultured in any of the sVPMS gels, regardless of initial stiffness. In sVPMS gels, NHLF were qualitatively more spread in the softer 60% gels. These differences in cell morphol ogy correlated to changes in matrix stiffness over time. All NHLF-only dVPMS gels significantly stiffened from day 1 to day 7, though the magnitude of stiffening was at least 2.5 times lower than gels containing co-cultures. Despite some cell spreading in 60% sVPMS gels compared to other crosslinking ratios, stiffening was not observed for any sVPMS crosslinking ratios, though the hydrogels maintained their initial stiffness, unlike the HUVEC monocultures.

As dVPMS hydrogels containing HUVEC-NHLF co-cultures exhibited increased rates of stiffening within the first 7 days, we evaluated microvascular network formation at earlier timepoints to investigate how material properties influence early vasculogenesis. After 3 days of culture, hydrogels crosslinked with sVPMS showed evidence of primitive vessel structures only in the softer 60% condition, while hydrogels crosslinked with dVPMS showed evidence of such structures across all formulations. A similar phenomenon was observed after 5 days, though higher crosslinking ratios of sVPMS started to exhibit very minimal evidence of vessel assembly. In the majority of conditions, dVPMS hydrogels were significantly stiffer than sVPMS gels at matched crosslinking ratios after 3 or 5 days. Greater crosslinked 90% dVPMS gels were not significantly stiffer than sVPMS gels by 5 days, possibly indicating that even in more degradable matrices there is a delay in matrix remodeling at higher densities. While 60% crosslinked gels had a greater rate of stiffening than other dVPMS hydrogels, vessel densities across all dVPMS hydrogels after 7

days were comparable. Taken together, these data suggest that while tuning bulk stiffness and degradability can enhance microvascular network assembly, neither alone is likely sufficient for rapid vascularization of engineered tissues.

5.5 Conclusions

Our findings illustrate a relationship between the degree to which a synthetic matrix can be remodeled and the assembly of microvascular networks *in vitro*. We demonstrated that cells' ability to effectively remodel a hydrogel is essential for robust vascularization and is facilitated, in part, through the co-culture of endothelial and stromal cells. While increasing the degradability promoted enhanced vascularization in more densely crosslinked hydrogels across a variety of stiffnesses, decreasing the local crosslinking density of less protease-susceptible gels also accomplished similar vessel densities. Further, we observed cell-mediated matrix stiffening that accompanied vascularization throughout the entirety of culture, which was more rapid in more degradable hydrogels. Importantly, we found that these matrix properties impact vessel morphogenesis and matrix remodeling as early as 3 days of culture, which is essential to identify materials that promote rapid vascularization upon transplantation *in vivo*. This work highlights the important interplay between stiffness and degradability, as well as the time-dependent changes in stiffness, in facilitating rapid vessel morphogenesis in synthetic 3D hydrogels. Future efforts should be made to assess how this initial increase in vessel morphogenesis influences vascular network functionality and how these more readily remodeled matrices facilitate vessel formation and inosculation *in vivo*.

5.6 Supplementary Manuscript Data
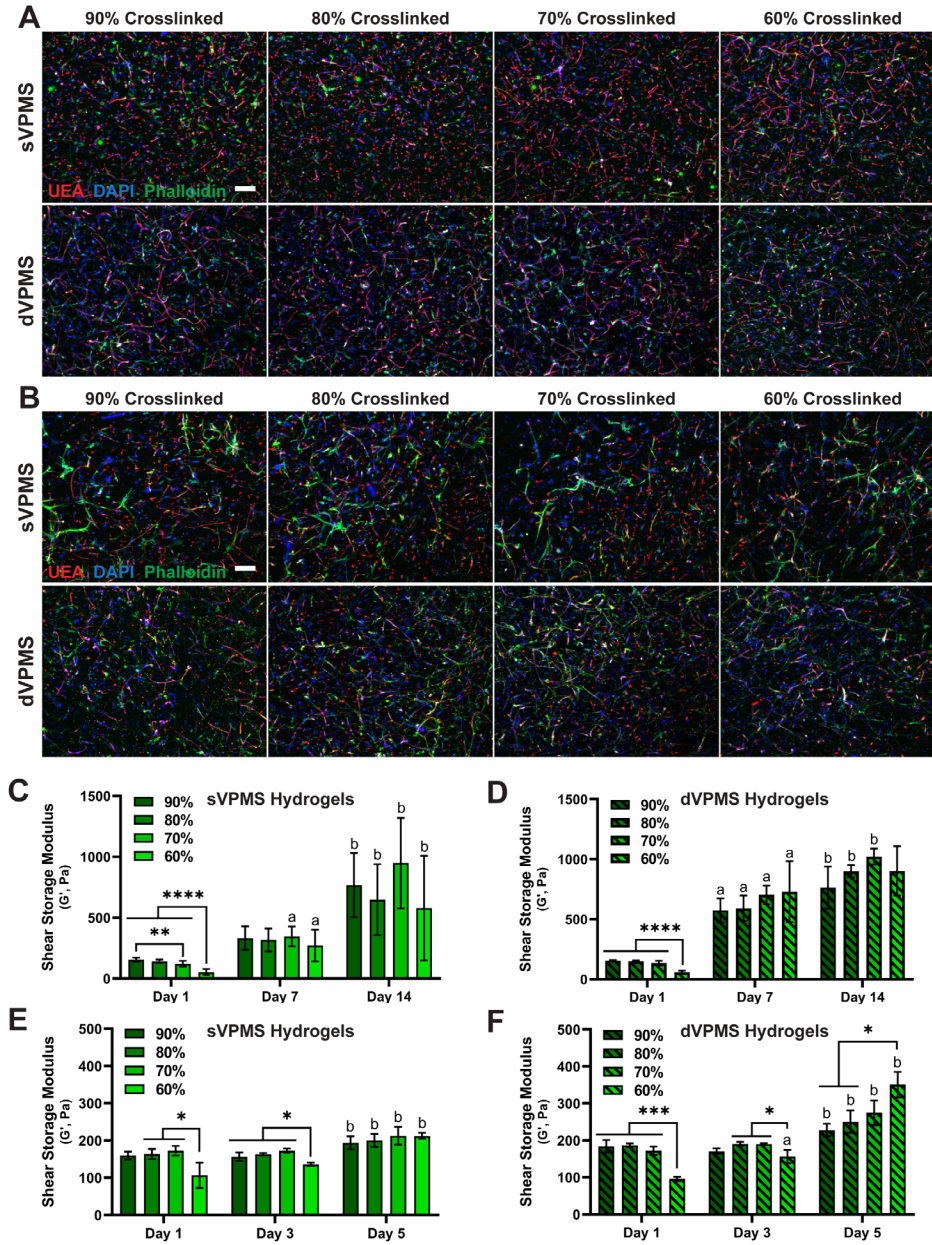
Figure 5.6: Matrix remodeling over time within each peptide. *Representative max intensity projections (Z = 300 μm) of vessel-like structures in hydrogels containing HUVEC-NHLF co-cultures after (A) 7 and (B) 14 days are shown stained with UEA (red), DAPI (blue), and phalloidin (green; scale bar = 200 μm). Day 1, 7, and 14 shear storage moduli of cellular (B) sVPMS and (C) dVPMS hydrogels. Note – this is identical data to that in Fig. 2C-F represented differently to more clearly show comparisons within a single peptide. a: p < 0.05 compared to day 1; b: p < 0.05 compared to day 7; **: p < 0.01; ****: p < 0.0001, N = 3-12. Day 1, 3, and 5 shear storage moduli of cellular (D) sVPMS and (E) dVPMS hydrogels. Note – this is identical data to that in Fig. 4A-D represented differently to more clearly show comparisons within a single peptide. a: p < 0.05 compared to day 1; b: p < 0.05 compared to day 3; *: p < 0.05; ***: p < 0.001, N = 3.*
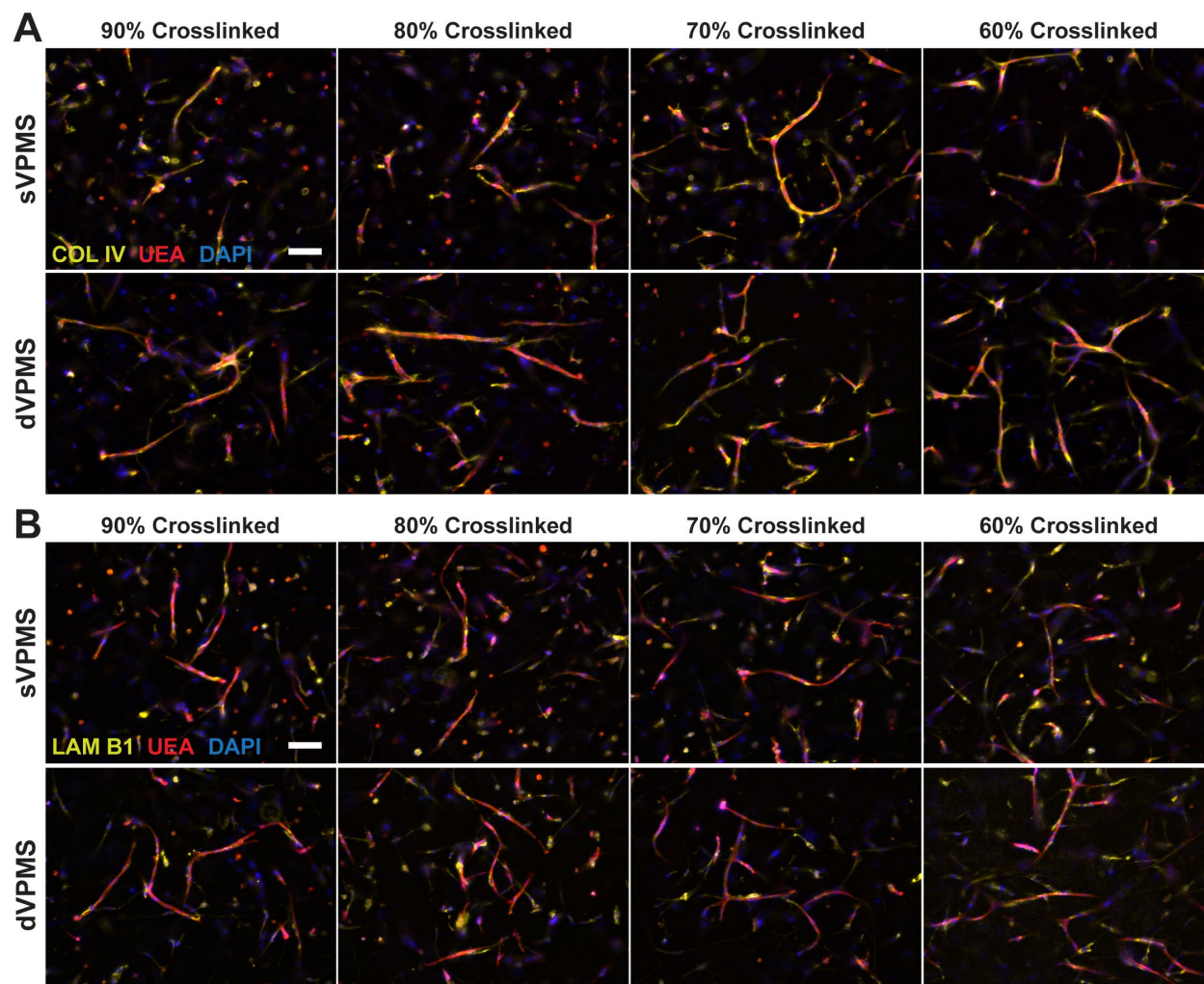
Figure 5.7: Day 7 basement membrane deposition. *Representative max intensity projections (Z = 30 µm) of (A) collagen IV and (B) laminin beta-1 localized to UEA-positive vessel-like structures after 7 days of culture (scale bar = 100 µm).*
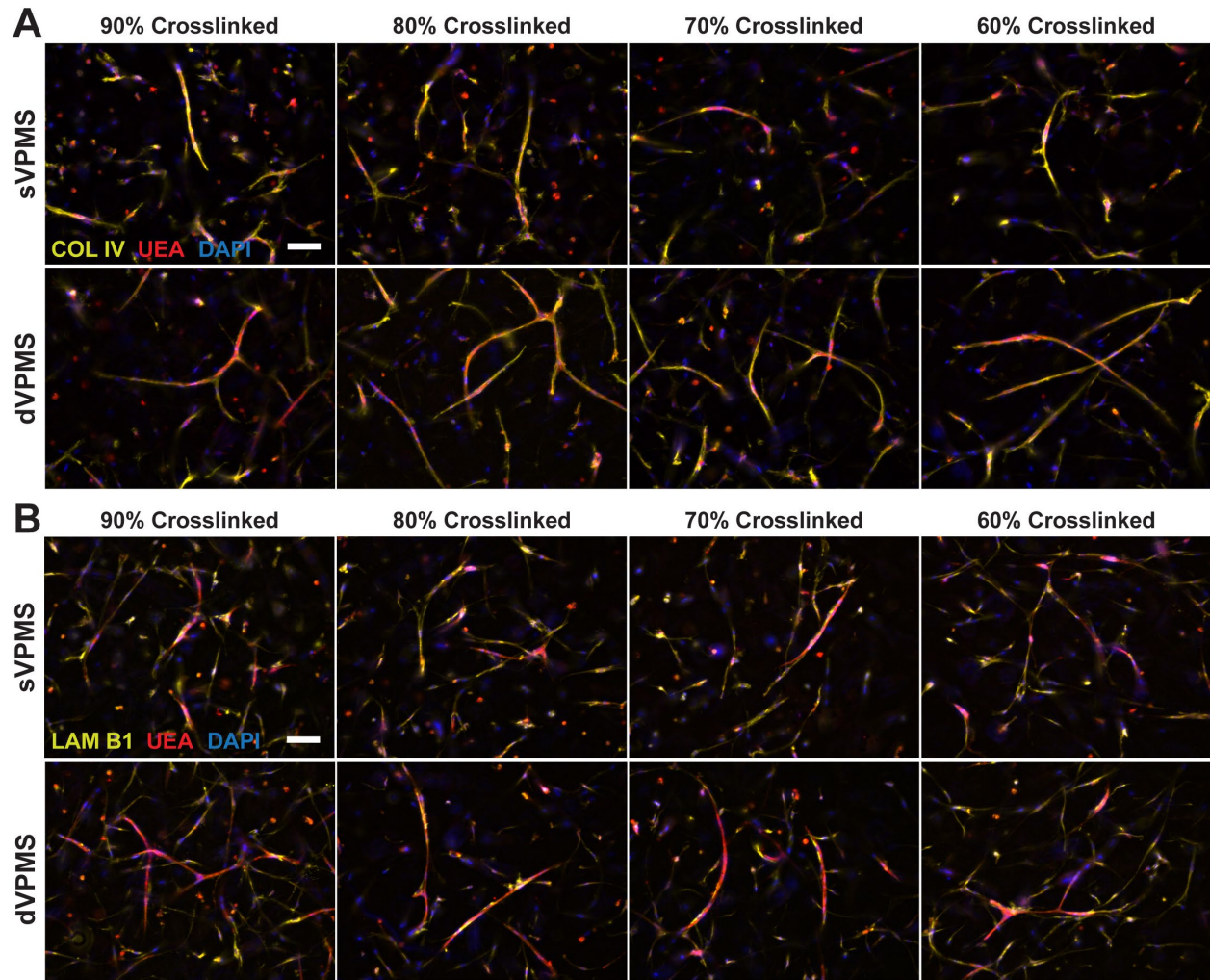
Figure 5.8: Day 14 basement membrane deposition. *Representative max intensity projections (Z = 30 μm) of (A) collagen IV and (B) laminin beta-1 localized to UEA-positive vessel-like structures after 14 days of culture (scale bar = 100 μm).*
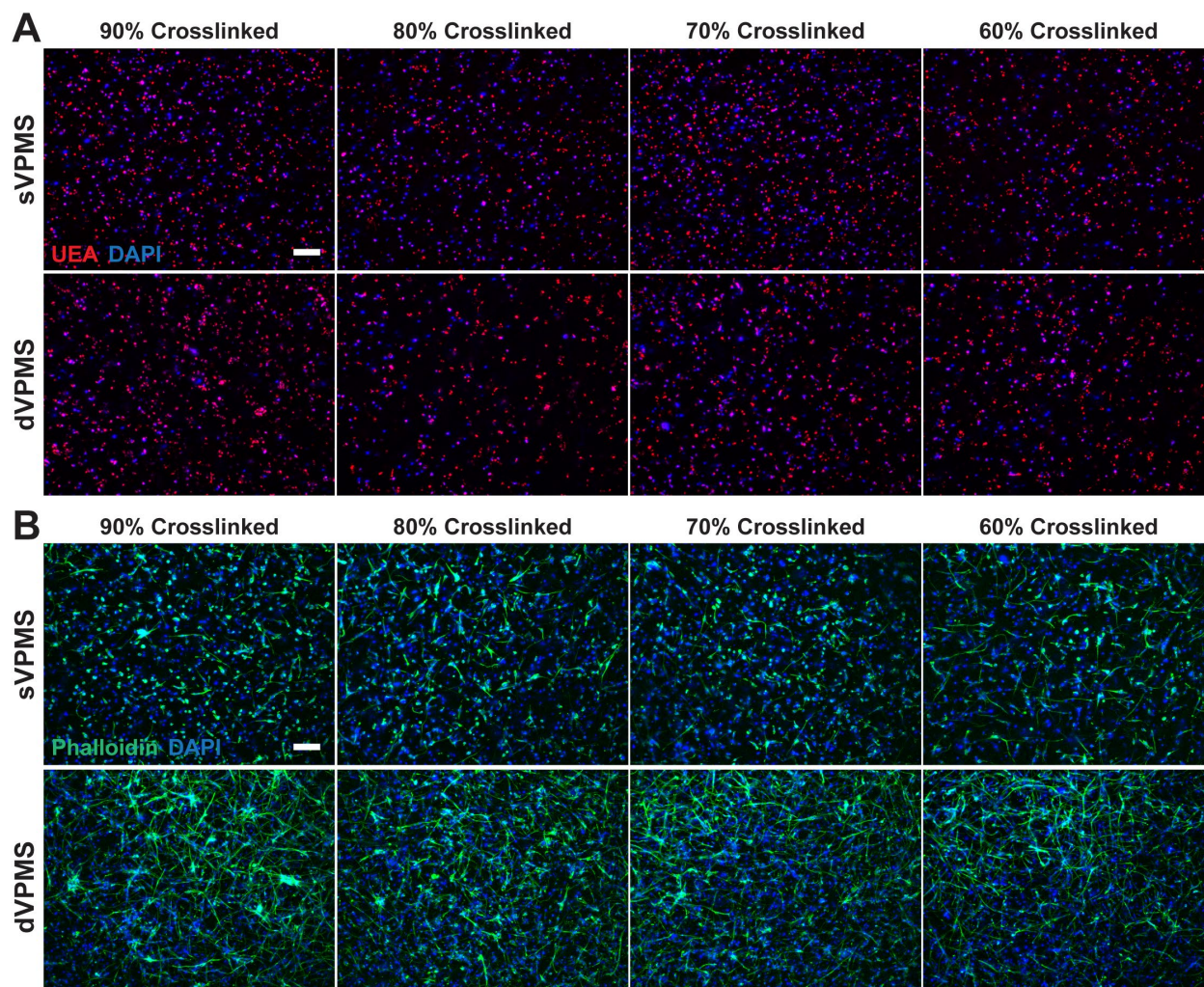
Figure 5.9: HUVEC and NHLF monocultures. *(A) Representative max intensity projections (Z = 300 μm) of HUVEC monoculture gels after 7 days of culture stained with UEA (red) and DAPI (blue). (B) Representative max intensity projections (Z = 300 μm) of NHLF monoculture gels after 7 days of culture stained with phalloidin (green) and DAPI (blue; scale bar = 200 μm).*

5.7 Additional Supplementary Data

5.7.1 RGD concentration influences vascularization and matrix remodeling

HUVEC and NHLF were encapsulated in PEGNB hydrogels that were formulated with varying concentrations of RGD (1.0, 1.5, 2.0, or 2.5 mM) and cultured for 7 days. Increasing RGD concentration did not have a significant effect on vessel density, though it trended toward 2.5 mM RGD supporting greater vessel morphogenesis (Fig. 5.10A-E). These findings algin with work from Brown et al., which found increasing adhesive ligand concentration from 0 to 1.0 mM facilitated greater endothelial cord length, but found diminishing returns between 1.0 and 3.0 mM [12]. Increasing RGD concentration resulted in significant cell-mediated matrix compaction, compacting gels to a diameter of ~4 mm compared to ~7 mm of other groups (Fig. 5.10F). These results led to the use of 1.0 mM RGD for all PEGNB-based experiments.
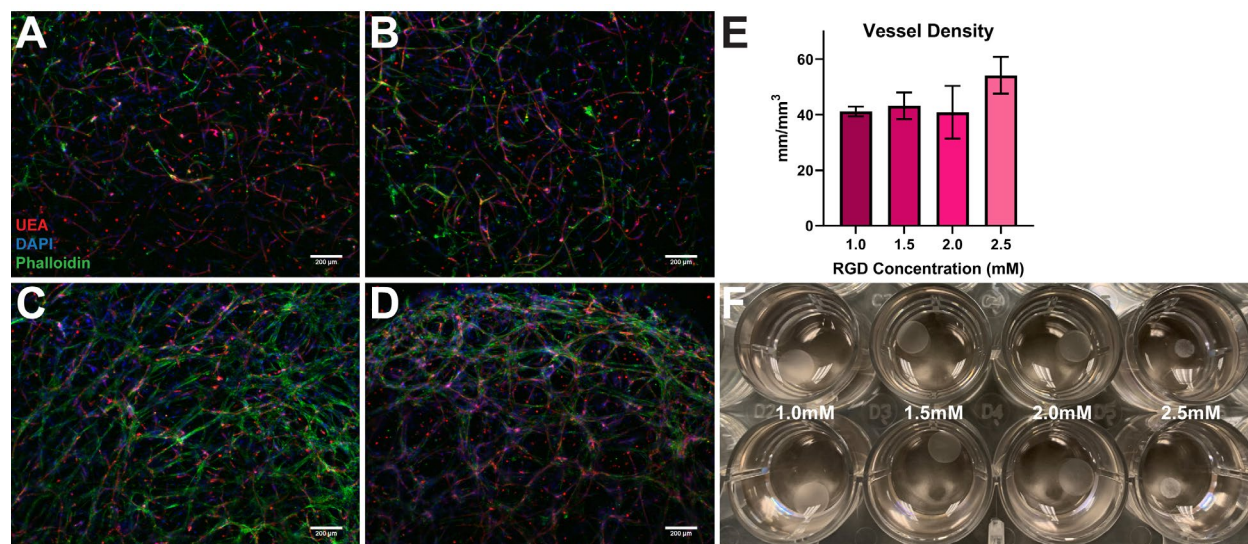
Figure 5.10: Increased RGD concentration improves vascularization but results in increased hydrogel compaction. *PEGNB (3 wt. %) hydrogels with (A) 1.0, (B), 1.5, (C) 2.0, and (D) 2.5 mM RGD 50% crosslinked (constant, regardless of RGD) with sVPMS cultured for 7 days. (E) Vessel density was quantified in cellular hydrogels of varying RGD concentrations; N = 3-4. (F) Cellular hydrogels after 7 days of culture.*

5.7.2 MSC as stromal cells facilitate vascularization of PEGNB matrices

HUVEC and MSC were encapsulated in 3 wt. % PEGNB hydrogels 90%, 80%, 70%, or 60% crosslinked with sVPMS and cultured for 7 days. MSC supported vessel morphogenesis in all hydrogel conditions (Fig. 5.11A-D). MSC-supported microvascular networks had comparable vessel densities (Fig. 5.11E) and matrix stiffening (Fig. 5.11F) to NHLF supported networks (Fig. 5.2) after 7 and 14 days across varying crosslinking ratios, with the exception of MSC not supporting increased vessel morphogenesis in initially softer 60% hydrogels.
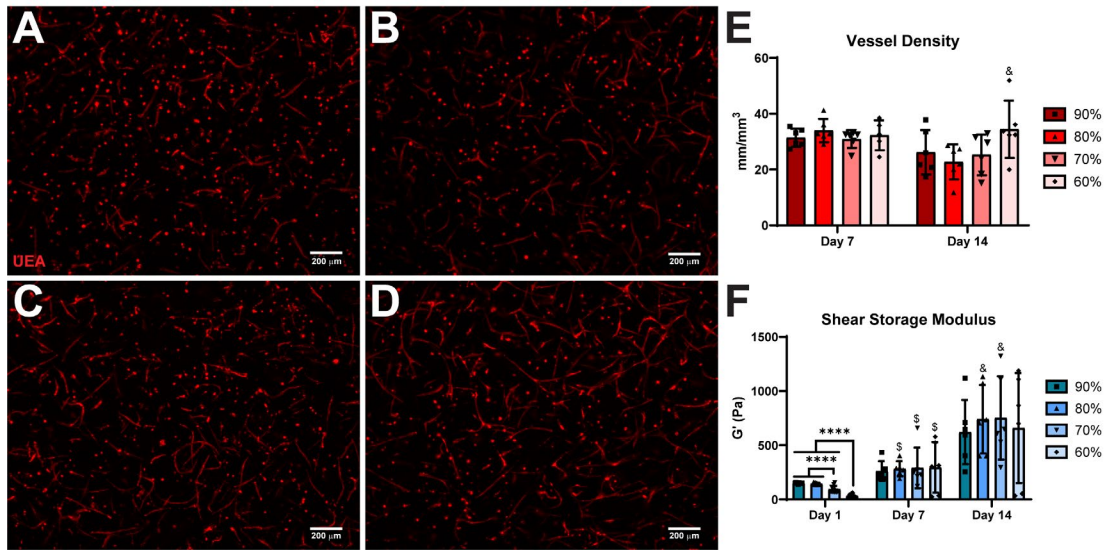
*Figure 5.11: MSC support the formation of microvascular networks and matrix remodeling in sVPMS-crosslinked PEGNB hydrogels. MSC-supported microvascular networks in (A) 90%, (B) 80%, (C) 70%, and (D) 60% crosslinked gels after 7 days of culture. (E) Vessel density was quantified in cellular hydrogels of varying crosslinking ratios after 7 and 14 days; N = 5-6. (F) Cellular hydrogels after 7 days of culture. (F) Day 1, 7, and 14 shear storage moduli of cellular hydrogels; $: p < 0.05 compared to day 1; &: p < 0.05 compared to day 7; ****: p < 0.0001, N = 6-12.*

5.7.3 Decreasing crosslinking ratio permits vascularization of higher wt. % PEGNB matrices

HUVEC and NHLF were encapsulated in 4 or 5 wt. % PEGNB hydrogels 70%, 60%, or 50% crosslinked (CL) with sVPMS and cultured for 7 days to assess if lower crosslinking ratios would facilitate vascularization in higher wt. % PEG hydrogels. Higher wt. % PEG hydrogels have the advantage of more rapid gelation kinetics but can be prohibitive to vessel assembly [16]. All tested hydrogel formulations supported vessel morphogenesis to a similar degree (Fig. 5.12A and

B), regardless of crosslinking ratio and initial stiffness (Fig. 5.12C). The majority of tested conditions, with the exception of 5% PEG 70% crosslinked, had similar vessel densities to 70-90% crosslinked 3 wt. % gels (Fig. 5.2A and B). Both wt. % PEG hydrogels that were 50% crosslinked significantly stiffened from day 1 to day 7 (Fig. 5.12C). While this small study showed that higher wt. % (and in some cases initially stiffer) hydrogels can be vascularized if crosslinking is reduced, this also led to greater variation within the data. Despite this, these hydrogel formulations warrant further investigation as an increased number of free arms could allow growth factors or proteins to be tethered to the matrix, permit secondary crosslinking/stiffening, or allow microbeads to be clicked together in a MAP-like scaffold.
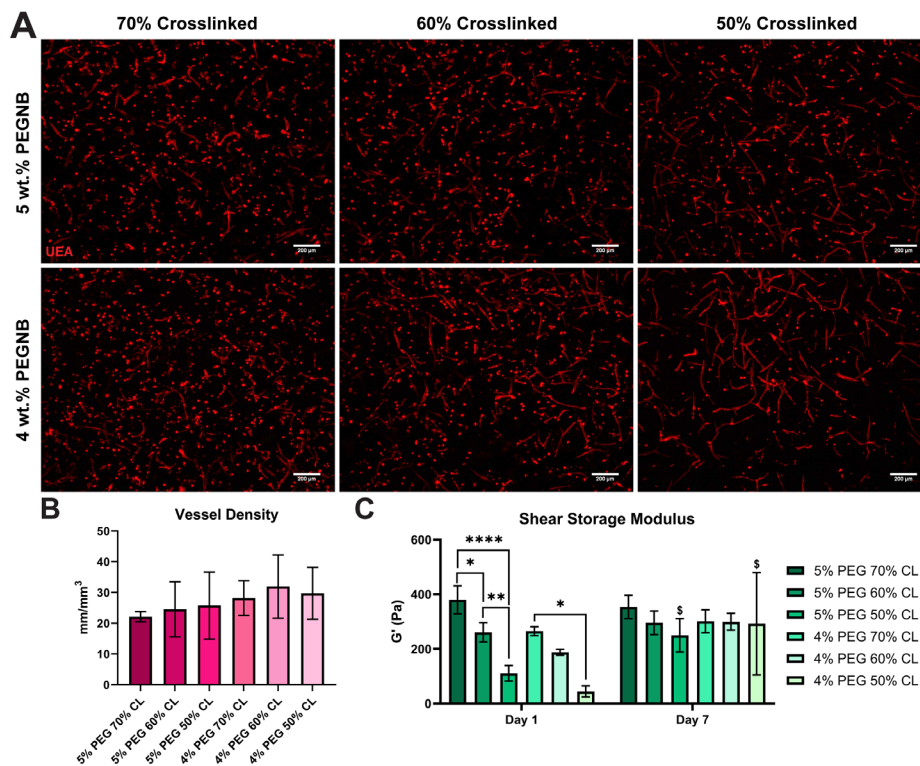
Figure 5.12: 4% and 5% PEGNB with reduced crosslinking ratio supports vessel morphogenesis. *(A) Microvascular networks in hydrogels after 7 days of culture. (B) Vessel density was quantified in cellular hydrogels of varying conditions after 7 days; N = 3. (C) Day 1 and 7 shear storage moduli of cellular hydrogels; *: p < 0.5; **: p < 0.01; ****: p < 0.0001; \$: p < 0.5 compared to day 1 of matched condition, N = 3.*

5.8 References

[1]   C. O'Connor, E. Brady, Y. Zheng, E. Moore, and K. R. Stevens, "Engineering the multiscale complexity of vascular networks," *Nat Rev Mater,* vol. 7, no. 9, pp. 702-716, 2022, doi: 10.1038/s41578-022-00447-8.

[2]   T. Rademakers, J. M. Horvath, C. A. van Blitterswijk, and V. L. S. LaPointe, "Oxygen and nutrient delivery in tissue engineering: Approaches to graft vascularization," *J Tissue Eng Regen Med,* vol. 13, no. 10, pp. 1815-1829, Oct 2019, doi: 10.1002/term.2932.

[3]   X. Chen *et al.*, "Prevascularization of a fibrin-based tissue construct accelerates the formation of functional anastomosis with host vasculature," *Tissue Eng Part A,* vol. 15, no. 6, pp. 1363-71, Jun 2009, doi: 10.1089/ten.tea.2008.0314.

[4]   T. Mirabella *et al.*, "3D-printed vascular networks direct therapeutic angiogenesis in ischaemia," *Nat Biomed Eng,* vol. 1, 2017, doi: 10.1038/s41551-017-0083.

[5]   N. E. Friend *et al.*, "Injectable pre-cultured tissue modules catalyze the formation of extensive functional microvasculature in vivo," *Sci Rep,* vol. 10, no. 1, p. 15562, Sep 23 2020, doi: 10.1038/s41598-020-72576-5.

[6]   R. Z. Lin *et al.*, "Host non-inflammatory neutrophils mediate the engraftment of bioengineered vascular networks," *Nat Biomed Eng,* vol. 1, 2017, doi: 10.1038/s41551-017-0081.

[7]   S. Ben-Shaul, S. Landau, U. Merdler, and S. Levenberg, "Mature vessel networks in engineered tissue promote graft-host anastomosis and prevent graft thrombosis," *Proc Natl Acad Sci U S A,* vol. 116, no. 8, pp. 2955-2960, Feb 19 2019, doi: 10.1073/pnas.1814238116.

[8]   J. Zhu, "Bioactive modification of poly(ethylene glycol) hydrogels for tissue engineering," *Biomaterials,* vol. 31, no. 17, pp. 4639-56, Jun 2010, doi: 10.1016/j.biomaterials.2010.02.044.

[9]   X. Li, Q. Sun, Q. Li, N. Kawazoe, and G. Chen, "Functional Hydrogels With Tunable Structures and Properties for Tissue Engineering Applications," *Front Chem,* vol. 6, p. 499, 2018, doi: 10.3389/fchem.2018.00499.

[10]   J. Patterson and J. A. Hubbell, "SPARC-derived protease substrates to enhance the plasmin sensitivity of molecularly engineered PEG hydrogels," *Biomaterials,* vol. 32, no. 5, pp. 1301-10, Feb 2011, doi: 10.1016/j.biomaterials.2010.10.016.

[11]   J. J. Moon *et al.*, "Biomimetic hydrogels with pro-angiogenic properties," *Biomaterials,* vol. 31, no. 14, pp. 3840-7, May 2010, doi: 10.1016/j.biomaterials.2010.01.104.

[12]   A. Brown, H. He, E. Trumper, J. Valdez, P. Hammond, and L. G. Griffith, "Engineering PEG-based hydrogels to foster efficient endothelial network formation in free-swelling and

confined microenvironments," *Biomaterials,* vol. 243, p. 119921, Jun 2020, doi: 10.1016/j.biomaterials.2020.119921.

[13] Y. J. He *et al.*, "Cell-Laden Gradient Hydrogel Scaffolds for Neovascularization of Engineered Tissues," *Adv Healthc Mater,* vol. 10, no. 7, p. e2001706, Apr 2021, doi: 10.1002/adhm.202001706.

[14] M. Vigen, J. Ceccarelli, and A. J. Putnam, "Protease-sensitive PEG hydrogels regulate vascularization in vitro and in vivo," *Macromol Biosci,* vol. 14, no. 10, pp. 1368-79, Oct 2014, doi: 10.1002/mabi.201400161.

[15] J. A. Beamish, B. A. Juliar, D. S. Cleveland, M. E. Busch, L. Nimmagadda, and A. J. Putnam, "Deciphering the relative roles of matrix metalloproteinase- and plasmin-mediated matrix degradation during capillary morphogenesis using engineered hydrogels," *J Biomed Mater Res B Appl Biomater,* vol. 107, no. 8, pp. 2507-2516, Nov 2019, doi: 10.1002/jbm.b.34341.

[16] B. A. Juliar, J. A. Beamish, M. E. Busch, D. S. Cleveland, L. Nimmagadda, and A. J. Putnam, "Cell-mediated matrix stiffening accompanies capillary morphogenesis in ultra-soft amorphous hydrogels," *Biomaterials,* vol. 230, p. 119634, Feb 2020, doi: 10.1016/j.biomaterials.2019.119634.

[17] C. C. Lin, C. S. Ki, and H. Shih, "Thiol-norbornene photo-click hydrogels for tissue engineering applications," *J Appl Polym Sci,* vol. 132, no. 8, Feb 20 2015, doi: 10.1002/app.41563.

[18] J. J. Roberts and S. J. Bryant, "Comparison of photopolymerizable thiol-ene PEG and acrylate-based PEG hydrogels for cartilage development," *Biomaterials,* vol. 34, no. 38, pp. 9969-79, Dec 2013, doi: 10.1016/j.biomaterials.2013.09.020.

[19] H. Shih and C. C. Lin, "Cross-linking and degradation of step-growth hydrogels formed by thiol-ene photoclick chemistry," *Biomacromolecules,* vol. 13, no. 7, pp. 2003-12, Jul 9 2012, doi: 10.1021/bm300752j.

[20] M. R. Zanotelli *et al.*, "Stable engineered vascular networks from human induced pluripotent stem cell-derived endothelial cells cultured in synthetic hydrogels," *Acta Biomater,* vol. 35, pp. 32-41, Apr 15 2016, doi: 10.1016/j.actbio.2016.03.001.

[21] M. Sofman, A. Brown, L. G. Griffith, and P. T. Hammond, "A modular polymer microbead angiogenesis scaffold to characterize the effects of adhesion ligand density on angiogenic sprouting," *Biomaterials,* vol. 264, p. 120231, Jan 2021, doi: 10.1016/j.biomaterials.2020.120231.

[22] D. G. Belair *et al.*, "Differential regulation of angiogenesis using degradable VEGF-binding microspheres," *Biomaterials,* vol. 93, pp. 27-37, Jul 2016, doi: 10.1016/j.biomaterials.2016.03.021.

[23] E. H. Nguyen, M. R. Zanotelli, M. P. Schwartz, and W. L. Murphy, "Differential effects of cell adhesion, modulus and VEGFR-2 inhibition on capillary network formation in synthetic hydrogel arrays," *Biomaterials,* vol. 35, no. 7, pp. 2149-61, Feb 2014, doi: 10.1016/j.biomaterials.2013.11.054.

[24] M. V. Turturro, M. C. Christenson, J. C. Larson, D. A. Young, E. M. Brey, and G. Papavasiliou, "MMP-sensitive PEG diacrylate hydrogels with spatial variations in matrix properties stimulate directional vascular sprout formation," *PLoS One,* vol. 8, no. 3, p. e58897, 2013, doi: 10.1371/journal.pone.0058897.

[25] F. Bordeleau *et al.*, "Matrix stiffening promotes a tumor vasculature phenotype," *Proc Natl Acad Sci U S A,* vol. 114, no. 3, pp. 492-497, Jan 17 2017, doi: 10.1073/pnas.1613855114.

[26] M. Ehrbar *et al.*, "Elucidating the role of matrix stiffness in 3D cell migration and remodeling," *Biophys J,* vol. 100, no. 2, pp. 284-93, Jan 19 2011, doi: 10.1016/j.bpj.2010.11.082.

[27] S. Sokic, M. C. Christenson, J. C. Larson, A. A. Appel, E. M. Brey, and G. Papavasiliou, "Evaluation of MMP substrate concentration and specificity for neovascularization of hydrogel scaffolds," *Biomater Sci,* vol. 2, no. 10, pp. 1343-1354, Oct 1 2014, doi: 10.1039/C4BM00088A.

[28] A. C. Newman, M. N. Nakatsu, W. Chou, P. D. Gershon, and C. C. Hughes, "The requirement for fibroblasts in angiogenesis: fibroblast-derived matrix proteins are essential for endothelial cell lumen formation," *Mol Biol Cell,* vol. 22, no. 20, pp. 3791-800, Oct 2011, doi: 10.1091/mbc.E11-05-0393.

[29] C. M. Ghajar, K. S. Blevins, C. C. Hughes, S. C. George, and A. J. Putnam, "Mesenchymal stem cells enhance angiogenesis in mechanically viable prevascularized tissues via early matrix metalloproteinase upregulation," *Tissue Eng,* vol. 12, no. 10, pp. 2875-88, Oct 2006, doi: 10.1089/ten.2006.12.2875.

[30] J. Schindelin *et al.*, "Fiji: an open-source platform for biological-image analysis," *Nat Methods,* vol. 9, no. 7, pp. 676-82, Jun 28 2012, doi: 10.1038/nmeth.2019.

[31] Y. J. He *et al.*, "Immobilized RGD concentration and proteolytic degradation synergistically enhance vascular sprouting within hydrogel scaffolds of varying modulus," *J Biomater Sci Polym Ed,* vol. 31, no. 3, pp. 324-349, Feb 2020, doi: 10.1080/09205063.2019.1692640.

[32] Y. J. He *et al.*, "Protease-Sensitive Hydrogel Biomaterials with Tunable Modulus and Adhesion Ligand Gradients for 3D Vascular Sprouting," *Biomacromolecules,* vol. 19, no. 11, pp. 4168-4181, Nov 12 2018, doi: 10.1021/acs.biomac.8b00519.

[33] R. M. Schweller and J. L. West, "Encoding Hydrogel Mechanics via Network Cross-Linking Structure," *ACS Biomater Sci Eng,* vol. 1, no. 5, pp. 335-344, May 11 2015, doi: 10.1021/acsbiomaterials.5b00064.

[34]   S. Sokic and G. Papavasiliou, "Controlled proteolytic cleavage site presentation in biomimetic PEGDA hydrogels enhances neovascularization in vitro," *Tissue Eng Part A,* vol. 18, no. 23-24, pp. 2477-86, Dec 2012, doi: 10.1089/ten.TEA.2012.0173.

[35]   S. Mahadevaiah, K. G. Robinson, P. M. Kharkar, K. L. Kiick, and R. E. Akins, "Decreasing matrix modulus of PEG hydrogels induces a vascular phenotype in human cord blood stem cells," *Biomaterials,* vol. 62, pp. 24-34, Sep 2015, doi: 10.1016/j.biomaterials.2015.05.021.

[36]   J. S. Miller, C. J. Shen, W. R. Legant, J. D. Baranski, B. L. Blakely, and C. S. Chen, "Bioactive hydrogels made from step-growth derived PEG-peptide macromers," *Biomaterials,* vol. 31, no. 13, pp. 3736-43, May 2010, doi: 10.1016/j.biomaterials.2010.01.058.

[37]   E. B. Peters, N. Christoforou, K. W. Leong, G. A. Truskey, and J. L. West, "Poly(ethylene glycol) Hydrogel Scaffolds Containing Cell-Adhesive and Protease-Sensitive Peptides Support Microvessel Formation by Endothelial Progenitor Cells," *Cell Mol Bioeng,* vol. 9, no. 1, pp. 38-54, Mar 1 2016, doi: 10.1007/s12195-015-0423-6.

[38]   R. M. Schweller, Z. J. Wu, B. Klitzman, and J. L. West, "Stiffness of Protease Sensitive and Cell Adhesive PEG Hydrogels Promotes Neovascularization In Vivo," *Ann Biomed Eng,* vol. 45, no. 6, pp. 1387-1398, Jun 2017, doi: 10.1007/s10439-017-1822-8.

[39]   K. Vats, G. Marsh, K. Harding, I. Zampetakis, R. E. Waugh, and D. S. Benoit, "Nanoscale physicochemical properties of chain- and step-growth polymerized PEG hydrogels affect cell-material interactions," *J Biomed Mater Res A,* vol. 105, no. 4, pp. 1112-1122, Apr 2017, doi: 10.1002/jbm.a.36007.

[40]   J. Kim, Y. P. Kong, S. M. Niedzielski, R. K. Singh, A. J. Putnam, and A. Shikanov, "Characterization of the crosslinking kinetics of multi-arm poly(ethylene glycol) hydrogels formed via Michael-type addition," *Soft Matter,* vol. 12, no. 7, pp. 2076-85, Feb 21 2016, doi: 10.1039/c5sm02668g.

[41]   S. J. Grainger, B. Carrion, J. Ceccarelli, and A. J. Putnam, "Stromal cell identity influences the in vivo functionality of engineered capillary networks formed by co-delivery of endothelial cells and stromal cells," *Tissue Eng Part A,* vol. 19, no. 9-10, pp. 1209-22, May 2013, doi: 10.1089/ten.TEA.2012.0281.

[42]   Y. C. Chiu *et al.*, "The role of pore size on vascularization and tissue remodeling in PEG hydrogels," *Biomaterials,* vol. 32, no. 26, pp. 6045-51, Sep 2011, doi: 10.1016/j.biomaterials.2011.04.066.

[43]   F. Mannello, "Serum or plasma samples? The "Cinderella" role of blood collection procedures: preanalytical methodological issues influence the release and activity of circulating matrix metalloproteinases and their tissue inhibitors, hampering diagnostic trueness and leading to misinterpretation," *Arterioscler Thromb Vasc Biol,* vol. 28, no. 4, pp. 611-4, Apr 2008, doi: 10.1161/ATVBAHA.107.159608.

[44]   X. Hu and C. Beeton, "Detection of functional matrix metalloproteinases by zymography," *J Vis Exp,* no. 45, Nov 8 2010, doi: 10.3791/2445.

Chapter 6 – Cell-encapsulating PEG-based Microbeads for Vascularization Applications

6.1 Introduction

Restoring blood flow to ischemic regions following tissue damage remains a significant clinical challenge in treating a variety of diseases and injuries, especially cardiovascular disease (CVD). CVD results from atherosclerotic plaque buildup in blood vessels, reducing blood flow to specific tissues, such as the heart in cases of coronary heart disease (CHD) or lower extremities in cases of peripheral artery disease (PAD). This lack of blood flow often results in cell death that progresses to loss of tissue function. In the United States alone, 20.1 million adults over the age of twenty have CHD and approximately 6.5 million adults over the age of forty have PAD, resulting in a high economic burden associated with disease management [1]. While revascularization strategies exist, such as bypass surgery or stenting, many patients are ineligible for these procedures due to high incidence of comorbidities, such as diabetes, coronary artery disease, neurological disorders, and cerebrovascular disease [2]. This has led to an increased demand for effective strategies for tissue repair and replacement; however, efforts to repair ischemic tissues utilizing drug therapies or direct cell delivery have been met with minimal clinical success [3-6]

Proangiogenic growth factor delivery strategies aimed at promoting new blood vessel formation in ischemic tissues have shown promising preclinical outcomes [7]; however, challenges regarding growth factor over expression, adverse health effects, sort half-life, limited retention at the injury sight, and a lack of knowledge of the appropriate route and dosage have limited the clinical potential of these therapies [8]. Furthermore, the delivery of only a single growth factor

may fail to recapitulate the complex growth factor cascade required for angiogenesis [8]. Cell delivery approaches have the potential to overcome some limitations of proangiogenic factors but have been plagued by low cell retention at the target site and reduced cell viability due to the harsh ischemic environment. To improve cell engraftment, researchers have explored the delivery of cells, some of which are capable of vasculogenic self-assembly, within hydrogels. Though, even when cell engraftment is improved, implanted cells can experience apoptosis as diffusion of the necessary nutrients is limited within large tissue constructs *in vivo* without timely supply of oxygen and nutrients [9, 10].

Microbeads may overcome some of the limitations of current cell-based therapies by minimizing mass transfer limitations and protecting cells during delivery via injection. Further, prevascularization of these microbeads *in vitro* may lead to more rapid microvascular network formation and inosculation with host blood supply upon implantation *in vivo* [11-14]. While previous studies have shown the potential to vascularize microbeads made of natural materials, these materials are often derived from animal sources and can exhibit batch-to-batch variability which may pose potential barriers to translation. Previous work from our group has shown the potential of pre-cultured fibrin-based microbeads to restore perfusion to ischemic tissue [11]. Despite these promising findings, cell-laden fibrin microbeads tended to aggregate with extended pre-culture, limiting injectability of prevascularized modules.

Synthetic materials offer advantages over natural materials, such as precise control over material properties and high reproducibility. Poly(ethylene glycol), or PEG, has emerged as a promising material for tissue engineering applications due to its ability to be functionalized with various end groups, affording relatively easy customization of hydrogel properties [15, 16]. PEG-based hydrogels have a demonstrated ability to support microvascular networks *in vitro* [17-22]

and *in vivo* [23]. PEG-based microbeads (also referred to as microgels, microspheres, or microparticles in the literature) are an established technology for tissue engineering applications such as biomolecule delivery [24-30] and as building blocks for larger hydrogel scaffolds, such as the increasingly popular microporous annealed particle (or MAP) hydrogels [31]; however, few studies utilize PEG microbeads for cell encapsulation or tissue development prior to transplantation, with even fewer in the focusing on vascularization efforts.

In this study, endothelial and stromal cells were encapsulated in degradable, cell-adhesive PEG-norbornene (PEGNB) microbeads via flow-focusing microfluidic droplet generation. We assessed the potential of these microbeads to support the formation of microvascular networks both within and emerging from the microbeads when embedded in larger tissue mimics *in vitro*. Microbeads were implanted into subcutaneous pockets on the dorsal flanks of SCID mice to evaluate the potential of these microbeads as a modular platform for cell delivery and vascularization.

6.2 Materials and Methods

6.2.1 Cell culture

Human umbilical vein endothelial cells (HUVEC) were isolated from umbilical cords from the University of Michigan Mott Children's Hospital as previously described [32]. Umbilical cords were obtained by a process considered exempt by the University of Michigan's Institutional Review Board (notice of determination dated August 21, 2014) because the tissue is normally discarded, and no identifying information is provided to the researchers who receive the cords. HUVEC were cultured in fully supplemented EGM2 (Lonza, Inc., Walkersville, MD). HUVEC were used from passages 4-7. Normal human lung fibroblasts (NHLF; Lonza) were cultured in

Dulbecco's modified eagle medium (DMEM; Gibco, Waltham, MA) supplemented with 10% fetal bovine serum (FBS; Gibco). NHLF were used from passage 10-15. All cells were cultured at 37 °C and 5% CO_2 with media replacement every two days.

6.2.2 Microfluidic droplet generation of PEGNB microbeads

Poly(ethylene glycol)-norbornene (PEGNB) microbeads were formed via thiol-ene photopolymerization [33]. 4-arm PEGNB (20 kDa; Creative PEGWorks, Durham, NC) and lithium phenyl-2,4,6-trimethylbenzoylphosphinate ("LAP"; Sigma-Aldrich, St. Louis, MO) were purchased from commercial sources that provide the percent substitution of norbornene by NMR and purity by HPLC, respectively. The thiol containing adhesive peptide Ac-CGRGDS-NH2 ("RGD"; AAPPTEC, Louisville, KY) and dithiol containing matrix metalloproteinase- (MMP-) sensitive crosslinking peptide Ac-GCRDVPMS↓MRGGDRCG-NH2 ("VPMS", cleavage site indicated by ↓; AAPPTEC), which contain an N-terminal acetylation and a C-terminal amidation, were dissolved in 25 mM acetic acid, filtered through 0.22 µm filters (Sigma-Aldrich), lyophilized for 48 h, and stored in a desiccator at -20 °C. The thiol content (purity) of each batch of peptide aliquots was determined using Ellman's reagent (Thermo Fisher, Waltham, MA). PEGNB and LAP were suspended in serum free EGM2 (SF-EGM2) and sterile filtered through 0.22 µm filters to create fresh stocks at desired concentrations for each experiment. Peptides were also resuspended in SF-EGM2 to reach desired concentrations.

A flow-focusing microfluidic device was used to encapsulate cells in PEGNB microbeads (Fig. 1). The discontinuous phase consisted of 20×10^6 total cells/mL in a 1:1 HUVEC:NHLF ratio suspended in a precursor solution comprised of 3 wt. % PEGNB (w/v), 0.1% LAP (w/v), 0.1% Pluronic F68 (v/v; Gibco), 1 mM RGD, 2.25 mM VPMS (90% crosslinked, 0.9 thiols per norbornene after accounting for RGD concentration), and SF-EGM2. The continuous phase

consisted of 0.5% FluoroSurfactant (008-FluoroSurfactant; RAN Biotechnologies, Beverly, MA) in NOVEC-7500 (Best Technology Inc., Minneapolis, MN). Microbead precursor solutions and fluorinated oil were loaded into glass syringes (Hamilton Company, Reno, NV) and injected into the microfluidic device via syringe pumps at constant flow rates of 15 µL/min and 30 µL/min, respectively. The syringe containing the cellular precursor solution was placed vertically and contained a small magnetic stir bar (6mm x 3mm; Big Science Inc., Huntersville, NC), which was continuously stirred using an adjacent stir plate to prevent cell settling throughout droplet generation. Microbeads were collected in a well of a standard 24-well plate and polymerized with a 6-Watt LED 365 nm Gooseneck Illuminator (AmScope, Feasterville, PA) set to max intensity for 90 s, corresponding to approximately 50 mW/cm^2.

Microbeads were collected via repeated on-strainer rinses. First, microbeads were rinsed three times with DMEM containing 10% FBS and 1% Pluronic F68 on a 40 µm cell strainer (Fisher). Then, microbeads were rinsed three times with DMEM containing 10% FBS on the strainer. Microbeads were transferred to a vented 50 mL conical tube with a filter (CELLTREAT Scientific Products, Shirley, MA) containing 20 mL of warmed fully supplemented EGM2. Microbeads were cultured in suspension for up to 7 days. Media was changed the day after, then every other day for 7 days.
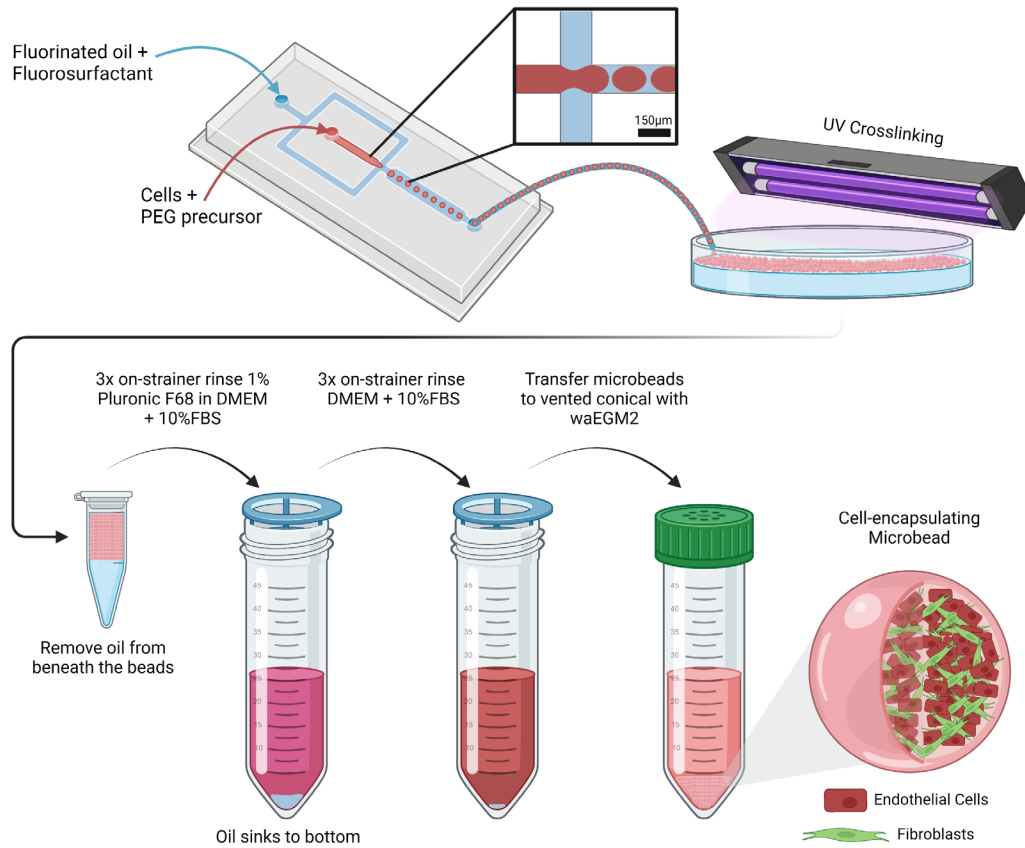
Figure 6.1:Fabrication of cell-encapsulating microbeads. *Microbeads were fabricated via microfluidic droplet generation. After UV crosslinking, microbeads were isolated from the oil using repeated on-strainer rinses before being cultured in EGM2.*

6.2.3 Vasculogenesis assay

Microbeads were embedded in bulk fibrin hydrogels to imitate a 3D model of vasculogenesis, as previously described [17, 18]. Culture media above the settled microbeads was aspirated, leaving only microbeads in a small volume of media. Constructs were made by mixing varying volumes of microbeads were with SF-EGM2, FBS (10% final), thrombin (1 U/mL final), and fibrinogen stock solution (2.5 mg/mL final clottable protein). Then, 500 μL or 250 μL of the microbead-protein mixture was added per well of a standard 24-well or 48-well culture plate, respectively, and incubated at room temperature for 5 min before being placed in the incubator for

25 min at 37 °C. EGM2 (0.5-1 mL/well) was added to each hydrogel after the complete gelation process. Media was changed the day after, then every other day for 7 days.

6.2.4 Fluorescent imaging and quantification

After overnight swelling, viability of cells encapsulated in the microbeads was assessed using a Live/Dead cell imaging kit (Fisher: Invitrogen). On days 1, 3, 5, or 7, microbeads in suspension and fibrin hydrogels were fixed with zinc formalin (Z-fix; Anatech, Battle Creek, MI) for 10 min, then washed three times with 1X Tris-buffered saline (TBS) for 5 min. Hydrogels were stained overnight with rhodamine-conjugated lectin from Ulex europaeus agglutinin I (UEA, 1:200; Vector Laboratories, Newark, CA), 4', 6-diamidino-2-phenylindol (DAPI, 1 μg/mL; Thermo Fisher, Waltham, MA), and AlexaFluor 488 phalloidin (1:200; Thermo Fisher, Waltham, MA) which label endothelial cells, cell nuclei, and F-actin, respectively. Samples were rinsed overnight with TBS prior to imaging. Confocal z-stacks (4x, 10x, 20x, 40x) were acquired using an Olympus IX81 microscope equipped with a disk-scanning unit (DSU; Olympus America, Center Valley, PA) and Metamorph Premier software (Molecular Devices, Sunnyvale, CA). Z-series stacks were collapsed into maximum intensity projections using Fiji [34]. Quantification of cell density was performed on 4x brightfield images. Quantification of preformed microvascular structures within pre-cultured microbeads was performed on 150 μm stacks (25 μm/slice, 7 slices/stack) imaged at 4x magnification. Quantification of angiogenic sprouting from microbeads cultured in fibrin bulk gels was performed on single-plain 4x scan slides of the entire 24- or 48-well plate wells.

6.2.5 Immunofluorescent staining and imaging

For immunofluorescent staining of basement membrane proteins, microbeads in suspension and fibrin hydrogels were fixed with Z-fix at days 1, 3, 5, or 7 as described above. Samples were permeabilized with 0.5% v/v Triton X-100 (Thermo Fisher) in TBS for one hour, rinsed four times for 5 min with 0.1% v/v Tween-20 (Thermo Fisher) in TBS (TBS-T), and blocked overnight at 4 °C in antibody diluting (AbDil) solution consisting of 2% w/v bovine serum albumin (BSA; Sigma-Aldrich, St. Louis, MO) in TBS-T. Gels were incubated with primary antibodies for collagen IV (1:500, mouse IgG1; Thermo Fisher) or laminin beta-1 (1:500, rabbit IgG; Thermo Fisher) diluted in AbDil solution overnight at 4 °C. Gels were washed three times for 5 min and rinsed overnight at 4 °C with TBS-T. Gels were stained with appropriate secondary antibodies, AlexaFluor 488 goat anti-mouse (1:200, IgGH+L; Thermo Fisher) or AlexaFluor 488 goat anti-rabbit (1:200, IgGH+L; Thermo Fisher), diluted in TBS-T and UEA and DAPI, as described above, overnight at 4 °C. Gels were rinsed overnight at 4 °C with TBS-T prior to imaging. Representative images were acquired at 4x and 10x magnification using the DSU and presented as maximum intensity projections.

6.2.6 Preparation of subcutaneous implants

Subcutaneous implants contained either a bulk suspension of HUVEC and NHLF or cellular microbeads in 500 µL fibrin hydrogels. Hydrogels were prepared as either precursor solutions for injection or preformed pucks for insertion. Fibrin hydrogel precursor solutions were comprised of SF-EGM2, FBS (10% final), thrombin (1 U/mL final), and fibrinogen stock solution (2.5 or 5.0 mg/mL final clottable protein). For injections, solutions were rapidly mixed, transferred into a 3 mL syringe fitted with a 23G needle, and injected into the animal. Preformed pucks were gelled in PDMS molds containing a 12 mm well (formed with a biopsy punch) on hydrophobic

coated (Sigmacote; Sigma-Aldrich) glass, the PDMS was removed, and the pucks were inserted into the animal.

6.2.7 Subcutaneous implants

Animals were anesthetized with vaporized isoflurane (1-5%) and prophylactic analgesia, carprofen (5 mg/kg), was administered to each animal via subcutaneous injection. Body temperature was maintained on a heating pad throughout the entirety of the surgical procedure. Ophthalmic ointment was added to the eyes of each mouse with a cotton swab. Dorsal lumbar flanks were shaved and depilatory agent (Nair; Fisher Scientific) was applied to remove remaining hair. The shaved area was sterilized by alternating Betadine (Thermo Fisher Scientific) and alcohol rinses, each repeated three times. A sterile surgical field was created using a sterile fenestrated drape, sterile tools were placed on the sterile field, and sterile gloves were donned prior to beginning the surgical procedure. For injections, the samples were prepared, mixed, and injected subcutaneously on the dorsal flank of the mouse under the skin tented with sterile forceps. The needle was left in the injection site for 30 s to allow for initial gelation of the solution prior to removal. Animals remained anesthetized for 20 min to allow for further gel polymerization. For preformed pucks, an incision (~1.5 cm) in the skin was made and surgical scissors were used to cut away the fascia from the skin. Pucks were inserted using a sterile spatula and cotton swab. Once inserted, the skin incision was closed using 5-0 nylon sutures (Oasis, Mettawa, IL). Mice were allowed to recover from the anesthesia before being placed in their normal housing. An additional dose of carprofen was administered to each animal 24 h after surgery, then daily as needed if animals had abnormal appearance.

6.2.8 Implant retrieval and post-processing

After 7 days, animals were euthanized via isoflurane overdose followed by secondary pneumothorax. Implants and the surrounding muscle tissue were excised with scissors and forceps, placed immediately in 20 mL glass scintillation vials with zinc formalin (Z-fix) and subsequently fixed for overnight at 4°C before being embedded in paraffin wax (for paraffin sectioning) or O.C.T. (for cryosectioning). For paraffin sectioning, implants were submerged in 70% ethanol and stored at 4°C until further processing. Samples were then placed in tissue cassettes (Unisette Tissue Cassettes, Simport, Canada), embedded in paraffin in a KD-BMII tissue embedding center (IHC World, Ellicott City, MD), and sectioned through their entire volume with a Thermo Scientific HM 325 rotary microtome (5 μm sections) for further analysis. For cryosectioning, implants were placed in 15% sucrose in PBS for 6 hours, then 30% sucrose in PBS overnight. Samples were then embedded in O.C.T. (Fisher Scientific) with 30% sucrose and flash frozen using dry ice pellets in 2-methyl butane (Fisher Scientific). Implants were sectioned through their entire volume with a Leica CM3050 S cryostat (10 μm sections) for further analysis.

6.2.9 Hematoxylin and eosin (H&E) staining

Paraffin sections were stained with Mayer's hematoxylin (Electron Microscopy Sciences, Hatfield, PA) and eosin Y (Sigma-Aldrich). Slides were deparaffinized with xylene twice (5 min/wash) and then transferred to 100%, 95%, 70% ethanol, and deionized water baths (3 min/wash, two baths per ethanol concentration). Slides were submerged in a hematoxylin bath for 15 min, and then rinsed with tap water for an additional 15 min. Slides were then placed in 95% ethanol for 30 s, followed by submersion in eosin Y for 1 min. Slides were subsequently transferred into a 95% ethanol bath for 1 min, and two separate 100% ethanol baths (1 min/bath) and two separate xylene baths (3 min/wash) to dehydrate the samples. Toluene mounting solution

(Permount; Electron Microscopy Sciences) was added to each slide prior to covering samples with coverslips. Slides dried overnight prior to imaging.

6.2.10 Human CD31 (hCD31) staining

The center of each implant paraffin embedded was determined by the largest cross-sectional area of H&E-stained explanted tissue sections. The subsequent serial section of each implant was then deparaffinized with xylene and rehydrated through a series of graded ethanol washes, ending with water. Slides were placed in 1x antigen retrieval solution (Agilent Dako, Santa Clara, CA) and placed in a steamer (95-99°C) for 35 min. The antigen retrieval solution and slides were removed and equilibrated to room temperature. Slides were rinsed 3x with 0.1% Tween-20 in tris-buffered saline (TBS-T) for 2 min. The area around the tissue was marked with an ImmEdge Hydrophobic Barrier PAP pen (Vector Laboratories). The Dako EnVision System-HRP kit (Agilent Dako, Santa Clara, CA) was utilized for hCD31 and α-SMA staining. First, tissues were incubated with peroxidase blocking solution for 5 min at room temperature. For human CD31 (hCD31) labeling, a mouse anti-human CD31 monoclonal antibody (Agilent Dako) diluted 1:50 in TBS-T was used as the primary antibody, incubated at 4 °C overnight. The HRP-conjugated secondary antibody solution was added to each sample and incubated at room temperature for 30 min. Samples were then incubated with DAB+ substrate-chromogen solution for 5 min at room temperature. Samples were counter-stained with hematoxylin for 15 min, washed in tap water for 15 min, then dehydrated with 95% ethanol, 100% ethanol, and xylene washes as described above. Toluene mounting solution was added prior to covering the samples with coverslips. Slides dried overnight prior to imaging.

6.2.11 Immunofluorescent staining of tissue sections

Cryosections were permeabilized with 0.5% v/v Triton X-100 (Thermo Fisher) in TBS with two 10 min washes, then rinsed three times with TBS for 1 min. Tissue sections were stained overnight with UEA (1:200), 4', DAPI (1 µg/mL), and AlexaFluor 488 phalloidin (1:200). Samples were rinsed three times with TBS for 1 min then overnight with TBS. SlowFade Gold Antifade Mountant (Fisher Scientific: Invitrogen) was added to the tissue sections prior to covering the samples with coverslips and sealing the edges with clearcoat nail polish.

6.2.12 Statistics

Statistical analysis was performed using Prism (GraphPAD, La Jolla, CA). Data are represented as mean ± standard deviation of at least three independent experimental replicates. Data were analyzed using one- or two-way ANOVA with Tukey post-hoc testing with pre-specified comparisons between conditions on a given day. A value of $p \leq 0.05$ was considered significant.

6.3 Results

6.3.1 PEGNB microbeads support high cell viability of encapsulated HUVEC and NHLF

A flow focusing microfluidic device was used to produce cell-laden PEGNB microbeads. After overnight swelling, referred to as day 1 pre-cultured (D1 PC), microbeads had an average diameter of 231.8 ± 9.7 µm. Microbeads contained both fibroblasts and UEA-positive endothelial cells distributed throughout the interior of the microbeads (Fig. 6.2D) that displayed high viability 24 h post-encapsulation (Fig. 6.2B). Cell density per microbead was quantified as high, medium, low, or empty if greater than 50%, between 25-50%, less than 25%, or none of the microbead was

occupied by cell bodies on phase imaging (Fig. 6.2A, C). Roughly half of all microbeads had medium or high cell density, with the greatest percentage of beads (40.8%) having low cell density.
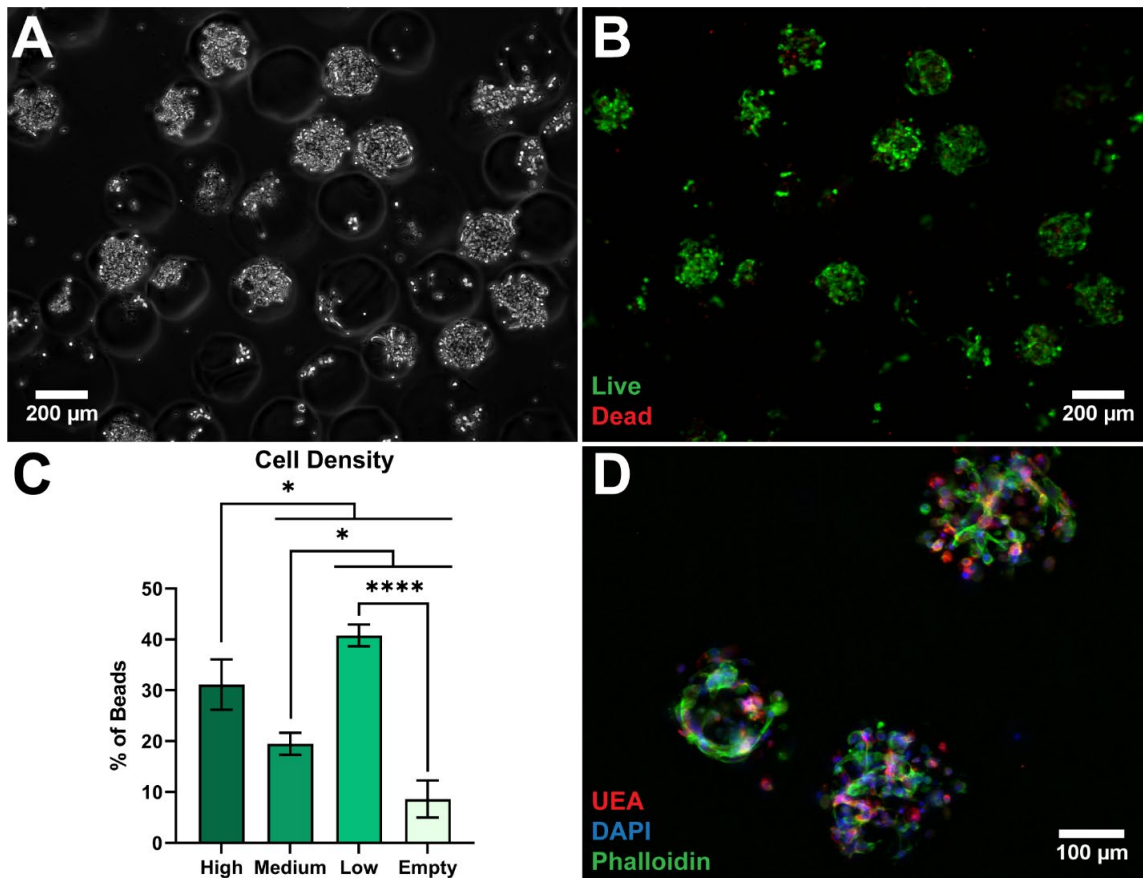
Figure 6.2: Endothelial and stromal cells were distributed throughout D1 PC microbeads. *(A) Phase and (B) live/dead staining of D1 PC microbeads. (C) Cell distribution throughout microbeads; *: p < 0.05, ****: p < 0.0001, N = 3 batches. (D) Representative max intensity projection (Z = 150 µm) of HUVEC and NHLF distributed throughout D1 PC microbeads.*

6.3.2 Microbeads catalyze the formation of microvascular networks in bulk fibrin hydrogels in vitro

D1 PC microbeads were embedded in larger tissue mimics and cultured *in vitro* for 7 days. Stromal cells and vessel-like structures invaded the surrounding matrix (Fig. 6.3A). The basement membrane component collagen IV was present and localized to UEA-positive vessel structures (Fig. 6.3B). Higher magnification images revealed close peri-vascular localization of stromal cells,

as evidence by UEA-negative DAPI and phalloidin along vessel-like structures (Fig. 6.3C and D).

Vessel structures also contained hollow lumens between UEA-positive vessel walls (Fig. 6.3E).
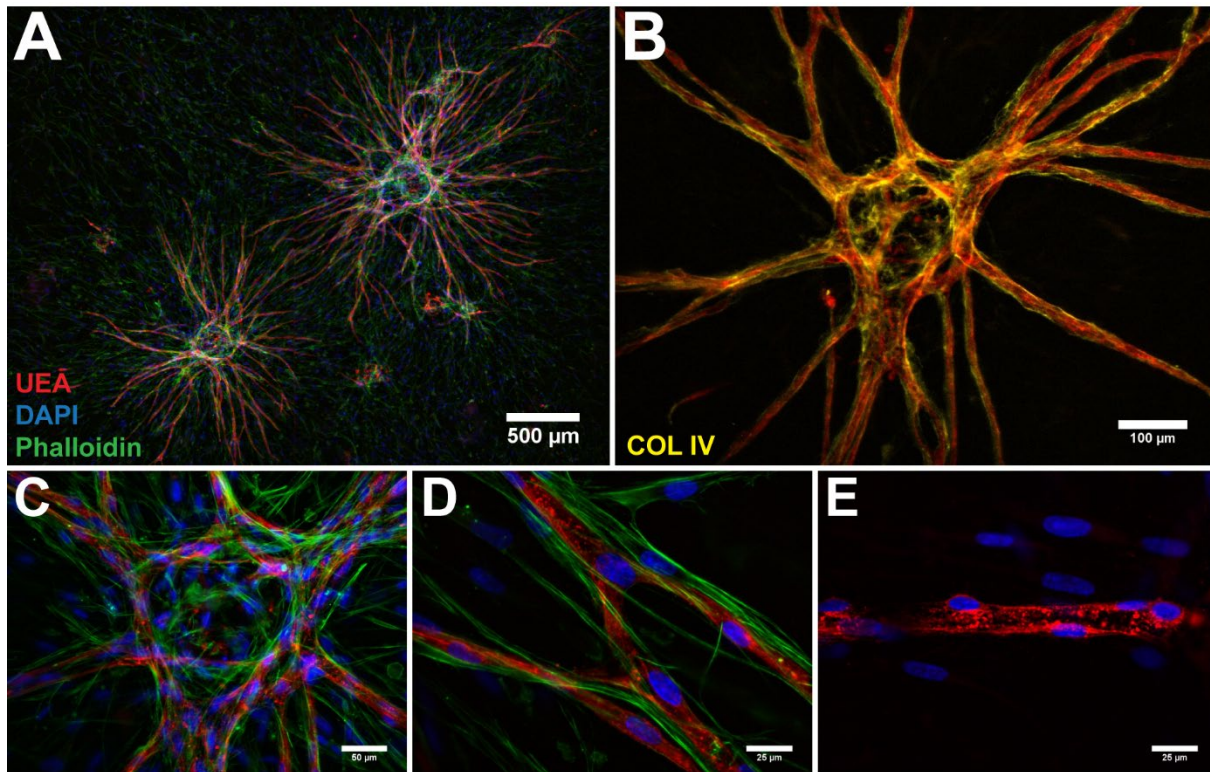
Figure 6.3: D1 PC microbeads vascularize tissue mimics in vitro. *(A) Vessel structures and stromal cells sprout from microbeads after 7 days of culture. (B) Basement membrane, COL IV, deposition was localized to vessel structures. (C, D) NHLF were closely associated with vessel structures. (E) Hollow lumen formation was demonstrated through laser confocal microscopy at middle slice of vessel structures.*

By increasing the volume fraction of microbeads encapsulated in bulk fibrin hydrogels, vessel density was increased within tissue constructs (Fig. 6.4). Including greater than 5% volume fraction of microbeads resulted in robust microvascular networks that were well-distributed throughout the entirety of the hydrogel.
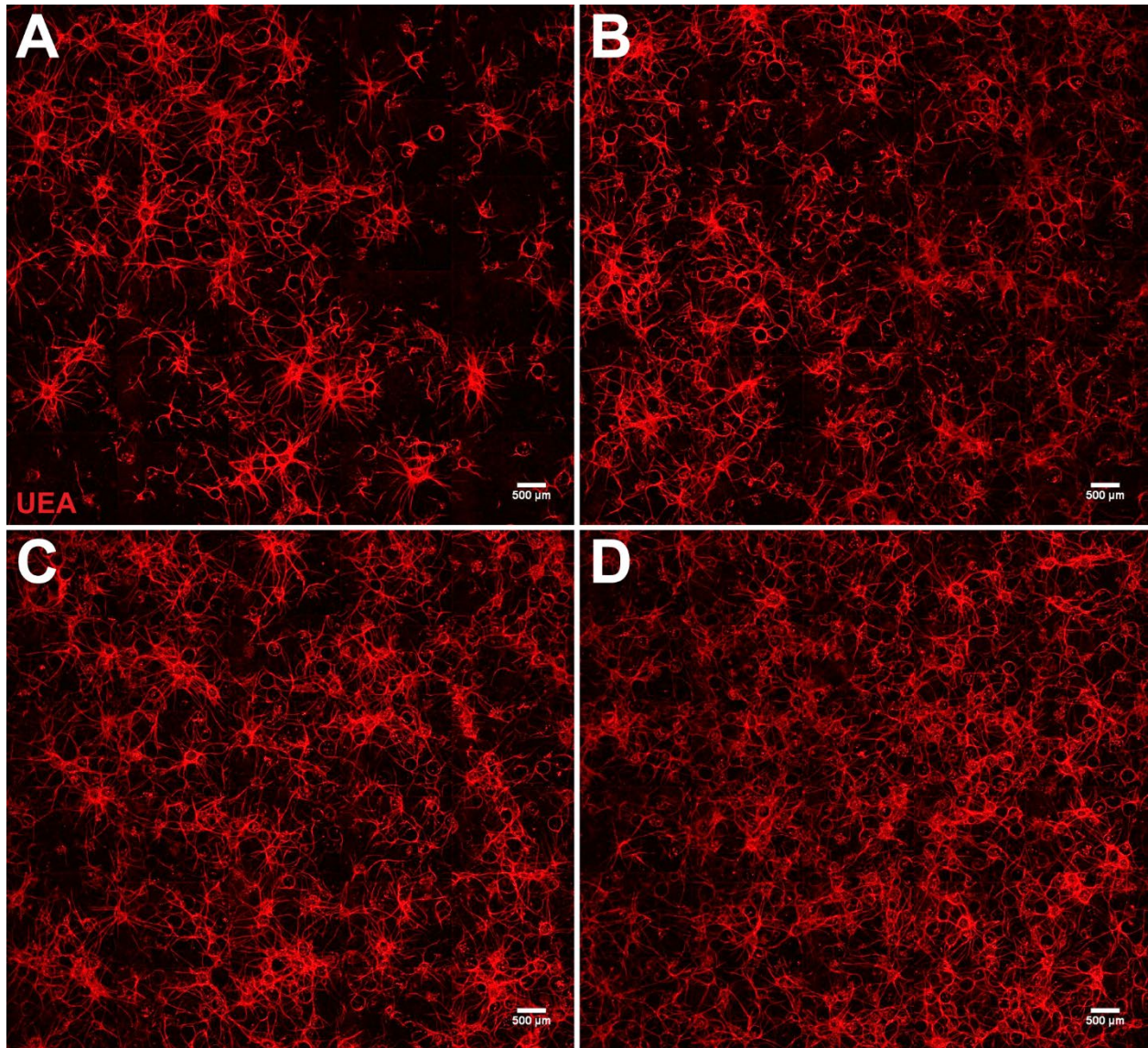
Figure 6.4: Microbeads form robust, well-distributed microvascular networks. *Whole gel scan slides of fibrin hydrogels containing (A) 5%, (B) 10%, (C) 15%, and (D) 20% volume fraction of microbeads.*

D1 PC microbeads were embedded in 2.5, 5.0, 7.5, and 10.0 mg/mL fibrin hydrogels to assess how the surround matrix density influenced vessel sprouting (Fig 6.5). Increased fibrin density attenuated overall sprouting; however, sprouting still occurred in the highest density fibrin (Fig. 6.5D). As fibrin density was increased, vessel structures remained more closely localized to the surface of microbeads despite the fibroblasts having invaded the matrix.
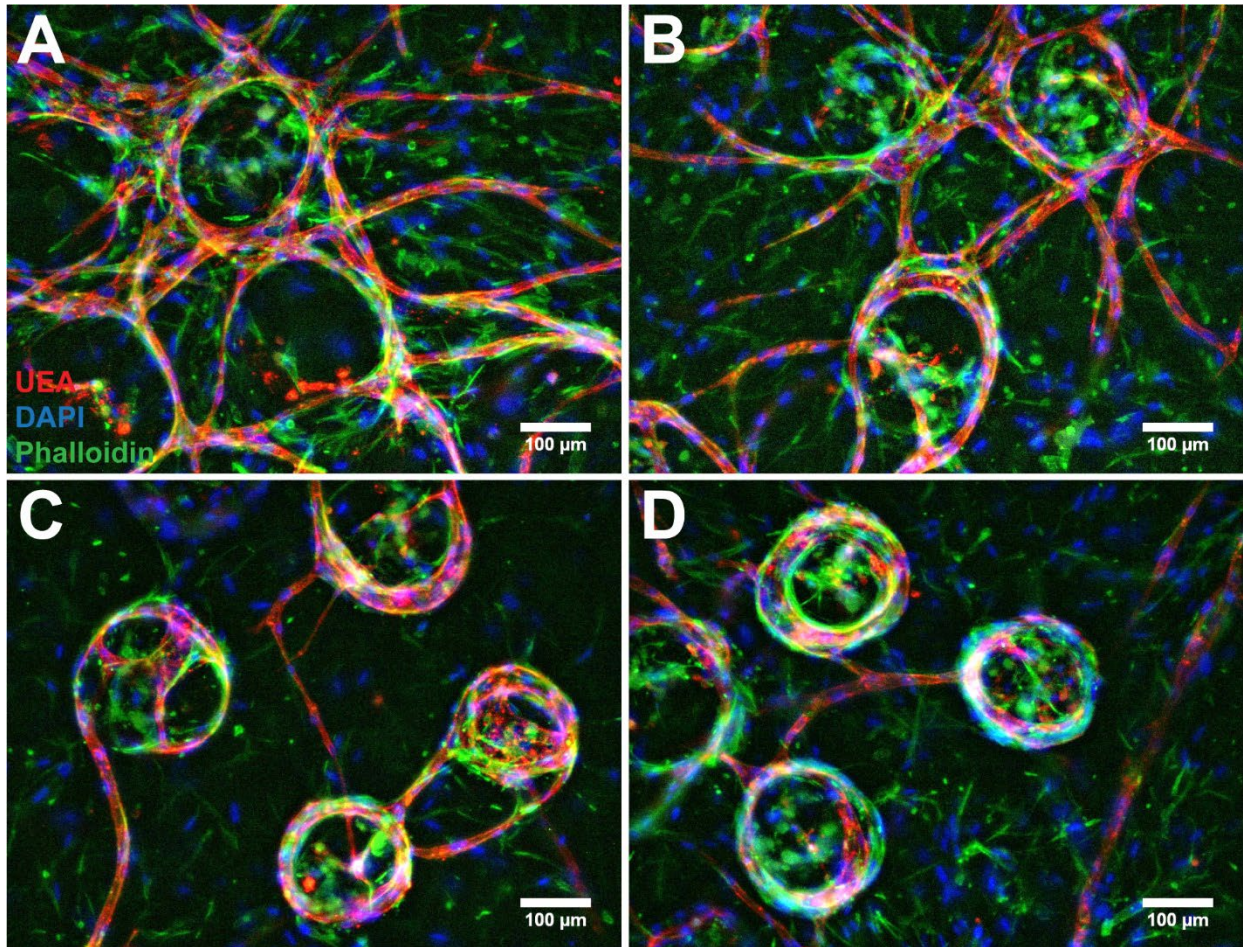
Figure 6.5: Microbeads vascularize high density fibrin hydrogels. *Representative max intensity projections (Z = 150 μm) of D1 PC microbeads cultured in (A) 2.5, (B) 5.0, (C) 7.5, and (D) 10.0 mg/mL fibrin hydrogels.*

6.3.3 Extended pre-culture of microbeads permits the formation of primitive microvascular networks within microbeads

To determine if microbeads have material properties that can support vessel formation within the microbead matrix prior to embedding or injecting them, microbeads were subjected to extended culture in suspension for up to 7 days. Quantification of the percentage of microbeads containing primitive vessel-like structures revealed that the majority (72%) of cell containing microbeads had evidence of primitive vessel-like structures present throughout the beads as early as 3 days (Fig. 6.6A and B). These structures persisted through 7 days of pre-culture (Fig. C and

D). UEA-negative phalloidin staining appeared mainly localized to the outside of the microbeads, suggesting fibroblast may have migrated to the exterior of the microbeads as the endothelial cells assembled into vessel-like structures inside.
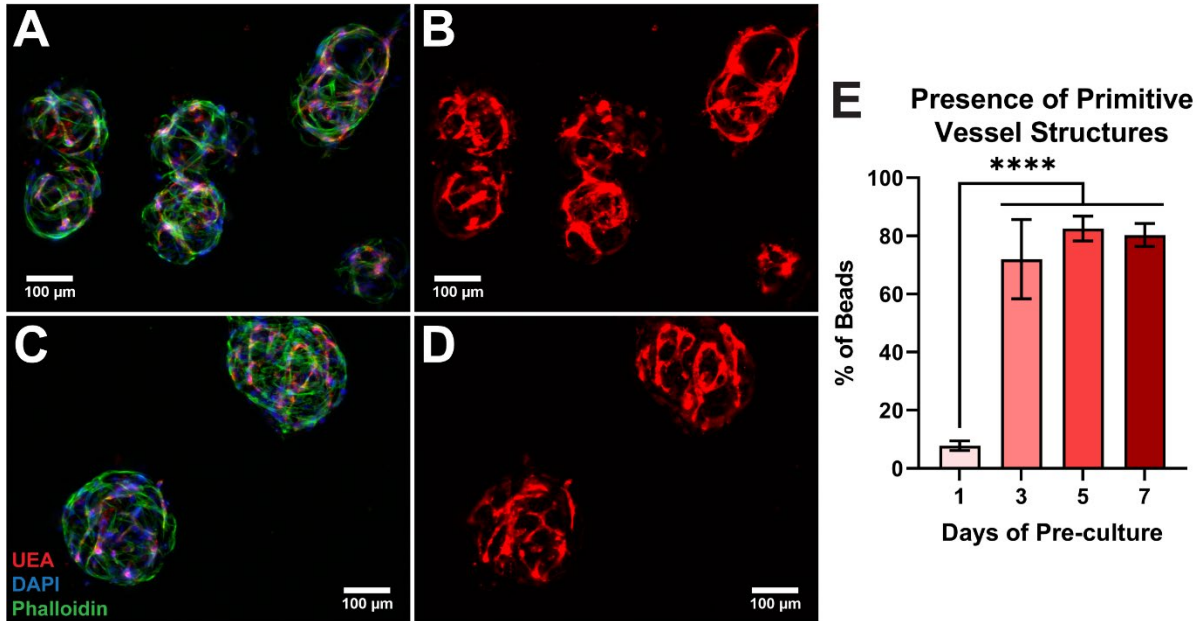
Figure 6.6: Microbeads support prevascularization through extended suspension culture. *Representative max intensity projections (Z = 100 μm) of microbeads cultured in suspension for (A, B) 3 and (C, D) 7 days. (E) Quantification of primitive vessel-like structures within cellular microbeads; ****: p < 0.0001, N = 3 batches.*

Furthermore, immunostaining for basement membrane components collagen IV (Fig. 6.7A) and laminin beta-1 (Fig. 6.7B) showed an increase in the presence of both proteins with increased pre-culture duration indicting an increase in vessel maturation. While laminin beta-1 was more broadly dispersed throughout microbeads, collagen IV was closely localized to UEA-positive vessel-like structures within the microbeads.
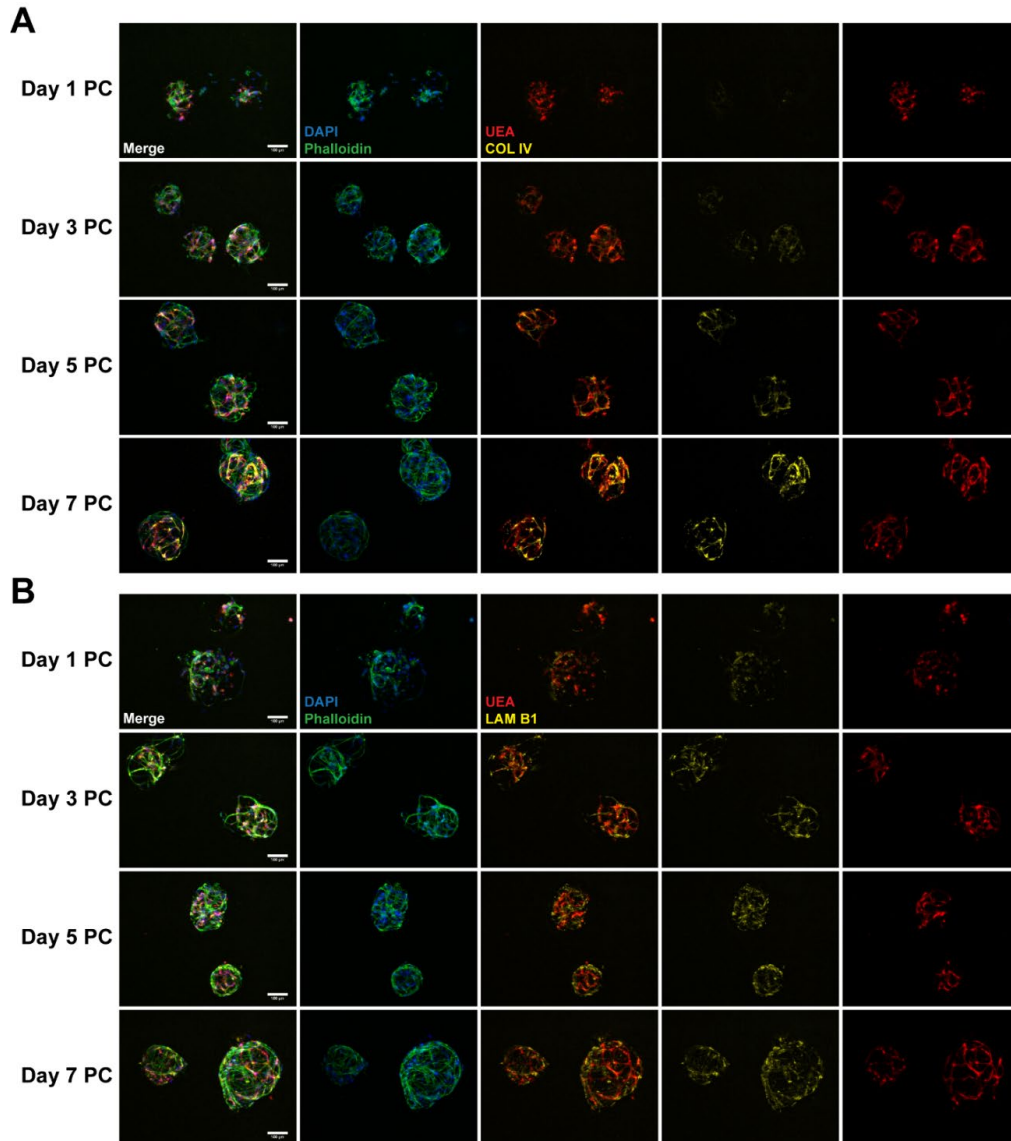
Figure 6.7: Prevascularization of microbeads enhances basement membrane deposition. Representative max intensity projections (Z = 100 μm) of (A) collagen IV and (B) laminin beta-1.

6.3.4 Increased pre-culture duration diminishes angiogenic sprouting in vitro

Pre-cultured microbeads were embedded in fibrin hydrogels and fixed after 3, 5 and 7 days of culture to determine if prevascularization facilitates earlier angiogenic sprouting compared to lesser pre-culture times. On the contrary, sprouting was attenuated as pre-culture duration was increased (Fig. 6.8A-H). Quantification of this sprouting revealed that increased pre-culture time delayed sprouting at early timepoints, and after a week of culture in fibrin, microbeads pre-cultured

for 7 days prior to embedded had significantly less sprouting than day 1 pre-cultured microbeads (Fig. 6.8I).
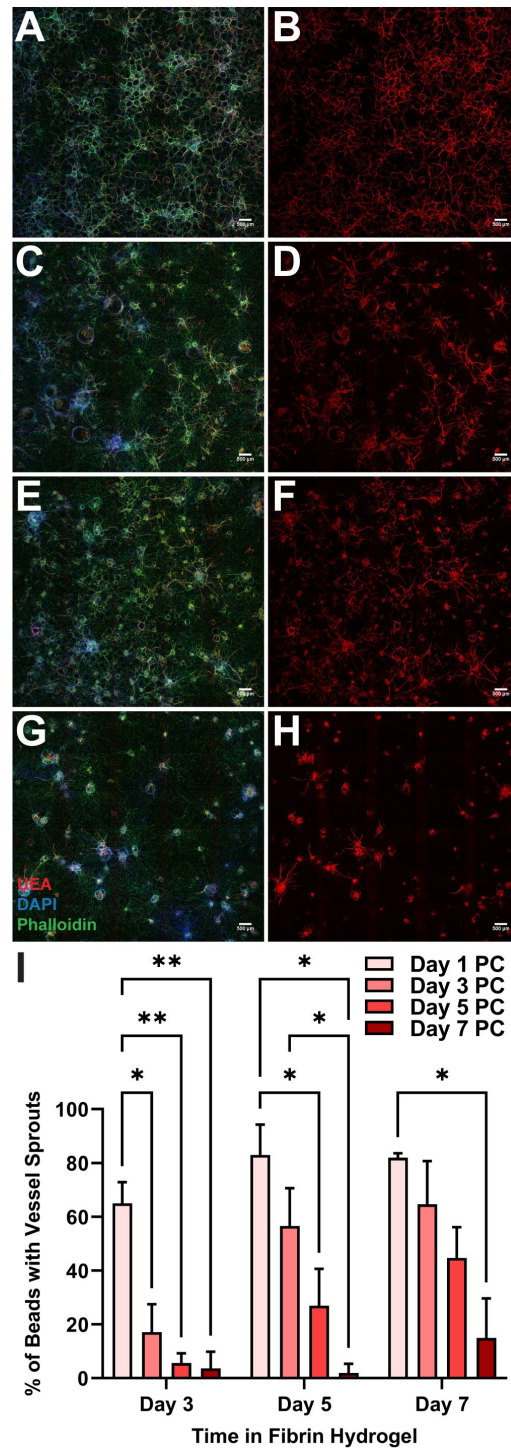
Figure 6.8: Prevascularized microbeads have decreased angiogenic sprouting. *Whole gel scan slides of (A, B) D1, (C, D) D3, (E, F) D5, and (G, H) D7 PC microbeads cultured in fibrin hydrogels for 7 days. (I)*

Quantification of angiogenic sprouting from pre-cultured microbeads; *: p < 0.05, **: p < 0.01, N = 3 batches.

Maximum intensity projection images of non-sprouting microbeads (Fig. 6.9) suggested that while vessels structures may have been present within pre-cultured microbeads at the time of embedding, which may have continued to develop shortly after, the UEA-positive structures within the microbeads appeared to collapse over culture time in fibrin hydrogels. This is seen within all pre-culture conditions, which appear to have more dispersed, puncti-like UEA staining in the interior of beads after extended culture in fibrin, despite fibroblasts invading the surrounding matrix.
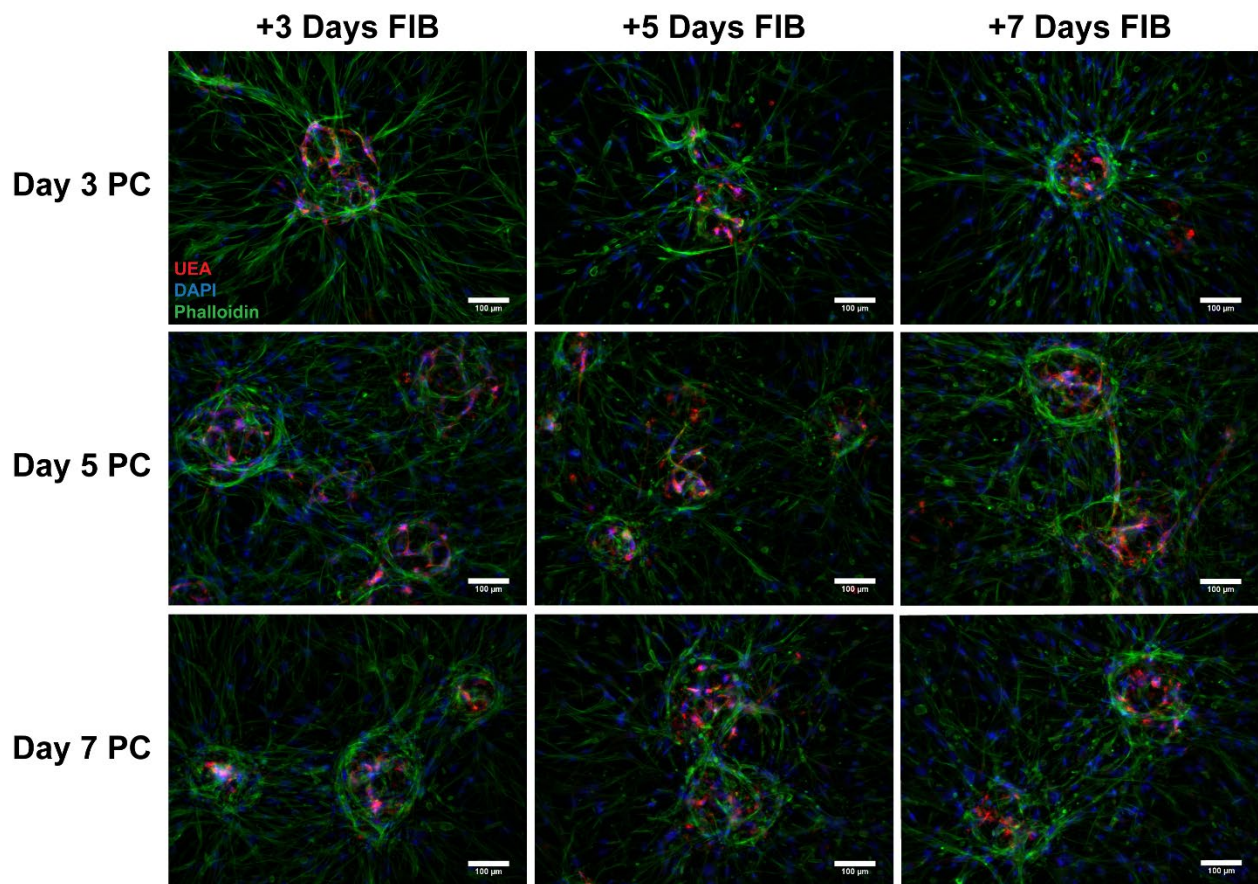
Figure 6.9: Vessel-like structures breakdown in non-sprouting pre-cultured microbeads. *Representative max intensity projections (Z = 100 μm) of non-sprouting microbeads.*

Non-sprouting microbeads were stained for collagen IV and laminin beta-1 (Fig. 6.10) to assess if fibroblasts had deposited basement membrane around the surface of microbeads throughout pre-culture, potentially creating a barrier that may contribute to the reduction of angiogenic sprouting. Collagen IV remained localized to the interior of microbeads and appeared to concurrently breakdown with the collapse of vessel-like structures throughout culture in fibrin hydrogels (Fig. 6.10A). Laminin beta-1was more closely localized to migrating fibroblasts that invaded the surrounding matrix (Fig. 6.10B).
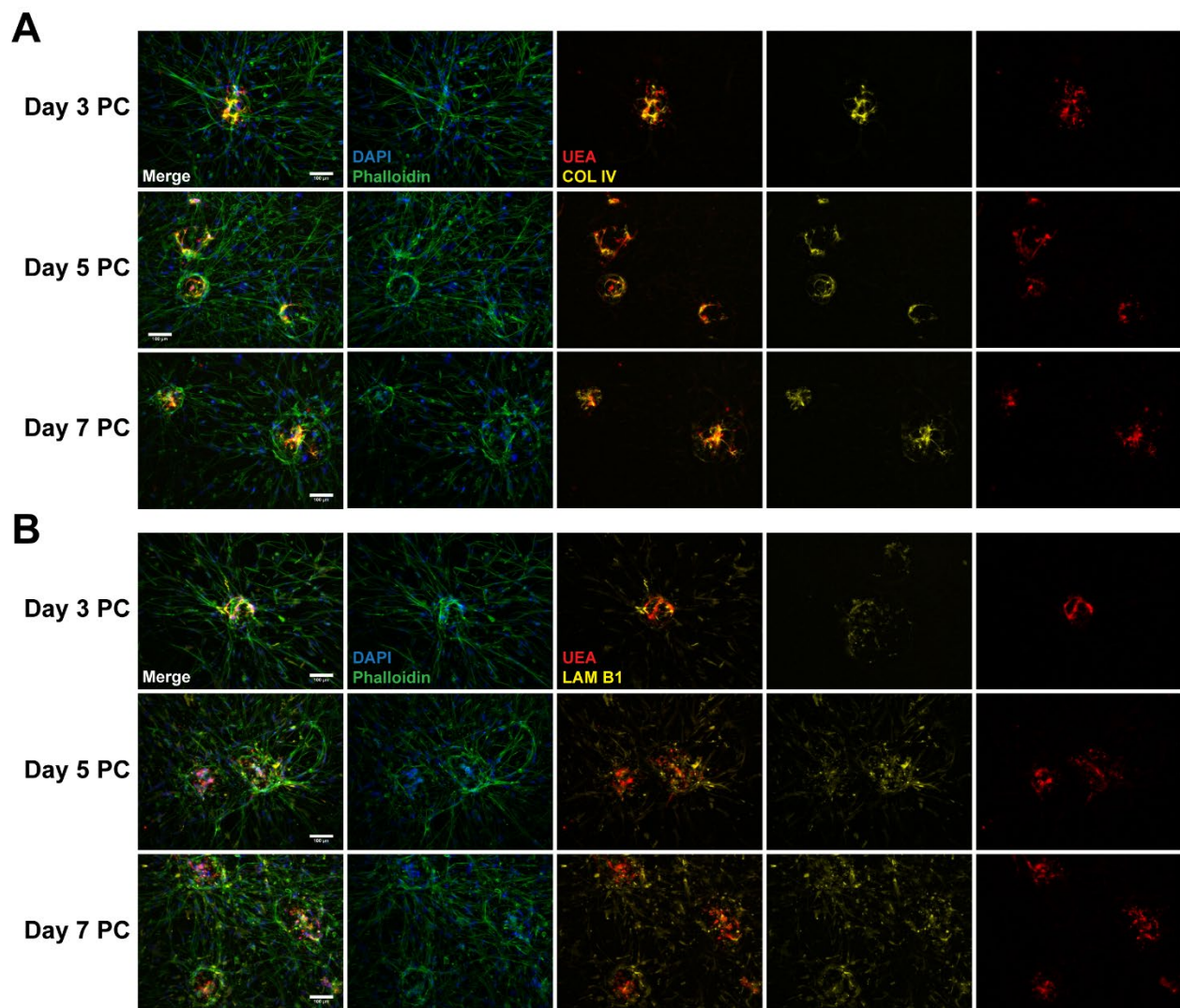
Figure 6.10: Non-sprouting microbeads exhibit dispersed basement membrane. *Representative max intensity projections (Z = 100 μm) of (A) collagen IV and (B) laminin beta-1 in pre-cultured microbeads cultured in fibrin hydrogels for up to 7 days.*

6.3.5 Microbeads support the formation of human-derived microvasculature in subcutaneous implants

Pre-cultured microbeads were delivered within acellular fibrin carrier gels into the subcutaneous space of SCID mice. In initial studies, 10% volume fraction of D1, D3, and D7 PC microbeads was injected in 2.5 mg/mL fibrin hydrogels that gelled *in situ* (Fig. 6.11A). Implants were heavily remodeled *in vivo*, which resulted in the majority of implants being complete degraded after 7 days. Only one sample containing D7 PC microbeads was successfully identified and retrieved. H&E staining was used to identify the implant region (Fig. 6.11B), which contained circular microbeads (asterisks) surrounded by the fibrin hydrogel. Somewhat unexpectedly, these microbeads appeared to contain significant ECM staining within the microbeads despite PEG hydrogels being amorphous. Human CD31 (hCD31) staining (Fig. 6.11C) identified microbeads that contained human-derived structures which appeared as non-perfused lumens (white arrows) as well as cord-like structures (black arrow).
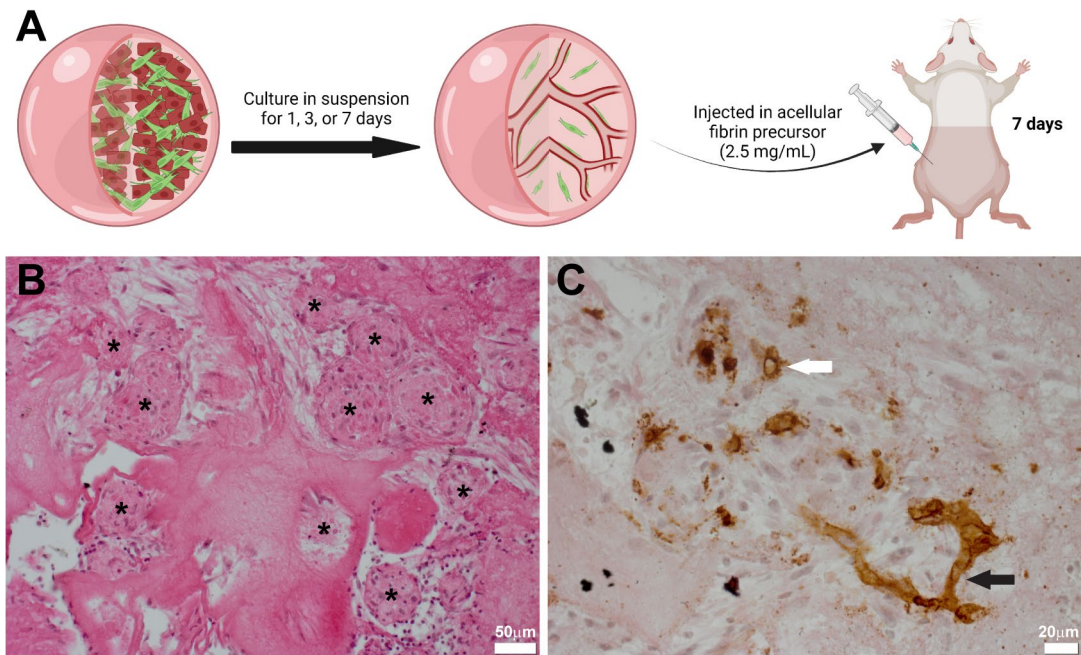
Figure 6.11: D7 PC microbeads contained significant ECM deposition and evidence of human-derived vessel-like structures after 7 days in vivo. *(A) Schematic representation of animal study, created with Biorender.com. (B) H&E and (C) hCD31 staining of microbead containing implants.*

In a secondary animal experiment, 15% volume fraction of D1 PC microbeads were encapsulated in preformed 5.0 mg/mL fibrin hydrogel pucks that were implanted into subcutaneous pockets (Fig. 6.12A). Increased fibrin density as well as implanting hydrogels with predefined boundaries resulted in implants that were more easily identified and retrieved after 7 days *in vivo*. Due to paraffin embedding, which requires sample dehydration, D1 PC microbeads (Fig. 6.12B, asterisks) essentially disappeared from the harvested implants as these microbeads are mainly composed of water and cells as the cells had not deposited ECM without extended pre-culture. Still, identified microbeads contained hCD31+ structures, identified as both non-perfused lumens (white arrows) as well as cord-like structures (Fig. 6.12C, black arrow).
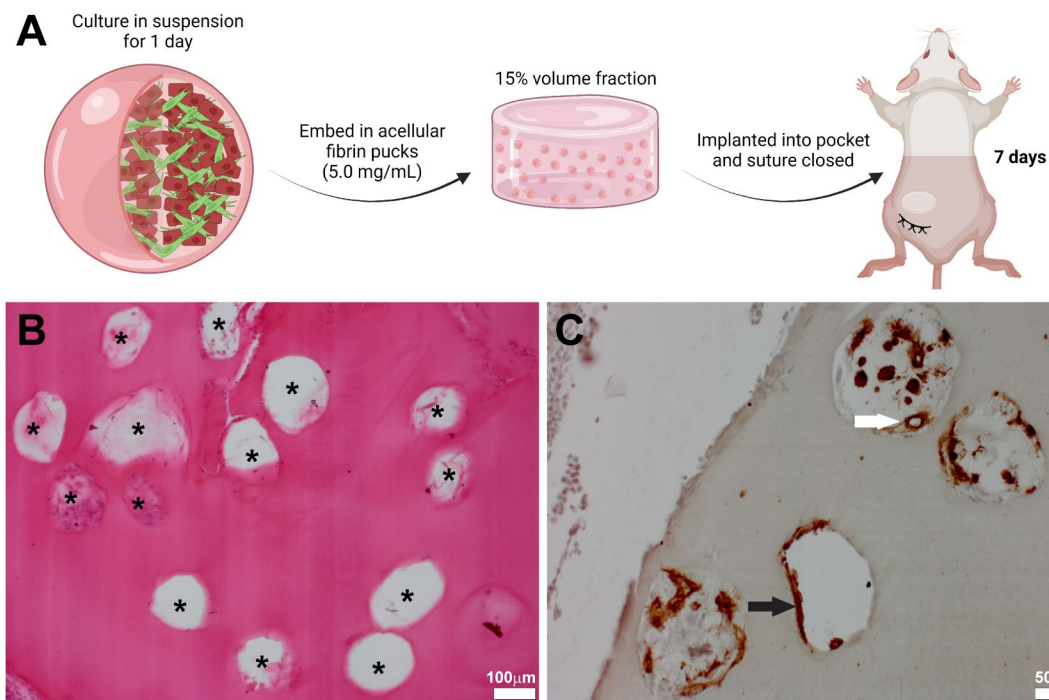
Figure 6.12: D1 PC microbeads contained minimal ECM deposition yet had some evidence of human-derived vessel-like structures after 7 days in vivo. *(A) Schematic representation of animal study, created with Biorender.com. (B) H&E and (C) hCD31 staining of microbead containing implants.*

In a tertiary animal experiment, 15% volume fraction of D1 PC microbeads were encapsulated in preformed 5.0 mg/mL fibrin hydrogel pucks that were implanted into subcutaneous pockets (Fig. 6.12A). Cellular bulk hydrogels containing 500 K/mL total cells of HUVEC and NHLF in a 1:1 ratio were included as a positive control for *in situ* vessel morphogenesis. These implants were processed for cryosectioning, which did not require dehydration of tissue samples, in an effort to more clearly analyze cellular behavior within microbeads. Control hydrogels, containing the same microbeads and cells implanted into the animal were cast on the day of surgery and cultured for 7 days *in vitro*. Both bulk cellular (Fig. 6.13A) and microbead (Fig. 6.13B) containing control gels formed robust microvascular networks *in vitro*. After 7 days *in vivo*, the same hydrogel conditions had strikingly different results. Cellular bulk hydrogel implants contained dispersed, short vessel segments (Fig. 6.13C). D1 PC microbead

implants showed minimal evidence of vascularization of the surrounding hydrogel (Fig. 6.13D). Higher magnification images illustrate that while some microbeads have vessel-like structures localized to the interior of the bead (Fig. 6.13E), some vessels successfully sprouted into the surrounding matrix (Fig. 6.13F). In some cases, these vessel-like structures appeared to contain hollow lumens (arrows).
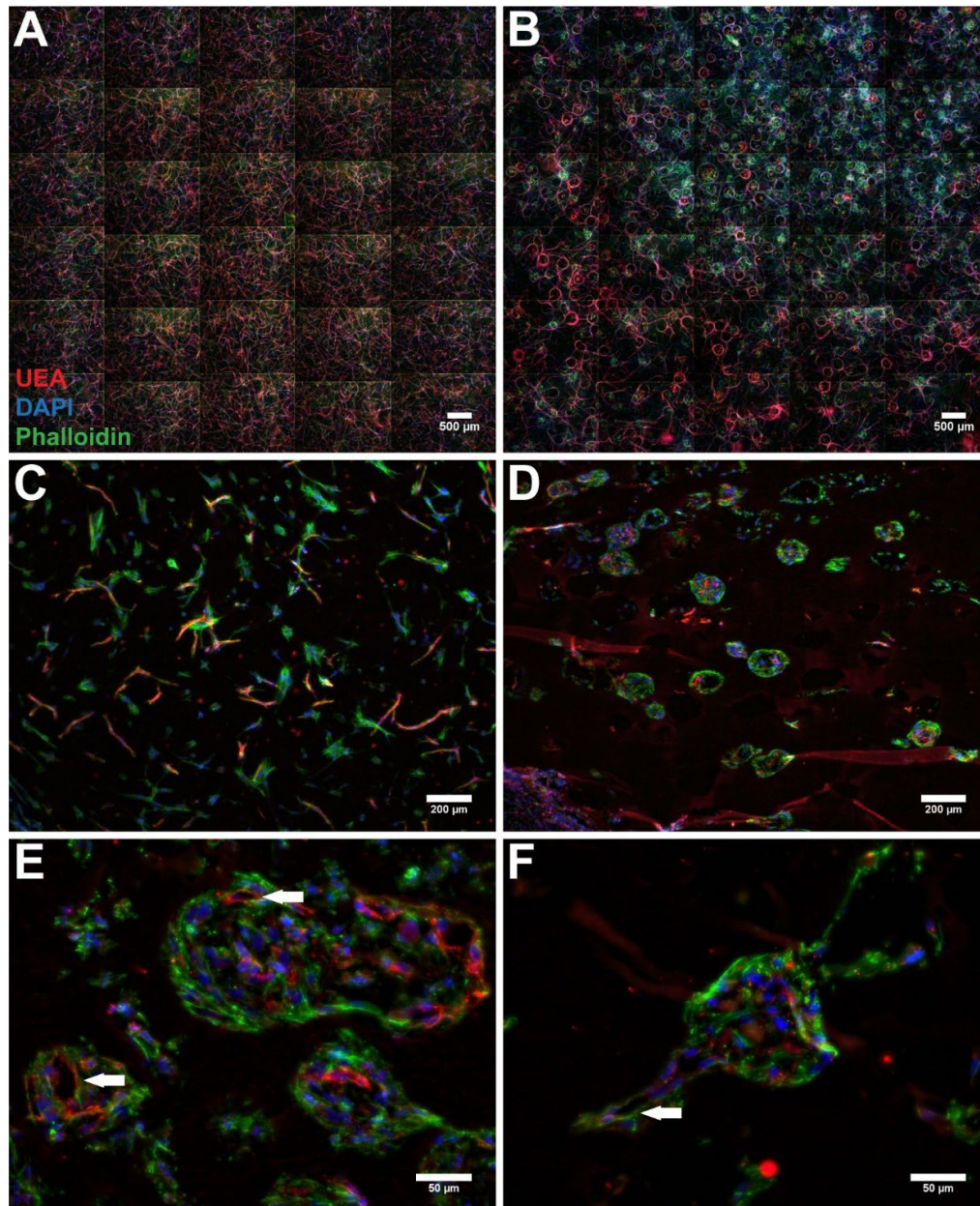
Figure 6.13: Conditions that support robust microvascular network formation in vitro do not translate to similar outcomes in vivo. *Whole hydrogel scan slides of control hydrogels cultured in vitro for 7 days*

In the final animal experiment, the volume fraction of microbeads as well as cell density of bulk cellular controls was increased to promote more robust vascularization *in vivo*. Preformed 5.0 mg/mL fibrin pucks contained either 50% volume fraction of D1 PC microbeads, which translates to roughly 3 million total cells per 500 µL implant, or 6 M/mL total cells of HUVEC and NHLF in a 1:1 ratio. Prevascularized pucks which contained 15% volume fraction of D1 PC microbeads or 500 K/mL total cells of HUVEC and NHLF in a 1:1 ratio cultured *in vitro* for 7 days were included as controls containing preformed microvascular networks present upon implantation (Fig. 6.14A).
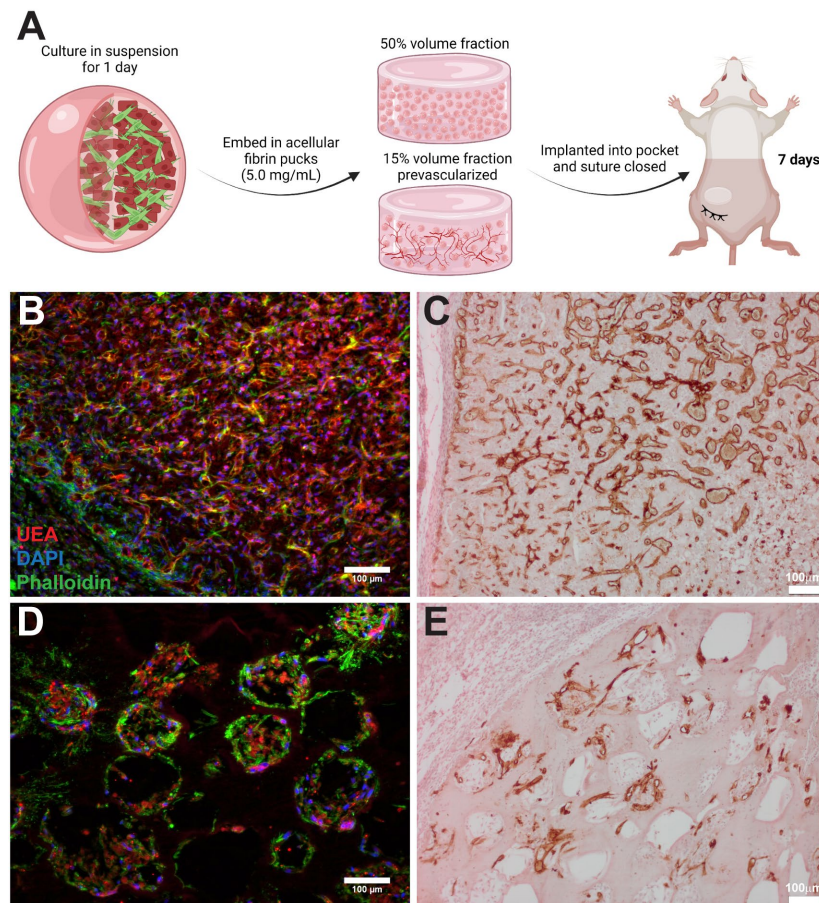
Figure 6.14: Increased cell density promotes in situ vessel morphogenesis in bulk control hydrogels. *(A) Schematic representation of animal study, created with Biorender.com. Subcutaneous implants containing*

(B, C) 6 M/mL HUVEC and NHLF and (D, C) 50% D1 PC microbeads after 7 days in vivo. (D, E) hCD31 staining of tissue implants.

Increasing the cell density of cellular bulk hydrogels promoted increased vessel morphogenesis *in vivo* (Fig. 6.14B and C). These vessels contained host erythrocyte, indicative of functional inosculation (Fig. 6.14C); however, the center of these tissue implants contained evidence of a necrotic core (Fig. 6.14D, bottom right, puncti hCD31+ staining). Increasing the volume fraction of microbeads did not yield similar results. Endothelial cell staining was still mainly localized to the interior of microbeads (Fig. 6.14D). Consistent with prior animal studies, microbeads contained hCD31+ structures, some of which were non-perfused lumens (Fig. 6.14E).
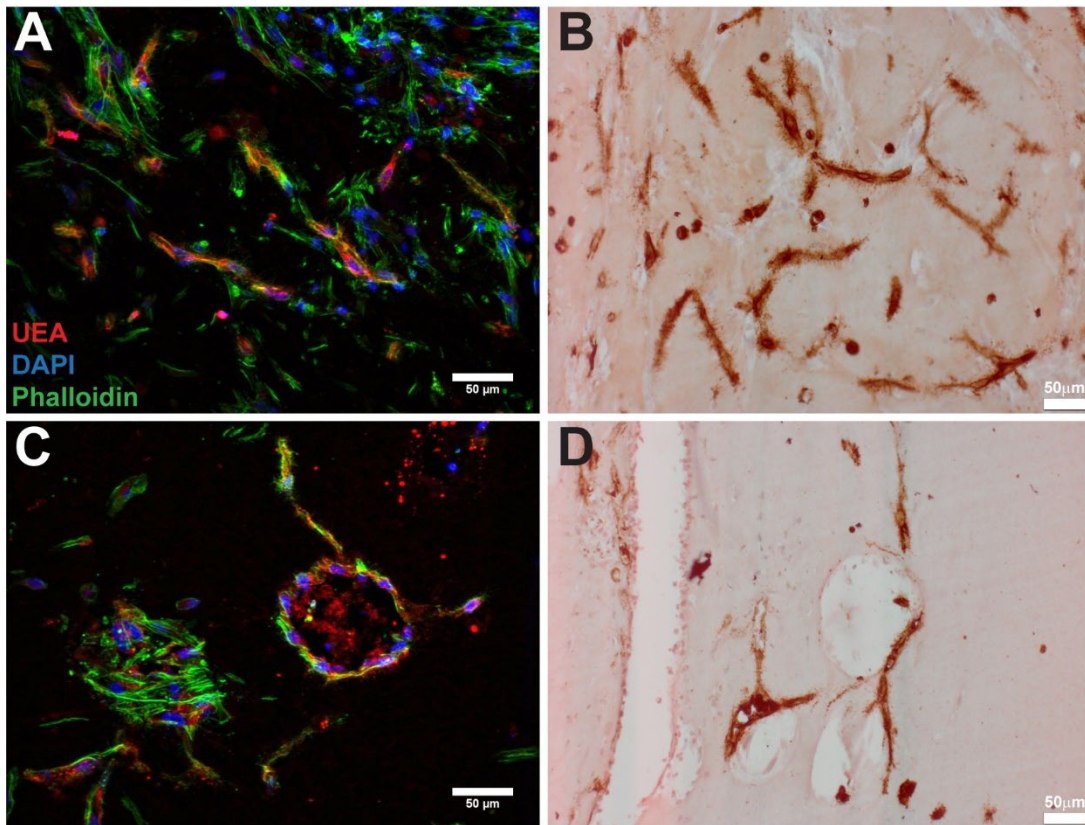
Figure 6.15: Prevascularized tissue implants maintain vessel density in bulk hydrogels. *Prevascularized subcutaneous implants containing (A, B) 500 K/mL HUVEC and NHLF and (C, D) 50% D1 PC microbeads after 7 days in vivo. (B, D) hCD31 staining of tissue implants.*

Prevascularized bulk hydrogels contained dispersed vessel segments (Fig. 6.15A and B). This microvascular network was less extensive than typical *in vitro* hydrogels (Fig. 6.13A) and

high cell density implants (Fig. 6.14B and C). In prevascularized microbead containing hydrogels, while some microbeads had evidence of vessel-like structures sprouting from microbeads (Fig. 6.15C and D), these vessel sprouts were more rarely observed and to lesser extent than typical *in vitro* D1 PC microbead containing hydrogels (Fig. 6.13B). These implants were more akin to results from previous animal studies (Fig. 6.13D-F) despite containing preformed structures prior to implantation.

6.4 Discussion

Modular tissue constructs (microgels, microspheres, microparticles, microbeads) are emerging as a promising cell culture platform for engineering micron-sized hydrogels with discrete microenvironments [35]. Previous studies have developed microbeads that support the *in vitro* culture [36-44] and delivery of endothelial cells *in vivo* [45-49]; however, only a small number of these studies focus on vascularization of these microbeads [11-14, 50]. Previous work from our group developed fibrin-based microbeads that supported prevascularization *in vitro* and the formation of functional microvascular networks *in vivo* after implantation in subcutaneous [12] and hindlimb ischemia [11] models. While these studies demonstrated a promising modular approach to vascularizing ischemic tissues, natural materials may have potential barriers to translation, including being derived from animal sources and potentially exhibiting batch-to-batch variability. Furthermore, fibrin microbeads experience aggregation during prevascularization [11, 12, 41], which can hinder injectability as well as overall vessel network coverage upon implantation [41].

PEG-based microbeads are an established technology for a variety of tissue engineering applications, though few studies utilize PEG microbeads for cell encapsulation and subsequent

tissue development prior to transplantation. Fewer studies utilize PEG microbeads for vascularization applications [38, 44, 46, 47, 51], none of which, to our knowledge, have focused on the development of prevascularized tissue modules. In this work, we fabricated cell-adhesive, degradable PEGNB microbeads containing HUVEC and NHLF, with the goal of developing a synthetic microbead platform that supports the formation of robust, well-distributed microvascular networks and prevascularization without microbead aggregation.

Microbeads supported high cell viability 24 h post-encapsulation. Both HUVEC and NHLF were distributed throughout the interior of microbeads. Despite variability in cell density across microbeads as a result of cell aggregation during droplet production, microbeads displayed relatively consistent diameters (coefficient of variance, CV = 4.18%; polydispersity index, PDI = 0.013). Though microfluidic droplet generation offers the ability to generate monodispersed droplets, cell settling and aggregation at high cell densities often leads to a more variable cell distribution within droplets [52-54]. Therefore, we optimized flow rates and cell concentration in the precursor to solution to increase the occurrence of higher cell density microbeads without disturbing droplet production, as large aggregates can result in flow fluctuations that effect the monodispersity of the droplets [54]. Future iterations of microbeads could be produced using microfluidic geometries that can produce large volumes of microbeads in a short period of time [55, 56], which may reduce cell aggregation and improve cell distribution across microbeads. Roughly half of all microbeads had a medium or high cell density which likely possess the threshold density of cells required for vascularization. Though the majority of microbeads contained only a few cells, it is feasible that these low density or empty microbeads could be beneficial in generating vascularized MAP hydrogels [31], in which the empty beads could be

utilized for secondary crosslinking given enough free, available norbornene arms remained after microbead polymerization.

Cellular microbeads catalyzed the formation of microvascular networks when embedded in bulk fibrin hydrogels *in vitro*. Both vessel structures and stromal cells invaded the surrounding matrix. These vessels contained hollow lumens and a close peri-vascular stromal cell localization. Furthermore, vessel structures were supported by basement protein, indicative of a mature vessel phenotype. Greater vessel densities were observed when the volume fraction of microbeads embedded in the bulk hydrogels was increased, forming well-distributed, robust microvascular networks. Microbeads even permitted sprouting in high concentration fibrin gels, though to a lesser extent, consistent with previous work from our group [57].

Extended suspension culture resulted in the formation of primitive vessel-like structures within the majority of microbeads as early as 3 days. As pre-culture time was increased, vessel-like structures continued to develop, achieving greater basement membrane deposition and more well-defined UEA-positive structures. Furthermore, microbeads were cultured for up to a week in suspension without signs of microbead aggregation, permitting extended pre-culture of discrete tissue modules. Other work has demonstrated prevascularization of discrete microbeads using fibrin [12], modified alginate [13, 14], and gelatin methacryloyl [50] matrices.

Despite the presence of preformed microvasculature within microbeads at the time of embedding, angiogenic sprouting was decreased as pre-culture time was increased. This could be a result of vascular remodeling during pre-culture, resulting in mature, quiescent small-scale microvascular networks that lack tip cells needed to initiate angiogenic sprouting [58-62]. Pre-cultured microbeads could be encapsulated in previously established microfluidic chips [58, 63] to assess if gradients of growth factors, such as VEGF or BMP, could encourage sprouting [64].

Fluorescent imaging confirmed that basement membrane proteins collage IV and laminin beta-1 were not localized to the surface of microbeads; however, other basement membrane proteins not stained for in this study could be creating a barrier to vessel sprouting. Similarly, while fibroblast bodies appear to leave the microbeads to invade the surround matrix, some cell bodies could remain strongly adhered to the surface of microbead, preventing vessels from sprouting. Core-shell microbeads [65-67], in which fibroblasts are localized to less rapidly degradable microbead cores surround by endothelial cells in a more readily degraded shell could be a feasible alternative approach, though such complex microfluidic fabrication approaches are outside the scope of this work.

The animal studies presented in this work primarily focused on optimizing implant formulation to support vessel morphogenesis *in situ* while still being retrievable for histological processing. Microbeads injected in acellular fibrin hydrogels were often completely remodeled after 7 days *in vivo*. Previous work from our group has demonstrated acellular fibrin gels were heavily infiltrated by host cells and degraded over time [11]. Preformed pucks were implanted into subcutaneous pockets in order to more easily retrieve implants. While this goal was accomplished, there are likely negative effects of creating a sharp interface between hydrogels and host tissue which could decreased integration and vascularization potential.

In vivo data suggests that pre-cultured microbeads support ECM deposition within the initially amorphous PEG matrix as result of pre-culture and subsequent time *in vivo*. Both early and later timepoint pre-cultured microbeads showed evidence of human-derived vessel-like structures in the form of hollow lumens and cord-like structures, though these structures lacked functional perfusion in the form of host erythrocytes within the lumen. This lack of perfusion likely resulted in vessel pruning *in vivo*. Even an increased volume fraction of microbeads, and thus an

increased cell density, in the implants did not significantly enhance vessel formation as it did in gels containing a bulk suspension of HUVEC and NHLF. As only half of each batch of microbeads may have sufficient cell density needed for vascularization, it is possible that the volume fraction needs to be increased further to generative microvascular networks *in vivo*.

Interestingly, implanting prevascularized pucks resulted in segmented vessel structures that were also not perfused. Compared to *in vitro* controls, vessels appeared to actually regress *in vivo* in prevascularized pucks for both microbeads and cell suspension containing implants. This could be a result of interfacial barriers between the tissue constructs and animal tissue [40] preventing integration of the preformed hydrogel pucks into the surrounding tissue, resulting in a lack of perfusion and thus vessel regression. Additional studies could include earlier timepoints to assess when this vessel regression occurs. Future studies could attempt to inject microbeads without a hydrogel carrier to determine if this could reduce potential interfacial barriers and promote inosculation between implanted vessels and host vessels. Additionally, previous studies have shown that prevascularization may actually inhibit functional inosculation due to an inability to engage non-inflammatory host neutrophils that are necessary for engraftment [68]. Furthermore, future studies could implant pre-cultured microbeads in a model of hindlimb ischemia to determine if an ischemic microenvironment may encourage sprouting as seen previously with fibrin-based microbeads [11].

6.5 Supplementary Data

6.5.1 Encapsulation of microbeads in microfluidic (30 µL) and microfluidic-like (500 µL) culture devices

D1 PC microbeads were encapsulated in two different types of devices to develop a platform to assess functional perfusion *in vitro*. First, microbeads were encapsulated in a previously utilized microvasculature-on-a-chip microfluidic device [69]. These devices were composed of microbeads resuspended in 30 µL of fibrin precursor solution that was injected around acupuncture needles into chambers between molded PDMS and a glass coverslip. After gelation, the needles were removed and the channels were coated with HUVEC (if necessitated by the experimental condition). Devices either lacked channels (no needles) or contained acellular or HUVEC-seeded channels.

Control bulk hydrogels (cast using the same batch of microbeads as in the devices) demonstrated robust vascularization as expected (Fig. 6.16A and B). Devices with no channels contained a more dispersed microvascular network (Fig. 6.16C). This could be a result of the small volume chamber receiving less microbeads than bulk gels (despite both theoretically having 20% microbead volume fraction). Devices containing both acellular (Fig. 6.16D) and cellular (Fig. 6.16E) channels had an even greater reduction of vessel morphogenesis in the surrounding hydrogel as the channels took up a considerable volume in the chambers. Microbeads localized next to the needles during fibrin polymerization often resulted in channel expansion, likely because microbeads were stuck to needles which tore the gel upon removal. Neither channel containing device exhibited perfusion of the surrounding network after 7 days of culture.
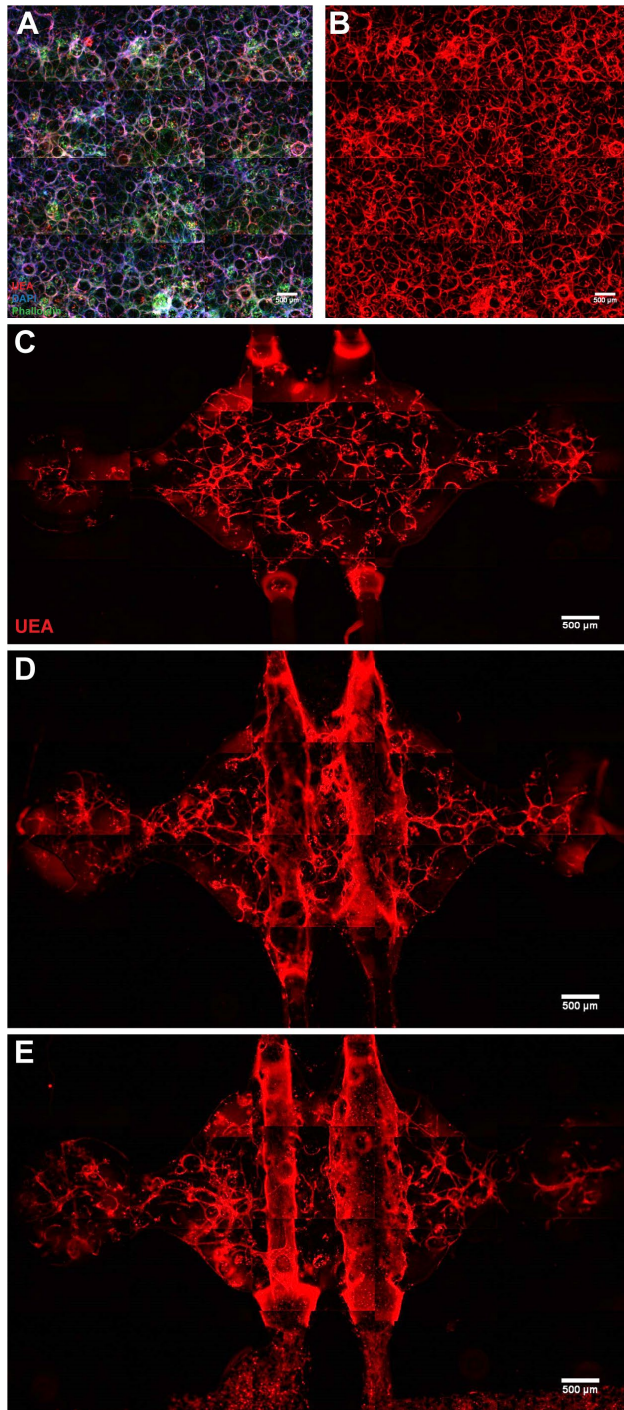
Figure 6.16: Microbeads cultured in microvasculature-on-a-chip device. *(A, B) Control bulk gels confirm expected vessel morphogenesis. Devices (B) without channels, (C) with acellular channels, and (D) with endothelialized channels after 7 days of culture.*

A new device was designed to fabricate larger volume (500-750 µL) fibrin hydrogels with endothelialized channels. A slab of PDMS with two overlapping 12 mm biopsy punched wells was bonded to a glass coverslip and needles were inserted to template the channels. Microbead containing fibrin precursor solutions were injected directly into the wells as the device was open on the top. After gelation, needles were removed, and endothelial cells were seeded into the channels. Sterile PBS was added to the top of the gel and media was added to the reservoirs, so nutrients were only provided to the gel from the channels.
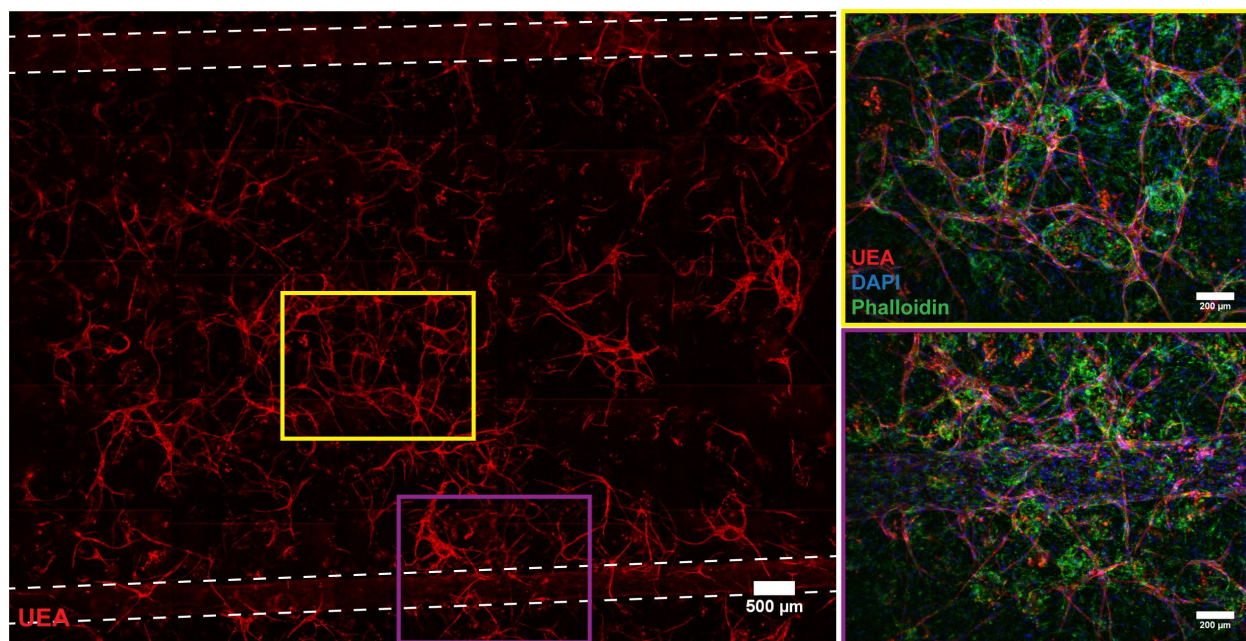
Figure 6.17: Microbeads cultured in fibrin gels containing endothelialized channels. *Microbeads were cultured in bulk fibrin hydrogels containing mesoscale endothelialized channels (dashed lines) for 7 days. Microvascular networks were formed between (yellow inset) and in close proximity to (purple inset) the channels.*

This platform supported microvascular network formation throughout the entire hydrogel (Fig. 6.17). While vessel formation occurred both between and in close proximity to the channels, functional perfusion was not yet observed after 7 or 14 days of culture. By 14 days of culture, there was some evidence of endothelial cells budding from the channels into the surrounding hydrogel; however, little evidence of sprouting was observed. This could be due to inefficient endothelial

cell seeding of the channels, as this device cannot be flipped over during seeding like the one previously described. This device offers a promising potential platform to assess functional perfusion of larger hydrogel constructs *in vitro* or to create growth factor gradients from the media channels, and thus should be further investigated to determine efficient ways to seed the channels to encourage sprouting and inosculation with the surrounding engineered vasculature.

6.5.2 Increasing the ratio of EC:LF (3:1) in encapsulated in microbeads

Previously, HUVEC-NHLF microbeads were formulated using 10 M/mL of each cell type (20 M/mL total). Increasing the ratio of HUVEC (15 M/mL) to NHLF (5 M/mL) within the PEG precursor solution was investigated to reduce the potential inhibitory effects of NHLF coating the outside of the microbeads. The goal was to have less NHLF overall which could reduce cell coating. Fluorescent staining revealed that some D1 PC microbeads had more UEA-negative phalloidin staining than others, indicating some microbeads had more NHLF encapsulated within them than others (Fig. 6.18A). After 3 days of suspension culture, microbeads supported the formation of primitive vessel-like structures (Fig. 6.18B), similar to what was observed in 1:1 ratio microbeads (Fig. 6.6A and B).

When embedded and cultured in bulk fibrin hydrogels for 7 days, D1 PC 3:1 formed microvascular networks throughout the entirety of gel (Fig. 6.18C and D), though they appeared more dispersed than those of 1:1 microbeads (Fig. 6.4). Vessel-like structures appeared more extensive when surrounded by UEA-negative phalloidin staining (Fig. 6.18C), which could indicate successful sprouting was more likely if the microbeads contained a threshold number of NHLF. As the NHLF are the "sticky" cell type during microfluidic droplet generation, decreasing the total number of NHLF more likely decreased the number of microbeads with both HUVEC and NHLF within them as fewer NHLF aggregates were distributed among microbeads.

Furthermore, D7 PC 3:1 microbeads also exhibited diminished angiogenic sprouting (Fig. 6.18 E and F) as was seen in 1:1 microbeads (Fig. 6.8G and H).
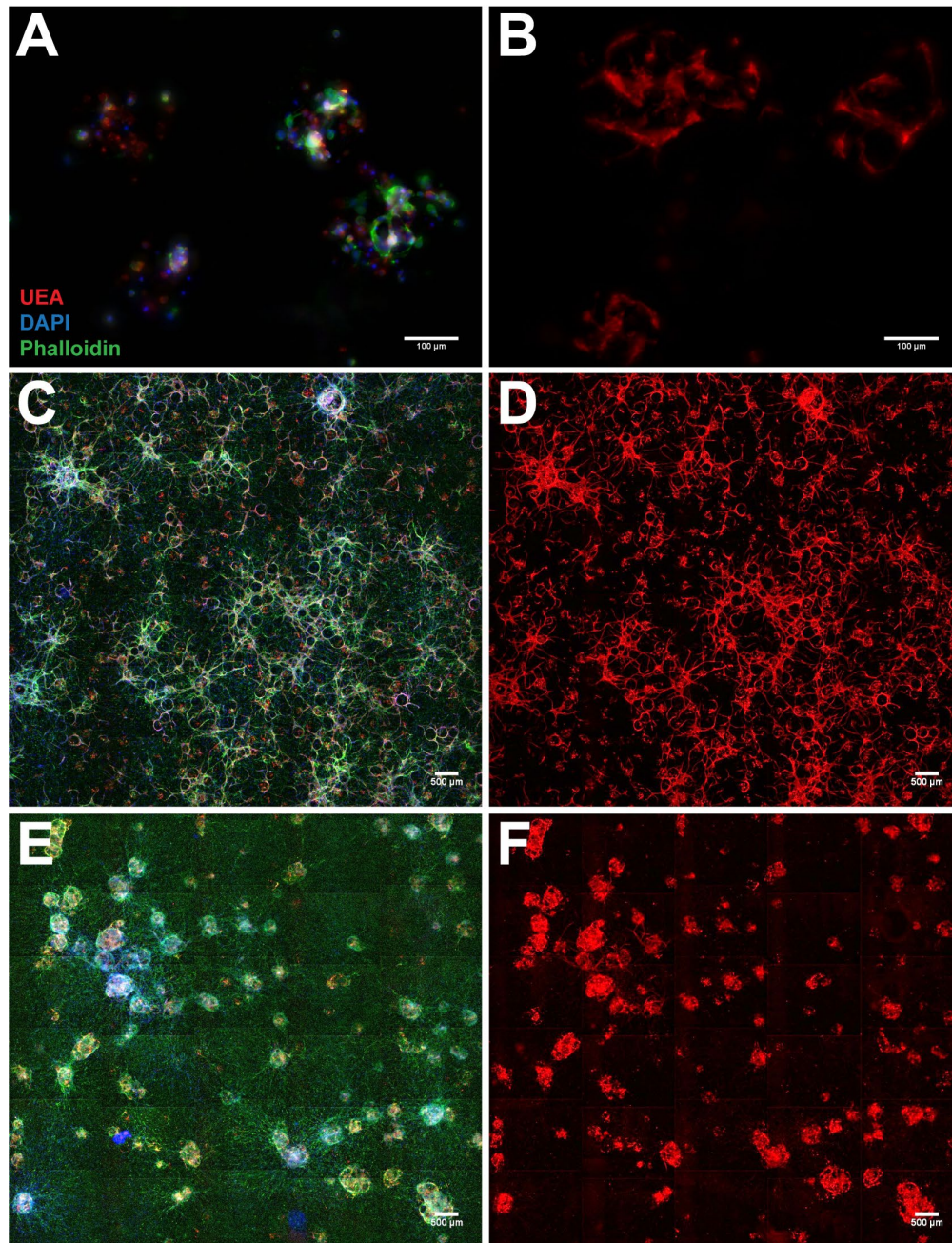
Figure 6.18: Increased ratio of EC:LF (3:1) within microbeads. *(A) D1 and (B) D3 PC microbeads in suspension. Whole gel scan slides of (C, D) D1 and (E, F) D7 PC microbeads cultured in bulk fibrin gels for 7 days.*

6.5.3 HUVEC monoculture microbeads

Previous literature has demonstrated vessel morphogenesis in PEG gels containing endothelial cell monocultures [19]. HUVEC monoculture microbeads (20 M/mL) were fabricated to assess if microbeads could be prevascularized in the absence of NHLF (or other stromal cells). D1 PC EC monoculture microbeads were embedded in bulk fibrin hydrogels containing 250 K/mL NHLF and cultured for 7 days. NHLF in the surrounding hydrogel supported angiogenic sprouting from the HUVEC monoculture microbeads (Fig. 6.19A and B). After 5 days of suspension culture, HUVEC monoculture microbeads showed no evidence of vessel morphogenesis within the microbeads (Fig. 6.19C and D). While HUVEC monocultures did not facilitate prevascularization in the absence of NHLF, this could be one approach to the delivery of only a single cell type with the expectation that host stromal cells could aid in *in vivo* vascularization.

A transwell setup, in which HUVEC monoculture microbeads were cultured on transwell inserts separated from NHLF cultured in the well plate (Fig. 6.20A), was evaluated to determine if NHLF paracrine signaling may support prevascularization of HUVEC monoculture microbeads. After 7 days of transwell culture, microbeads showed minimal evidence of HUVEC spreading or assembly (Fig. 6.20B and C).

HUVEC monoculture microbeads were then added to fibrin hydrogels beneath transwell inserts containing NHLF (Fig. 6.21A) to determine if NHLF paracrine signaling could induce angiogenic sprouting. After 7 days of culture, only microbeads near or in direct contact with the transwell showed evidence of vessel sprouting, while microbeads near the edges of the hydrogel did not sprout (Fig. 6.21B, C).
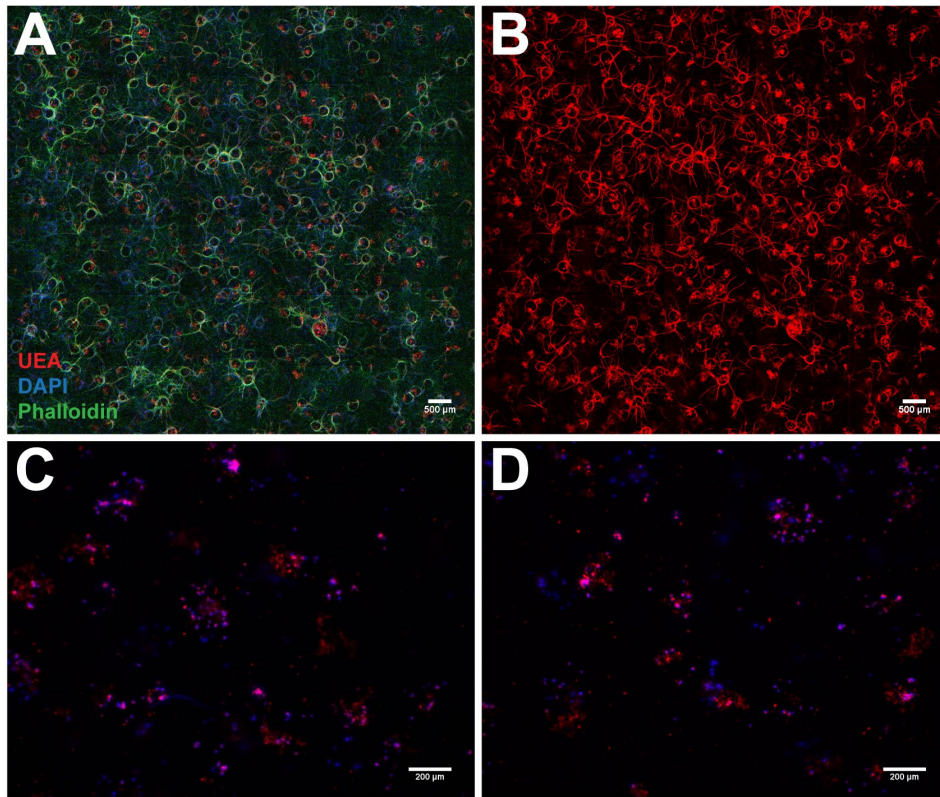
Figure 6.19: EC monoculture microbeads. *(A, B) Whole gel scan slides of D1 PC EC monoculture microbeads embedded with 250 K/mL NHLF in bulk fibrin hydrogels cultured for 7 days. (C, D) D5 PC EC monoculture microbeads in suspension.*
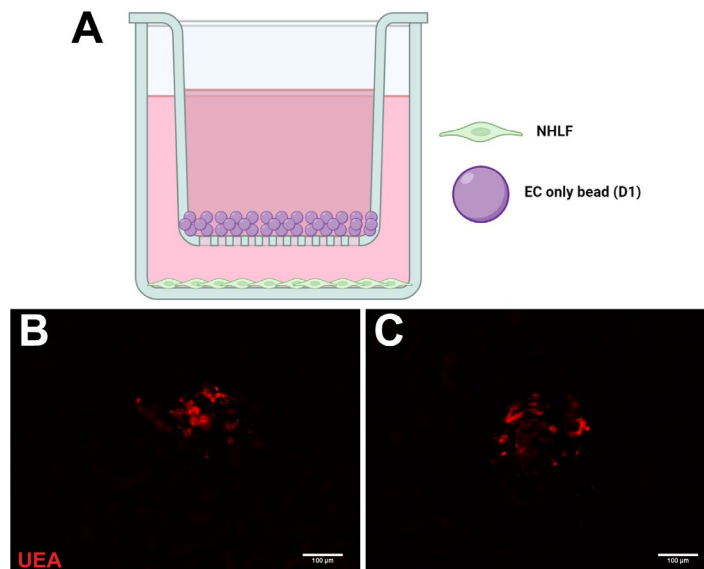
Figure 6.20: EC monoculture microbeads cultured on transwell separated from NHLF. *(A) Schematic representation of experimental setup (Created with Biorender.com). (B, C) EC monoculture microbeads after 7 days of transwell culture.*
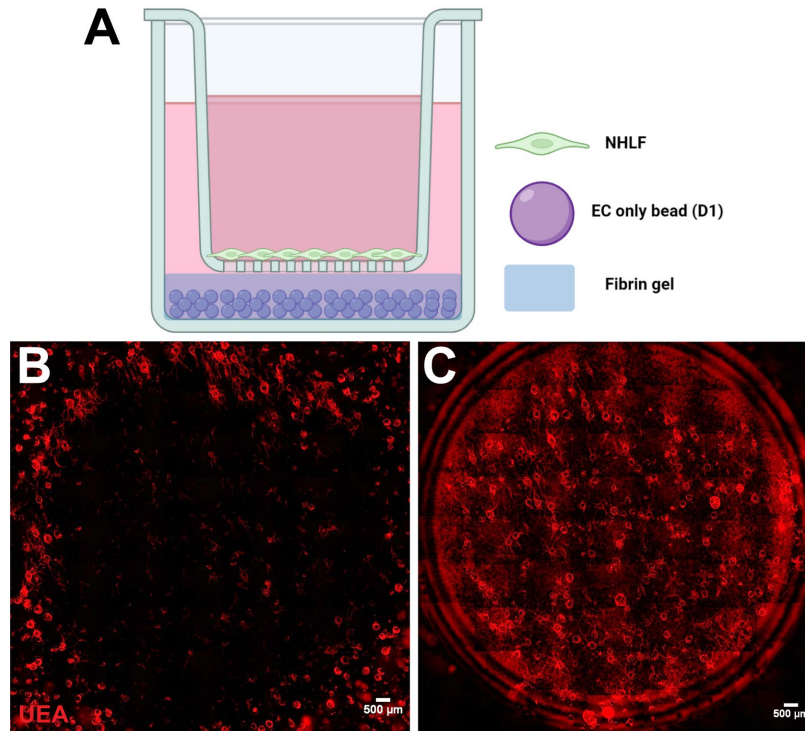
Figure 6.21: EC monoculture microbeads cultured in fibrin bulk gel separated from NHLF on transwell. *(A) Schematic representation of experimental setup (Created with Biorender.com). (B) Surrounding hydrogel containing EC monoculture microbeads after 7 days of culture. (C) Hydrogel directly beneath (and adhered to) transwell containing NHLF.*

This data suggests that NHLF needed to be in direct (or very close) contact with HUVEC monoculture microbeads to support vessel morphogenesis and angiogenic sprouting. NHLF monoculture microbeads were co-cultured in suspension with HUVEC monoculture microbeads in a single bioreaction tube to determine if this approach would facilitate prevascularization of HUVEC microbeads while keeping NHLF isolated to their own microbeads. After 7 days of suspension culture, some HUVEC monoculture microbeads had evidence of primitive vessel-like structures (Fig. 6.22, arrows); however, these microbeads were also encapsulated in a sheath of UEA-negative phalloidin staining, indicating NHLF had migrated from their microbeads onto the HUVEC microbeads. HUVEC microbeads without this phalloidin staining contained unassembled HUVEC as evidenced by individual circles of UEA staining. This suggests that stromal cells must

be in direct contact, by way of being in/on the same microbead, with HUVEC for prevascularization to occur.
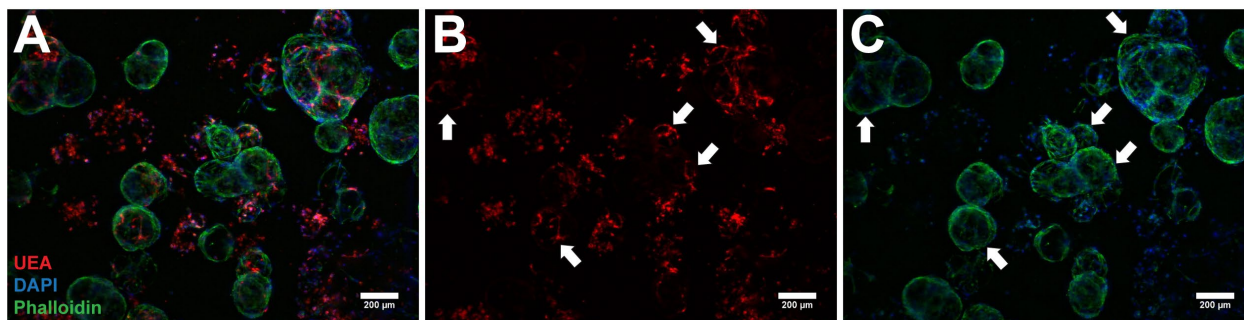
Figure 6.22: EC monoculture and LF monoculture microbeads cultured together in suspension. (A) UEA-DAPI-Phalloidin, (B) UEA only, and (C) DAPI-Phalloidin staining of monoculture microbeads after 7 days of co-culture in suspension in a single bioreaction tube (arrows indicate microbeads that appear to contain vessel-like structures).

6.5.4 Alternative stromal cells (MSC, NHDF, HASMC)

NHLF formed aggregates during microfluidic droplet generation, resulting in uneven distribution of cells within microbeads. Other stromal cells were incorporated into microbeads under the same conditions (flow rate, PEG formulation, cell density, etc.) to determine if they would aggregate less and therefore enable a more homogenous cell distribution throughout microbeads. HUVEC-MSC microbeads containing 20 M/mL total cells in a 1:1 ratio were generated. During droplet generation, MSC did not appear to aggregate in the inlet tubing. D1 PC microbeads contained both UEA-positive HUVEC and UEA-negative MSC (Fig. 6.23A). D5 PC microbeads showed little evidence of HUVEC spreading and assembly (Fig. 6.23B).

When embedded and cultured in fibrin hydrogels for 7 days, D1 PC microbeads did not support the formation of microvascular networks (Fig. 6.23D), despite the MSC remaining active (migrating, proliferating) in the surrounding matrix (Fig. 6.23C). Now that cell distribution throughout microbeads was improved, cell density was increased to 30 M/mL in a 1:1 ratio to increase the overall cell number in each microbead. After 7 days of culture in fibrin hydrogels, D1

PC microbeads showed minimal evidence of vessel morphogenesis, with only a few microbeads surrounded by UEA-positive vessel-like structures (Fig. 6.23F). Again, the MSC appeared proliferative and migratory in the surrounding fibrin hydrogel, while HUVEC mostly remain contained to the interior of microbeads (Fig. 6.23E).
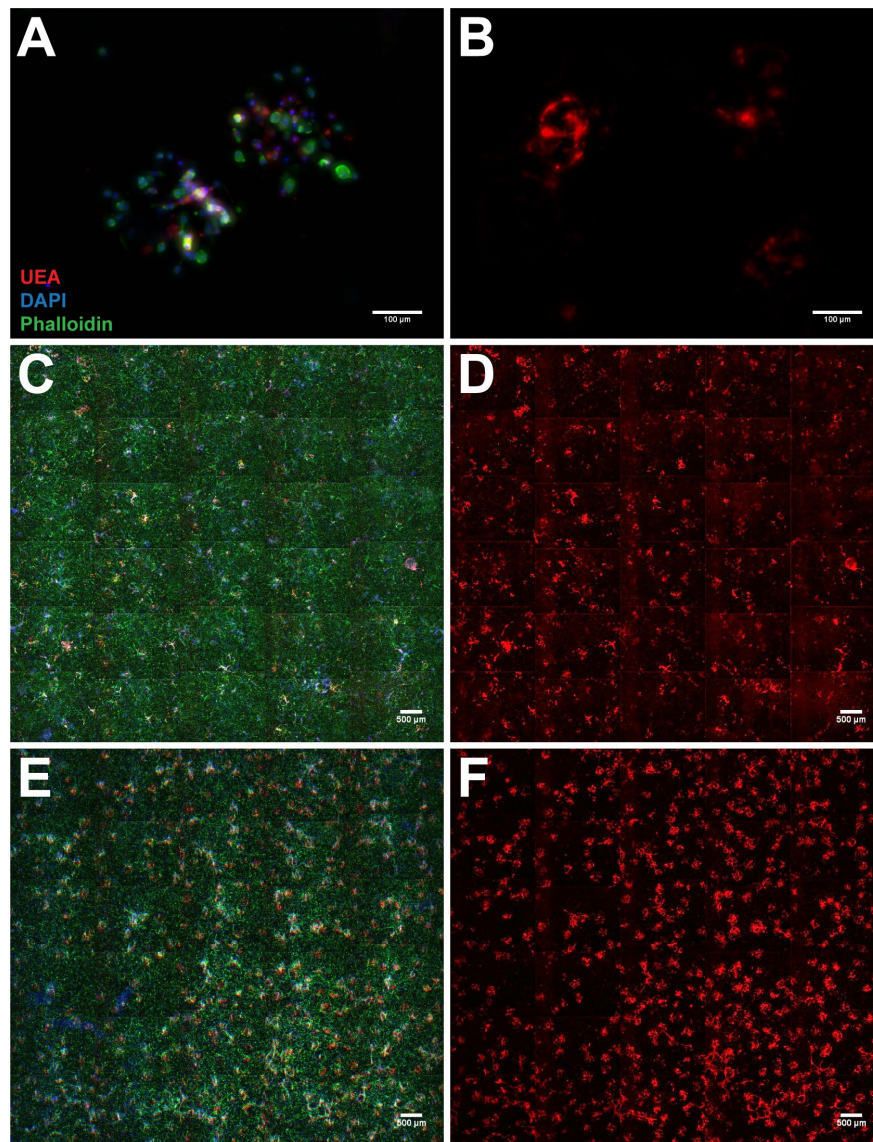
Figure 6.23: HUVEC-MSC microbeads. *(A) D1 and (B) D5 PC microbeads. (C) UEA-DAPI-Phalloidin and (D) UEA only staining of whole gel scan slides of D1 PC 20 M/mL HUVEC-MSC microbeads cultured in bulk fibrin hydrogels for 7 days. (E) UEA-DAPI-Phalloidin and (F) UEA only staining of whole gel scan slides of D1 PC 30 M/mL HUVEC-MSC microbeads cultured in bulk fibrin hydrogels for 7 days.*

A similar phenomenon was observed in HUVEC-NHDF and HUVEC-HASMC microbeads. Minimal cell aggregation occurred during microbead fabrication, but microbeads failed to supported vessel morphogenesis and angiogenic sprouting. HUVEC-NHDF appeared similar to HUVEC-MSC microbeads in that NHDF were active in the surrounding fibrin matrix (Fig. 6.24). HUVEC-HASMC microbeads had UEA-negative phalloidin localized to the microbead surface (Fig. 6.25), indicating neither HUVEC nor HASMC invaded the surrounding matrix. Though alternative stromal cell sources did not produce as robust vessel morphogenesis as NHLF under the same conditions, modifications to the microbeads or their fabrication could potentially improve this outcome and should be explored.
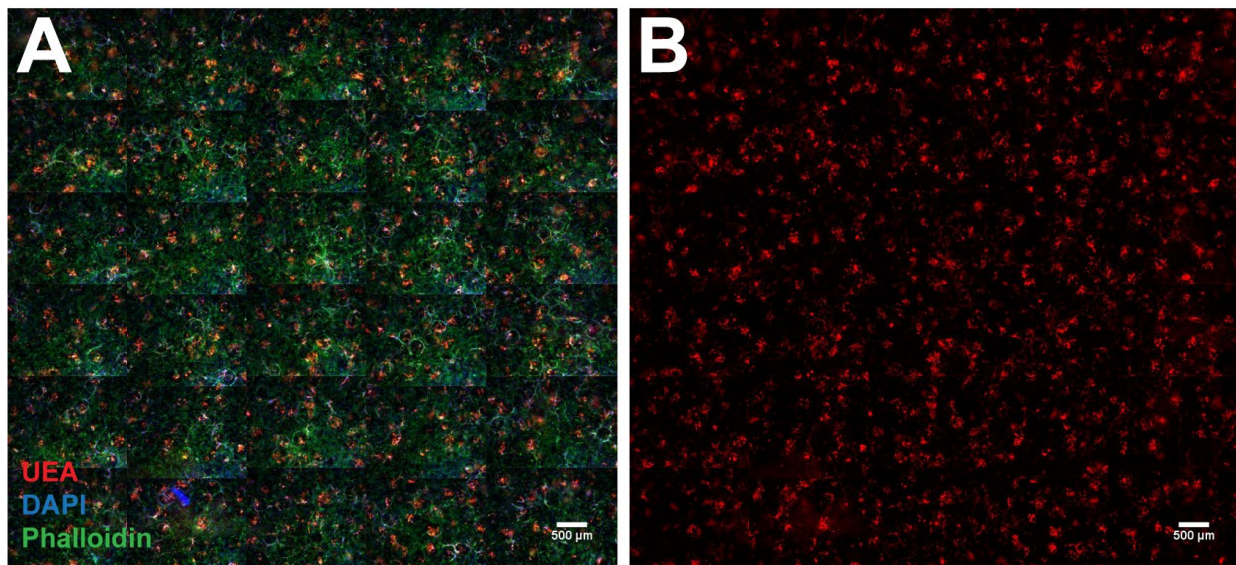
Figure 6.24: HUVEC-NHDF microbeads. (A) UEA-DAPI-Phalloidin and (B) UEA only staining of whole gel scan slides of D1 PC HUVEC-NHDF microbeads cultured in bulk fibrin hydrogels for 7 days.
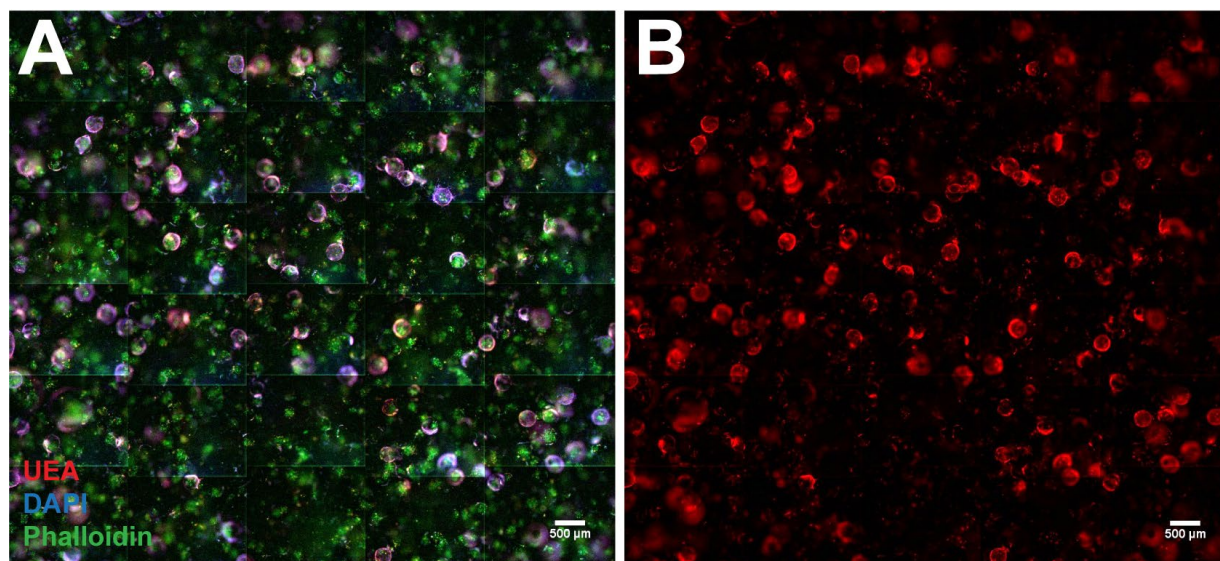
Figure 6.25: HUVEC-HASMC microbeads. *(A) UEA-DAPI-Phalloidin and (B) UEA only staining of whole gel scan slides of D1 PC HUVEC-HASMC microbeads cultured in bulk fibrin hydrogels for 7 days.*

6.5.5 Increased degradability (dVPMS-crosslinked) microbeads

Chapter 5 demonstrated that increasing the degradability, by way of crosslinking with dVPMS, increased the vascularization potential of PEGNB-based matrices. HUVEC and NHLF were encapsulated in PEGNB microbeads crosslinked with dVPMS. D1 PC microbeads contained both cell types distributed throughout (Fig. 6.26A and B) and supported microvascular network assembly when embedded and cultured in fibrin hydrogels for 7 days (Fig. 6.26C and D).

dVPMS-crosslinked microbeads were cultured in suspension for up to 5 days. As with sVPMS-crosslinked microbeads, dVPMS-crosslinked microbeads supported vessel morphogenesis as early as 3 days (Fig. 6.27A, B) which persisted over time (Fig. 6.27C-F). Further investigation is needed to determine how matrix degradability influences prevascularization and subsequent angiogenic sprouting. It is possible that the use of dVPMS as a crosslinker can support earlier vessel morphogenesis within microbeads than sVPMS.
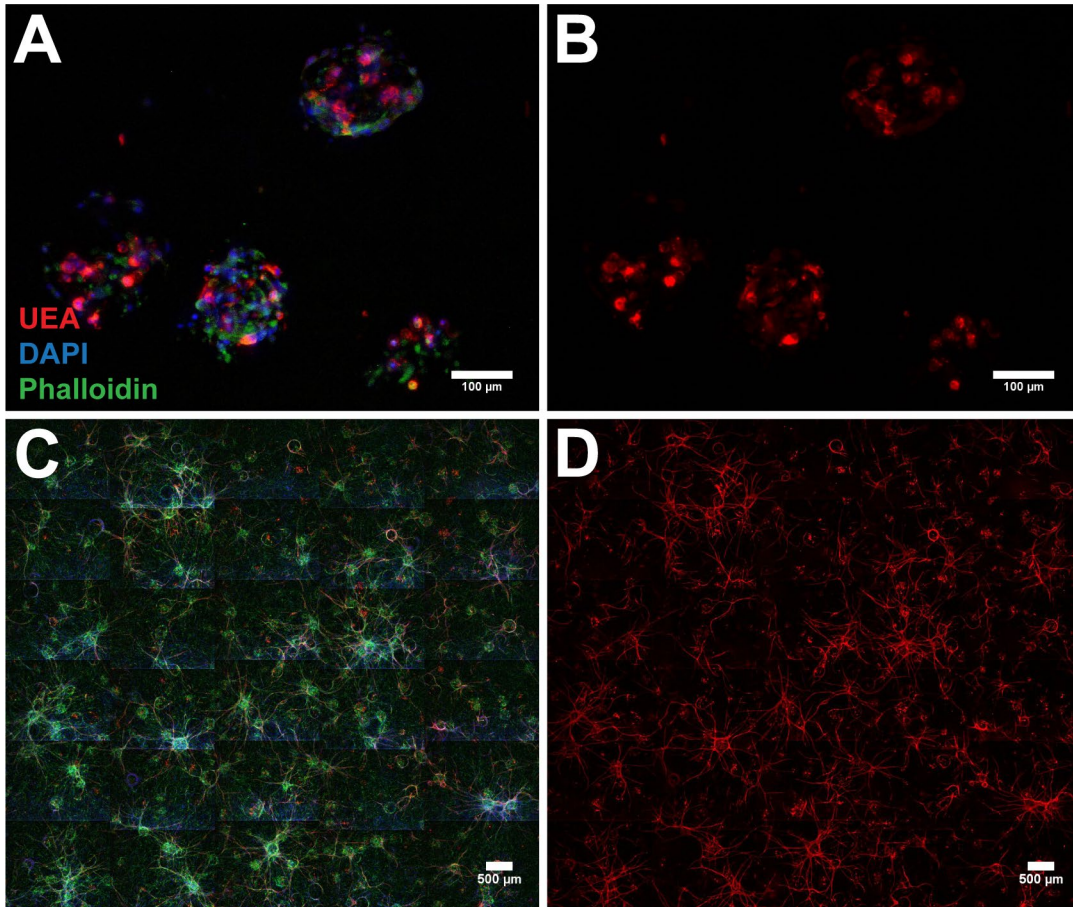
Figure 6.26: HUVEC-NHLF microbeads crosslinked with dVPMS. *(A) UEA-DAPI-Phalloidin and (B) UEA only staining of D1 PC dVPMS microbeads in suspension. (C) UEA-DAPI-Phalloidin and (D) UEA only staining of whole gel scan slides of D1 PC dVPMS microbeads cultured in bulk fibrin hydrogels for 7 days.*
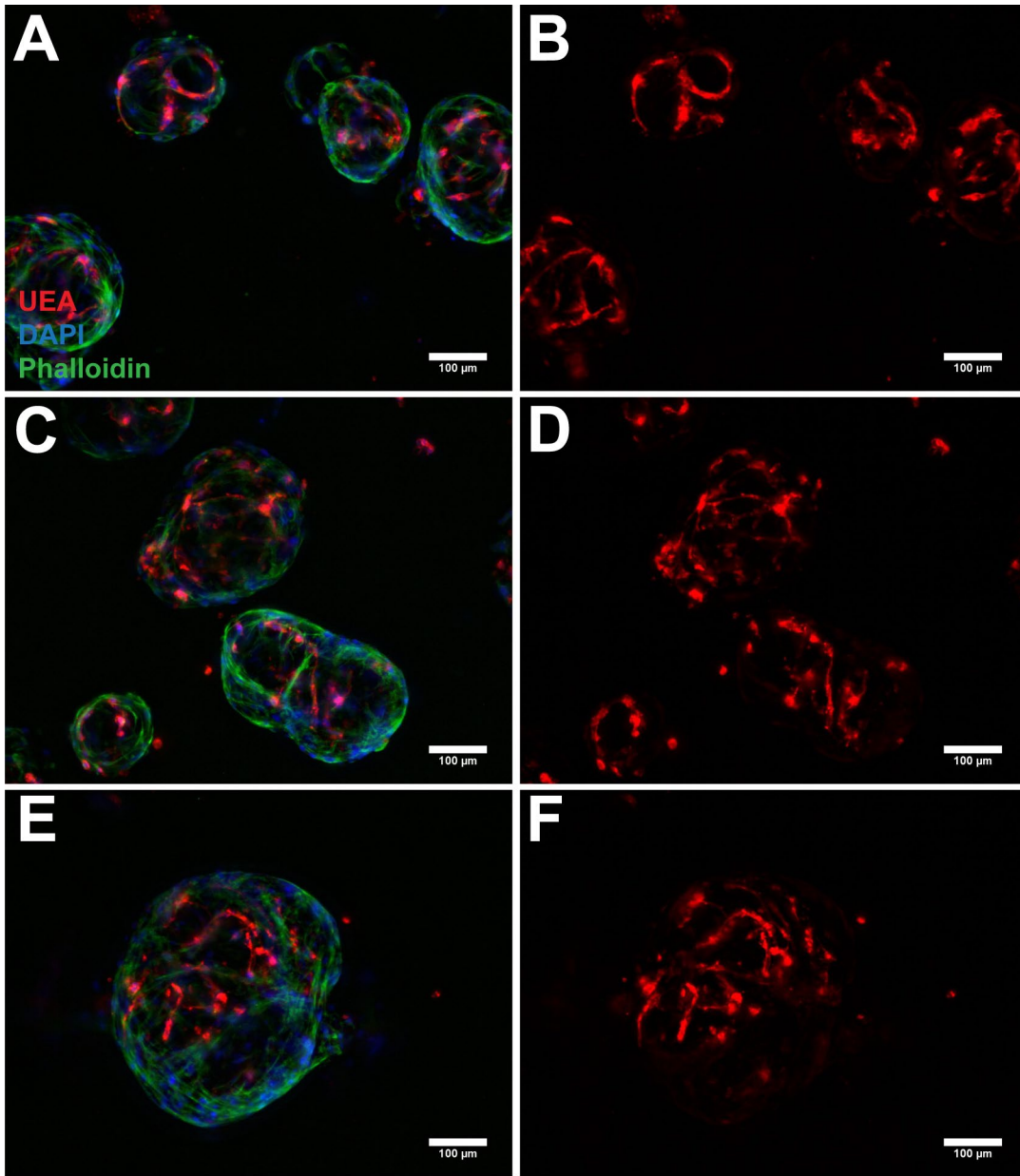
Figure 6.27: Pre-cultured HUVEC-NHLF dVPMS-crosslinked microbeads. *(A, C, D) UEA-DAPI-Phalloidin and (B, D, E) UEA only staining of (A, B) D1, (C, D) D3, and (E, F) D5 PC dVPMS microbeads in suspension.*

6.5.6 Vortex emulsion PEGNB microbeads

An alternative PEGNB microbead fabrication technique commonly used in the literature is vortex emulsification, in which PEG precursor solutions are added to oil in a microcentrifuge tube and vortexed to emulsify the PEG solution before exposure to UV for crosslinking. HUVEC-

NHLF (20 M/mL, 1:1 ratio) microbeads were fabricated using this technique to assess if vortex emulsification could more rapidly generate larger volumes of microbeads that may have a more homogeneous cell distribution. Compared to microfluidic droplet generation, which takes 20 min to produce microbeads from 300 µL of precursor solution, vortex emulsification produced the same volume of microbeads in ~10 s. Microbeads had a greater variation in diameter compared to microfluidic droplet generation. Live/dead staining 24 h post-encapsulation revealed that some microbeads contained a high density of viable cells, while others did not (Fig. 6.28 A and B).
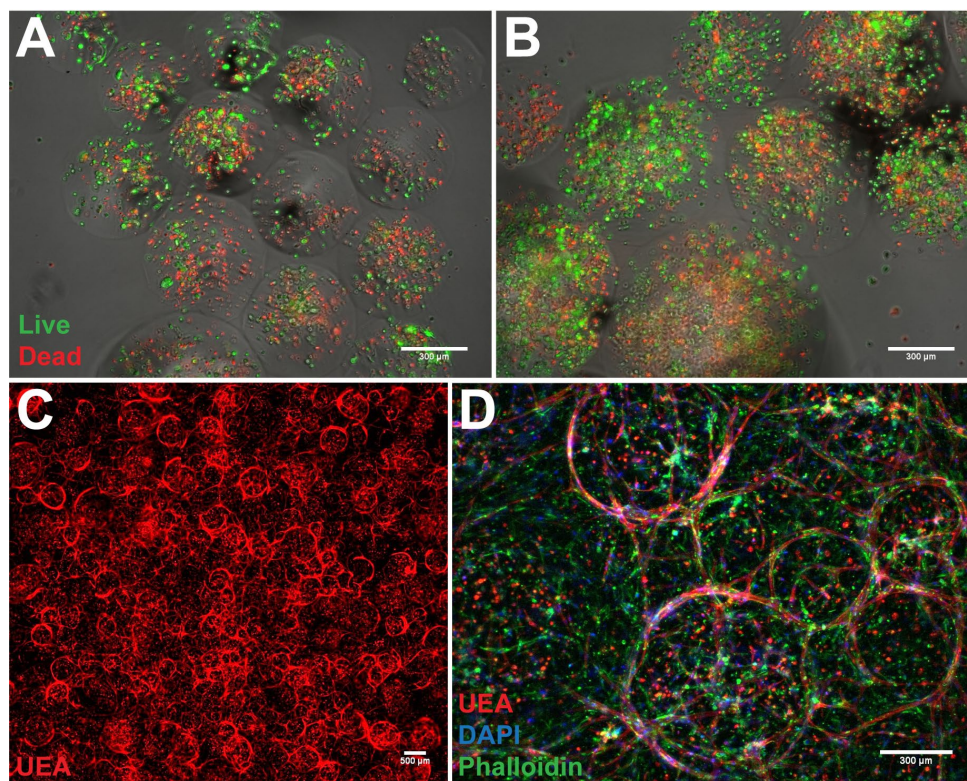
Figure 6.28: PEGNB microbeads formed via vortex emulsification. *(A, B) Live/dead staining of HUVEC and NHLF 24 h post-encapsulation. (C) Whole gel scan slide of D1 PC vortex microbeads cultured in bulk fibrin hydrogels for 7 days. (D) Select region of whole gel scan slide.*

Microbeads were embedded and cultured in fibrin hydrogels for 7 days. The sprouting profile of vortex microbeads was different from that of microfluidic microbeads. While some vessel sprouting from the microbeads was observed, HUVEC tended to form vessel-like structures on the surface of microbeads as opposed to sprouting out into the surrounding matrix (Fig. 6.28 C

and D). A large majority of HUVEC remain as individual cells, as evidenced by UEA staining, which could indicate that HUVEC were the cell type with lower viability post-encapsulation. Repeated vortexing to emulsify the precursor solution may not be suitable for HUVEC encapsulation.

6.5.7 Alternate PEG macromer (PEGVS) microbeads

As our group had previous experience vascularizing PEG-vinyl sulfone (PEGVS) bulk hydrogels [17, 18, 20], this macromer was investigated for use in microbeads using the same water-in-oil emulsification approach that was used for the fibrin-based beads in Chapters 3 and 4. PEGVS hydrogels are formed via a click chemistry known as Michael type addition (MTA), a reaction that is highly dependent on the pH of the reaction as well as the concentration of PEG and crosslinker. Higher wt. % 5.5% PEGVS supported the formation of individual microbeads containing highly viable cells; however, over time some cells migrated to the exterior of the microbeads while others in the center of the microbeads died (Fig. 6.29). Since previous literature on vascularized PEG matrices has demonstrated lower wt. % PEG hydrogels facilitates greater vessel morphogenesis, the wt. % PEGVS was decreased to 5%, which generated microbeads that yielded similar results to 5.5%. Decreasing the wt. % of PEGVS further to 4.5% led to aggregation between microbeads that were not fully polymerized during the emulsification process. Microbeads started to crosslink as spheres, but then became aggregated before collection. Further, these microbeads also had diminished cell viability and cell spreading by day 7.
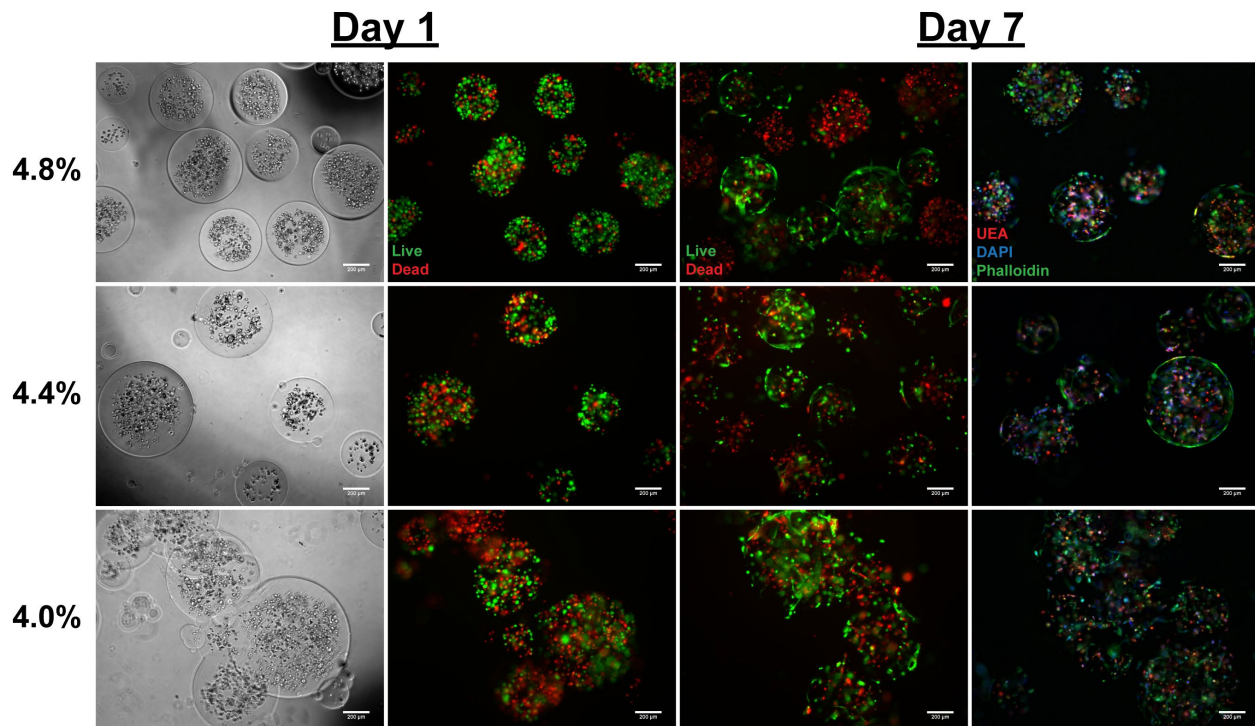
Figure 6.29: PEGVS microbeads formed via bulk emulsification. *HUVEC and NHLF were encapsulated in microbeads formulated with 4.8, 4.4, or 4.0% PEGVS and cultured for up to a week in suspension.*

A flow-focusing device with fluorinated oil was used to produce 3 wt. % PEGVS microbeads. PEGVS flowed through the center channel and the crosslinker flowed through two parallel channels (Fig. 6.30A) where they met just before the pinching junction (Fig. 6.30B). Small fluorospheres (2 μm diameter) were incorporated into the crosslinker to assess how well it was distributed through the microbeads. Fluorospheres (and thus crosslinker) were unevenly distributed of crosslinker across microbeads (Fig. 6.30C and D). Further, small fluctuations led to large microbeads being produced due to coalescence. While this could be a larger problem when working with cells that could cause these flow fluctuations due to aggregation, the ability to generate soft/lower wt. % MTA formed microbeads is an exciting approach as it allows the formation of microbeads from a variety of PEG macromers.
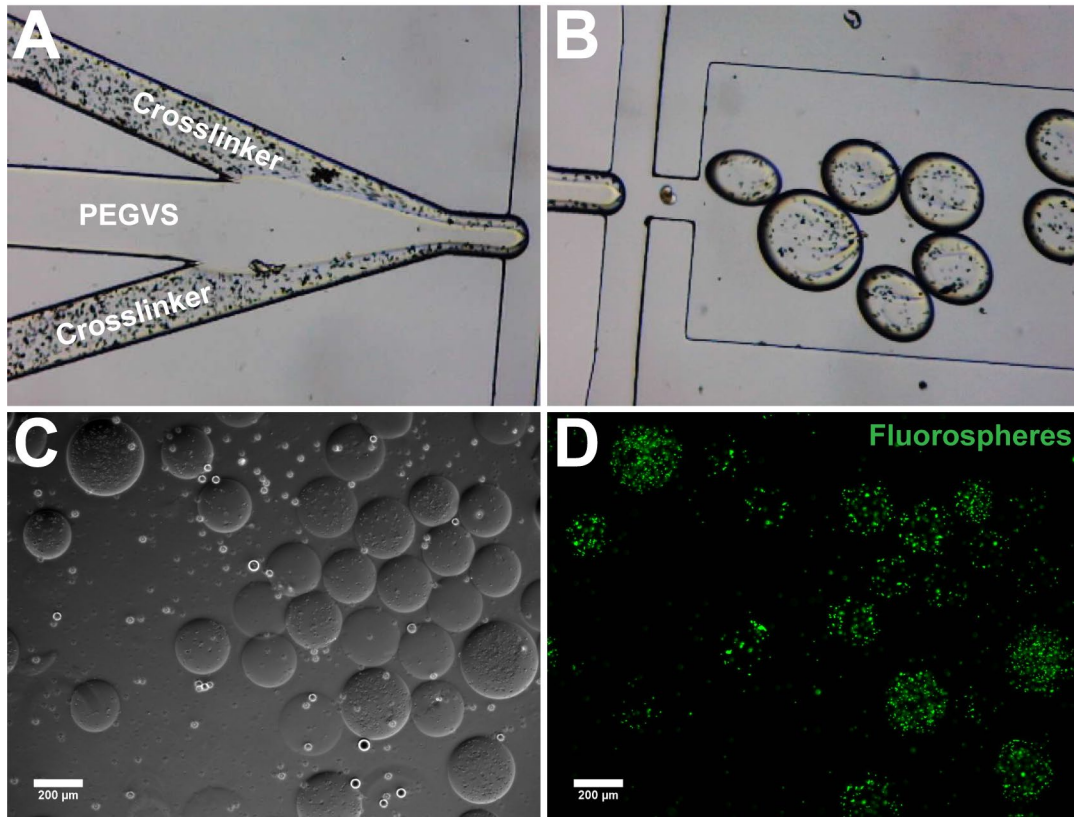
Figure 6.30: Acellular PEGVS microbeads formed via microfluidic droplet generation. *(A) PEGVS and crosslinker (VPMS) met at the flow-focusing junction (B) where droplets were pinched by fluorinated oil. (C) Phase and (D) fluorescent imaging of microbeads 24 h post-fabrication.*

6.6 References

[1]   C. W. Tsao *et al.*, "Heart Disease and Stroke Statistics-2022 Update: A Report From the American Heart Association," *Circulation,* vol. 145, no. 8, pp. e153-e639, Feb 22 2022, doi: 10.1161/CIR.0000000000001052.

[2]   L. Beltran-Camacho, M. Rojas-Torres, and M. C. Duran-Ruiz, "Current Status of Angiogenic Cell Therapy and Related Strategies Applied in Critical Limb Ischemia," *Int J Mol Sci,* vol. 22, no. 5, Feb 26 2021, doi: 10.3390/ijms22052335.

[3]   T. J. Cahill, R. P. Choudhury, and P. R. Riley, "Heart regeneration and repair after myocardial infarction: translational opportunities for novel therapeutics," *Nat Rev Drug Discov,* vol. 16, no. 10, pp. 699-717, Oct 2017, doi: 10.1038/nrd.2017.106.

[4]   L. Uccioli, M. Meloni, V. Izzo, L. Giurato, S. Merolla, and R. Gandini, "Critical limb ischemia: current challenges and future prospects," *Vasc Health Risk Manag,* vol. 14, pp. 63-74, 2018, doi: 10.2147/VHRM.S125065.

[5]   M. Qadura, D. C. Terenzi, S. Verma, M. Al-Omran, and D. A. Hess, "Concise Review: Cell Therapy for Critical Limb Ischemia: An Integrated Review of Preclinical and Clinical Studies," *Stem Cells,* vol. 36, no. 2, pp. 161-171, Feb 2018, doi: 10.1002/stem.2751.

[6]   G. Marsico, S. Martin-Saldana, and A. Pandit, "Therapeutic Biomaterial Approaches to Alleviate Chronic Limb Threatening Ischemia," *Adv Sci (Weinh),* vol. 8, no. 7, p. 2003119, Apr 2021, doi: 10.1002/advs.202003119.

[7]   Y. Pan *et al.*, "Advances for the treatment of lower extremity arterial disease associated with diabetes mellitus," *Front Mol Biosci,* vol. 9, p. 929718, 2022, doi: 10.3389/fmolb.2022.929718.

[8]   M. Hassanshahi *et al.*, "Critical limb ischemia: Current and novel therapeutic strategies," *Journal of Cellular Physiology,* vol. 234, no. 9, pp. 14445-14459, 2019, doi: 10.1002/jcp.28141.

[9]   R. K. Jain, P. Au, J. Tam, D. G. Duda, and D. Fukumura, "Engineering vascularized tissue," *Nature Biotechnology,* vol. 23, no. 7, pp. 821-823, 2005, doi: 10.1038/nbt0705-821.

[10]   T. L. Place, F. E. Domann, and A. J. Case, "Limitations of oxygen delivery to cells in culture: An underappreciated problem in basic and translational research," *Free Radic Biol Med,* vol. 113, pp. 311-322, Dec 2017, doi: 10.1016/j.freeradbiomed.2017.10.003.

[11]   N. E. Friend, J. A. Beamish, E. A. Margolis, N. G. Schott, J. P. Stegemann, and A. J. Putnam, "Pre-cultured, cell-encapsulating fibrin microbeads for the vascularization of ischemic tissues," *J Biomed Mater Res A,* Jun 16 2023, doi: 10.1002/jbm.a.37580.

[12]   N. E. Friend *et al.*, "Injectable pre-cultured tissue modules catalyze the formation of extensive functional microvasculature in vivo," *Sci Rep,* vol. 10, no. 1, p. 15562, Sep 23 2020, doi: 10.1038/s41598-020-72576-5.

[13]   A. L. Torres, S. J. Bidarra, M. T. Pinto, P. C. Aguiar, E. A. Silva, and C. C. Barrias, "Guiding morphogenesis in cell-instructive microgels for therapeutic angiogenesis," *Biomaterials,* vol. 154, pp. 34-47, Feb 2018, doi: 10.1016/j.biomaterials.2017.10.051.

[14]   A. L. Torres *et al.*, "Microvascular engineering: Dynamic changes in microgel-entrapped vascular cells correlates with higher vasculogenic/angiogenic potential," *Biomaterials,* vol. 228, p. 119554, Jan 2020, doi: 10.1016/j.biomaterials.2019.119554.

[15]   J. Zhu, "Bioactive modification of poly(ethylene glycol) hydrogels for tissue engineering," *Biomaterials,* vol. 31, no. 17, pp. 4639-56, Jun 2010, doi: 10.1016/j.biomaterials.2010.02.044.

[16]   X. Li, Q. Sun, Q. Li, N. Kawazoe, and G. Chen, "Functional Hydrogels With Tunable Structures and Properties for Tissue Engineering Applications," *Front Chem,* vol. 6, p. 499, 2018, doi: 10.3389/fchem.2018.00499.

[17]   J. A. Beamish, B. A. Juliar, D. S. Cleveland, M. E. Busch, L. Nimmagadda, and A. J. Putnam, "Deciphering the relative roles of matrix metalloproteinase- and plasmin-mediated matrix degradation during capillary morphogenesis using engineered hydrogels," *J Biomed Mater Res B Appl Biomater,* vol. 107, no. 8, pp. 2507-2516, Nov 2019, doi: 10.1002/jbm.b.34341.

[18]   B. A. Juliar, J. A. Beamish, M. E. Busch, D. S. Cleveland, L. Nimmagadda, and A. J. Putnam, "Cell-mediated matrix stiffening accompanies capillary morphogenesis in ultra-soft amorphous hydrogels," *Biomaterials,* vol. 230, p. 119634, Feb 2020, doi: 10.1016/j.biomaterials.2019.119634.

[19]   A. Brown, H. He, E. Trumper, J. Valdez, P. Hammond, and L. G. Griffith, "Engineering PEG-based hydrogels to foster efficient endothelial network formation in free-swelling and confined microenvironments," *Biomaterials,* vol. 243, p. 119921, Jun 2020, doi: 10.1016/j.biomaterials.2020.119921.

[20]   M. Vigen, J. Ceccarelli, and A. J. Putnam, "Protease-sensitive PEG hydrogels regulate vascularization in vitro and in vivo," *Macromol Biosci,* vol. 14, no. 10, pp. 1368-79, Oct 2014, doi: 10.1002/mabi.201400161.

[21]   M. R. Zanotelli *et al.*, "Stable engineered vascular networks from human induced pluripotent stem cell-derived endothelial cells cultured in synthetic hydrogels," *Acta Biomater,* vol. 35, pp. 32-41, Apr 15 2016, doi: 10.1016/j.actbio.2016.03.001.

[22]   E. B. Peters, N. Christoforou, K. W. Leong, G. A. Truskey, and J. L. West, "Poly(ethylene glycol) Hydrogel Scaffolds Containing Cell-Adhesive and Protease-Sensitive Peptides Support Microvessel Formation by Endothelial Progenitor Cells," *Cell Mol Bioeng,* vol. 9, no. 1, pp. 38-54, Mar 1 2016, doi: 10.1007/s12195-015-0423-6.

[23]   R. M. Schweller, Z. J. Wu, B. Klitzman, and J. L. West, "Stiffness of Protease Sensitive and Cell Adhesive PEG Hydrogels Promotes Neovascularization In Vivo," *Ann Biomed Eng,* vol. 45, no. 6, pp. 1387-1398, Jun 2017, doi: 10.1007/s10439-017-1822-8.

[24]   F. Jivan *et al.*, "Sequential Thiol-Ene and Tetrazine Click Reactions for the Polymerization and Functionalization of Hydrogel Microparticles," *Biomacromolecules,* vol. 17, no. 11, pp. 3516-3523, Nov 14 2016, doi: 10.1021/acs.biomac.6b00990.

[25]   N. A. Impellitteri, M. W. Toepke, S. K. Lan Levengood, and W. L. Murphy, "Specific VEGF sequestering and release using peptide-functionalized hydrogel microspheres," *Biomaterials,* vol. 33, no. 12, pp. 3475-84, Apr 2012, doi: 10.1016/j.biomaterials.2012.01.032.

[26]   M. W. Toepke, N. A. Impellitteri, S. K. Lan Levengood, D. S. Boeldt, I. M. Bird, and W. L. Murphy, "Regulating specific growth factor signaling using immobilized branched ligands," *Adv Healthc Mater,* vol. 1, no. 4, pp. 457-60, Jul 2012, doi: 10.1002/adhm.201200077.

[27]   D. G. Belair, A. S. Khalil, M. J. Miller, and W. L. Murphy, "Serum-dependence of affinity-mediated VEGF release from biomimetic microspheres," *Biomacromolecules,* vol. 15, no. 6, pp. 2038-48, Jun 9 2014, doi: 10.1021/bm500177c.

[28]   D. G. Belair *et al.*, "Differential regulation of angiogenesis using degradable VEGF-binding microspheres," *Biomaterials,* vol. 93, pp. 27-37, Jul 2016, doi: 10.1016/j.biomaterials.2016.03.021.

[29]   D. G. Belair and W. L. Murphy, "Specific VEGF sequestering to biomaterials: influence of serum stability," *Acta Biomater,* vol. 9, no. 11, pp. 8823-31, Nov 2013, doi: 10.1016/j.actbio.2013.06.033.

[30]   G. A. Foster, D. M. Headen, C. Gonzalez-Garcia, M. Salmeron-Sanchez, H. Shirwan, and A. J. Garcia, "Protease-degradable microgels for protein delivery for vascularization," *Biomaterials,* vol. 113, pp. 170-175, Jan 2017, doi: 10.1016/j.biomaterials.2016.10.044.

[31]   D. R. Griffin, W. M. Weaver, P. O. Scumpia, D. Di Carlo, and T. Segura, "Accelerated wound healing by injectable microporous gel scaffolds assembled from annealed building blocks," *Nat Mater,* vol. 14, no. 7, pp. 737-44, Jul 2015, doi: 10.1038/nmat4294.

[32]   C. M. Ghajar, K. S. Blevins, C. C. Hughes, S. C. George, and A. J. Putnam, "Mesenchymal stem cells enhance angiogenesis in mechanically viable prevascularized tissues via early matrix metalloproteinase upregulation," *Tissue Eng,* vol. 12, no. 10, pp. 2875-88, Oct 2006, doi: 10.1089/ten.2006.12.2875.

[33]   C. C. Lin, C. S. Ki, and H. Shih, "Thiol-norbornene photo-click hydrogels for tissue engineering applications," *J Appl Polym Sci,* vol. 132, no. 8, Feb 20 2015, doi: 10.1002/app.41563.

[34]   J. Schindelin *et al.*, "Fiji: an open-source platform for biological-image analysis," *Nat Methods,* vol. 9, no. 7, pp. 676-82, Jun 28 2012, doi: 10.1038/nmeth.2019.

[35]   A. S. Caldwell, B. A. Aguado, and K. S. Anseth, "Designing Microgels for Cell Culture and Controlled Assembly of Tissue Microenvironments," *Adv Funct Mater,* vol. 30, no. 37, Sep 10 2020, doi: 10.1002/adfm.201907670.

[36]   J. K. Gandhi, L. Zivkovic, J. P. Fisher, M. C. Yoder, and E. M. Brey, "Enhanced Viability of Endothelial Colony Forming Cells in Fibrin Microbeads for Sensor Vascularization," *Sensors (Basel),* vol. 15, no. 9, pp. 23886-902, Sep 18 2015, doi: 10.3390/s150923886.

[37]   C. Zhang *et al.*, "Novel hiPSC-based tri-culture for pre-vascularization of calcium phosphate scaffold to enhance bone and vessel formation," *Mater Sci Eng C Mater Biol Appl,* vol. 79, pp. 296-304, Oct 1 2017, doi: 10.1016/j.msec.2017.05.035.

[38]   C. L. Franco, J. Price, and J. L. West, "Development and optimization of a dual-photoinitiator, emulsion-based technique for rapid generation of cell-laden hydrogel microspheres," *Acta Biomater,* vol. 7, no. 9, pp. 3267-76, Sep 2011, doi: 10.1016/j.actbio.2011.06.011.

[39]   G. Ramirez-Calderon, H. H. Susapto, and C. A. E. Hauser, "Delivery of Endothelial Cell-Laden Microgel Elicits Angiogenesis in Self-Assembling Ultrashort Peptide Hydrogels In Vitro," *ACS Appl Mater Interfaces,* vol. 13, no. 25, pp. 29281-29292, Jun 30 2021, doi: 10.1021/acsami.1c03787.

[40]   M. Sofman, A. Brown, L. G. Griffith, and P. T. Hammond, "A modular polymer microbead angiogenesis scaffold to characterize the effects of adhesion ligand density on angiogenic sprouting," *Biomaterials,* vol. 264, p. 120231, Jan 2021, doi: 10.1016/j.biomaterials.2020.120231.

[41]   A. Y. Rioja, E. L. H. Daley, J. C. Habif, A. J. Putnam, and J. P. Stegemann, "Distributed vasculogenesis from modular agarose-hydroxyapatite-fibrinogen microbeads," *Acta Biomater,* vol. 55, pp. 144-152, Jun 2017, doi: 10.1016/j.actbio.2017.03.050.

[42]   A. Y. Rioja, R. Tiruvannamalai Annamalai, S. Paris, A. J. Putnam, and J. P. Stegemann, "Endothelial sprouting and network formation in collagen- and fibrin-based modular microbeads," *Acta Biomater,* vol. 29, pp. 33-41, Jan 2016, doi: 10.1016/j.actbio.2015.10.022.

[43]   R. Tiruvannamalai Annamalai, A. Y. Rioja, A. J. Putnam, and J. P. Stegemann, "Vascular Network Formation by Human Microvascular Endothelial Cells in Modular Fibrin Microtissues," *ACS Biomater Sci Eng,* vol. 2, no. 11, pp. 1914-1925, Nov 14 2016, doi: 10.1021/acsbiomaterials.6b00274.

[44]   W. J. Seeto, Y. Tian, S. Pradhan, P. Kerscher, and E. A. Lipke, "Rapid Production of Cell-Laden Microspheres Using a Flexible Microfluidic Encapsulation Platform," *Small,* vol. 15, no. 47, p. e1902058, Nov 2019, doi: 10.1002/smll.201902058.

[45]   P. H. Kim *et al.*, "Injectable multifunctional microgel encapsulating outgrowth endothelial cells and growth factors for enhanced neovascularization," *J Control Release,* vol. 187, pp. 1-13, Aug 10 2014, doi: 10.1016/j.jconrel.2014.05.010.

[46]   W. J. Seeto, Y. Tian, R. L. Winter, F. J. Caldwell, A. A. Wooldridge, and E. A. Lipke, "Encapsulation of Equine Endothelial Colony Forming Cells in Highly Uniform, Injectable Hydrogel Microspheres for Local Cell Delivery," *Tissue Eng Part C Methods,* vol. 23, no. 11, pp. 815-825, Nov 2017, doi: 10.1089/ten.TEC.2017.0233.

[47]   R. L. Winter *et al.*, "Cell engraftment, vascularization, and inflammation after treatment of equine distal limb wounds with endothelial colony forming cells encapsulated within hydrogel microspheres," *BMC Vet Res,* vol. 16, no. 1, p. 43, Feb 4 2020, doi: 10.1186/s12917-020-2269-y.

[48]   H. Zhao, Wang, Z., Jiang, S., Wang, J., Hu, Z., Lobie, P. E., Ma, S. , "Microfluidic Synthesis of Injectable Angiogenic Microgels," *Cell Reports Physical Science,* vol. 1, no. 5, p. 100047, 20 May 2020 2020, doi: 10.1016/j.xcrp.2020.100047.

[49]   P. Du, A. D. S. Da Costa, C. Savitri, S. S. Ha, P. Y. Wang, and K. Park, "An injectable, self-assembled multicellular microsphere with the incorporation of fibroblast-derived

extracellular matrix for therapeutic angiogenesis," *Mater Sci Eng C Mater Biol Appl,* vol. 113, p. 110961, Aug 2020, doi: 10.1016/j.msec.2020.110961.

[50]   C. M. Franca *et al.*, "High-Throughput Bioprinting of Geometrically-Controlled Pre-Vascularized Injectable Microgels for Accelerated Tissue Regeneration," *Adv Healthc Mater,* p. e2202840, May 23 2023, doi: 10.1002/adhm.202202840.

[51]   R. Matta, S. Lee, N. Genet, K. K. Hirschi, J. L. Thomas, and A. L. Gonzalez, "Minimally Invasive Delivery of Microbeads with Encapsulated, Viable and Quiescent Neural Stem Cells to the Adult Subventricular Zone," *Sci Rep,* vol. 9, no. 1, p. 17798, Nov 28 2019, doi: 10.1038/s41598-019-54167-1.

[52]   C. Y. Li, D. K. Wood, J. H. Huang, and S. N. Bhatia, "Flow-based pipeline for systematic modulation and analysis of 3D tumor microenvironments," *Lab Chip,* vol. 13, no. 10, pp. 1969-78, May 21 2013, doi: 10.1039/c3lc41300d.

[53]   S. Allazetta, L. Kolb, S. Zerbib, J. Bardy, and M. P. Lutolf, "Cell-Instructive Microgels with Tailor-Made Physicochemical Properties," *Small,* vol. 11, no. 42, pp. 5647-56, Nov 11 2015, doi: 10.1002/smll.201501001.

[54]   M. G. A. Mohamed, S. Kheiri, S. Islam, H. Kumar, A. Yang, and K. Kim, "An integrated microfluidic flow-focusing platform for on-chip fabrication and filtration of cell-laden microgels," *Lab Chip,* vol. 19, no. 9, pp. 1621-1632, Apr 23 2019, doi: 10.1039/c9lc00073a.

[55]   J. M. De Rutte, J. Koh, and D. Di Carlo, "Scalable High-Throughput Production of Modular Microgels for In Situ Assembly of Microporous Tissue Scaffolds," *Advanced Functional Materials,* vol. 29, no. 25, p. 1900071, 2019, doi: 10.1002/adfm.201900071.

[56]   H. Zhang *et al.*, "Large-scale single-cell encapsulation in microgels through metastable droplet-templating combined with microfluidic-integration," *Biofabrication,* vol. 14, no. 3, Jun 6 2022, doi: 10.1088/1758-5090/ac7168.

[57]   E. Kniazeva, S. Kachgal, and A. J. Putnam, "Effects of extracellular matrix density and mesenchymal stem cells on neovascularization in vivo," *Tissue Eng Part A,* vol. 17, no. 7-8, pp. 905-14, Apr 2011, doi: 10.1089/ten.TEA.2010.0275.

[58]   W. Y. Wang, D. Lin, E. H. Jarman, W. J. Polacheck, and B. M. Baker, "Functional angiogenesis requires microenvironmental cues balancing endothelial cell migration and proliferation," *Lab on a Chip,* vol. 20, no. 6, pp. 1153-1166, 2020, doi: 10.1039/c9lc01170f.

[59]   K. S. Okuda and B. M. Hogan, "Endothelial Cell Dynamics in Vascular Development: Insights From Live-Imaging in Zebrafish," *Front Physiol,* vol. 11, p. 842, 2020, doi: 10.3389/fphys.2020.00842.

[60] C. G. Fonseca, P. Barbacena, and C. A. Franco, "Endothelial cells on the move: dynamics in vascular morphogenesis and disease," *Vasc Biol,* vol. 2, no. 1, pp. H29-H43, 2020, doi: 10.1530/VB-20-0007.

[61] L. Jakobsson *et al.*, "Endothelial cells dynamically compete for the tip cell position during angiogenic sprouting," *Nat Cell Biol,* vol. 12, no. 10, pp. 943-53, Oct 2010, doi: 10.1038/ncb2103.

[62] B. L. Macklin *et al.*, "Intrinsic epigenetic control of angiogenesis in induced pluripotent stem cell-derived endothelium regulates vascular regeneration," *NPJ Regen Med,* vol. 7, no. 1, p. 28, May 12 2022, doi: 10.1038/s41536-022-00223-w.

[63] D. H. Nguyen *et al.*, "Biomimetic model to reconstitute angiogenic sprouting morphogenesis in vitro," *Proc Natl Acad Sci U S A,* vol. 110, no. 17, pp. 6712-7, Apr 23 2013, doi: 10.1073/pnas.1221526110.

[64] K. E. Johnson and T. A. Wilgus, "Vascular Endothelial Growth Factor and Angiogenesis in the Regulation of Cutaneous Wound Repair," *Adv Wound Care (New Rochelle),* vol. 3, no. 10, pp. 647-661, Oct 1 2014, doi: 10.1089/wound.2013.0517.

[65] H. Li, Y. Shang, Q. Feng, Y. Liu, J. Chen, and H. Dong, "A novel bioartificial pancreas fabricated via islets microencapsulation in anti-adhesive core-shell microgels and macroencapsulation in a hydrogel scaffold prevascularized in vivo," *Bioact Mater,* vol. 27, pp. 362-376, Sep 2023, doi: 10.1016/j.bioactmat.2023.04.011.

[66] E. M. Kim *et al.*, "Fabrication of core-shell spheroids as building blocks for engineering 3D complex vascularized tissue," *Acta Biomater,* vol. 100, pp. 158-172, Dec 2019, doi: 10.1016/j.actbio.2019.09.028.

[67] H. Wang, H. Liu, H. Liu, W. Su, W. Chen, and J. Qin, "One-Step Generation of Core–Shell Gelatin Methacrylate (GelMA) Microgels Using a Droplet Microfluidic System," *Advanced Materials Technologies,* vol. 4, no. 6, p. 1800632, 2019, doi: 10.1002/admt.201800632.

[68] R. Z. Lin *et al.*, "Host non-inflammatory neutrophils mediate the engraftment of bioengineered vascular networks," *Nat Biomed Eng,* vol. 1, 2017, doi: 10.1038/s41551-017-0081.

[69] E. A. Margolis *et al.*, "Stromal cell identity modulates vascular morphogenesis in a microvasculature-on-a-chip platform," *Lab Chip,* vol. 21, no. 6, pp. 1150-1163, Mar 21 2021, doi: 10.1039/d0lc01092h.

Chapter 7 – Summary, Conclusions, and Future Directions

7.1 Summary of Findings and Conclusions

This chapter summarizes the research conducted in this dissertation, including contributions to the field of tissue engineering and future work that may improve current technologies and enhance therapeutic potential. The overall goal of this dissertation was to develop injectable, modular, vascularizing microbeads capable of supporting the development of robust microvascular networks to address the overarching hypothesis that prevascularized microbeads can jump-start inosculation with host vasculature upon implantation, rapidly revascularizing ischemic tissues. The following subsections summarize the key findings and conclusions of each aim to highlight progress made toward achieving this goal.

7.1.1 Aim 1 – Evaluate the vascularization capability of established fibrin-based microbeads in vivo in a subcutaneous implant and hindlimb ischemia model.

Fibrin-based microbeads had been previously developed by our group [1]. This work (Chapter 3 [2], Chapter 4 [3]) analyzed how prevascularization of fibrin microbeads influenced vessel network formation *in vitro* as well as *in vivo* in immunocompromised mice in subcutaneous implant and hindlimb ischemia models. These *in vivo* models allowed the assessment of how this microbead platform and prevascularization thereof influences the formation of functional microvascular networks *in situ*. Furthermore, the hindlimb ischemia model provided a platform to test if pre-cultured microbeads could restore perfusion to ischemic tissues.

Key findings and conclusions: This work showed that pre-cultured microbeads can form functional microvascular networks within 3 days of being implanted *in vivo*, as evidenced by the presence of host erythrocytes in the lumen of human-derived vessels. By 14 days post-surgery, animals treated with pre-cultured microbeads showed increased macroscopic reperfusion of ischemic foot pads and improved limb salvage compared to the cellular controls. These findings highlight the potential therapeutic benefit of developing modular, prevascularized microbeads as a minimally invasive therapeutic for treating ischemic tissues.
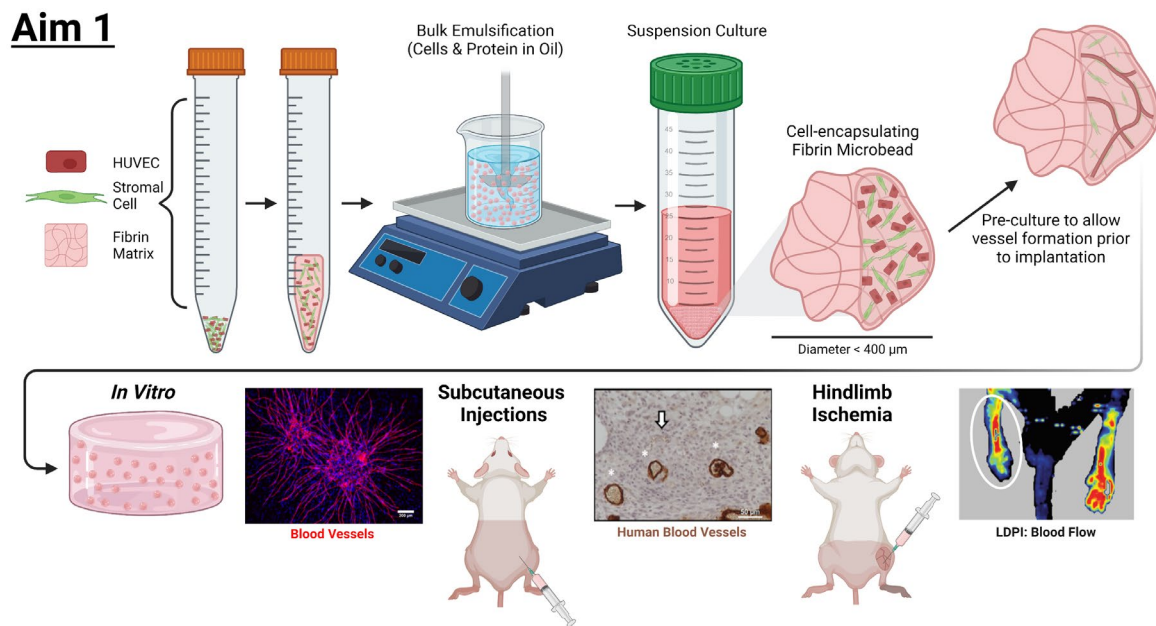
Figure 7.1: Aim 1 summary.

7.1.2 Aim 2 – Develop PEG-based microbeads that facilitate the formation of well-distributed microvascular networks within a tissue mimic in vitro.

While fibrin-based microbeads demonstrated great promise for revascularization applications, microbead aggregation during prevascularization hindered injectability and reduced overall vessel network coverage in larger constructs. PEG-based matrices were investigated for use as non-aggregating, injectable microbeads. Our group had prior experience vascularizing bulk

PEGVS hydrogels formed via Michael type addition [4-6]; however, the relatively slow gelation kinetics of this PEG macromer would necessitate more complex geometries for microfluidic droplet generation. Therefore, thiol-ene photopolymerized PEGNB was explored as it enables more control over microbead gelation without significantly increasing the complexity of fabrication [7]. PEGNB bulk hydrogel formulations that supported vessel formation were first identified, with a focus on how material physicochemical cues influence the rate and degree of microvascular network formation (Chapter 5 [8]).

Next, cell-laden PEGNB microbeads were developed via flow-focusing microfluidic biofabrication (Chapter 6). While there is a sizeable body of literature surrounding PEG-based microbeads/microgels/microspheres/microparticles, few actually encapsulate cells within the microbead matrix, and fewer do so via microfluidic droplet generation (compared to electrospray or vortex emulsion methods). Flow rates, initial cell concentration, buffers, and the microbead collection and isolation protocol were optimized to improve cell encapsulation efficiency. Cell distribution and viability 24 h post-encapsulation as well as the ability of microbeads to vascularize fibrin hydrogels *in vitro* were analyzed.

Key findings and conclusions: Enhanced cell-mediated remodeling of bulk PEGNB hydrogels, achieved either by reduced crosslinking (and thereby stiffness) or increased degradability, led to more rapid vessel formation and higher degrees of cell-mediated stiffening. PEGNB microbeads supported HUVEC and NHLF encapsulation with high viability and catalyzed the formation of robust, well-distributed microvascular networks in the surrounding matrix *in vitro*. These findings highlight the suitability of PEGNB as a biomaterial for the generation of vascularizing microbeads.
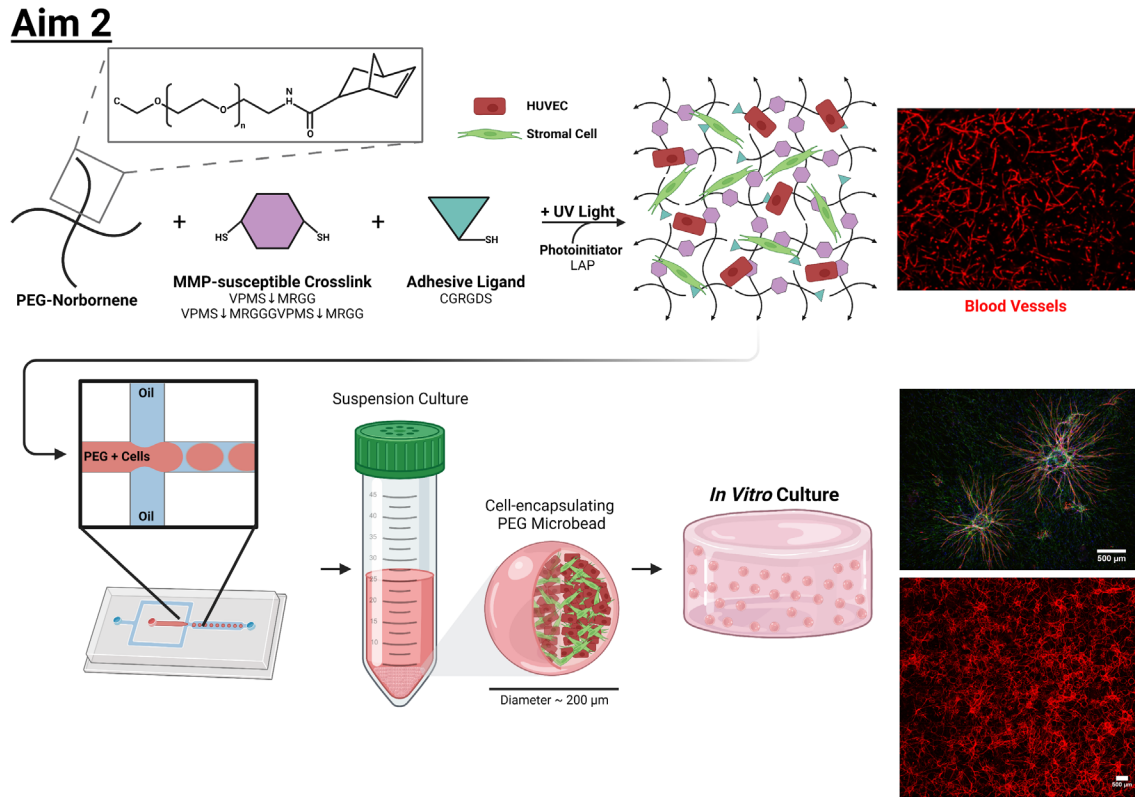
Figure 7.2: Aim 2 summary.

7.1.3 Aim 3 – Assess the prevascularization potential and subsequent performance of PEG-based microbeads in vitro and in vivo.

Few studies have encapsulated endothelial cells in PEG-based microbeads [9-13], focusing only on cell delivery post-encapsulation. Other work has demonstrated prevascularization of discrete microbeads using modified agarose [14], customized alginate [15, 16], and gelatin methacryloyl [17] matrices. Inspired by these works as well as our prior fibrin-based microbead results mentioned previously, PEGNB microbeads were subjected to extended pre-culture to determine if this platform could support prevascularization without microbead aggregation, and if so, how does this influence *in vitro* and *in vivo* vascularization potential. Microbeads were cultured in suspension to determine if microbeads would support prevascularization prior to being

embedded in larger fibrin hydrogels or implanted in subcutaneous pockets in immunocompromised mice.

Key findings and conclusions: Extended pre-culture of PEGNB microbeads enabled the formation of basement membrane supported vessel-like structures within the microbead matrix without aggregation, achieving the goal of developing non-aggregating, injectable prevascularized microbeads. However, increased pre-culture time unexpectedly led to decreased angiogenic sprouting *in vitro*. *In vivo* data revealed human-derived capillary-like structures as well as some evidence of lumen formation within microbeads; however, in most cases these structures failed to vascularize the surrounding implant region. These findings highlight the potential of PEGNB microbeads to support discrete prevascularized tissue models; however, further studies are needed to understand why preformed vessels are not sprouting from prevascularized microbeads.

Aim 3
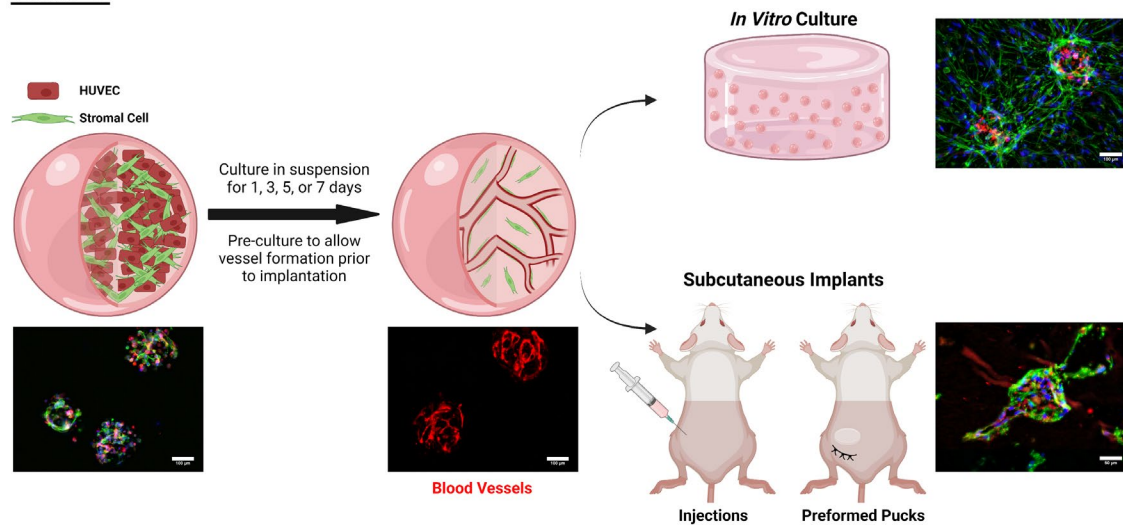
Figure 7.3: Aim 3 summary.

7.2 Impact

Cell-based tissue engineering strategies have demonstrated tremendous potential to develop effective therapeutics, functional tissue constructs, and perhaps one day, whole organs. Modular constructs with discrete microenvironments are becoming increasingly popular as platforms to deliver functional tissue units or engineer complex tissue structures [18]. This work contributes to the growing body of research centered on developing modular tissue constructs for vascularization applications. This dissertation described two different types of cell-encapsulating microbeads, each with attractive properties for vascular tissue engineering.

Fibrin-based microbeads utilize a relatively abundant and well-characterized matrix material that is naturally bioactive and vasculogenic, requiring little modification for tissue engineering applications [19]. The batch emulsification process used to fabricate fibrin microbeads generated a large volume of microbeads in a relatively short time. While previous studies have demonstrated prevascularized microbeads form microvascular networks *in vivo* [15-17], to our knowledge, none have applied cell-encapsulating microbeads toward the vascularization of ischemic tissues. The fibrin microbeads presented in this work rapidly formed functional microvasculature networks when implanted *in vivo*, including when delivered in a model of hindlimb ischemia. Further, pre-cultured microbeads supported the reperfusion of ischemia tissues, increasing limb salvage compared to bulk cellular controls. These results demonstrate the potential therapeutic benefit of developing prevascularized microbeads as a novel approach to vascularizing ischemic tissues.

PEG-based microbeads offer a "blank slate" that can be modified to include tissue-specific peptides or bioactive molecules. As such, PEG microbeads can be easily customized for encapsulation of different cell types without changing the manner of microbead production, more

easily producing tissue-specific modules. The flow-focusing microfluidic biofabrication used to generate PEG microbeads produced relatively homogenous droplets with a tight size distribution. The non-aggregating nature of PEG microbeads permitted the formation of well-distributed microvascular networks and prevascularization of discrete modular constructs. MAP hydrogels are a rapidly emerging class of porous hydrogels formed from secondary crosslinked microbeads, often which are made from PEG [20]. The cellular PEG microbeads developed here could improve current MAP scaffolds by acting as nodes of vascularization throughout the scaffold [21, 22].

Regardless of material type, vascularized microbeads could be combined with other constructs to form complex, multiphasic tissues. This has been previously shown by our group in the case of vascularized bone constructs [23], and future efforts are being made to generate cardiac and muscle microbeads to be combined with vascularizing microbeads with the goal of treating ischemic heart tissue after myocardial infarction or regenerating muscle tissue after volumetric muscle loss injuries (Fig. 7.1). Furthermore, as 3D printing becomes a more accessible tool for engineering complex tissues, microbeads could be integrated into this approach to increase the complexity of the printed constructs. Microbeads have been modified for use as extrudable inks [24-26] and support baths for extrusion printing [27-29]. Wang et al. printed endothelialized channels into a suspension bath of GelMA microbeads, which was secondarily crosslinked together. Endothelial cells from these channels sprouted into the surrounding microbeads after 3 days of culture [29]. Inspired by studies like this, our research group is attempting to print endothelialized channels into a suspension bead bath containing the vascularizing microbeads developed in this dissertation, with the goal of creating hierarchical vascular structures to support engineering large-scale tissues.
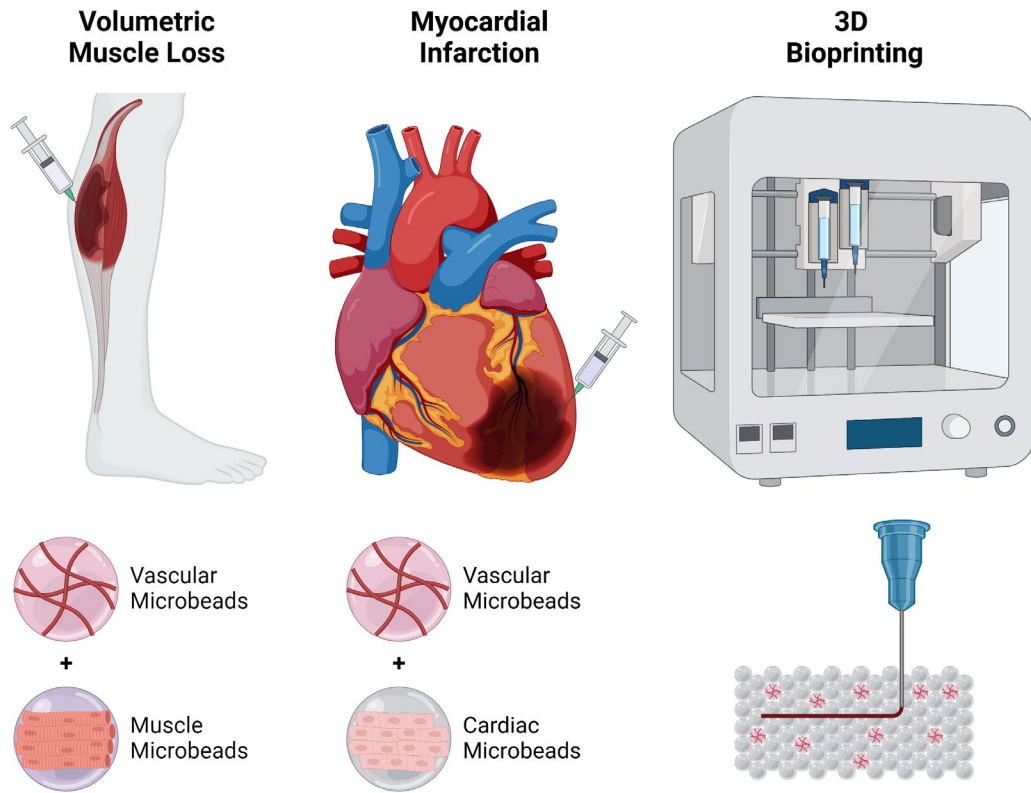
Figure 7.4: Potential future applications of vascularized microbeads.

7.3 Future Directions

Future work could focus on methods to encourage sprouting from prevascularized PEG microbeads. One potential method to induce angiogenic sprouting is the encapsulation of pre-cultured microbeads in previously established microfluidic chips [30, 31] (Fig. 6.17) or newly developed culture platforms (Figs. 6.18 and 7.2) to assess if growth factor gradients will encourage vessel sprouting. Growth factors, such as VEGF and BMP, are important in inducing a tip cell phenotype, which is required for angiogenic sprouting from established microvascular networks [32]. It is possible that the vessels within pre-cultured PEG microbeads have become too mature, resulting in endothelial cell quiescence and thus lack of sprouting [31-35]. Furthermore, it is possible that the disruption of the aggregated fibrin microbead matrix during microbead

resuspension prior to embedding or injecting them causes microvascular network disruption, inducting a tip cell phenotype and permitting sprouting from pre-cultured microbeads. If this approach revealed promising results (i.e., increased sprouting), pre-cultured microbeads could be co-encapsulated in bulk hydrogels or co-delivered *in vivo* with degradable growth factor (e.g., VEGF [34, 36]) releasing microbeads to encourage sprouting. This platform could also be used to assess functional perfusion of the microvasculature *in vitro* [37], which could provide an alternative approach to costly and timely animal model studies. Lastly, an ischemic microenvironment, such as the hindlimb ischemia model used in Chapter 4, may also provide additional cues necessary to encourage vessel structures to migrate out of the pre-cultured microbeads and vascularize the surroundings. Delivering PEG microbeads without a fibrin carrier gel could be considered to eliminate potential interfacial boundary issues [38] between the PEG and fibrin, allowing the PEG to be better integrated with the host tissue.
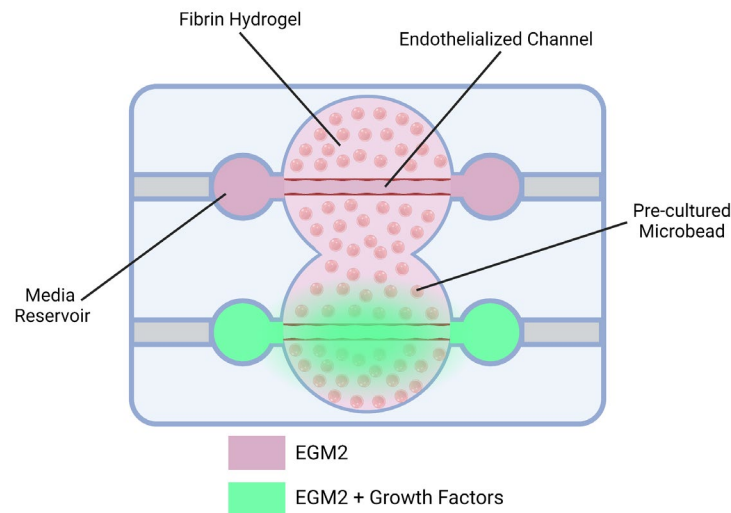
Figure 7.5: Proposed microfluidic device to encouraging angiogenic sprouting from pre-cultured microbeads. Pre-cultured microbeads are encapsulated in bulk fibrin hydrogels (500-750 µL) containing endothelialized channels. Growth factors could be added to the media to create a chemokine gradient, encouraging sprouting from the microbeads.

Different microbead formulations could also be explored to achieve enhanced angiogenic potential. In Chapter 4, PEGNB bulk hydrogels crosslinked with dVPMS supported vessel morphogenesis as early as 3 days in all crosslinking conditions. If applied to microbeads, dVPMS may facilitate sufficient prevascularization within shorter time periods to overcome the significant inhibitory effects of prolonged pre-culture on sprouting in sVPMS-crosslinked microbeads described in Chapter 6. Furthermore, a core-shell approach [26, 39-41] to microbead design could improve the implementation of both fibrin and PEG microbeads. PEG microbeads could be developed to have fibroblasts localized within less rapidly degradable cores surrounded by endothelial cells in a more readily degradable shell (Fig. 7.6). This could prevent fibroblasts from potentially forming a barrier around microbeads that inhibits vessel sprouting, but still localizes fibroblasts in close proximity to endothelial cells to provide the necessary paracrine signaling for prevascularization of the microbead shell. The core could be composed of higher wt. % PEG formulated with a higher crosslinking ratio to decreased degradability, while the shell could be composed of 3 wt. % PEGNB crosslinked with dVPMS to facilitate faster remodeling. Other more slowly degradable peptides could be explored to further slow core degradation [42]. Core-shell microbeads would require more complex microfluidic fabrication approaches but could have impactful results on microbead vascularization potential.
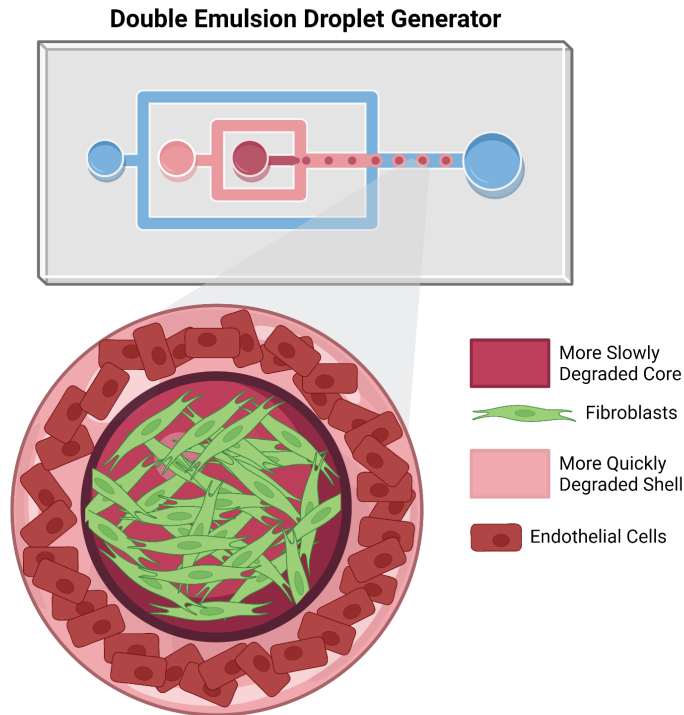
Figure 7.6: Proposed core-shell PEG-based microbeads. *A double emulsion flow-focusing microfluidic device would be used to encapsulate NHLF in a more slowly degraded core and HUVEC in a more quickly degraded shell.*

Fibrin microbeads could similarly by coated in a secondary matrix (degradable PEG, alginate, agarose, etc.) to prevent aggregation during pre-culture, though material selection must be appropriate to permit subsequent vascularization and avoid creating interfacial boundary issues [38] or a culture platform similar to immunoisolating capsules [43]. Hybrid materials could be explored to leverage the advantageous properties of both natural and synthetic matrices presented here. Winter et al. have successfully encapsulated equine ECFC within PEG-fibrinogen microbeads for cell delivery to dermal wounds [11]. Rioja et al. developed non-aggregating microbeads from composite materials including various combinations of agarose, hydroxyapatite, and fibrinogen, some of which supported prevascularization and enhanced vessel network length [14].

Lastly, other microbead fabrication techniques could be explored to generate large volumes of microbeads for therapeutic applications. In this work, only 300 µL of precursor solution was used to produce a single batch of microbeads at a time (at 0.9 mL/h). This was done to reduce the effects of cell aggregation over time, which resulted in a wide distribution of cell densities throughout microbeads. Zhang et al. [44] have developed a microfluidic strategy based on metastable emulsion-templating combined with microfluidic integration that supported the production of microbeads at 10 mL/h, while de Rutte et al. [45] have developed a microfluidic strategy using a parallelized step emulsification device that supported the production of microbeads at 7.2-19.2 mL/h with low coefficient of variance. More rapidly generating microbeads could potentially improve the cell distribution by reducing the time cells have to aggregate in the inlet tubing before entering the device. Additionally, these methods of rapid droplet production may advance the clinical realization of microbead approaches by generating volumes necessary for larger animal models and clinical application.

7.4 Overall Conclusions and Impact

The work presented in this dissertation examines the benefits and limitations of multiple biomaterial and cell-based vascularization approaches to create a novel strategy for restoring perfusion to ischemic tissues. The result of this body of work is the development of modular, cell-encapsulating, vascularizing microbeads using both natural and synthetic matrices. Fibrin-based microbeads catalyzed the formation of functional microvascular networks within 3 days *in vivo* and restored perfusion to ischemic tissues to promote limb salvage, supporting the overall hypothesis that prevascularized microbeads can jump-start inosculation with host vasculature upon implantation to rapidly revascularize ischemic tissues.

Despite these promising results, the tendency of fibrin microbeads to aggregate during pre-culture limited their injectability and thus their ability to be implemented as a minimally invasive therapeutic. PEGNB-based microbeads overcame this issue, permitting extended pre-culture without microbead aggregation, improving the injectability of this microbead approach. While day 1 pre-cultured microbeads formed robust, well-distributed microvascular networks *in vitro*, increased pre-culture time unexpectedly led to decreased sprouting from microbeads, partially refuting the originally proposed hypothesis. This motivates the need to investigate future directions that can harness the positive aspects of both microbead approaches presented here.

This work also highlights the trade-offs of each material approach and emphasizes future work that could lead to significant improvements toward the fabrication and implementation of vascularizing microbeads. Overall, these findings demonstrate the potential of modular, prevascularized microbeads as a minimally invasive therapeutic for restoring blood flow to ischemic tissues. While this dissertation focuses on the use of microbeads for the therapeutic vascularization of ischemic tissues, vascularizing microbeads can also contribute to other exciting areas of tissue engineering, including as a combinatorial therapeutic for *in situ* regeneration of diseased or injured tissues or as a building block in the development of complex, multiphasic tissues.

7.5 References

[1] A. Y. Rioja, R. Tiruvannamalai Annamalai, S. Paris, A. J. Putnam, and J. P. Stegemann, "Endothelial sprouting and network formation in collagen- and fibrin-based modular microbeads," *Acta Biomater,* vol. 29, pp. 33-41, Jan 2016, doi: 10.1016/j.actbio.2015.10.022.

[2]   N. E. Friend *et al.*, "Injectable pre-cultured tissue modules catalyze the formation of extensive functional microvasculature in vivo," *Sci Rep,* vol. 10, no. 1, p. 15562, Sep 23 2020, doi: 10.1038/s41598-020-72576-5.

[3]   N. E. Friend, J. A. Beamish, E. A. Margolis, N. G. Schott, J. P. Stegemann, and A. J. Putnam, "Pre-cultured, cell-encapsulating fibrin microbeads for the vascularization of ischemic tissues," *J Biomed Mater Res A,* Jun 16 2023, doi: 10.1002/jbm.a.37580.

[4]   J. A. Beamish, B. A. Juliar, D. S. Cleveland, M. E. Busch, L. Nimmagadda, and A. J. Putnam, "Deciphering the relative roles of matrix metalloproteinase- and plasmin-mediated matrix degradation during capillary morphogenesis using engineered hydrogels," *J Biomed Mater Res B Appl Biomater,* vol. 107, no. 8, pp. 2507-2516, Nov 2019, doi: 10.1002/jbm.b.34341.

[5]   B. A. Juliar, J. A. Beamish, M. E. Busch, D. S. Cleveland, L. Nimmagadda, and A. J. Putnam, "Cell-mediated matrix stiffening accompanies capillary morphogenesis in ultra-soft amorphous hydrogels," *Biomaterials,* vol. 230, p. 119634, Feb 2020, doi: 10.1016/j.biomaterials.2019.119634.

[6]   M. Vigen, J. Ceccarelli, and A. J. Putnam, "Protease-sensitive PEG hydrogels regulate vascularization in vitro and in vivo," *Macromol Biosci,* vol. 14, no. 10, pp. 1368-79, Oct 2014, doi: 10.1002/mabi.201400161.

[7]   Z. Jiang, B. Xia, R. McBride, and J. Oakey, "A microfluidic-based cell encapsulation platform to achieve high long-term cell viability in photopolymerized PEGNB hydrogel microspheres," *J Mater Chem B,* vol. 5, no. 1, pp. 173-180, Jan 7 2017, doi: 10.1039/C6TB02551J.

[8]   N. E. Friend, A. J. McCoy, J. P. Stegemann, and A. J. Putnam, "A combination of matrix stiffness and degradability dictate microvascular network assembly and remodeling in cell-laden poly(ethylene glycol) hydrogels," *Biomaterials,* vol. 295, p. 122050, Apr 2023, doi: 10.1016/j.biomaterials.2023.122050.

[9]   W. J. Seeto, Y. Tian, S. Pradhan, P. Kerscher, and E. A. Lipke, "Rapid Production of Cell-Laden Microspheres Using a Flexible Microfluidic Encapsulation Platform," *Small,* vol. 15, no. 47, p. e1902058, Nov 2019, doi: 10.1002/smll.201902058.

[10]   W. J. Seeto, Y. Tian, R. L. Winter, F. J. Caldwell, A. A. Wooldridge, and E. A. Lipke, "Encapsulation of Equine Endothelial Colony Forming Cells in Highly Uniform, Injectable Hydrogel Microspheres for Local Cell Delivery," *Tissue Eng Part C Methods,* vol. 23, no. 11, pp. 815-825, Nov 2017, doi: 10.1089/ten.TEC.2017.0233.

[11]   R. L. Winter *et al.*, "Cell engraftment, vascularization, and inflammation after treatment of equine distal limb wounds with endothelial colony forming cells encapsulated within hydrogel microspheres," *BMC Vet Res,* vol. 16, no. 1, p. 43, Feb 4 2020, doi: 10.1186/s12917-020-2269-y.

[12] R. Matta, S. Lee, N. Genet, K. K. Hirschi, J. L. Thomas, and A. L. Gonzalez, "Minimally Invasive Delivery of Microbeads with Encapsulated, Viable and Quiescent Neural Stem Cells to the Adult Subventricular Zone," *Sci Rep,* vol. 9, no. 1, p. 17798, Nov 28 2019, doi: 10.1038/s41598-019-54167-1.

[13] C. L. Franco, J. Price, and J. L. West, "Development and optimization of a dual-photoinitiator, emulsion-based technique for rapid generation of cell-laden hydrogel microspheres," *Acta Biomater,* vol. 7, no. 9, pp. 3267-76, Sep 2011, doi: 10.1016/j.actbio.2011.06.011.

[14] A. Y. Rioja, E. L. H. Daley, J. C. Habif, A. J. Putnam, and J. P. Stegemann, "Distributed vasculogenesis from modular agarose-hydroxyapatite-fibrinogen microbeads," *Acta Biomater,* vol. 55, pp. 144-152, Jun 2017, doi: 10.1016/j.actbio.2017.03.050.

[15] A. L. Torres, S. J. Bidarra, M. T. Pinto, P. C. Aguiar, E. A. Silva, and C. C. Barrias, "Guiding morphogenesis in cell-instructive microgels for therapeutic angiogenesis," *Biomaterials,* vol. 154, pp. 34-47, Feb 2018, doi: 10.1016/j.biomaterials.2017.10.051.

[16] A. L. Torres *et al.*, "Microvascular engineering: Dynamic changes in microgel-entrapped vascular cells correlates with higher vasculogenic/angiogenic potential," *Biomaterials,* vol. 228, p. 119554, Jan 2020, doi: 10.1016/j.biomaterials.2019.119554.

[17] C. M. Franca *et al.*, "High-Throughput Bioprinting of Geometrically-Controlled Pre-Vascularized Injectable Microgels for Accelerated Tissue Regeneration," *Adv Healthc Mater,* p. e2202840, May 23 2023, doi: 10.1002/adhm.202202840.

[18] A. S. Caldwell, B. A. Aguado, and K. S. Anseth, "Designing Microgels for Cell Culture and Controlled Assembly of Tissue Microenvironments," *Adv Funct Mater,* vol. 30, no. 37, Sep 10 2020, doi: 10.1002/adfm.201907670.

[19] J. Ceccarelli and A. J. Putnam, "Sculpting the blank slate: how fibrin's support of vascularization can inspire biomaterial design," *Acta Biomater,* vol. 10, no. 4, pp. 1515-23, Apr 2014, doi: 10.1016/j.actbio.2013.07.043.

[20] D. R. Griffin, W. M. Weaver, P. O. Scumpia, D. Di Carlo, and T. Segura, "Accelerated wound healing by injectable microporous gel scaffolds assembled from annealed building blocks," *Nat Mater,* vol. 14, no. 7, pp. 737-44, Jul 2015, doi: 10.1038/nmat4294.

[21] J. M. Lowen, G. C. Bond, K. H. Griffin, N. K. Shimamoto, V. L. Thai, and J. K. Leach, "Multisized Photoannealable Microgels Regulate Cell Spreading, Aggregation, and Macrophage Phenotype through Microporous Void Space," *Adv Healthc Mater,* vol. 12, no. 13, p. e2202239, May 2023, doi: 10.1002/adhm.202202239.

[22] S. Xin, O. M. Wyman, and D. L. Alge, "Assembly of PEG Microgels into Porous Cell-Instructive 3D Scaffolds via Thiol-Ene Click Chemistry," *Adv Healthc Mater,* vol. 7, no. 11, p. e1800160, Jun 2018, doi: 10.1002/adhm.201800160.

[23] N. G. Schott, H. Vu, and J. P. Stegemann, "Multimodular vascularized bone construct comprised of vasculogenic and osteogenic microtissues," *Biotechnol Bioeng,* vol. 119, no. 11, pp. 3284-3296, Nov 2022, doi: 10.1002/bit.28201.

[24] Y. Fang *et al.*, "3D Printing of Cell-Laden Microgel-Based Biphasic Bioink with Heterogeneous Microenvironment for Biomedical Applications," *Advanced Functional Materials,* vol. 32, no. 13, p. 2109810, 2022, doi: 10.1002/adfm.202109810.

[25] C. E. Miksch *et al.*, "4D Printing of Extrudable and Degradable Poly(Ethylene Glycol) Microgel Scaffolds for Multidimensional Cell Culture," *Small,* vol. 18, no. 36, p. e2200951, Sep 2022, doi: 10.1002/smll.202200951.

[26] Y. Ou *et al.*, "Bioprinting microporous functional living materials from protein-based core-shell microgels," *Nat Commun,* vol. 14, no. 1, p. 322, Jan 19 2023, doi: 10.1038/s41467-022-35140-5.

[27] G. Yang *et al.*, "Fabrication of centimeter-sized 3D constructs with patterned endothelial cells through assembly of cell-laden microbeads as a potential bone graft," *Acta Biomater,* vol. 121, pp. 204-213, Feb 2021, doi: 10.1016/j.actbio.2020.11.040.

[28] A. Lee *et al.*, "3D bioprinting of collagen to rebuild components of the human heart," *Science,* vol. 365, no. 6452, pp. 482-487, Aug 2 2019, doi: 10.1126/science.aav9051.

[29] X. Wang *et al.*, "3D bioprinting microgels to construct implantable vascular tissue," *Cell Prolif,* vol. 56, no. 5, p. e13456, May 2023, doi: 10.1111/cpr.13456.

[30] D. H. Nguyen *et al.*, "Biomimetic model to reconstitute angiogenic sprouting morphogenesis in vitro," *Proc Natl Acad Sci U S A,* vol. 110, no. 17, pp. 6712-7, Apr 23 2013, doi: 10.1073/pnas.1221526110.

[31] W. Y. Wang, D. Lin, E. H. Jarman, W. J. Polacheck, and B. M. Baker, "Functional angiogenesis requires microenvironmental cues balancing endothelial cell migration and proliferation," *Lab on a Chip,* vol. 20, no. 6, pp. 1153-1166, 2020, doi: 10.1039/c9lc01170f.

[32] C. G. Fonseca, P. Barbacena, and C. A. Franco, "Endothelial cells on the move: dynamics in vascular morphogenesis and disease," *Vasc Biol,* vol. 2, no. 1, pp. H29-H43, 2020, doi: 10.1530/VB-20-0007.

[33] K. S. Okuda and B. M. Hogan, "Endothelial Cell Dynamics in Vascular Development: Insights From Live-Imaging in Zebrafish," *Front Physiol,* vol. 11, p. 842, 2020, doi: 10.3389/fphys.2020.00842.

[34] L. Jakobsson *et al.*, "Endothelial cells dynamically compete for the tip cell position during angiogenic sprouting," *Nat Cell Biol,* vol. 12, no. 10, pp. 943-53, Oct 2010, doi: 10.1038/ncb2103.

[35] B. L. Macklin *et al.*, "Intrinsic epigenetic control of angiogenesis in induced pluripotent stem cell-derived endothelium regulates vascular regeneration," *NPJ Regen Med,* vol. 7, no. 1, p. 28, May 12 2022, doi: 10.1038/s41536-022-00223-w.

[36] G. A. Foster, D. M. Headen, C. Gonzalez-Garcia, M. Salmeron-Sanchez, H. Shirwan, and A. J. Garcia, "Protease-degradable microgels for protein delivery for vascularization," *Biomaterials,* vol. 113, pp. 170-175, Jan 2017, doi: 10.1016/j.biomaterials.2016.10.044.

[37] E. A. Margolis *et al.*, "Stromal cell identity modulates vascular morphogenesis in a microvasculature-on-a-chip platform," *Lab Chip,* vol. 21, no. 6, pp. 1150-1163, Mar 21 2021, doi: 10.1039/d0lc01092h.

[38] M. Sofman, A. Brown, L. G. Griffith, and P. T. Hammond, "A modular polymer microbead angiogenesis scaffold to characterize the effects of adhesion ligand density on angiogenic sprouting," *Biomaterials,* vol. 264, p. 120231, Jan 2021, doi: 10.1016/j.biomaterials.2020.120231.

[39] H. Wang, H. Liu, H. Liu, W. Su, W. Chen, and J. Qin, "One-Step Generation of Core–Shell Gelatin Methacrylate (GelMA) Microgels Using a Droplet Microfluidic System," *Advanced Materials Technologies,* vol. 4, no. 6, p. 1800632, 2019, doi: 10.1002/admt.201800632.

[40] H. Li, Y. Shang, Q. Feng, Y. Liu, J. Chen, and H. Dong, "A novel bioartificial pancreas fabricated via islets microencapsulation in anti-adhesive core-shell microgels and macroencapsulation in a hydrogel scaffold prevascularized in vivo," *Bioact Mater,* vol. 27, pp. 362-376, Sep 2023, doi: 10.1016/j.bioactmat.2023.04.011.

[41] E. M. Kim *et al.*, "Fabrication of core-shell spheroids as building blocks for engineering 3D complex vascularized tissue," *Acta Biomater,* vol. 100, pp. 158-172, Dec 2019, doi: 10.1016/j.actbio.2019.09.028.

[42] J. Patterson and J. A. Hubbell, "Enhanced proteolytic degradation of molecularly engineered PEG hydrogels in response to MMP-1 and MMP-2," *Biomaterials,* vol. 31, no. 30, pp. 7836-45, Oct 2010, doi: 10.1016/j.biomaterials.2010.06.061.

[43] M. A. Brunette *et al.*, "Human Ovarian Follicles Xenografted in Immunoisolating Capsules Survive Long Term Implantation in Mice," *Front Endocrinol (Lausanne),* vol. 13, p. 886678, 2022, doi: 10.3389/fendo.2022.886678.

[44] H. Zhang *et al.*, "Large-scale single-cell encapsulation in microgels through metastable droplet-templating combined with microfluidic-integration," *Biofabrication,* vol. 14, no. 3, Jun 6 2022, doi: 10.1088/1758-5090/ac7168.

[45] J. M. De Rutte, J. Koh, and D. Di Carlo, "Scalable High-Throughput Production of Modular Microgels for In Situ Assembly of Microporous Tissue Scaffolds," *Advanced Functional Materials,* vol. 29, no. 25, p. 1900071, 2019, doi: 10.1002/adfm.201900071.

Appendices

The following appendices contain protocols that were critical for carrying out the research

presented in this dissertation.

Appendix A – Cell Culture

<u>Materials:</u>
- 15 mL and 50 mL conical tubes
- 70% ethanol
- Autoclaved, non-filtered P-200 tips
- Autoclaved pasteur pipets
- Cell freezing vials
- Culture flasks
- Culture media
- DMSO
- FBS
- Ice bucket with crushed ice
- Pipette tips
- Serological pipets
- Sterile PBS
- Trypsin

<u>Equipment:</u>
- Automatic pipette aid
- BSC
- Hemocytometer
- Incubator
- Microscope
- Mr. Frosty
- Pipettes
- Tally counter

<u>Overview:</u>
This protocol describes the general process of culturing cells, from thaw to harvest for experiments and freezing for long term storage.

<u>Notes:</u>
- All cell culture reagents should be kept sterile, and all cell culture work should be conducted in the Biological Safety Cabinet (BSC). Any items brought into the BSC should be sprayed with 70% ethanol to sterilize. Exceptions: cell culture flasks, well plates, and bioreaction tubes.
- Cells are stored in the liquid nitrogen dewar. A cell log is maintained to keep a record of the type and number of cells vials we have. As you remove or replace cell vials in the

dewar please update the cell log. This will help you keep track of your cell stocks and inform lab members when we may need to obtain new cells for expansion.

- While the glass pasteur are autoclaved prior to use, I like to attach a yellow autoclaved P-200 tip to the end of the class as well for extra sterility. I change the tip every time before I aspirate in case it had touched anything in the hood while I was working.
- It is important to know at what percent confluence your cells should be passaged at. Some cells can start to differentiate or become quiescent if they become too confluent. If your cells run out of room to grow, they will start to apoptose. Though you do not want your cells to become over-confluent, if you passage them when they are at a low confluence you will not be optimizing resources or the cells' proliferative lifespan.
- In general, cells are happier when kept on ice as it slows their metabolic activity. They are even happier if they are in a pellet while on ice to further slow their activity. Keep cells on ice when they are not actively being worked with.

Thawing and plating cells:

1. Prepare two aliquots of media in conical tubes and place in 37°C water bath.
   a. One for resuspending cell vial(s).
      i. I use as much media as will add to 10 mL total when combined with the cell vial(s) into a 15 mL conical tube.
         1. Example: Thawing and combining two vials (which will be 2 mL) means I will prepare an 8 mL aliquot of media.
      ii. Regardless of cell type, I use DMEM+FBS for this step to preserve the more expensive media used to actually culture the cells.
   b. One for plating cells.
      i. This will be the specific culture media for your cell type and the volume will depend on the flask you will be using.

         T-75 → 10 mL
         T-175 → 23 mL
         T-182 → 24 mL
         T-225 → 30 mL
         NHLF/NHDF → DMEM + 10%FBS + 1x Anti-Anti
         HUVEC → EGM-2/VascuLife + 1x Anti-Anti
         MSC → RoosterBio MSC Media

2. Retrieve cell vial from liquid nitrogen dewar and place in 37°C water bath in foam holder.
   a. It should only take a few minutes for the vial to thaw.
   b. You will want to remove the vial from the water bath when there is a small amount of frozen solution left.
3. Take cell vial and media aliquot for resuspension into BSC.
4. Using a P-1000 pipette, transfer the cell vial into the media aliquot.
   a. I also like to rinse the inside of the vials with a little media and transfer it to the aliquot to ensure I am getting the maximum number of cells.
5. Tightly close cap and centrifuge cells at 200g for 5 min.
6. While cells are centrifuging, bring flasks and other media aliquot into BSC.
7. Label the flask with the following information
   a. Cell type, passage number, total cell number, your initials, and the date.

      b. I also like to add the date the vial was frozen just in case the flask becomes contaminated immediately after thaw. If you suspect it was the vial that was contaminated (not the media you used) then you can toss the remaining vials from that date to ensure it does not keep happening.

8. Attach glass pasteur pipette to vacuum hose.
9. Retrieve cells from centrifuge and bring into BSC.
      a. Be careful not to shake the conical tube and disturb the cell pellet.
10. Aspirate media above the cell pellet.
      a. Be very careful not to aspirate the cell pellet, which will appear as a faint layer at the bottom of the tube.
      b. Tip: Aspirate the majority of the media, then tilt the tube to move the liquid toward the pipet tip to avoid placing your pipet tip too close to your cell pellet.
11. Using automatic pipet, resuspend the cell pellet in culture media (only use 10 mL of media so you can use a 10 mL serological).
      a. Gently pipet media onto the pellet and pipet up and down a few times to break up pellet, until pellet is no longer visible.
      b. Start with only 1 mL of media, then add a few more and mix, then add the rest and mix.
12. Transfer entire cell suspension to flask.
13. Add the remaining media in the aliquot to the flask if needed.
14. Close flask tightly, gently tilt flask back and forth to distribute cell suspension over surface, and transfer to incubator.
      a. It is always a good idea to check the flask under the microscope before placing into the incubator to ensure you did not accidentally aspirate the cell pellet.

Changing culture media:
1. Prepare aliquot with appropriate volume of culture media and place in 37°C water bath.
2. Attach glass pasteur pipette to vacuum hose.
3. While media is warming, check cells under microscope..
      a. Check for signs of contamination and note confluency.
4. Bring warmed media and flask into the BSC.
5. Tilt the flask and aspirate the media from the side of the flask.
      a. Avoid scraping the bottom of the flask with the pipet as this can remove your cells from the surface and aspirate them.
6. Transfer new media to flask using automatic pipet.
7. Close flask tightly, gently tilt flask back and forth to distribute media over surface, and transfer to incubator.

Passaging/Harvesting cells:
1. Prepare aliquots of media in conical tubes and place in 37 °C water bath.
      a. Prepare an aliquot of DMEM+FBS for quenching.
            i. This will need to be equal to the amount of trypsin/TriplE that will be used (see below).
            ii. Media used for quenching must have serum to quench the enzymes.
      b. Prepare an aliquot(s) of media for replating cells.
2. Bring flask with cells into the BSC.

3. Aspirate the media from the flask.
4. Add PBS to flask and gently rinse the flask by tilting back and forth then aspirate.
5. Add appropriate volume of trypsin/TriplE to flask.
   > T-75 → 3 mL
   > T-175 → 7 mL
   > T-182 → 8 mL
   > T-225 → 10 mL
6. Gently tilt flask back and forth to cover surface.
7. Tightly close flask and place in incubator for 5 min.
   a. During incubation, bring conical tubes and hemocytometer into BSC. Label tubes for cell type and passage number.
8. Remove the flask from incubator and check under the microscope to ensure cells are rounded and lifted from the flask (floating).
   a. If there are still cells attached, gently tap the bottom of the flask to dislodge any cells still adhered. If a large number of cells are still attached, consider putting back in the incubator for another minute.
9. Bring flask and media for quenching into the BSC.
10. Add same volume of media to flask as trypsin/TriplE.
11. Repeatedly rinse the entire bottom of the flask with cell suspension to dislodge any cells that are still adhered.
12. Transfer the entire volume of cell suspension to a conical tube.
13. Remove sample for cell counting.
    a. 10 uL for using the hemocytometer (use P-20)
    b. 200 uL for the Coulter Counter
    c. Tip: You will want to do this quickly and sample from the middle of the solution to get an accurate sample before the cells settle. If cells have been sitting, I like to re-cap the conical tube and invert it a few times before taking my sample.
14. Check that there are cells in the hemocytometer. If the number seems unusually low, you may need to take and count another sample.
15. Tightly close cap and centrifuge cells at 200g for 5 min.
16. While cells are centrifuging, count cells from sample (see below).
17. Bring new flasks and other media aliquot into the BSC.
18. Label the new flasks with the following information:
    a. Cell type, passage number, total cell number, your initials, and the date.
19. Retrieve cells from centrifuge and bring into the BSC.
    a. Be careful not to shake the conical tube and disturb the cell pellet.
20. Aspirate media above cell pellet.
    a. Be very careful not to aspirate the cell pellet.
    b. Tip: Aspirate the majority of the media, then tilt the tube to move the liquid toward the pipette tip to avoid placing your pipette tip too close to your cell pellet.
21. Using automatic pipet, resuspend the cell pellet in culture media at desired concentration.
    a. Gently pipet media onto the pellet and pipet up and down a few times to break up pellet, until pellet is no longer visible.
    b. Tip: Progressively pipette more media onto the cell pellet (e.g., dispense 1 mL, then 3 mL, etc.). This will prevent the pellet from floating in a large volume making it harder to effectively resuspend.

22. Distribute cell suspension to new flask(s).
23. Add additional media to flasks for necessary culture volume if needed.
24. Close flask tightly, gently tilt flask back and forth to distribute cell suspension over surface.
25. Check the flask under the microscope to make sure cells are present, then transfer to incubator.

Cell counting (using the hemocytometer):

1. Place glass coverslip on hemocytometer.
2. Collect 10 uL sample of cell suspension.
3. Pipette sample of cell suspension into hemocytometer grove beneath coverslip.
    a. Capillary action will wick the sample into the chamber.
4. Place hemocytometer on microscope under 10x magnification.
5. Count all cells in the four corner squares with larger grids.
    a. In each square, if cells fall on the outer lines only count the cells that fall on the top and left line, not the right and bottom line.
    b. Keep track of the total number of cells counted using the tally counter.

Count cells in squares **1 - 4**
Count cells on top and left lines
DO NOT count cells on right and bottom lines
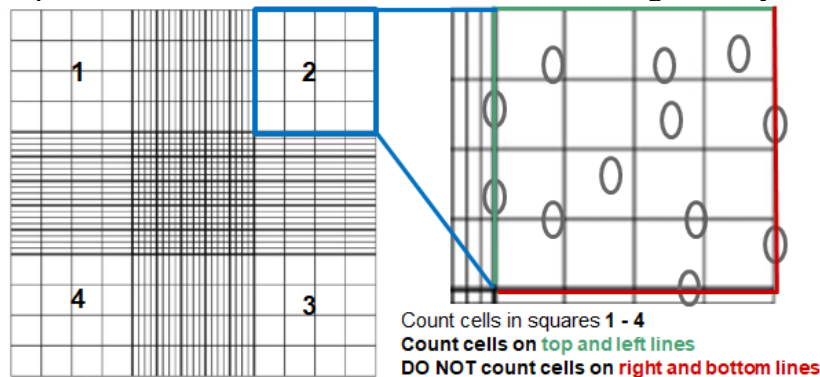
6. Once you have the cell count, use the equation below to calculate total cell number

$$\frac{Cell\ count}{4} * 10^4 * total\ volume\ of\ bulk\ cell\ suspension\ =\ total\ cell\ number$$

Counting cells using the Coulter Counter (Stegemann Lab):

1. Collect a 200uL sample of cell suspension and mix it with 19.8mL of Isoton-II Diluent solution in plastic Coulter Counter cuvette and cover.
    a. 19.8L is one dispense (preset volume) of the bottle using the white plastic cap/cover.
    b. Remove the white stopper from the end of the dispensing tube, gently pull the white plastic cap/cover all the way up, and release while holding the cuvette under the tube to allow the liquid to flow in.
    c. Note: The use of 200 uL and 19.8 mL of solutions are pre-set, if you change these values for any reason, please notify the lab
2. Turn on Coulter Counter (switch on right side).
3. Turn on the laptop using power button.
4. Open the Multisizer 3 program.
5. Enter info for cell sample:
    a. Group ID: Your name or initials

b. Sample ID: cell type and passage number
6. Open door, lower stage, and remove blue Coulter Clenz solution.
    a. Be careful to not touch the aperture/glass probe as they are very delicate and critical for the device.
7. Mix the cell suspension (by holding the cap on tightly and inverting back and forth a few times).
8. Remove cap then place cuvette in holder on stage and carefully raise so the aperture/probe are both submerged in the solution.
9. Run the program.
10. Select area under the curve by clicking at the start of the curve and drag end line to the end of the curve (typically use 10-30 um for most cells).
11. Calculate total cell number by the following equation:

$$200 * volume\ of\ bulk\ cell\ suspension * area\ under\ the\ curve$$
$$= total\ cell\ number$$

12. Remove the cell suspension solution, place the beaker containing the blue Coulter Clenz solution back on stage, and raise stage.
    a. Note: If the blue Coulter Clenz solution is getting low then please refill.
13. Turn off Coulter Counter and software
14. Bleach sample, pour down sink, rinse cuvette.

Cell Freezing:
1. Place Mr. Frosty in the fridge (if not already in the fridge).
2. Prepare reagents for harvesting cells.
3. Passage cells as described above and take sample for counting cells.
4. Centrifuge cells at 200g for 5 mins.
5. While cells are centrifuging, count cells from sample.
6. Once done centrifuging, you can resuspend cells in culture media to replate some for continued culture if needed.
    a. If this is done, re-centrifuge the cells into another pellet after you have removed what you will replate (and remember to subtract that number of cells from total cell count remaining in pellet).
7. Place cells in pellet on ice.
8. Prepare enough freeze media for freezing cells at desired density (make at least 0.5 mL extra) and place on ice.
    a. I typically make freeze media composed of 70% culture media, 20% FBS, and 10% DMSO.
    b. This may need to be adjusted for your specific cell type as some cell types may require higher FBS concentrations to improve post-thaw viability.
        i. You can often find recommended freeze media on the supplier website.
9. Label desired number of cryovials with the following information:
    Cell type
    P# → P#   (passage now → passage when plating)
    Total cell number   (e.g., 500K, 1M)
    Initials
    Date

Note: Account for volume loss that will occur when distributing cell suspension into vials, roughly 0.5 mL of cell suspension will be lost

10. Aspirate media above cell pellet.
11. Resuspend cell pellet in freeze media for desired cell density (number of cells/mL).
12. Distribute 1 mL of cell suspension into each cryovial, being sure to pipette up and down between vials to ensure the suspension is well-mixed and cells do not settle.
    a. This is very important if you have a larger volume of cell suspension as cells can settle quickly, especially if they are larger cells.
    b. If there is a large volume, you will want to twirl the flask in between taking aliquot volumes.
13. Place cryovials in Mr. Frosty, mark out number with date and initials on top of Mr. Frosty, and place in -80°C freezer.
14. The next day, move cells from Mr. Frosty to liquid nitrogen dewar.
15. Update the cell log to keep record of your cell inventory.
16. Place Mr. Frosty back in fridge.
    a. Please replace the isopropanol if you were then one to use the Mr. Frosty for its fifth use.
    b. There is a waste container in the large flammables cabinet for the isopropanol.

Appendix B – Isolation of HUVEC from Fresh Umbilical Cords
Adapted from Jonathan Bezenah

*Protocol amended from Davis J., Crampton S.P., Hughes C.C.W. (2007). Isolation of Human Umbilical Vein Endothelial Cells (HUVEC). JoVE. 3. doi: 10.3791/183.

Materials:
- 1 pair of scissors
- 18 G needle (or 16 G needle)
- 2 Hemostats
- 2 L beaker
- 33 mm 0.22 um filter
- 5 mL and 20 mL syringes
- Autoclave tape
- Butterfly needle
- Collagenase
- EGM-2
- Foil
- Paper towels
- Sterile PBS
- T-25 and 75 flasks

Equipment:
- Automatic pipette aid
- BSC
- Incubator
- Microscope
- Pipettes
- Scale

Overview:
This protocol describes the process of harvesting HUVEC from fresh umbilical cords obtained from the university hospital.

Notes:
- Cords should be used within 1 week or less from birth (hospital collection).
- You can do two cords at one time, but you will need to double everything.
- If possible, use the <u>right</u> BSC as the surface of the BSC already has some bleach erosion.

Procedure:

The day before cell isolation:

1. Place 2 hemostats and 1 pair of scissors in a 2 L beaker.
2. Cover the beaker with aluminum foil and then tape one side of the aluminum foil to the beaker using autoclave tape.
3. Autoclave beaker using the textiles setting.
    a. Sterilization time: 45 min
    b. Drying time: 10 min

The day of cell isolation:

1. Place the umbilical cord and the sterile PBS in the water bath.
    a. Make sure that the cord is in the biohazard delivery bag to avoid contaminating the water bath.
2. Prepare 0.1% collagenase in PBS.
    a. Add 5 mg of collagenase to 5 mL of PBS.
    b. Make sure to make this solution every time this protocol is repeated.
3. Sterile filter the collagenase solution using a 5 mL syringe with a 33 mm 0.22 um filter.
4. Attach an 18G needle to a 5 mL syringe and aspirate the 5 mL of the filtered collagenase solution.
5. Remove the needle from the syringe carefully and throw it in the biohazardous sharps container.
    a. Place the syringe back in its wrapper for storage.
6. Aspirate 20 mL of PBS each into two 20 mL syringes.
    a. Put the syringes back in their wrappers for storage.
7. Place paper towels inside the BSC.
    a. Use enough to cover your working area properly.
8. Soak the towels with bleach (make sure surface is completely wet with bleach) starting at the edges.
9. Put on a second pair of gloves.
10. Take out the umbilical cord and PBS from the water bath and bring into the BSC.
11. Take out the umbilical cord from its container and wipe off the clotted blood in the paper towels.
    a. Role the cord around on the bleach soaked towels.
12. Locate the lines where they clamped the hemostats on both ends of the cord and cut the cord below the clamp marks.
    a. Use cord container as a waste container for the pieces cut from the cord.
    b. The cleaner the cut is the easier it is to locate the veins and arteries.
13. Gently slide half of the butterfly needle into the vein and clamp the cord with the needle using the hemostat.
    a. There will be two arteries and one vein, locate the artery wall for both arteries then the vein will be the vessel with the smaller diameter.
    b. You must spiral the needle around because vein spirals around the outside.
    c. NOTE – Leave the plastic casing of the butterfly needle covering the needle when inserting it into the vein. The vein looks like a stretch mark. You shouldn't have to put a lot of force when inserting the needle into the vein, there should be no resistance.

14. Remove the extra part of the butterfly needle so that you only have the tube connected to the butterfly needle.
15. Attach the first 20 mL syringe of PBS and inject all of it slowly into the vein making sure there are no clots.
    a. Make sure the cord is on top of the waste container.
16. Attach the collagenase syringe and begin injecting the solution until the liquid coming down changes its color to gold.
    a. It takes approximately 1 mL of collagenase of color change to occur.
    b. Make sure to put the cord on top of the white towel to make it easier to notice the liquid color change.
17. Clamp the other end of the cord and very carefully re-inflate the vein with the ~4 mL of collagenase remaining in the syringe.
18. Carefully place everything in the autoclaved beaker which initially contained the hemostats and scissors. Cover the top with the aluminum foil taped at one side of the beaker. Be careful not to puncture the cord at any point.
19. Remove your outer pair of gloves and take the 2 L beaker to the bottom incubator.
20. Leave the cord in the incubator for 20 min.
21. Put on a second pair of gloves and take out the cord from the incubator and bring into the BSC.
22. Remove the hemostat that is <u>not</u> holding the needle and then attach the last 20 mL syringe of PBS.
23. Place the cord on top of a 50 mL centrifuge tube and begin injecting the PBS in the vein very slowly to wash off the cells but avoid bursting the vein. Collect the entire solution in the 50 mL tube.
24. Discard the cord in the waste container after removing the needle and the hemostat holding it in place.
25. Centrifuge the tube at 200g for 5 mi.
26. Dispose of butterfly needle in biohazardous sharp.
27. Make sure all waste goes in the biohazard bag.
28. Clean up the BSC with bleach and ethanol.
29. Bring a T-25 flask into the BSC.
    a. Label it: "HUVEC P.0, date, your initials, date of cord harvest".
30. Remove the 50 mL tube from the centrifuge and aspirate off the supernatant.
    a. Make sure to do it carefully to avoid aspirating off the HUVEC.
31. Resuspend cell pellet with 5 mL EGM-2.
32. Put the cell-media solution into the flask.
33. Place the flask in the incubator overnight.
----
34. Check flask under microscope. This is especially important to make sure there are no signs of contamination.
35. Place flask in the BSC and aspirate off the media.
36. Add 5 mL of PBS and gently rock the flask.
37. Aspirate off the PBS and add another 5 mL of PBS.
38. Remove PBS and add 5 mL of fresh EGM-2.
39. Make sure to check on HUVEC under the microscope every day. Cells should be confluent (~80%) in less than 1 week. If not, throw the cells away.

40. Once the cells are confluent, trypsinize and passage them into two T-75 flasks (P0 → P1).
41. Grow to confluency and freeze them down. Label them P1 → P2. This means they will be P2 when plated.

Appendix C – Encapsulating Cells in a 3D Fibrin Matrix

<u>Materials:</u>
- 15 mL and 50 mL conical tubes
- 2 mL microcentrifuge tubes
- Fibrinogen, thrombin, FBS, SF media
- Ice bucket with crushed ice
- Pipette tips
- Serological pipets
- Trypsin, PBS, culture media
- Well plates of desired size (usually 24)

<u>Equipment:</u>
- Automatic pipette aid
- BSC
- Hemocytometer
- Incubator
- Microscope
- Pipettes
- Scale
- Tally counter

<u>Overview:</u>
This protocol describes the process of encapsulating cells in a bulk 3D fibrin hydrogel.

<u>Notes:</u>
- I would recommend calculating the necessary masses and volumes needed for the following procedure based on the number of conditions and gels you will be making.
    - Determine the amount of fibrinogen, cell density, and total cell number required, and calculate volumes of each component in the gel precursor solution.

<u>Procedure:</u>
1. Remove fibrinogen from the freezer to warm to room temperature.
2. Prepare cell culture supplies.
    a. Trypsin, quenching media, etc.
3. Place reagents for making fibrin gels in ice bucket.
    a. Serum free media, FBS, and thrombin.
    b. Thrombin often takes a while to thaw so it is best to thaw prior to placing on ice.
4. Prepare fibrinogen solution.
    a. Calculate desired concentration of clottable protein (taking into account the dilution in other precursor components), the necessary volume fibrinogen stock solution, and then mass of fibrinogen needed.

     b.   Weight out fibrinogen and transfer to 15 mL conical tube.
     c.   Resuspend fibrinogen in SF media at desired stock concentration.
     d.   Place fibrinogen solution in water bath.
          i.   Tap tube on counter to dislodge the fibrinogen clot from bottom of tube.
         ii.   Gently swirl tube every 5 mins for 15-20 mins to dissolve completely.

5.   Harvest cells as you normally would, collecting the desired number of cells for each condition into a microcentrifuge tube.
     a.   It is common to make 1000 uL of fibrin precursor solution and split it to make two 500uL gels yielding two technical replicates.
     b.   Note: If you are doing co-cultures of ECs and stromal cells then both cell types should be combined into a single tube.
     c.   Place cell pellets on ice while you prepare the gel components.
     d.   Set aside extra cells on ice to be frozen down or plated after making gels.

6.   Centrifuge the cells for 5 min at 200g.

7.   Filter the fibrinogen using a 5 mL syringe and 0.22 um filter then place on ice.
     a.   Note: Do not move the fibrinogen solution from hot to cold too quickly as this could potentially cause some gelation. Make sure the fibrinogen solution comes to room temp before being placed on ice.
     b.   You can also filter earlier if there is time during cell collection process.

8.   Vortex thrombin.

9.   Label well plate with the experimental details and conditions, the date, and your initials.

10. Bring gel precursor components into the BSC.

11. Aspirate media above cell pellets.

12. Add serum free media to the cell pellets.

13. Add thrombin to the cell pellets.

14. Add FBS to the cell pellets and gently resuspend.

15. Add fibrinogen stock solution and mix solution 4-5 times.
     a.   Try to not create bubbles during mixing.
     b.   You will want to be quick with mixing as the gel will start to polymerize within ~1 min.

16. Transfer desired volume of cell mixture to well of well plate and repeat with remaining precursor.
     a.   Again, avoid making bubbles in your gel as this will make imaging harder in the future. To do this, consider not ejecting the last bit of solution, and definitely do not push past the first stop on the pipette.

17. Let gels begin to polymerize undisturbed at room temperature for 5 min.

18. Carefully move gels to incubator for 25 minutes to complete gelation.
     a.   During this time, it would be ideal to plate or freeze remaining cells.
     b.   You will also want to prepare an aliquot of media to feed your gels once they have polymerized.

19. Add media to fully formed gels.

20. Change gel media the next day, then every other day following.

Appendix D – Fabricating Fibrin Microbeads
Adapted from Ana Rioja

Materials:
- 15 mL and 50 mL conical tubes
- 2 glass bowls (ideally 4.5" and 5.5" diameter Pyrex bowls)
- Autoclaved 100 mL beaker
- Autoclaved propeller
- Autoclaved water
- Fibrinogen, thrombin, FBS, SF media
- Ice bucket with crushed ice (two if one is needed for cell culture)
- Parafilm
- Pipette tips
- Serological pipets
- Sterile PDMS (PSF-100cSt viscosity silicone fluid)
- Sterile 0.1% L101 in PBS
- Trypsin, PBS, culture media
- Vented conical tubes (if planning to culture beads in suspension)

Equipment:
- Automatic pipette aid
- BSC
- Hemocytometer
- Hot plate
- Incubator
- Laminar flow cabinet
- Microscope
- Overhead stirrer with stand
- Pipettes
- Scale
- Tally counter

Overview:
This protocol describes the process of fabricating cell-encapsulating fibrin microbeads using bulk emulsification.

Notes:
- Make sure there are autoclaved beakers, impellers, and water **the day before** you plan to make beads.

- Make sure there is enough 0.1% L101 in PBS for the wash steps **the day before**. If there isn't, you will need to make more at least the day before as the L101 will need time to go into solution overnight. This is stored in the fridge.
  - Add 500 uL of Pluronic L101 to an unopened 500 mL container of PBS.
- While 3 mL of precursor solution is typically used to make one batch of beads, lab members have successfully made beads batches with up to 6 mL of precursor solution without noticing differences in bead properties.
- Vascular microbeads for *in vitro* experiments typically have a cell density of 2 M/ml total cells in a 1:1 ratio of EC:stromal cells, but this can be changed depending on desired microbead properties.
- Vascular microbeads usually have a final concentration of 2.5 mg/ml fibrin, but this can be altered depending on desired microbead properties.
- Desired culture media volume and media changes will depend on the experiment and total cell number in batch.
  - Keep this consistent for comparison experiments as giving more/less media more/less frequently could change cell behavior in pre-culture.
- Acellular beads should be stored in the fridge in 10% FBS in PBS to prevent some sticking, but this should not have to be changed prior to use.

Tips:
These tips are found throughout the protocol, but please look these over before starting the process.
- It can take a while for the water to reach 40°C so make sure this preparation is done early in your process.
- ALWAYS coat serological pipets and pipette tips with pure serum or serum containing media before touching beads or else you will lose a lot of beads that get stuck in the serological or pipette tip.

Procedure:
1. Remove fibrinogen from the freezer to warm to room temperature.
2. Prepare cell culture supplies.
   a. Trypsin, quenching media, etc.
3. Prepare laminar hood (LH).
   a. Remove blue cover, turn on the hood with the ON button, and turn on light.
      i. Give the hood a few minutes to establish proper air flow.
4. In LH, prepare water bath: Autoclaved water in 4.5" glass bowl on hot plate set to 40°C
   a. Turn on hot plate then click "set" button once to select temperature, increase/decrease temperature with knob, then click "set" button again to set temperature.
   b. Make sure temperature prob is inserted into water bath.
5. Bring bucket of crushed ice into LH.
   a. Place FBS, serum free media, and thrombin on ice.
   b. Thrombin often takes a while to thaw so it is best to thaw prior to placing on ice.
6. Bring sterile PDMS and autoclaved 100 mL beaker and impeller into LH.
7. Place 75 mL of sterile PDMS in beaker and cover beaker with parafilm.

a. Note: PDMS is very viscous, so when pipetting volume expel the entire volume, wait a few seconds for more PDMS to build up in the tip and expel again.
8. Place beaker of PDMS into ice bath, being careful to not splash PDMS onto parafilm.
   a. Make sure beaker is covered in ice up to meniscus of PDMS.
9. Prepare fibrinogen solution.
   a. Calculate desired concentration of clottable protein (taking into account the dilution in other precursor components), the necessary volume fibrinogen stock solution, and then mass of fibrinogen needed.
      i. Don't forget to prepare fibrinogen for bulk gels as well if you will be encapsulating D0 beads.
   b. Weight out fibrinogen and transfer to 15 mL conical tube.
   c. Resuspend fibrinogen in SF media at desired stock concentration.
   d. Place fibrinogen solution in water bath.
      i. Tap tube on counter to dislodge the fibrinogen clot from bottom of tube.
      ii. Gently swirl tube every 5 mins for 15-20 mins to dissolve completely.
10. Harvest cells as you normally would, collecting the desired number of cells for the intended cell density for the entire bead batch in one 15 mL conical tube.
    a. Note: If you are doing co-cultures of ECs and stromal cells then both cell types should be combined into a single tube.
    b. Place cell pellet on ice while you prepare the gel components.
    c. Set aside extra cells on ice to be frozen down or plated after making beads.
11. Centrifuge the cells for 5 min at 200g.
12. Filter the fibrinogen using a 5 mL syringe and 0.22 um filter then place on ice in LH.
    a. Note: Do not move the fibrinogen solution from hot to cold too quickly as this could potentially cause some gelation. Make sure the fibrinogen solution comes to room temp before being placed on ice.
    b. You can also filter earlier if there is time during cell collection process.
13. Vortex thrombin.
14. Set up the mixer and PDMS bath in LH.
    a. Move ice from the ice bucket to the 5.5" glass bowl to create a smaller ice bath.
    b. Move the PDMS to the smaller ice bath being careful to not splash PDMS on parafilm.
    c. Attach the impeller, being careful not to accidentally touch the arms on the clamp.
    d. Remove the parafilm from the beaker.
    e. Place the small ice bath with the beaker of PDMS on the stage and raise until you can clamp the beaker just below the lip of the beaker.
       i. Make sure the beaker is secure as later it will need to be well attached during the ice to water bath transition.
    f. Adjust the impeller so both arms of the impeller are submerged in the PDMS.
       i. Make sure the impeller isn't directly on the bottom of the beaker.
    g. Turn on the mixer controller with the switch on the back.
    h. Check that the mixer controls are set to 30 mins, 600 RPM, 0 torque by clicking the respective buttons – adjust using the + and - buttons as needed.

      i. Note: These parameters can be changed to modify microbead properties, such as size distribution.

    i. Check that the impeller spins unimpeded by starting the mixer with the "start" button.

      i. Adjust impeller if necessary and check again.

    j. Reset the time back to 30 mins by pressing the time button twice.

15. Attach a 5 mL serological pipet to the automatic pipettor.
16. Aspirate media from the cell pellet and bring into LH.
17. Add serum free media to the cell pellet.
18. Add thrombin to the cell pellet.
19. Add FBS to the cell pellet and gently resuspend.
20. The next three steps will need to happen **quickly** so review first before moving forward.
21. Next you will need to add fibrinogen to the cell mixture, which will likely need to be done using two P-1000 pipettes as the volume will be greater than 1000 uL.
    a. Set the volume on both P-1000 pipettes and attach tips to both.
    b. First, add the smaller volume of fibrinogen to the side of the tube – DO NOT MIX.
    c. Then, add the remaining and mix three times.
22. Aspirate all of the cell suspension using the 5 mL serological pipet, turn on mixer, then expel entirety of precursor into the PDMS bath.
23. Turn on the mixer.
    a. Start and stop the mixer three times <u>within the first minute</u> to ensure solution is mixed.
24. After 5 mins, stop the mixer and replace ice bath with the water bath.
    a. Lower stage (do not go too low or it will get stuck).
    b. Remove ice bath.
    c. Hold bowl of warm water under beaker with left hand then move hot plate under the bowl with the right hand and place on stage.
    d. Raise stage.
    e. Make sure temperature probe is stable in water bath (can place in slot between clamp and beaker).
25. Start the mixer again and set the temperature of the hot plate to 37° C.
26. During the 25 mins, prepare aliquot of media for suspension culture and place in water bath.
27. After the remaining 25 mins, turn off the mixer.
28. Loosen impeller until it freely falls into the beaker.
29. Securely holding the beaker, remove it from the clamp and carefully transfer beaker with impeller to a comfortable work area within the LH.
30. Slowly swirl impeller over beaker to remove as much PDMS-bead solution as possible.
    a. Leave impeller on top of Kimwipe to prevent PDMS from getting everywhere.
31. Coat a 25 mL pipet with 0.1% L101 in PBS all the way up to the top of the pipet, then transfer 5 mL into two 50 mL tubes.
    a. Keep 0.1% L101 in PBS in fridge between wash steps (if possible).

32. Using the same pipet, first add 25 mL of bead solution into each 50 mL tube, then split the remaining bead solution between the two tubes.
    a. Note: You will want to rinse off the beads from the side of the beaker and hold the beaker at an angle so that the beads settle in one spot to improve yield.
    b. Save the 25 mL pipet in the empty beaker.
33. Tilt tubes back and forth in your hands for 5 mins (or you can put them on a rotisserie).
34. Centrifuge 50 mL tubes for 5 mins at 200g.
    a. Note: Other lab members have tried 175g with success to try to lessen aggregation.
35. Using 25 mL pipet from before, remove the PDMS layer from the beads and collect this and future rinse waste in the beaker.
    a. Remove the first 30 mL of PDMS using the fast "F" setting on the pipet, then switch to the slow "S" setting to slowly remove the remaining PDMS without aspirating the bead solution layer.
    b. Try to remove as much PDMS as possible, but if you cannot get all of it that is ok.
36. Coat a 10 mL pipet with 0.1% L101, then transfer 4 mL into two 15 mL tubes.
37. Using the same pipet, transfer bead solution to two 15 mL tubes (one 50 mL tube unto one 15 mL tube).
    a. Beads float at the top of the bead solution layer and get slightly stuck on the sides of the bottom of the tube, so try to gently scrape off the residual beads with the pipet tip as you aspirate up the solution and move it to the new tube.
    b. If there is a remaining PDMS layer, avoid aspirating it as much as possible when collecting the beads so it does not get moved to the new tube.
    c. Save to 10 mL pipet.
38. Centrifuge 15 mL tubes for 5 mins at 200g.
39. Using the 10 mL pipet from before, remove all solution above the beads.
40. Coat another 10 mL pipet in 0.1% L101 and transfer 5 mL to one of the 15 mL tubes, then transfer beads from that tube to other 15 mL tube to combine.
    a. You do not need to break up the bead pellet to move it, but once beads are combined into one tube gently breaking up the bead pellets with the pipet.
    b. Doing this now will help them aggregate less when moving to media.
    c. Save 10 mL pipet.
41. Centrifuge the 15 mL tube for 5 mins at 200g.
42. Remove as much 0.1% L101 from bead pellet as possible.
    a. You can use a smaller pipette, such as a P-1000 or P-200 to remove any remaining 0.1% L101 around the bead pellet.
43. Coat a 5 mL pipet with serum containing medium (or pure serum) and add desired volume to beads.
    a. First add only 1-3 mL of medium for transferring to vented conical tube, then add remaining volume once transferred to the vented tube.
44. Using same pipet, break up beads, then transfer beads to filter cap conical tube.
45. At this point, I would recommend breaking up the beads further with a P-1000 pipette (remember to coat).

a. If you are going to embed D0 beads or Nattokinase digest, you will want to take your sample before adding the rest of the culture media.
46. Add remaining media to beads and place in incubator in tube rack for culture.
47. Empty waste of PDMS/0.1% L101 into waste container, clean impeller, and leave beaker soaking in soap and water over night before cleaning the next day.
48. Clean cell culture hoods.
49. For media changes: Aspirate as much media as possible above stagnant beads (you do not need to get every last drop) and then add desired media.
    a. I do not centrifuge the beads if they are already settled at the bottom.
    b. You can try to gently break up the bead aggregate, but not recommended to put a lot of shear on the beads.
    c. COAT PIPET with serum containing media before breaking up aggregate.
50. For embedding the microbeads, centrifuge the beads briefly, aspirate all the media above the beads, resuspend the beads in a known volume, take samples for each condition into microcentrifuge tubes, centrifuge for 5 min at 200g, then make gels as you normally would with cell pellets.
    a. COAT PIPET with serum containing media before breaking up aggregate.
    b. If you are going embed beads after multiple pre-culture timepoints, take into account the volume of beads already taken.
        i. For example, if I resuspended the beads in 2 mL of media and took 300 uL of beads, the next timepoint I would resuspend them in 1.5 mL of media before taking my sample.

Nattokinase (NTK) digestion for counting cells in beads

1. In step 45 above, resuspend beads in only 1 mL of media.
2. To make NTK solution, prepare NTK in 1 mM EDTA at a 2.5 mg/mL concentration.
3. Combine 100 uL of bead solution and 100 uL of NTK solution in one well of a 96 well plate.
4. Incubate at 37° C for 30 min.
5. Count using hemocytometer.
    a. Note: If you are expecting a lot of cells to be present in the beads, I would recommend diluting the mixture with 200 uL of media or PBS before counting cells.

$$\frac{total\ cell\ number\ in\ four\ corner\ squares}{4} * 10 * 400$$

$$= \#\ cells\ per\ 100\ uL\ of\ bead\ solution$$

$$\#\ cells\ per\ 100\ uL\ of\ bead\ solution * 10 = total\ \#\ cells\ per\ batch\ of\ beads$$

$$(must\ subtract\ the\ \#\ of\ cells\ used\ in\ NTK\ digestion\ to\ determine\ \#\ of\ cells\ remaining\ in\ batch)$$

Appendix E – Preparing Peptide and PEG Aliquots

Materials:
- 13 mm 0.22 um filter
- 15 and 50 mL conical tubes
- 20-22G needle (1 ½ inch length recommended)
- 28G insulin syringe
- 3 mL syringe
- ddH2O
- Ethanol wipes
- Glacial acetic acid
- Kimwipes
- Rubber bands
- Sterile 0.5 mL (for peptides) or 1.5 mL (for PEG) microcentrifuge tubes
- Sterile 2 mL microcentrifuge tubes
- Sterile forceps (usually kept in BSCs)
- Stock vials of peptides or PEG

Equipment:
- BSC
- Bunsen burner
- Flint spark
- Fume hood

Overview:
This procedure describes the process of preparing peptides and PEG aliquots from stock vials for use and short-term storage.

Notes:
- It is helpful to keep aliquots made on the same day in the same color tubes. Therefore, you should try to determine how many of each color microcentrifuge tubes you will need at least one day before this process so you can autoclave a pouch of tubes in time, otherwise, you may need to search through the boxes of autoclaved tubes to get enough of the right tube color.
  - I personally like to keep pouches of same color tubes autoclaved. I write the number of tubes on the autoclave pouch for future reference.
- It is also helpful to not repeat the same color twice in a row, so dates/purity does not get mixed up.
  - I typically survey what colors are currently in use in the box and pick a different one when possible.

- Whenever removing peptides or PEG from stock containers allow them to warm to room temperature for <u>at least</u> 30 min before opening to prevent condensation inside the containers.
  - **<u>Do not</u>** open container until there is no longer moisture on the sides.
- You should not lyophilize peptides and PEG at the same time to prevent cross-contamination.
- RGD is typically aliquoted in 0.5-3 mg per aliquot. VPMS is typically aliquoted in 1-10 mg depending on the needs of the experiment.
  - If you have a thorough experimental plan you will know how what masses you should aliquot to avoid combining aliquots when possible.
  - Include at least two-three 1 mg aliquots in all batches for Ellman's testing.
- When peptides are ordered, we request that they are aliquoted in specified masses that are intended to be resuspended in full in the stock tube to prevent loss of expensive peptide.
- Try to work relatively quickly once peptides are resuspended to preserve purity.

<u>Peptide aliquots:</u>
1. Retrieve DesiVac box containing necessary molecules from the -20°C freezer.
2. This process should be done in the BSC.
3. Pre-label 0.5 mL microcentrifuge tubes and place in tube rack.
   a. Use all tubes of the same color (will be very helpful finding them later in the aliquot box). I write the peptide abbreviation and the mg in the aliquot on the top (e.g., "VPMS 5" for 5 mg of VPMS peptide) and on the side write the mass out fully (e.g., "5 mg") and the date.
4. Prepare 2 mL microcentrifuge tube per peptide to be aliquoted.
   a. E.g., one for VPMS and one for RGD
5. Make fresh 25 mM acetic acid (37 uL of glacial acetic acid per 25 mL ddH2O) in the fume hood.
   a. This should be made fresh every time.
6. Remove stock peptide from DesiVac box (after allowing box to warm to room temperature).
   a. If you are not going to resuspend the full stock vial (though this is not recommended) then remove desired mass and purge the vial of oxygen with argon.
7. Store stocks back in DesiVac box and place back in -20°C freezer.
8. In the BSC, add 25 mM acetic acid solution to the peptide stock vial to achieve <u>50 mg/mL</u> (i.e., 500 uL for a 25 mg or 1000 uL for a 50 mg stock vial).
9. Vortex vigorously until dissolved (about 0.5-2 min).
10. Centrifuge to collect all liquid from sides at bottom.
11. If dissolving multiple vials thoroughly exchange solution between all containers to ensure a uniform and complete dissolution for all aliquots.
12. Use a 3 mL syringe equipped with a 1 ½" needle (20-22G) to draw up all the solution.
13. Filter through a <u>13 mm 0.22 um syringe filter</u> into the sterile 2 mL microcentrifuge tube.
14. Centrifuge to collect all liquid from sides at bottom.
15. Dispense the appropriate volume of the solution to each of the labelled 0.5 mL tubes, being careful to pipette solution to bottom of tube, avoiding getting liquid on the side of the tube.

a. It is important at this stage that you have very careful pipette technique. Ensure that you eject the full volume into each tube. IT IS ESSENTIAL THAT THIS STEP IS DONE PRECISELY!
      i. For 15 mg/tube – 300 uL (use P-1000 pipette)
      ii. For 10 mg/tube – 200 uL (use P-200 pipette)
      iii. For 5 mg/tube – 100 uL (use P-200 pipette)
      iv. For 1 mg/tube – 20 uL (use P-20 pipette)
   b. I always start with the larger volumes first so you are sure there is enough volume to complete those.
   c. Note: You will lose some volume (1-3 mg worth) as a result of filtering.
16. If solution is present on sides of tube, centrifuge the tubes briefly to collect all the liquid in the bottom. At this point be very careful with the tubes so the liquid does not splash up onto the side again. All the liquid must stay in the bottom of the tube so when they are lyophilized all of the mass is together.
17. Move the tubes to the main lab area.
18. Gently dab an ethanol wipe on the top of the tubes, being careful not to rub off the marker on the top.
19. Ignite a Bunsen burner.
20. Heat the needle of a 28G insulin needle red hot then quickly puncture a small hole in each of the 0.5 mL tubes containing the aliquots. You will need to reheat the need between every tube. This hole will allow the sample to be lyophilized but will keep the contents relatively clean/sterile.
21. Move back to the BSC.
22. Use sterile tweezers to place all the tubes in 50 mL conical tubes.
   a. You can place up to twelve 0.5 uL tubes per 50 mL tube.
23. Cover the top of the tubes with a Kimwipe folded over on itself four times (so there are 8 ply)
   a. It should be a small square that is a little bigger than the opening of the conical tube.
24. Carefully secure with rubber band by wrapping it twice around the edges of the Kimwipe/tube.
25. Move all the covered 50 mL tubes to a glass lyophilization flask(s), cover with foil, and place in -80°C freezer for at least 4-6 h (or overnight).
   a. The maximum number of 50 mL tubes that can be done in a single lyophilization flask is 4.
26. Remove the labels from the peptide vials and stick on a white paper with any notes to keep track of when the stocks are being used.
   a. I like to put the date, color of tubes, and number of tubes.

PAUSE POINT – samples freezing over night

1. The next day prepare the lyophilizer per instruction on the wall.
2. Prepare the lyophilizer flask (BE CAREFUL THESE ARE VERY EXPENSIVE DESPITE THEIR SIMPLE APPEARANCE!) and the rubber cover.
3. <u>Very quickly</u> the lyophilization flask from the freezer, remove the foil cover with rubber cover, place on lyopilizer and turn to vacuum.

a. Maximum time to do this should be about 15-30 seconds. You need to do this quickly to avoid peptides melting.
b. The glass will be slippery, so move fast, but not so fast that you will lose control of it.
4. Lyophilize for 48 hours.
5. If a lot of people have been using the lyophilizer, place a sign on it that <u>no other samples should be added while the peptides are on the machine.</u> They are very sensitive to melting if the lyophilizer fails and will be ruined.

PAUSE POINT – samples on lyophilizer

1. After ~48 hours the aliquots should be ready to be taken off the lyophilizer.
2. Get the aliquot storage box out at least 30 min prior to removing samples from lyophilizer so it will be ready to add samples to.
3. Prepare ~1 cm wide strips of parafilm for each tube.
4. Remove samples from lyophilizer and shut down lyophilizer according to instructions.
5. Remove 50 mL conical tube from lyphilization flask and bring into BCS.
6. Remove rubber bands and Kimwipes.
7. Remove 0.5 mL microcentrifuge tubes from the conical tube and arrange in tube rack according to mass.
8. Wrap each vial lid with parafilm.
    a. I start by covering the top (and the hole), then go around the edge of the tube then back across the top in a figure 8. Make sure hole on the top and the sides of the tube are well sealed.
9. Place aliquots in the DesiVac box.
10. Take a picture of the current set of aliquots.
11. Update the Google Drive file for the box layout.
12. Also update the Google Drive file for the aliquot information.

<u>PEG aliquots (PEGVS):</u>
The procedure is essentially the same as above EXCEPT:
1. Dissolve the PEG in <u>ddH2O</u> at <u>50 mg/mL</u> (will take more time to dissolve before filtering). This can be done at a lower concentration than 50 mg/mL, but it depends on the highest aliquot mass you wish to make (i.e., it must be able to fit in a 1.5 mL tube).
    a. For 50 mg/tube – 1000 uL (use 1000 uL pipette)
    b. For 30 mg/tube – 600 uL (use 1000 uL pipette)
    c. For 20 mg/tube – 400 uL (use 1000 uL pipette)
    d. For 10 mg/tube – 200 uL (use 200 uL pipette)
2. Weigh out PEG into 15 mL conical tube.
3. Before placing stock bottle back into DesiVac box, purge with argon gas.
    a. Open the argon gas valve outside of the fume hood.
    b. Open the regulator.
        i. You should hear a hissing noise from the cone in the fume hood.
    c. Uncap the stock bottle and place under the cone.
        i. Leave the cone slightly tilted open.
    d. After ~30 sec, quickly cap the bottle while keeping it under the cone

          i.   Hold cone with one hand hovering over the bottle and cap with other hand.
     e.   Tighten cap and wrap with parafilm.
     f.   Turn of regulator and close argon gas valve.
4. <u>Protect from light at all steps.</u>
5. Place aliquots in 1.5 mL (not 0.5 mL) tubes.
6. It is even more essential to move samples very quickly from -80°C to lyophilizer (15 s max! PEG will melt very quickly)

Samples need to be lyophilized for at least 48h, **<u>covered with aluminum foil to protect from light.</u>** IT IS ESSENTIAL THAT PEPTIDES AND PEG ARE NOT LYOPHILIZED AT THE SAME TIME!

Appendix F – Casting Cellular Photopolymerized PEGNB Hydrogels

Materials:
- 13 mm syringe filters
- 15 mL and 50 mL conical tubes
- 2 mL microcentrifuge tubes
- 24 well plate
- 3 mL syringes
- Cell culture reagents (PBS, trypsin, media, etc.)
- Crosslinking molecule (PEGDT, DTT, degradable peptide aliquots, etc.)
- Cutoff 1 mL Syringes
- Hydrophobic coated 96 well plate (for ultrasound characterization)
- Hydrophobic coated glass slides and PDMS (for gels of different volumes/dimensions)
- Ice bucket with crushed ice
- LAP (or other photoinitiator)
- PBS (or other buffer of interest)
- PEGNB (stock, to be weighed out)
- Pipettes tips (P-20, P-200, P-1000)
- RGD aliquots (if applicable)
- Serological pipets

Equipment:
- 15 mL conical tube rack (with tape covering bottom holes so syringes do not fall through)
- Automatic pipette aid
- BSC
- Hemocytometer
- Incubator
- Microscope
- Pipettes
- Tally counter
- UV lamp (365 nm)

Overview:
This procedure describes the process of forming (cellular) thiol-ene photopolymerized PEGNB hydrogels via stepwise copolymerization using cysteine flanked crosslinking molecules.

Notes:
- If making cellular gels, UV sterilize the cutoff syringes in the hood before use. I try to do this the night before, by placing the syringes cut side up in a microcentrifuge tube rack and letting the UV cycle finish. If you do not remember to do this the day before, you can

do it the day of experiments while you prepare the cells (only if you have the option of using both TC hoods).
- Record the amount of PEGNB/PEGDT/DTT/LAP, degradable peptide (if applicable), and RGD (if applicable) used in each experiment in the shared Google Drive sheets so we can keep track of how much of each molecule is remaining.
- WHENEVER REMOVING PEG OR PEPTIDES FROM STOCK CONTAINERS ALLOW THEM TO WARM TO ROOM TEMPERATURE FOR <u>AT LEAST</u> 30 MIN BEFORE OPENING TO PREVENT CONDENSATION INSIDE THE CONTAINERS (i.e., **<u>do not</u>** open containers until there is no longer moisture on the sides).

Tips:
These tips are found throughout the protocol as reminders, but please look these over before starting the process.
- I recommend always making at least 100 uL (ideally 150 uL) of gel precursor at a time to avoid working with really small volumes.
  - DO NOT make individual gels as small errors in pipetting can make each gel have very different mechanical properties.
- Try to work with more dilute starting concentrations (within reason) to avoid using really small volumes as well.
  - This can be adjusted in the "Component Stock Solutions" in the recipe sheet.
- Precise volumes are crucial for experiment accuracy and reproducibility.
  - Make sure you are always ejecting the full volume of the solutions by pushing to the second stop of the pipette.
- It is also critical to make sure your solutions (at all stages) are well-mixed.
  - With the exception of cells, vortex, vortex, vortex!
- When mixing a solution with the pipette, make sure you do so slowly to avoid any volume loss of solution stuck up in the tip.
  - Again, make sure to eject the full volume after mixing.
- Try to remove as much of the media above the cell pellet as possible as to not dilute out the precursor components with extraneous media.
  - If you leave a little more media in one group than another, it will be hard to determine if mechanical properties and thus cellular response were as a result of the intended gel properties or the resulting properties from diluted concentrations.

Procedure:
1. Retrieve DesiVac box containing necessary molecules from the -20C freezer and the glass jar containing necessary molecules from the fridge below the freezer.
2. Allow DesiVac and glass jar to come to room temperature (no condensation on the exterior of the containers) before opening.
   a. In the summer this usually takes 45-75 min
   b. In the winter this usually takes 30-45 min
3. While the containers are coming to room temperature, harvest cells as you normally would, collecting the desired cell number for the specified number of gels per condition in 2 mL microcentrifuge tubes.
   a. For HUVEC-NHLF microbeads I typically use 4 M/mL cells in a 1:1 ratio.

    b. Note: DO NOT make gels individually as working with small volumes can lead to small errors that have substantial impacts on the stiffness of the gels. Instead, mix all the precursor components for all of the gels of a desired condition in one tube and distribute into multiple syringes.

        i. For example, if you want to make three 50ul gels of one condition then you will pellet enough cells for three gels into one tube and resuspend that pellet in 150ul precursor solution. Then, you will distribute that solution by pipetting 50ul into each cutoff syringe.

        ii. To avoid ending up with a gel smaller than the others due to volume loss, I recommend preparing ~10ul extra of precursor solution and cells.

            1. I.e., make 160ul of precursor solution plus cells, and be sure to account for this increased volume when calculating the number of cells you need per tube.

4. Place cell pellets on ice while you prepare the gel components.

5. Complete the PEGNB **recipe sheet** (specific to type of PEG and the crosslinking molecule, example below) to calculate weight of molecules needed.

    a. The ==yellow== cells are ones that require user input (and checking) but may not change from experiment to experiment. The red cells vary from experiment to experiment and need more careful checking. The gray ones are calculated from the yellow and red ones.

        i. Calculate enough PEGNB and LAP to account for some volume loss during sterile filtering (~50ul extra).

        ii. Always make sure the purity for the molecules is accurate for each lot/batch of aliquots you will be working with or else all of the calculations will be off.

            1. This can be found within the Google Drive on various sheets (short term box with aliquots as well as Ellman's sheet).

            2. An Ellman's test will need to be done for each batch of aliquoted peptides to determine batch purity.

        iii. If you will be combining multiple peptide aliquots, make a note on how much volume each peptide would need individually.

            1. For example, if you need 7 mg of peptide and will combining a 4 mg and 3 mg aliquot – note how much volume each tube would need individually so you can resuspend them separately prior to combining them to make the peptides are not accidentally more concentrated due to losing any volume when combining tubes.

6. Retrieve peptide aliquots from box.

    a. RGD and degradable peptides (VPMS, usually) are stored as prepared aliquots of specific masses (1-10 mg, usually) so they do not need to be weighed out each time (or sterile filtered). It is important that you make sure there is enough of each peptide already aliquoted for your planned experiment.

        i. If peptides are running low (~10 mg or so remaining), then new ones will need to be prepared. This process takes 4 days so DO NOT wait until the last minute to prepare new peptide aliquots or experiments will be delayed.

7. Weigh out PEGNB and LAP into 2mL microcentrifuge tubes.

       a. In the winter, it is critically important to use the static gun to reduce loss of molecules and accurately measure out masses.
           i. Use the static gun on the microcentrifuge tube, spatula, and stock container.

8. Purge stocks with Argon in the chemical hood and parafilm them.
9. Return stocks to containers and place containers back in their respective storage locations.
       a. Note: You will need to pump the lid of the DesiVac container to remove as much air as possible. Don't overdo it, just enough to make sure the top button is fully lowered into its slot in the lid.
10. Update recipe sheet with exact weighed out masses for any components that were not previously stored as lyophilized aliquots.
11. Print the recipe sheet.
       a. I like to save them in a binder for future reference and record stiffness directly on the sheet to keep track of each batch of gels.
12. Resuspend the freshly weighed out molecules (PEGNB, LAP) in PBS (or another buffer) according to the recipe sheet.
       a. Resuspension is done using the vortex, NOT pipetting up and down. Some of the solutions can be viscous and you want to avoid volume loss.
       b. Resuspend the PEGNB first as it takes longer to fully dissolve. You will need to vortex it and let it rest a few times. You can try to constantly vortex to dissolve, but I have found that it doesn't work much quicker then mixing and letting the solution rest. If you have a sonicator bath, this will speed up the process.
       c. Next, resuspend the LAP and vortex.
       d. Wait to resuspend the peptides as these will begin to degrade once resuspended so you want to do this just before you are going to use them.
13. Briefly centrifuge the PEGNB and LAP to collect at the bottom of the microcentrifuge tubes.
14. Sterile filter the PEGNB and LAP.
       a. Use 3 mL syringes and 13 mm filters.
       b. I like to also use a P-200 to pull any remaining solution out of the ejecting side of the filter just to make sure I have enough for all of the gels.
15. Arrange cutoff syringes for first set of gels in taped 15 mL conical tube rack with UV lamp at the appropriate distance (usually ~1 inch above the gels for ~50 mW/cm^2).
       a. I place the syringes cutoff side up in one opening of a 15ml conical tube rack, such that up to 4 syringes are in one opening. As the gooseneck lamp has two UV sources, you can cast 8 gels at a time.
       b. Make sure the plunger is pulled back enough for the gel to fit into the syringe. Try to keep this distance consistent between syringes. I typically cut the syringes around the 0.1 mark and pull the plunger down to the 0.2 mark.
16. Resuspend the aliquoted peptides (VPMS, RGD) in PBS (or another buffer) according to the recipe sheet.
       a. If you are combining aliquots for the needed mass, then resuspend one aliquot at a time in the volume needed for that individual mass prior to combining.
17. Vortex all solution so they are well mixed.

a. PEGNB is stable at room temp for many hours, however, the crosslinking molecules will degrade more quickly once resuspended.
   b. If you are going to be making a lot of gels or going more slowly on your first few attempts then you should keep solutions on ice to slow degradation and use within 30-60 min, if possible, though I have used solutions that were kept at room temp for a little over an hour and they crosslinked just fine.
   c. If solutions have been sitting for a while, vortex again before using.
18. Aspirate media from cell pellet.
   a. Make sure you get as much media off of the cell pellet as possible as any extra media will dilute out your precursor and you won't have the concentrations you calculated.
   b. Note: The cells do dilute the solution also, so cellular gels will often be softer than acellular gels.
19. Add gel components (push to the second stop on the pipette to eject full volume) to the bottom side of the tube containing the cell pellet in the following order (do not resuspend the cell pellet until step e):
   a. PEGNB – slowly draw up and expel as PEG is more viscous, be sure that all PEG is pipetted into the tube
   b. LAP
   c. RGD – pipette up and down a few times to mix the peptide, expel any volume in the tip, then take needed volume
   d. VPMS – pipette up and down a few times to mix the peptide, expel any volume in the tip, then take needed volume
   e. PBS/buffer – gently and slowly resuspend the cell pellet now, be sure that all precursor solution is pipetted into the tube when done
   Note: Some rounding may be needed depending on the precision of the pipettes. I follow standard rounding rules.
20. Set P-200 pipette to 50 uL and attach tip.
21. Quickly vortex the solution.
   a. You do not want to add too much stress on the cells, so I do 3 quick pulses on the vortex, just enough to mix each time.
   b. THIS IS IMPORTANT as well mixed solutions are necessary for consistent stiffness between gels.
22. Distribute 50 uL of solution to each cutoff syringe (or 96 well plate or PDMS mold).
23. To crosslink the gels, expose them to UV light using the gooseneck UV light source.
   a. Time duration for crosslinking will depend on a variety of variables, including wt. % PEG, crosslinking density, LAP concentration, and UV intensity.
   b. UV intensity can be measured using the radiometer.
   c. It is important to keep UV time and intensity constant between different experimental groups even if some formulations crosslink faster than others, as you want the cells in each group to receive the same amount of UV exposure. I do this by making sure the UV light is always the same distance from the gels during exposure.
24. Pop the gels out of the syringes (or scoop them out of the PDMS molds with a spatula) into a 24 well plate containing 1 mL of warm media per well.

a. Try to pop the gels directly into the solution, submerging them while they are still on the plunger. Then, use a spatula to pop the gel off if needed.

b. You want to be as close to the media in the well as possible when popping the gels out as sometimes they want to fly off the plunger.

c. DO NOT let the gel hit the side of the well before it has been moistened in solution. It will stick to the side of the well and ruin the gel.

d. If necessary, you can confirm your gel has formed by slowing moving the plunger upward until the top of the gel is showing just above the syringe.

25. Repeat steps 18-23 for remaining conditions.

a. Be sure you are mixing your peptides before taking needed volume.

26. Change media, now using 2 mL, the next day and then every other day after that.

a. To change media, tilt the plate on its lid so the gels settle toward the bottom of the well. Use a micro spatula to hold down the gel so it does not get sucked up by the aspirator.

b. If you are scared of losing gels because it is too soft, consider manually aspirating the media from those wells.

Short Description of Experiment Date

Component Properties

Abbreviation		Lot	MW	Aliquot Date	Gross Mass in Aliquot (mg)	Reactive Mass in Aliquot (mg)	Purity		
PEG-NB	4-arm PEG norbornene	FY05073	20021	Fresh	34.0	33.66	0.99	< Assumed from supplier information	
RGD	AC-CGRGDS-NH2	CP-L-501006-1	634.67	4/1/2022	1.0	0.6285	0.625	< Ellman's test from date (initials of person who did Ellman's)	Buffer: resuspended in PBS or SF-EGM2
VPMS	Ac-GCRDVPMSMRGGDRCG-NH2	CP-H-500216-1	1738.01	3/17/2022	4.0	2.9524	0.738	< Ellman's test from date (initials of person who did Ellman's)	
LAP	Lithium phenyl-2,4,6-trimethylbenzoylphosphinate	MKCM1930	294.1	Fresh	1.0	0.983	0.983	< Assumed from supplier information	

Common Stock solutions:

	Active Concentration		Filter loss		Mass used			
	mg/ml	mM	ul	Gross (mg)	Active (mg)	ul		
PEG-NB	75.0	3.7	0	34.0	33.7	448.8	ADEQUATE	
RGD	6.3	10.0	0	1.000	0.629	99.0	ADEQUATE	
VPMS	41.7	24.0	0	4.000	2.952	70.8	ADEQUATE	
LAP	2.9	10.0	0	1.000	0.983	334.2	ADEQUATE	

Gel Description	Molar XS mol SH/mol VS post RGD	Total Solids	Mass Composition (mg/ml)				Molar Composition (mM)				Total Volume	Recipe Volumes Per Gel (ul, for measured concentrations)				
			PEG-NB	RGD	VPMS	LAP	PEG-NB	RGD	VPMS	LAP		PEG-NB Stock	RGD Stock	VPMS Stock	LAP Stock	Buffer
3% PEG, 90% CL	0.900	35.5	30.0	0.6	3.9	1.0	1.50	1.000	2.25	3.400	210	84.00	21.000	19.66	71.40	13.94
3% PEG, 80% CL	0.800	35.1	30.0	0.6	3.5	1.0	1.50	1.000	2.00	3.400	210	84.00	21.000	17.48	71.40	16.12
3% PEG, 70% CL	0.700	34.7	30.0	0.6	3.0	1.0	1.50	1.000	1.75	3.400	210	84.00	21.000	15.29	71.40	18.31
3% PEG, 60% CL	0.600	34.2	30.0	0.6	2.6	1.0	1.50	1.000	1.50	3.400	210	84.00	21.000	13.11	71.40	20.49
										Totals	840.00	336.00	84.00	65.54	285.60	68.86

Appendix G – Rheology of Bulk Hydrogels
Adapted from Yen Kong

Materials:
- Glass plate to balance well plates (if measuring directly in well)
- Double sided scotch tape
- Course grit wet sandpaper (800 grit or lower is best)
- 8 mm biopsy punch
- Micro lab spoon (if measuring PEG hydrogels)

Equipment:
- AR-G2 shear rheometer with Peltier stage attached for standard measurements
- UV stage if performing in situ UV curing
- 8 mm measurement head with adapter and longer spindle rod for preformed hydrogel characterization
- 20 mm measurement head for in situ gelation measurements

Overview:
This protocol describes the use of a parallel plate rheometer for characterizing hydrogel material properties.

Notes:
- Experiments for characterizing material properties in preformed hydrogels, either in a well plate or as a puck, are done with the 8mm measurement head.
- Experiments for characterizing the gelation kinetics, either on the Peltier plate or UV stage, are typically best performed with the 20 mm measurement head. The greater surface area provides a more accurate measurement and reduces slippage for gels that are cast in situ.
- Getting a transducer initialization error has become more common over the last couple years. This error is most likely caused by a problem with the rotary optical encoder that keeps track of the displacement and velocity of the bearing spindle. If you receive this error quickly turn off the instrument because rotation of the spindle starts to accelerate out of control. Usually restarting the instrument and software a couple times will fix the problem. The error only occurs at start up. When simply restarting doesn't work, I have had some success with starting the instrument with the measurement lowered to be in contact with the measurement plate to hold it in place, which seems to allow the encoder to register the spindle more easily. You will get a magnetic bearing instability warning however, at which point, raise the measurement head and restart the software, but not the instrument.

- TA instruments suggestions for dealing with transducer initialization failure: Transducer initialization is reporting a problem with the rotary optical encoder that keeps track of the displacement and velocity of the bearing spindle. The rotary encoder is positioned at the top of the air bearing motor/transducer assembly. When it fails to report a position change the error will be posted. There could be some dust in and around the encoder, try blowing compressed air thru the opening where the draw rod sits. If you are comfortable taking things apart you could remove the cowl cover and top encoder cover to better inspect and blow out any dust. If the error is persistent, I would recommend a service call.
  - To avoid initialization failure, it is ok to **leave the instrument running for long periods of time**, however, it is important to **turn off the cooling pump when not in use** because the pump will overheat if left running over night, this is bad for the pump, and also heats the water bath, such that the Peltier stage can't cool down to an appropriate temperature to perform experiments. Only leave the rheometer and air on.
- Measurement parameters for collagen/fibrin are typically performed in a 24-well plate or larger, using the 8 mm measurement head indented into the hydrogel ~300 um, 0 N normal force, 6% strain, 1 rad/sec.
- Measurement parameters for PEG hydrogel pucks are typically performed using the 8 mm measurements head indented into the hydrogel at 0.05 N normal force, 5% strain, 1 rad/sec. If the gels are quite soft, they may not ever reach 0.05 N normal force, and instead we measure them at 1000 um gap height. DO NOT go less than 1mm gap height.

Procedure:
1. Log in to the "Rheometer" profile on the rheometer computer in the Putnam lab space
2. Plug in the water pump to the power strip.
   a. Check water bath level for Peltier stage cooling pump and add water if necessary, exchange with fresh water if cleaning is needed.
3. Open the Rheological Advantages software to control the AR-G2 rheometer.
4. If the rheometer already has the necessary stage and geometry attached, or you were the last one to use the rheometer, you can skip to step 7.
5. If a stage swap is necessary between the Peltier and UV stage swap now by removing the cooling tubes (pinch the white clasps on the side) and unplug the smart swap connector (the multipronged metal connection). Press the right most button on the rheometer front panel twice to release the stage. Attach the cooling tubes and re-plug the smart swap connector for the desired stage.
   a. If performing a UV experiment, at this point calibrate the UV irradiance with the radiometer and remote sensor. Wizard -> UV irradiance calibration.
6. If a geometry swap is necessary:
   a. First remove the original geometry and perform the inertial calibration. Options -> Instrument -> Inertia Tab. This is done without a geometry attached.
   b. Screw on the desired testing geometry components
      i. The 20mm diameter measurement head geometry uses the shorter spindle rod.
      ii. The 8mm diameter measurement head geometry needs an adapter and the longer spindle rod.

c. If smart swap is enabled, the instrument will automatically recognize the geometry and give the option to load the geometry file that corresponds to the geometry's serial number. If not, then manually load the appropriate geometry file. Geometry → Open → select correct geometry in "Geometry" folder.

d. Invalidate all zero point and select "NO" to map when asked.

e. Calibrate geometry inertia. Settings tab -> geometry inertia calibrate.

f. Calibrate bearing friction. Options -> Instrument -> Miscellaneous.

g. Perform rotational mapping. Use 'two' iteration and 'standard' type. Instrument -> Rotational mapping.

7. Load or create new test procedure. Procedure -> open, or Procedure -> new.

a. Procedures are typically "oscillation" procedures. When you click new procedure, it will open the default tab to input procedure steps and test parameters. New oscillation procedures will default to have 3 steps: 1) conditioning 2) frequency sweep 3) post-experiment. You can right click on a step to add another step to the procedure. You can uncheck the box to turn off a particular step. In addition to oscillation frequency sweep, we commonly perform an oscillation strain sweep for initial characterization of a hydrogel, then oscillation time sweeps as the primary measure for comparison between conditions for a particular type of hydrogel/material.

b. To input parameters for each step; click on the step in the procedure, then fill in the desired parameters for the step in the tabs that appear to the right.

c. To save a procedure go to File-> Save As

*** For new materials, it is recommended to first perform an oscillation frequency sweep (0.1 -> 10 rad/sec, at least 5 points per decade) at low strain (0.5 – 1 % strain) to determine the viscoelastic limit. Then selecting an appropriate oscillation frequency based on this first test, perform a strain sweep (0.1 - 10%) to determine the strain stiffening limit. You should be ready to report these results as it is most common for materials to be characterized with frequency and strain parameters in their linear viscoelastic limit.

* If you are UV curing you will need to do a time sweep first to determine how long to cure your gels before frequency and strain sweeps. Add an event step for switching on/off the UV to your procedure.

* After determining parameters that are within the LVE range, we typically just perform a 30-60 second time sweep at the appropriate strain and frequency.

8. If you are doing gelation tests, perform oscillation mapping. Mapping needs to be done with the appropriate geometry, at the approximate gap of the test, and needs to cover all the parameters you included in your procedure. Instrument -> Oscillatory mapping.

i. If the instrument is not well mapped you may get inertial artifacts in your measurement, such as negative values.

9. Prepare the stage for hydrogel measurement:

a. Pre-cast PEG hydrogels will be measured directly on the Peltier stage but require sandpaper on the stage and measurement head to prevent it from slipping out from under the measurement head. Put double sided tape on the back of the sandpaper, cut out an 8 mm punch, then apply the sandpaper to the measuring face of the measurement head and the stage, being careful to center the sandpaper under the

measurement head. Sandpaper is usually good for multiple days, replace when sandpaper is no longer adhered. Use a razor blade to remove, if needed.

b. If you are measuring hydrogels directly in the well plate (typically fibrin or collagen) you will still need sandpaper on the measurement head to reduce slipping over the surface. You will also need to find the glass plate that is kept under the rheometer (~ 0.1 x 14 x 18 cm) and place on the Peltier stage to keep the well plate level.

c. If you are going to use a specific temperature for your measurement, you can set the stage to this temperature now to save time at the start of your first measurement run. Samples containing cells should be tested at 37°C.

d. If you are UV curing your hydrogels, make sure the UV stage is well cleaned. You will also want to wear the UV protectant safety glasses.

10. Zero the geometry gap . If you are doing in-well measurements, make sure to zero into an empty well. Say "NO" to move head to back off distance, this moves the head all the way up and wastes time. Move head up manually using arrow buttons on rheometer or in the software.

11. Zero the normal force . You may need to press the zero button a few times for it to give a negligible value (< 0.01 N, usually in the E-10 range)

12. Sample loading:

a. For PEG hydrogel pucks, use a micro lab spoon to transfer the gel from the well plate and center it on the sandpaper on the stage with a flat side face down.

b. For in-well hydrogels, make sure the well of the plate is well centered under the measurement head. If the head is off to the side, it could give false measurements because of the extra contact area with the sides of the well.

c. For in situ gelation, lower the head to the measurement height (typically 100 – 1000 um). The approximate volume of the sample depends on the gap value and the geometry (should be using 20 mm) and can be found at the Geometry -> settings tab -> dimensions tab. Mix the precursor solution then pipette the approximate volume + 10% into the gap. Seal around the outside with mineral oil so it doesn't dry out if you will be taking long measurements.

13. Sample measurement: Before lowering the measurement head or pipetting in sample for in situ gelation STOP ROTATION of measurement head to prevent shearing

a. For PEG hydrogels: Zero the normal force. Manually lower the head until the normal force reads ~0.05 N. If gels are very soft and this normal force is not reached, stop at 1000 um, because you will destroy your gel if the gap is too small.

b. For hydrogels that have a large viscous component (unlike PEG hydrogels that are primarily elastic) the normal force will quickly dissipate after lowering the measurement head onto them, so measurement at a constant normal force is not feasible. To address this, it is common to perform measurements at a constant gap height (which is appropriate for in situ gelation) but cellular hydrogels contract over time so a constant gap height is also not appropriate. Instead, you will want

to ident a constant depth into the hydrogel. Bring the measurement head into contact with the hydrogel, then input a gap height 300 um lower to indent into the hydrogel.

    c. For in situ gelation: work quickly to start measurement as soon as possible after mixing and pipetting in precursor solution.

14. When you press the start measurement button in the top left corner you will be prompted to put in run information. Include all important information in the file name, and make sure it is saving to the appropriate directory to find the file.

    a. Repeat for all samples, zeroing the normal force between samples if it does not return to < 0.01 after removing samples from stage.

15. Data can be loaded in the TA data analysis program.

    a. When you open a file, nothing will immediately happen, and you will need to select view as table. You can then select all, copy, and paste into an Excel document.

16. Do not shut down the instrument.

    a. We are currently leaving the instrument on between uses, but require **the pump be turned off**. To do so, set the required stage temperature to room temp (20-25°C), wait for the stage to reach this value and remain there for a few minutes, then instrument → set temperature system idle. After, unplug the pump for the pump.

    b. Shut down the software and log off of the Rheometer profile.

Appendix H – Collagenase Digestion of Bulk PEG Hydrogels
Adapted from Ben Juliar

Materials:
- 15 mL and 50 mL conical tubes
- 2 mL microcentrifuge tubes
- Collagenase I (or IV) from *Clostridium histolyticum*
- Microspoon/spatula
- Phosphate buffered saline supplemented with 0.4 mM CaCl$_2$ and 0.1 mM MgCl$_2$
- Pipette tips
- Serological pipets
- Surgical scalpel (if fully dissolving gels)

Equipment:
- Automatic pipette aid
- Incubator shaker plate
- Microcentrifuge tube rack
- Scale

Overview:
This protocol describes the process of degrading/digesting MMP-degradable PEG hydrogels using collagenase, either for rheological measurements or cell isolation.

Notes:
- If this protocol is being performed on samples for degradation properties (i.e., you will be measuring their stiffness over time) then you will want a at least two gels for each timepoint.
  - While you could measure the same gels over and over, they spend a decent amount of time outside of the collagenase solution which could influence your results.
- You will want to use the shaker plate with the incubation chamber in the Stegemann lab for measuring degradation properties so the hydrogels are evenly degraded, but if you are degrading the entire gels this can be done in a standard incubator with timed inversion mixing of the tubes.
- It is a good idea to do practice degradation on acellular PEG hydrogels of the same formulation (wt. %, crosslinking, etc.) as your cellular gels to check if you need to increase/decrease collagenase concentration for ideal hydrogel degradation.
  - Hydrogels should completely degrade in 30-45 min for cell isolation. If your gels do not fully degrade in this time period, test higher concentrations of collagenase.

- If this procedure is intended to be used for RNA isolation, immediately after cell pelleting you will need to move forward with biomolecular isolation, so you should also prepare for that before initiating this procedure.
- To recover a decent pellet for RNA isolation you will want at least 300k total cells per centrifuge tube (closer to 500k is preferred). If there are not enough cells you will not be able to see your pellet to aspirate and you will get a poor yield. Keep this in mind when designing your experiments (e.g., cell seeding density and number of gels to pool together per replicate).

Procedure:
1. Prepare fresh collagenase solution:
    a. Calculate the amount of Collagenase solution needed
        i. 400 µL per 50 µL hydrogel for cell isolation
        ii. 1 mL per 50 µL hydrogel for degradation kinetics
    b. Calculate the amount of Collagenase powder resuspended in the necessary volume of PBS (0.4 mM $CaCl_2$ and 0.1 mM $MgCl_2$) to achieve the desired U/ml (U = digestion units)
        i. U/mg varies by lot, so check the current lot
2. Warm up Collagenase solution in water bath to 37 °C until fully dissolved
    a. Do not leave in water bath longer than needed, it will start to lose activity if left for too long (hours)
3. Aspirate media from PEG gels
    a. If using automatic aspiration, use a sterile microspoon/spatula to hold the PEG gel against the side of the well so you do not accidentally suck it up
4. Rinse gels with PBS (0.4 mM $CaCl_2$ and 0.1 mM $MgCl_2$)
    a. It is best to fill the wells to maximize the rinse
5. Aspirate off PBS
6. For degradation kinetics, add 1 mL of Collagenase solution to each well then incubate at 37 °C in Stegemann incubator shaker plate
    a. Vortex Collagenase solution prior to adding to wells
    b. Use microspoon/spatual to submerge the gel fully
    c. Remove gels for rheology then place back into incubation chamber
7. For cell isolation, cut up the hydrogels into quarters or smaller using a scalpel and transfer pieces to microcentrifuge tubes and add Collagenase solution
    a. You will probably need 2-3 gels per tube to recover enough cells for a decent pellet
    b. You may choose to transfer gels first then cut up in the microcentrifuge tube, if you find it more convenient this way
    c. Add is 400 µL of Collagenase per gel
        i. Despite hydrogel swelling, you should be able to add 1200 µL of collagenase solution to 3 hydrogels (50 ul hydrogels swell to ~200 µL)
8. Incubate tubes at 37 °C until gels fully degrade
    a. Mix via inversion every 5-10 min
    b. Typically, 30-45 mins, but it could vary and should not take more than an hour
9. Once gels are degraded, spin down solution and cells at 500g for 5 min
10. Aspirate off collagenase solution from cells

     a.   Thorough aspiration is not essential; it is more important to ensure that your pellet remains undisturbed to maximize yield

11. Rinse cells in PBS and spin down at 500g for 5 min
     a.   If your pellets are very faint, it is ok to skip the wash step to minimize the risk of losing them (I usually skip this step and the next)

12. Aspirate off PBS and proceed with experiment
     a.   Again, thorough aspiration is not essential; it is more important to ensure that your pellet remains undisturbed to maximize yield

Appendix I – Fabricating PDMS Microfluidic Devices

Materials:
- 21G needle (blunt preferred)
- Ethanol (EtOH. 100%)
- Foil
- Glass slides
- Isopropanol (IPA, 70% and 100%)
- Kimwipes
- Mini aluminum dishes (77 mm for 3' wafers)
- NOVEC 7500
- PDMS kit (Sylgard 184 Kit – base & curing agent)
- Plastic cup
- Plastic stir stick (or 2 mL serological pipette)
- Plastic syringes
- Polyethylene tubing
- Scotch Tape
- SU-8 wafer(s)
- Trichloro(1H, 1H, 2H, 2H-perfluorooctyl) silane (97% stock)

Equipment:
- Desiccation chamber
- Fume hood
- Oven
- Pipettes
- Plasma etcher

Overview:
The protocol describes the process of fabricating PDMS devices for microfluidic droplet generation. SU8 wafers were previously prepared in the Lurie Nanofabrication Facility or generously provided by the Baker lab.

Notes:
- The SU-8 wafers are VERY *delicate*. When cleaning wafers and removing PDMS it is essential to be as gentle as possible as to avoid cracking the wafers.
- This protocol takes 3-4 days to complete, so plan ahead if you need devices in the near future.

Procedure:
1. Turn on the oven to 70° C.

       a.   Use arrows to adjust temperature.
2. Place plastic cup on scale and tare weight.
3. Dispense PDMS base into cup.
       a.   You will need 20-22g of PDMS per 3' wafer.
4. Tare weight again.
5. Add 10% (by weight) PDMS curing agent.
       a.   For example, 44g of base requires 4.4g of curing agent.
       b.   If you pour too much curing agent, tare the weight again and add the necessary amount of base such that the curing agent is ~10% of the weight.
       c.   It doesn't have to be exact, but make sure you have at least 10% curing agent.
6. Using a plastic stir stick, vigorously mix the PDMS.
       a.   This will create a lot of bubbles such that the mixture will appear more white than clear.
7. Place the cup into the vacuum chamber to desiccate (remove the air from) the solution.
       a.   Remove lid, place cup in chamber, and turn on the pump.
       b.   Turn the red knob so that arrow is pointing towards the inlet to the chamber.
       c.   The vacuum should start to increase on the meter on the pump. To ensure that the vacuum is working, after a few seconds lift the chamber slightly by the lid to make sure the seal holds. If not, the lid placement likely needs to be adjusted before trying to establish the vacuum again.
       d.   After a few minutes you can slowly turn the red knob so that the arrow is pointing towards the tubing/pump to release the pressure and pop the large bubbles that initially form. Then turn on the pump and turn the red knob to re-establish the vacuum.
       e.   The time taken to fully remove all bubbles from the solution is dependent on the volume of the solution. Larger volumes take longer to desiccate.
8. While PDMS is being desiccated, gently clean the surface of the wafer with 70% isopropanol.
       a.   Waterfall isopropanol over the surface of the wafer with the squirt bottle, being sure to focus on rinsing the features, then dry with compressed air, again, focusing on the features.
9. Place the wafer in a small aluminum dish and cover with foil to keep clean until the PDMS is ready.
10. Once the bubbles have been purged from the PDMS, turn the vacuum pump off, turn the red knob perpendicular with the white inlet to release the pressure, then remove the lid.
11. Remove the foil covering the wafer, place the dish on the scale, and tare the weight.
12. Pour 20-22g of PDMS onto the wafer.
       a.   Any leftover PDMS could be poured into a petri dish to make PDMS molds for gels later.
13. Desiccate the wafer in the vacuum chamber again to remove any bubbles that may have formed during the pouring.
       a.   This shouldn't take nearly as long (only a few minutes).

b. If bubbles are at the surface of the PDMS you can pop them or move them with a pipette tip.
c. If no bubbles were generated during the pouring this step can be skipped.
14. Carefully move the dishes to the oven and place on a level surface.
15. Bake the PDMS overnight at 70° C in the oven.

----

16. Carefully remove the dish from the oven and place upside down on the lab bench to cool at room temperature.
    a. You want to make sure the wafer is not cooled too quickly as faster thermal cycling will reduce the lifespan of the wafer.
    b. If you are going to bond the devices today make sure you leave the oven on. If not, remember to turn the oven off.
17. Using scissors, **carefully** cut away the aluminum from the sides of the PDMS.
    a. You want to avoid any sort of bending of the wafer as this will lead to it cracking.
    b. Cut the sides of the dish down to the PDMS in a few locations, then peel the aluminum away sideways.
18. Using a razor, **carefully** cut away the aluminum and PDMS from the bottom of the wafer
    a. Carefully peel away the aluminum at the bottom of the wafer circumferentially a little at a time until the aluminum is fully released from the PDMS.
    b. There will likely be a thin layer of PDMS under the wafer as well, so you want to try to get the razor flush with the wafer and cut away the PDMS as well.
    c. Again, you want to avoid any sort of bending of the wafer as this will lead to it cracking.
19. **Carefully** remove the PDMS from the wafer.
    a. To do this, you will want to place the wafer/PDMS wafer-side down on the bench, very gently apply light pressure to the center of the wafer/PDMS just to hold it down on the bench, and circumferentially pull the PDMS from the wafer a little at a time until the PDMS is fully released from the wafer.
    b. At this point you want to avoid place the PDMS feature-side down on any surface.
20. Cut out the individual devices from the PDMS slab using a razor.
    a. Be careful not to cut the features.
21. Use a biopsy punch (typically 1 mm) to punch out the tubing inlets and outlets.
    a. Do this with the PDMS feature-side up. You should be able to feel the punch slot into the grove for the hole. This is very important as misaligned holes will not connect to channels.
    b. Do not rotate the biopsy punch to get it through as this may tear the PDMS.
    c. Make sure you try to keep the biopsy punch as straight as possible it goes through the PDMS to avoid odd angles or damaging the channels.
22. Store the devices feature-side up until you are ready to bond them to glass slides.

----

23. If you have turned the oven off prior, turn it back on to 70° C.
24. Clean the PDMS devices.
    a. Waterfall 100% IPA over the PDMS and vigorously rub the features with your fingers.
    b. Wash away IPA residue by water falling 100% EtOH over the surface.
    c. Place the devices into a jar with 100% EtOH and sonicate for 2-5 min.
25. Clean the glass slides using the same steps as the devices, without the sonication step.
26. Dry the PDMS and glass completely with compressed air.
27. Place PDMS devices feature-side up and glass slides in 70° C for 15-20 min to remove any residual EtOH.
28. Remove PDMS devices and glass from oven and allow to cool to at room temperature.
29. Optional (recommended): Add scotch tape to the feature-side of the devices and surface of the glass slides that you plan to bond the devices to. This will be removed before plasma bonding but will help avoid any particulates getting onto the bonding surfaces and remove any remaining particulates after the rinses.
30. On one well plate lid, place 4 glass slides and 4 PDMS devices feature-side up.
31. Put the well plate lid into the plasma chamber and close the chamber door.
    a. If you put on tape, remove this before placing in the plasma chamber.
32. Plasma treat the devices and slides for 1min at 10% O_2 (O_2 should be preset).
    a. Select Commands → Plasma
    b. If you need to change the time, first select Commands → Plasma time then Commands → Plasma
33. After the treatment is done, remove the devices and glass from the chamber.
    a. The chamber needs to repressurize first, so I often unlatch the door then wait for it to pop open.
34. Line up the PDMS feature-side down with the center of treated surface of the glass slide and carefully make contact at one edge, then let the rest flop down on the glass.
    a. I recommend lining up the long edge, so the device stays mostly center on the slide.
    b. DO NOT apply pressure to the device when you are dropping it onto the glass slide as you can end up with internal stresses at the interface if you try to guide it down, which can warp the features
    c. Once the device is down, *gently* press on the device to initially adhere it to the glass slide.
35. Turn the device over onto a Kimwipe (so it doesn't stick to the bench) and apply uniform pressure to the stiff, glass backing.
    a. Pressure on the soft, PDMS side can be more focused and lead to cave-in since the 'ceilings' inside the device channels are still sticky.
    b. You want to apply sufficient pressure such that you are sure the device is well-bonded, but not so much pressure that you crack the glass slide.
36. Put the devices (glass directly on metal rack) in the 80° C oven in the for 5 min.
37. Remove devices from oven and cool to RT with light pressure on the glass back (again on a Kimwipe).

a. There are weights and other various items that you can use to apply pressure, so you do not burn yourself on the hot glass.
38. Repeat steps 31-37 with the remaining devices.
39. Place scotch tape on top of the PDMS to protect the inlets and outlets from dust.
40. Put the devices in 70° C oven overnight.
   a. This helps internalize remaining -OH groups and restore surface hydrophobicity.
----

41. Move devices into the fume hood on a paper towel.
42. Prepare the surface treatment solution (to render the devices hydrophobic) by diluting the Trichloro(1H, 1H, 2H, 2H-perfluorooctyl) silane to a 2% solution in NOVEC 7500 (1:50 dilution) in a microcentrifuge tube and vortex.
   a. Volume to prepare: A general rule of thumb is you will use ~100uL per device.
   b. Prepare this solution fresh before each use as it is oxygen-sensitive and will form a precipitate after a while (~1hr).
   c. Immediately following mixing by vortex, run nitrogen gas over the top of the stock bottle to flush out oxygen, seal the bottle, and parafilm it to protect against oxygen.
43. Transfer the surface treatment into a syringe via an attached 21G needle, then flip upside down and attach tubing to the needle.
   a. Be VERY careful not to push the needle through the wall of the tubing (this is why a blunt needle is preferred).
44. Connect the tubing to the aqueous inlet of the device and slowly fill the device with the silane solution.
45. When it begins to come out of the device outlet, cover the outlet with your finger to force the solution through the PEG inlet. Essentially the goal here is to fill every bit of the device.
   a. You want to inject slowly because too much pressure can force leaking and make the device appear defective.
   b. You should not experience resistance when injecting the silane solution. If it is difficult to get the solution to flow, the most likely explanation is that one of the inlet channels is blocked and is causing a pressure build-up, and it is unlikely the device will be usable, and you should probably just discard it (bet let it air out in the fume hood overnight first).
46. Repeat Steps 44 and 46 with all devices you are treating.
47. Allow treatment to proceed for 10min at RT.
   a. This timing is not critical and could be extended slightly when working with a lot of devices. However, do not allow to treat too long as precipitates may form. Longer than ~15min is not advisable.
48. Aspirate the surface treatment out of the device outlet using the same tubing and syringe.
49. Flush the device completely with NOVEC 7500 oil by repeating steps 45 and 46 with a syringe filled with pure NOVEC 7500.

a. If you intend to keep and reuse the tubing from the surface treatment, make sure you thoroughly flush it with oil to ensure no precipitates form.

b. It is completely fine to continue flowing the oil even after it fills the device. This will ensure that any remaining surface treatment gets pushed out and cannot form precipitates.

50. Aspirate the oil out of the device. If oil is still remaining, you can try to push air through the devices using a clean syringe.

51. Place the device in the 70° C oven for ~30 min to evaporate remaining oil.

52. Clean up the fume hood, disposing of the surface treatment and oil in the designated waste container and leaving the other materials used to dry out in the hood overnight.

53. Remove from oven and place scotch tape on top of the PDMS to protect the inlets and outlets from dust.

54. Label the device with date of surface treatment. Store at room temperature.

55. Turn off the oven.

----

56. Sterilize the devices before using to make sterile microbeads.

a. You can use UV ozone, but I have found that this leaves an odd residue in the channels that comes off into the beads, so I have avoided using this method.

b. Instead, I use EtOH and UV in the BSC.

i. Using a syringe, needle, and tubing, fill each device with 70% EtOH.

ii. Let the EtOH sit for ~5 min in the devices, then rinse with sterile PBS, then try to push the liquid out of the devices so the channels are empty.

iii. Leave devices in the BSC for one UV cycle.

iv. Store devices in a sterile container (e.g., autoclaved empty pipette tip box).

57. Lastly, you may want to check the flow profiles of each device. I have noticed that some do not pinch as effectively as others. I do this by running sterile PBS and oil through the devices and monitor the flow profile on the microscope.

Appendix J – Microfluidic Droplet Generation of Cell-laden PEGNB Microbeads

<u>Materials:</u>
- 13 mm syringe filters
- 15 mL and 50 mL conical tubes
- 2 mL microcentrifuge tubes
- 23G needle
- 23 mL 1% Pluronic F-68 in DMEM10 (1% F-68; or other culture media with FBS)
- 23 mL DMEM10 (or other culture media with FBS)
- 24 well plate
- 3 mL syringes
- 40 um cell strainer
- 50 mL bioreaction conical tube
- Autoclaved 6 mm x 3 mm stir bar
- Autoclaved blunt tip 21G needles (x2)
- Autoclaved micro spoon
- Cell culture reagents (PBS, trypsin, media, etc.)
- Crosslinking molecule (PEGDT, DTT, degradable peptide aliquots, etc.)
- Glass syringes (2.5 and 5 mL)
- Ice bucket with crushed ice
- LAP (or other photoinitiator)
- Microfluidic device
- PEGNB (stock, to be weighed out)
- Pipettes tips (P-20, P-200, P-1000)
- RGD aliquots (if applicable)
- Serological pipets
- SF media (for type of cells being used)
- Sterile 0.5% fluorosurfactant [RAN Biotechnologies] in NOVEC 7500
  - Can be filtered and used up to 5 times (4 additional filters after the initial)
- Sterile Pluronic F-68
- Tubing

<u>Equipment:</u>
- Automatic pipette aid
- BSC
- Hemocytometer
- Incubator
- Microscope
- Pipettes

- Small microscope
- Small stir plate
- Syringe pumps
- Tally counter
- UV lamp (365 nm)

Overview:
This procedure describes the process of fabricating cellular thiol-ene photopolymerized PEGNB microbeads via microfluidic droplet generation.

Notes:
- Record the amount of PEGNB/PEGDT/DTT/LAP, degradable peptide (if applicable), and RGD (if applicable) used in each experiment in the shared Google Drive sheets so we can keep track of how much of each molecule is remaining.
- WHENEVER REMOVING PEG OR PEPTIDES FROM STOCK CONTAINERS ALLOW THEM TO WARM TO ROOM TEMPERATURE FOR <u>AT LEAST</u> 30 MIN BEFORE OPENING TO PREVENT CONDENSATION INSIDE THE CONTAINERS (i.e., **<u>do not</u>** open containers until there is no longer moisture on the sides).

Tips:
These tips are found throughout the protocol as reminders, but please look these over before starting the process.
- Precise volumes are crucial for experiment accuracy and reproducibility.
  - Make sure you are always ejecting the full volume of the solutions by pushing to the second stop of the pipette.
- It is also critical to make sure your solutions (at all stages) are well-mixed.
  - With the exception of cells, vortex, vortex, vortex!
- When mixing a solution with the pipette, make sure you do so slowly to avoid any volume loss of solution stuck up in the tip.
  - Again, make sure to eject the full volume after mixing.
- Try to remove as much of the media above the cell pellet as possible as to not dilute out the precursor components with extraneous media.
  - If you leave a little more media in one group than another, it will be hard to determine if mechanical properties and thus cellular response were as a result of the intended gel properties or the resulting properties from diluted concentrations.
- I recommend starting with a lower density (10 M/mL) of cells in the precursor for the first time you make beads to figure out if your cells aggregate in the inlet tubing.
  - If your cells aggregate, keep batches small (I typically do 300 uL).
- You will likely need to optimize various parameters throughout this protocol (cell density, flow rates, etc.) for your specific cell type and application.
- I like to sterilize (soak in 70% ethanol) the syringes and tubing the day before so there is enough time for all of the ethanol to evaporate.
- Always use glass syringes as these will have less flow fluctuations.

Procedure:
27. UV the syringes and tubing in the BSC.

28. Retrieve DesiVac box containing necessary molecules from the -20C freezer and the glass jar containing necessary molecules from the fridge below the freezer.
29. Allow DesiVac and glass jar to come to room temperature (no condensation on the exterior of the containers) before opening.
    a. In the summer this usually takes 45-75 min
    b. In the winter this usually takes 30-45 min
30. While the containers are coming to room temperature, harvest cells as you normally would, collecting the desired cell number in 2 mL microcentrifuge tubes.
    a. For HUVEC-NHLF microbeads I typically use 20 M/mL cells in a 1:1 ratio.
31. Place cell pellet on ice while you prepare the microbead components.
32. Place DMEM10 and 1% F-68 in water bath.
33. Place media in bioreaction tube in incubator.
34. Complete the PEGNB **recipe sheet** (specific to type of PEG and the crosslinking molecule, example below) to calculate weight of molecules needed.
    a. The <mark>yellow</mark> cells are ones that require user input (and checking) but may not change from experiment to experiment. The <mark>red</mark> cells vary from experiment to experiment and need more careful checking. The gray ones are calculated from the yellow and red ones.
        i. Calculate enough PEGNB and LAP to account for some volume loss during sterile filtering (~50 uL extra).
        ii. Always make sure the purity for the molecules is accurate for each lot/batch of aliquots you will be working with or else all of the calculations will be off.
            1. This can be found within the Google Drive on various sheets (short term box with aliquots as well as Ellman's sheet).
            2. An Ellman's test will need to be done for each batch of aliquoted peptides to determine batch purity.
        iii. If you will be combining multiple peptide aliquots, make a note on how much volume each peptide would need individually.
            1. For example, if you need 7 mg of peptide and will combining a 4 mg and 3 mg aliquot – note how much volume each tube would need individually so you can resuspend them separately prior to combining them to make the peptides are not accidentally more concentrated due to losing any volume when combining tubes.
35. Retrieve peptide aliquots from box.
    a. RGD and degradable peptides (VPMS, usually) are stored as prepared aliquots of specific masses (1-10 mg, usually) so they do not need to be weighed out each time (or sterile filtered). It is important that you make sure there is enough of each peptide already aliquoted for your planned experiment.
        i. If peptides are running low (~10 mg or so remaining), then new ones will need to be prepared. This process takes 4 days so DO NOT wait until the last minute to prepare new peptide aliquots or experiments will be delayed.
36. Weigh out PEGNB and LAP into 2 mL microcentrifuge tubes.
    a. In the winter, it is critically important to use the static gun to reduce loss of molecules and accurately measure out masses.

      i.   Use the static gun on the microcentrifuge tube, spatula, and stock container.

37. Purge stocks with Argon in the chemical hood and parafilm them.
38. Return stocks to containers and place containers back in their respective storage locations.
    a.   Note: You will need to pump the lid of the DesiVac container to remove as much air as possible. Don't overdo it, just enough to make sure the top button is fully lowered into its slot in the lid.
39. Update recipe sheet with exact weighed out masses for any components that were not previously stored as lyophilized aliquots.
40. Print the recipe sheet.
    a.   I like to save them in a binder for future reference and record important details like cell passage, cell density, flow rates, etc. on the sheet to keep track of each batch of microbeads.
41. Resuspend the freshly weighed out molecules (PEGNB, LAP) in SF media according to the recipe sheet.
    a.   Resuspension is done using the vortex, NOT pipetting up and down. Some of the solutions can be viscous and you want to avoid volume loss.
    b.   Resuspend the PEGNB first as it takes longer to fully dissolve. You will need to vortex it and let it rest a few times. You can try to constantly vortex to dissolve, but I have found that it doesn't work much quicker then mixing and letting the solution rest. If you have a sonicator bath, this will speed up the process.
    c.   Next, resuspend the LAP and vortex.
    d.   Wait to resuspend the peptides as these will begin to degrade once resuspended so you want to do this just before you are going to use them.
42. While the PEGNB and LAP are dissolving, prepare the BSC with the microfluidic setup.
    a.   Turn off the UV.
    b.   Bring in 24 well plate, needles, stir bar.
    c.   Turn on the syringe pumps – set syringe diameter and flow rate (if needed).
    d.   Make sure stir plate is plugged in and on its side facing the syringe pump (do not turn on yet).
    e.   Turn on small microscope (set to video if needed by pressing the "M" button).
    f.   Infuse oil into 5 mL syringe through tubing, invert and remove any air bubbles from syringe and tubing, then place into syringe pump.
    g.   Connect oil and outlet tubing to the microfluidic device.
        i.   Flow a little oil through the device to prime the channels.
    h.   Using forceps, place the stir bar into the 2.5 mL syringe and attach plunger, decompressing until it is at the 1 mL demarcation.
    i.   Attached 23G needle to 2.5 mL syringe (KEEP CAPPED).
    j.   Place 2.5 mL syringe into pump, then remove and decompress the plunger the rest of the way.
        i.   This is so the pump is adjusted to where the plunger will be when you draw up our precursor solution to reduce the time the cells are sitting in the syringe.
    k.   Attach the inlet tubing to the 21G blunt needle and set aside.

43. Briefly centrifuge the PEGNB and LAP to collect at the bottom of the microcentrifuge tubes.
44. Sterile filter the PEGNB and LAP.
    a. Use 3 mL syringes and 13 mm filters.
    b. I like to also use a P-200 to pull any remaining solution out of the ejecting side of the filter just to make sure I have enough.
45. Resuspend the aliquoted peptides (VPMS, RGD) in SF media according to the recipe sheet.
    a. If you are combining aliquots for the needed mass, then resuspend one aliquot at a time in the volume needed for that individual mass prior to combining.
46. Vortex all solution so they are well mixed.
47. Aspirate media from cell pellet.
    a. Make sure you get as much media off of the cell pellet as possible as any extra media will dilute out your precursor and you won't have the concentrations you calculated.
48. Add gel components (push to the second stop on the pipette to eject full volume) to the bottom side of the tube containing the cell pellet in the following order (do not resuspend the cell pellet until all reagents are added):
    a. PEGNB – slowly draw up and expel as PEG is more viscous, be sure that all PEG is pipetted into the tube.
    b. LAP
    c. RGD – pipette up and down a few times to mix the peptide, expel any volume in the tip, then take needed volume.
    d. VPMS – pipette up and down a few times to mix the peptide, expel any volume in the tip, then take needed volume.
    e. SF media
    f. Pluronic F-68
    g. Mix solution with P-200, making sure to expel all solution from tip when done.
    Note: Some rounding may be needed depending on the precision of the pipettes. I follow standard rounding rules.
49. Quickly vortex the solution.
    a. You do not want to add too much stress on the cells, so I do 3 quick pulses on the vortex, just enough to mix each time.
    b. THIS IS IMPORTANT as well mixed solutions are necessary for consistent results between batches.
50. Take precursor solution into microfluidic hood.
51. Uncap needle on 2.5 mL syringe, draw up precursor solution, and pull up plunger until it is at 1he 1 mL demarcation.
52. Remove 23G needle and replace with blunt needle attached to tubing.
53. Place 2.5 mL syringe onto inverted syringe pump.
54. Turn on stir plate, set to 5, and make sure it is close enough for the stir bar to be stirring.
55. Using the syringe pump controls, quick infuse the precursor solution until it is almost to the tip of the inlet tubing.
56. Attach inlet tubing.
57. Start the flow of the oil then the precursor.

58. Place the microfluidic device on the small microscope and adjust the stage so you can see the junction.
59. Place the outlet tubing into a well of the 24 well plate with the lid used to hold the tubing in place.
60. Turn off BSC lights and monitor droplet production at the junction.
    a. If a clog in the device occurs, it is best to let the pumps continue to run until they clear the clog. This may result in a rush of precursor solution and loss of droplet production in response to increased pressure buildup. If this happens, stop the pump for the precursor solution then use the double arrow to infuse oil into the device and turn the oil pump back on. Once droplet production resumes, turn back on the syringe pump for the precursor solution.
61. Once all of the precursor solution has run through the device (you see air bubbles entering the junction), detached the outlet tubing but keep the end in the 24 well plate so all the solution pours into the well.
62. Crosslink the beads with UV for 1.5 min.
    a. While this is happening, I like to start cleaning up the hood.
        i. Flush device with a little oil if planning to reuse.
        ii. Detach precursor syringe.
        iii. Dispose of tubing in biohazardous waste (oil tubing can stay attached to needle tip and device).
        iv. Turn off syringe pumps, microscope, stir plate.
        v. Flip str plate right side up.
63. Remove 24 well plate from hood, spray, and turn on UV.
64. Move 24 well plate to other BSC, bring DMEM10, 1% F-68, and bioreaction tube from the incubator.
65. Place 40 um strainer on 50 mL conical tube.
66. Using P-1000, transfer beads in oil to a 2 mL microcentrifuge tube.
67. Gently tape the tube to encourage beads to float to top of oil.
68. Remove as much oil as you can from below bead layer, collecting it in a separate vial to be filtered and reused later.
    a. I like to first use a P-1000 to get the majority of the oil, tap again, then use a P-200 to get the rest.
69. Add 1 mL of 1% F-68 to the beads and pipet up and down to mix the beads until there are no clear aggregates in oil left.
70. Transfer to strainer.
71. Waterfall 5-7 mL of 1% F-68 over beads 1 mL at a time to rinse them.
    a. In between 1 mL rinses I like the tilt the strainer back and forth, kind of like panning for gold, to encourage the media to flow through.
    b. Then, use the 1 mL to rinse the beads from the side of the strainer.
    c. I also like to use a P-200 to pull the media through if it seems like it is not going through with gravity.
72. Using micro spoon, transfer beads to new 2 mL microcentrifuge tube containing 1% F-68.
    a. First, hold the strainer at an angle, tilted toward you.
    b. Waterfall 1% F-68 over beads to collect them at the bottom of the strainer.

c. Use the spoon to continue to collect the beads into one clump then scoop them into the microcentrifuge tube.

d. If beads still seem present, add another ~300 uL 1% F-68 onto the bead clump then aspirate into the P-1000 and transfer to microcentrifuge tube.

73. Repeat steps 43-46 two more times (for a total of three 1% F-68 rinses).

74. Now with DMEM10, repeat steps 43-46 three times.

Note: As the beads get cleaner, they also become more sticky, so make sure you are coating pipet tips with serum containing media first (I try to use the same pipet tip throughout if I can keep it sterile to prevent loss of bead sin each new tip).

75. After last rinse, use micro spoon to transfer beads to media in bioreaction tube.

76. Cap bioreaction tube and move to incubator.

77. Change media the next day and then every other day after that.

a. To change media, I will twirl the tube to dislodge beads from the side and allow them 10-20 min to settle at the bottom.

b. Slowly aspirate media from the top (try not to submerge tip) down to ~5 mL and add fresh media.

c. If using beads in gels, do the same steps as above, then use a P-1000 to manually remove as much media as you can above the loose bead pellet.

d. DO NOT centrifuge microbeads if they are soft enough that cells could be pulled from them.

Short Description of Experiment — **Date**

Component Properties

Abbreviation		Lot	MW	Aliquot Date	Gross Mass in Aliquot (mg)	Reactive Mass in Aliquot (mg)	Purity			
PEG-NB	4-arm PEG norbornene	FY05073	20021	Fresh	34.0	33.66	0.99	< Assumed from supplier information		
RGD	AC-CGRGDS-NH2	CP-L-501006-1	634.67	4/1/2022	1.0	0.6285	0.629	< Ellman's test from date (initials of person who did Ellman's)	Buffer: resuspended in PBS or SF-EGM2	
VPMS	Ac-GCRDVPMSMRGGDRCG-NH2	CP-H-500216-1	1738.01	3/17/2022	4.0	2.9524	0.738	< Ellman's test from date (initials of person who did Ellman's)		
LAP	Lithium phenyl-2,4,6-trimethylbenzoylphosphinate	MKCM1930	294.1	Fresh	1.0	0.983	0.983	< Assumed from supplier information		

Common Stock solutions:

	Active Concentration		Filter loss		Mass used			
	mg/ml	mM	ul	Gross (mg)	Active (mg)	ul		
PEG-NB	75.0	3.7	0	34.0	33.7	448.8	ADEQUATE	
RGD	6.3	10.0	0	1.000	0.629	99.0	ADEQUATE	
VPMS	41.7	24.0	0	4.000	2.952	70.8	ADEQUATE	
LAP	2.9	10.0	0	1.000	0.983	334.2	ADEQUATE	

Gel	Molar XS		Mass Composition (mg/ml)				Molar Composition (mM)				Total	Recipe Volumes Per Gel (ul, for measured concentrations)				
Description	mol SH/mol VS post RGD	Total Solids	PEG-NB	RGD	VPMS	LAP	PEG-NB	RGD	VPMS	LAP	Volume	PEG-NB Stock	RGD Stock	VPMS Stock	LAP Stock	Buffer
3% PEG, 90% CL	0.900	35.5	30.0	0.6	3.9	1.0	1.50	1.000	2.25	3.400	210	84.00	21.000	19.66	71.40	13.94
3% PEG, 80% CL	0.800	35.1	30.0	0.6	3.5	1.0	1.50	1.000	2.00	3.400	210	84.00	21.000	17.48	71.40	16.12
3% PEG, 70% CL	0.700	34.7	30.0	0.6	3.0	1.0	1.50	1.000	1.75	3.400	210	84.00	21.000	15.29	71.40	18.31
3% PEG, 60% CL	0.600	34.2	30.0	0.6	2.6	1.0	1.50	1.000	1.50	3.400	210	84.00	21.000	13.11	71.40	20.49
										Totals	840.00	336.00	84.00	65.54	285.60	68.86

15 μL/min

Cells + PEG precursor

150μm

Fluorinated oil +
Fluorosurfactant

30 μL/min

UV Crosslinking

3x on-strainer rinse 1%
Pluronic F68 in DMEM
+ 10%FBS

3x on-strainer rinse
DMEM + 10%FBS

Transfer microbeads
to vented conical with
warmed EGM2

Cell-encapsulating
Microbead

Remove oil from
beneath the beads

Oil sinks to bottom

Endothelial Cells

Fibroblasts

Appendix K – Subcutaneous Implant Model

Materials:
- 5-0 nylon sutures
- 70% ethanol
- Betadine
- Blank surgical records
- Carprofen
- Cotton applicators
- Enzol
- Ethanol wipes
- Eye lube
- Gauze pads
- Insulin syringes
- Isoflurane
- Isoflurane scavenging charcoal filter
- Lab tape
- Nair
- Oxygen
- Sterile fenestrated and non-fenestrated drapes
- Sterile PBS
- Windex + vinegar

Equipment:
- Anesthesia vaporizer (chamber and nose cone)
- Bead sterilizer
- BSC
- Electric razor
- Exhaust snorkel
- Heating pads (x3)
- LDPI
- Scale and weighing cup
- Sharpies (multiple colors)
- Stereomicroscope
- Surgical tools:

Overview:
This procedure describes the process of injecting hydrogel precursor solutions or implanted preform hydrogel pucks in the subcutaneous space on the backs of immunocompromised mice.

Notes:
- This procedure requires the help of an additional lab member as they must prepare the implants and inject them or insert them in order for the surgeon to remain sterile.
- We have tried to reinforce the sutures with surgical glue, but this seemed to irritate the skin around the sutures. We also tried surgical clips, but they were quite large compared to the incision and didn't work well.

Preparation:
1. Before the day of surgery, autoclave surgical tools.
   a. Non-delicate tools and the retractors can be autoclaved in standard autoclave pouches.
   b. The delicate tools should be autoclaved directly in the stainless-steel storage box wrapped in sterilization wrap.
   c. The retractor holders should be autoclaved wrapped in sterilization wrap
2. Spray down counter with 70% ethanol.
3. Spray and wipe induction chamber with Windex + vinegar solution (you must also do this between cages).
4. Weigh isoflurane scavenging charcoal filter (this can be done the day before). The maximum weight gain per filter is 50 g.
5. Make sure isoflurane vaporizer is filled with isoflurane.
6. Check oxygen level on tank.
7. Dilute carprofen 1:100 in PBS (this gives a 500 µg/ml solution). The injection can then be 10 µL per g (250 µL for a 25 g mouse) which is easier to measure and dose appropriately.
   a. Note: carprofen is good for 7 days once diluted (store at room temp) and the stock vial expires after 28 days once punctured (stored at room temperature after opening and at 4°C prior to opening).
8. Prepare 10-15 mL of sterile PBS in 50 mL conical tubes, one per animal.
9. Turn on bead sterilizer.
   a. Switch is in the back, once on you need to push the knob in twice to set the temperature.
10. Plug in heating pads.
    a. The temperature-controlled pad will be used during surgery, the two other pads will be used during LDPI and under the recovery cage.
11. Place sterile drape over temperature-controlled heating pad.
12. Turn on temperature-controlled heating pad set on low (one green light).
13. Place paper towel in the induction chamber.
14. Place wood under the door.
15. Turn on exhaust snorkel.
16. Make sure the flow of isoflurane and oxygen is directed into the induction chamber.
17. Turn on isoflurane vaporizer set to 1 O_2 and 5% iso just before getting the mouse.

Induction of Anesthesia:
1. Pick up mice by tail and place in induction chamber. Record time on the surgical records.

      a. While waiting for mouse to fall asleep, set up scale with weighing cup and turn on.
2. Once breaths have been reduced to 1 breath per second, pinch the mouse's toe to make sure they do not have a stimuli response, then transfer to scale.
3. Record weight on surgical records and move mouse back to induction chamber for about 30 s.
4. Change the flow of oxygen and isoflurane to be directed to the nose cone, then decrease the iso to 2%.
5. Move the mouse from the induction chamber to the nose cone with the mouse on its stomach.

Mouse Preparation:
1. Appy a generous amount of eye lube to each eye using a cotton applicator.
2. Sharpie the mouse's tail with the desire color and note on surgical records.
3. Administer Carprofen subcutaneously by scruffing the neck skin and injecting it beneath and record time on surgical records.
      a. If the mouse weighs 25 g it needs 250 cc of diluted Carprofen.
4. Shave the mouse from the mid back to the bilateral feet.
5. Apply Nair to the shaved area.
6. Wait ~ 30 s then use a dry gauze pad to remove the Nair.
7. Use a wet gauze pad to further remove the Nair from the skin.
8. Use a dry gauze pad to dry the skin and limb.
9. Transfer mouse to a new sterile drape.
10. Tape down limbs with lab tape.
11. Do three alternating rinses of betadine and ethanol.
      a. Apply betadine with cotton applicators, then rinse away with ethanol wipes.
12. Place sterile fenestrated drape over the mouse with the widest part of the opening over the left hindlimb.
13. Wipe down microscope knobs with ethanol.
14. Drop sterile surgical tools, cotton swabs, and sutured onto the sterile field. Open the toolbox containing additional sterile surgical tools. Uncap one of the conical tubes of sterile PBS and place near surgical field.
15. Don sterile gloves.

Surgery:
For injections:
1. Have the assisting person prepare the hydrogel precursor solutions one implant at a time and load into a 3 mL syringes equipped with a 23G needle.
2. Tent the skin using sterile forceps and inject the precursor solution beneath the skin.
3. Leave needle inside for 30 s to allow for initial polymerization.
4. Repeat for second implant.
5. Allow animal to remain anesthetized for 20 min before recovery to allow for hydrogel polymerization.
For implanting preformed pucks:
6. Create two ~1.5 cm incisions low down on opposite sides of the spine.
7. Separate the skin from the facia.

8. Use a sterile cotton applicator soaked with sterile PBS to investigate if the incisions are open and deep enough for hydrogel implants.
9. Have the assisting person load the hydrogel puck onto a sterile spatula and bring it over to the incision.
10. Using the cotton applicator, push the implant into the incision, making sure it does not fall out.
11. Using forceps, tent skin over wound and then close the wound using interrupted sutures with 5-0 nylon sutures (8 throws per knot). Tie sutures every ~2 mm (typically 4-5 total).

Recovery:
1. Remove mouse from nose cone and transfer to recovery cage.
2. Note the time the mouse was removed from anesthesia and placed in recovery cage on surgical records.
3. Allow mouse to recover in a separate cage with no bedding on a separate warming pad.
4. Note the time the animal fully recovered (awake and mobile) on the surgical records and check the box if recovery was normal.
5. Complete the remaining section of the surgery sheet with the time, date, and observations about the surgical site and mouse's behavior post-op and add initials.
6. Once mouse has fully recovered it can be placed into a new cage for subsequent housing.
   a. Remember to move food, water, and cage card to new cage.
   b. New cage should have soft bedding and some food pellets placed on the floor of the cage.
7. When mice are returned to vivarium post-surgery, place yellow surgical acetate with date of surgery and date of suture removal over cage card. Add a dissolvable biohazard sticker to the cage with the label "HDS" and add a non-dissolvable biohazardous sticker to the yellow acetate with the date and "human-derived substance."

Post-Surgery Monitoring and Imaging:
1. Carprofen will be administered 24 hours after surgery. This is best done with someone to help you hold the mice while you inject the carprofen.
2. Bring diluted carprofen and insulin syringes down to vivarium.
3. In the ABSL2 room BSC, open the cage and survey animals' incision.
4. Score each animal condition on the surgical records.
5. One animal at a time, have the assisting person scruff the mouse while you inject the correct dose of Carprofen beneath the skin on the neck. Return animal to cage and note time Carprofen was administer on surgical records.
6. Animals need to be monitored daily, noting animal health on the surgical records.

Appendix L – Hindlimb Ischemia Model
Adapted from Jeffrey Beamish

Materials:
- 5-0 silk and nylon sutures
- 70% ethanol
- Betadine
- Blank surgical records
- Carprofen
- Enzol
- Ethanol wipes
- Eye lube
- Fine tipped cotton applicators
- Gauze pads
- Insulin syringes
- Isoflurane
- Isoflurane scavenging charcoal filter
- Lab tape
- Nair
- Oxygen
- Regular cotton applicators
- Sterile fenestrated and non-fenestrated drapes
- Sterile PBS
- Windex + vinegar

Equipment:
- Anesthesia vaporizer (chamber and nose cone)
- Bead sterilizer
- BSC
- Electric razor
- Exhaust snorkel
- Heating pads (x3)
- LDPI
- Scale and weighing cup
- Sharpies (multiple colors)
- Stereomicroscope
- Surgical tools:

Overview:
This procedure describes the process of inducing hindlimb ischemia via ligation and excision of the femoral artery followed by implantation of tissue constructs in an intramuscular pocket adjacent to the ligation site.

Notes:
- This procedure requires the help of an additional lab member as they must prepare the implants and inject them into the muscle in order for the surgeon to remain sterile.
- It is very important to make sure you can clearly identify the vascular structures so you can accurately and reliably produce ischemia between mice.
- We have tried to reinforce the sutures with surgical glue, but this seemed to irritate the skin around the sutures. We also tried surgical clips, but they were quite large compared to the incision and didn't work well.
- Animals should receive carprofen daily until limb tissue appear normal.

Preparation:
18. Before the day of surgery, autoclave surgical tools.
    a. Non-delicate tools and the retractors can be autoclaved in standard autoclave pouches.
    b. The delicate tools should be autoclaved directly in the stainless-steel storage box wrapped in sterilization wrap.
    c. The retractor holders should be autoclaved wrapped in sterilization wrap
19. Spray down counter with 70% ethanol.
20. Spray and wipe induction chamber with Windex + vinegar solution (you must also do this between cages).
21. Weigh isoflurane scavenging charcoal filter (this can be done the day before). The maximum weight gain per filter is 50 g.
22. Make sure isoflurane vaporizer is filled with isoflurane.
23. Check oxygen level on tank.
24. Dilute carprofen 1:100 in PBS (this gives a 500 µg/ml solution). The injection can then be 10 µL per g (250 µL for a 25 g mouse) which is easier to measure and dose appropriately.
    a. Note: carprofen is good for 7 days once diluted (store at room temp) and the stock vial expires after 28 days once punctured (stored at room temperature after opening and at 4°C prior to opening).
25. Prepare 10-15 mL of sterile PBS in 50 mL conical tubes, one per animal.
26. Turn on bead sterilizer.
    a. Switch is in the back, once on you need to push the knob in twice to set the temperature.
27. Plug in heating pads.
    a. The temperature-controlled pad will be used during surgery, the two other pads will be used during LDPI and under the recovery cage.
28. Place sterile drape over temperature-controlled heating pad.
29. Turn on temperature-controlled heating pad set on low (one green light).
30. Place paper towel in the induction chamber.

31. Place wood under the door.
32. Turn on exhaust snorkel.
33. Make sure the flow of isoflurane and oxygen is directed into the induction chamber.
34. Turn on isoflurane vaporizer set to 1 O_2 and 5% iso just before getting the mouse.

Induction of Anesthesia:
6. Pick up mice by tail and place in induction chamber. Record time on the surgical records.
    a. While waiting for mouse to fall asleep, set up scale with weighing cup and turn on.
7. Once breaths have been reduced to 1 breath per second, pinch the mouse's toe to make sure they do not have a stimuli response, then transfer to scale.
8. Record weight on surgical records and move mouse back to induction chamber for about 30 s.
9. Change the flow of oxygen and isoflurane to be directed to the nose cone, then decrease the iso to 2%.
10. Move the mouse from the induction chamber to the nose cone with the mouse on its stomach.

Mouse Preparation:
16. Appy a generous amount of eye lube to each eye using a cotton applicator.
17. Sharpie the mouse's tail with the desire color and note on surgical records.
18. Administer Carprofen subcutaneously by scruffing the neck skin and injecting it beneath and record time on surgical records.
    a. If the mouse weighs 25 g it needs 250 cc of diluted Carprofen.
19. Flip mouse over onto back.
20. Shave the mouse from the mid abdomen to the bilateral feet.
21. Apply Nair to the shaved area.
22. Wait ~ 30 s then use a dry gauze pad to remove the Nair.
23. Use a wet gauze pad to further remove the Nair from the skin.
24. Use a dry gauze pad to dry the skin and limb.
25. Transfer mouse to a new sterile drape.
26. Tape down limbs with lab tape.
27. Do three alternating rinses of betadine and ethanol.
    a. Apply betadine with cotton applicators, then rinse away with ethanol wipes.
28. Place sterile fenestrated drape over the mouse with the widest part of the opening over the left hindlimb.
29. Wipe down microscope knobs with ethanol.
30. Drop sterile surgical tools, cotton swabs, and sutured onto the sterile field. Open the toolbox containing additional sterile surgical tools. Uncap one of the conical tubes of sterile PBS and place near surgical field.
31. Don sterile gloves.

Surgery:
12. Position stereomicroscope above mouse such that field of view contains lower ventral region.
    a. Use a 4x setting with a 0.5X extending objective.

13. Using curved micro surgical scissors, make an ~1.5 cm incision from popliteal fossa to the inguinal ligament. Use fine forceps to tent skin during incision.

14. Retract superiorly and medially at the top of the incision to expose the inguinal fat pad. Place two additional counter traction retractors at the bottom of the incision.

15. Carefully dissect through inguinal fat pad. There is usually a branch of the superficial epigastric artery that traverses this fat pad. Pinch with tweezers for 30 seconds then cut. After dissecting through the inguinal fat pad, replace the retractor in this area to better expose the target triangle formed from the inguinal ligament, the femoral nerve, and the femoral artery/vein pair.

16. Use fine forceps and a fine tipped cotton swab to remove overlying fascia and fat to expose and gently separate the femoral artery, vein, and nerve. NOTE there is often a large vein branch just below the top layer of this triangle. DO NOT disturb it.

17. Prepare 5-0 silk suture. Cut off the needle as it is not needed and use only a short length to avoid getting it tangled up. Place this on one of the retractor holders where it is easier to grab with the forceps. Grasp the suture so it can be fed to the other forceps.

18. Use curved fine forceps to loop under the artery only just below the superficial epigastric and proximal coddle bifurcation. Pass the suture from the other forceps to this pair then gently pull the suture under the artery. Tie off x 3 (I think this is best done under the scope with forceps (may need to zoom out).

19. Periodically, moisten the surgical site with a fine pointed cotton swab dipped in sterile PBS.

20. If bleeding occurs at any time, use a fine pointed cotton swab to absorb the blood at the surgical site and to apply gentle pressure.

21. Repeat step 6-7 for the distal ligation site, ligating just about the saphenous popliteal bifurcation.

RETRACTOR PLACEMENT

INGUINAL LIGAMENT

FEMORAL NERVE
(PROXIMAL TO JOINING THE FEMORAL NEUROVASCULAR BUNDLE)

FEMORAL ARTERY
FEMORAL VEIN

272
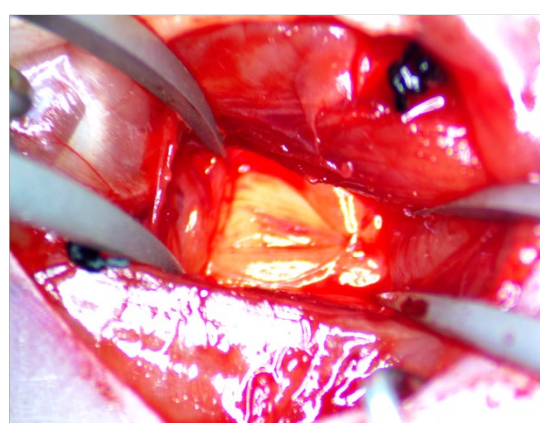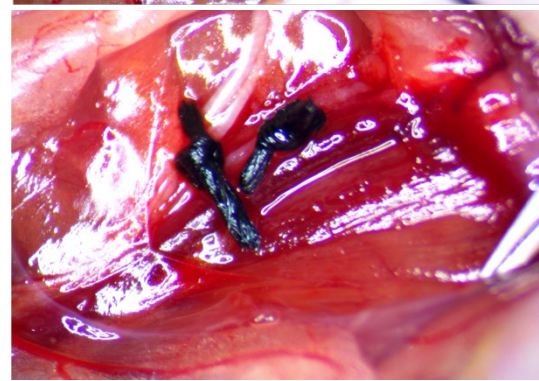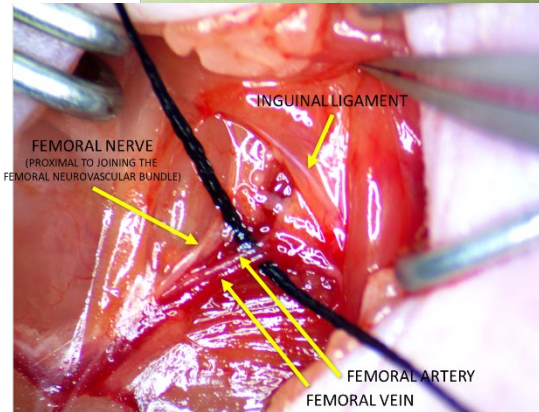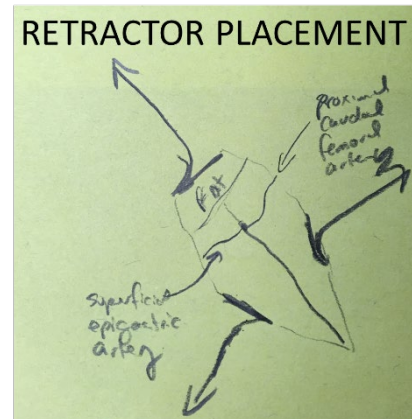
22. Around this time assistant should start preparing the implant solutions in the BSC
23. Transect the femoral artery in between the distal and proximal knots.
24. After ligation use the forceps to gently separate the tissue medial to the femoral artery, proximal to the distal ligation site and just distal to the superficial epigastric artery. Use the forceps to create a small cuboidal void.
25. Just before implantation, have the assistant firmly place a regular size cotton applicator in the void to absorb any liquid or blood.
26. Immediately after this, pipette implant solution using a P-1000 pipette tip into the void.
27. Hold this implant area open for 3 min to allow the gel to form (for 2.5 mg/ml fibrin gel)
28. Carefully remove the retractors. Using forceps, tent skin over wound and then close the wound using interrupted sutures with 5-0 nylon sutures (8 throws per knot). Tie sutures every ~2 mm (typically 7-8 total).
29. Move mouse to LDPI area and verify that the ligation was successful using LDPI.
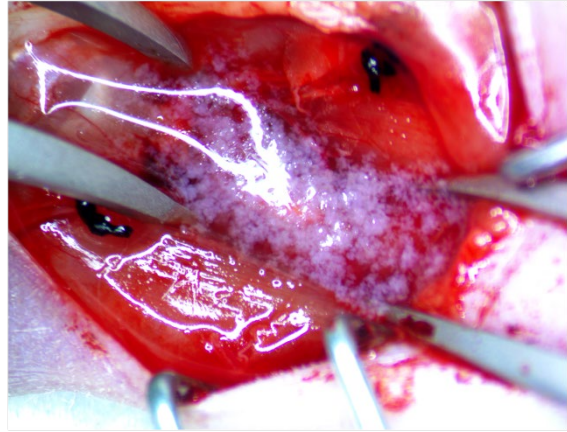
LDPI:
1. Move mouse to LDPI area (black mat) with nose cone.
2. Place mouse on stomach and pull legs out so the foot pads are flat.
3. Adjust black mat so that the mouse is under the laser.
4. In PIMSoft program
   a. Go to file --> new recording
   b. On left-hand side of the screen:
      i. Select Project --> New
      ii. Enter procedure and date e.g., "Ischemic Limb xx-xx-20xx"
      iii. Select Subject --> New
      iv. Enter date and mouse number/color e.g., " xx-xx-20xx BLUE 2"
5. Adjust the region of interest (ROI) box on the bottom right image to include the entirety of both foot pads.
   a. This can be done using the "Outline" option of the program and readjusting the animal; however, it seems to be more time efficient to adjust the ROI box manually.
6. Hit the record bottom in the bottom center of the screen.
7. Allow one full recording to occur, then let a second recording start.
8. Hit the stop button to the left of the record button.
9. When prompted, select "End after recording"
10. Let second recording finish.
    a. Note: Program saves recordings automatically as they occur.
11. Make a summary PPT for each day of surgery that describes the animals' experimental conditions and LDPI and tissue condition over time.

Post-LDPI:

8. Remove mouse from nose cone and transfer to recovery cage.
9. Note the time the mouse was removed from anesthesia and placed in recovery cage on surgical records.
10. Allow mouse to recover in a separate cage with no bedding on a separate warming pad.
11. Note the time the animal fully recovered (awake and mobile) on the surgical records and check the box if recovery was normal.
12. Complete the remaining section of the surgery sheet with the time, date, and observations about the surgical site and mouse's behavior post-op and add initials.
13. Once mouse has fully recovered it can be placed into a new cage for subsequent housing.
    a. Remember to move food, water, and cage card to new cage.
    b. New cage should have soft bedding and some food pellets placed on the floor of the cage.
14. When mice are returned to vivarium post-surgery, place yellow surgical acetate with date of surgery and date of suture removal over cage card. Add a dissolvable biohazard sticker to the cage with the label "HDS" and add a non-dissolvable biohazardous sticker to the yellow acetate with the date and "human-derived substance."

Post-Surgery Monitoring and Imaging:

7. Carprofen will be administered 24 hours after surgery, then every day as needed to manage pain. This is easier to do under anesthesia if you are doing it alone. Further, animals will have post-op LDPI measurements on days 1, 3, 5, 7, 10 and 14.
8. Bring cage and surgical records up to surgery room.
9. Anesthetize each mouse, administer Carprofen, and measure LDPI of footpads as described above. Also acquire a color image on the AmScope software for later description of hindlimb ischemia severity.
10. Allow animal to recovery in separate recovery cage before moving it back to its original cage.
11. Note that carprofen was administer and score animal condition on the surgical records for each animal before returning the cage and records back to the vivarium.
12. Animals need to be monitored daily, noting animal health on the surgical records.
.

Appendix M – Histological Processing of Implants

Materials:
- 1x PBS
- 10% ethanol
- 15% sucrose in PBS
- 2-methyl butane
- 30% sucrose in PBS
- 70% ethanol
- Blades
- Cassettes (pink or white depending on implant size)
- Dry ice pellets
- Foil
- Glass slides
- Ice cubes (square, use ice tray in freezer)
- MilliQ water
- O.C.T (one bottle with 30% sucrose)
- PAP pen
- Paper towels
- Peel away molds
- Pencil
- Razor
- Z-fix

Equipment:
- Cryostat (Baker)
- Hot blocks (Shikanov)
- Ice bucket
- Microtome (Shikanov)
- Slide box(es)
- Small glass Pyrex bowl
- Static gun
- Styrofoam container
- Tissue dehydrator (Coleman)
- Tissue embedding center (Coleman)
- Tongs

Overview:
This protocol describes the process embedding tissue samples in paraffin for paraffin sectioning and O.C.T. for cryosectioning followed by the appropriate sectioning techniques.

Notes:
- This is a multiday process so you will need to plan accordingly. It will take 2 days to prepare and embed samples before you can section.
- Prepare sucrose solutions ahead of time (~ 1 week) to ensure sucrose is properly dissolved.
  - 30% sucrose in PBS
    - Add 150 g sucrose to 500 mL bottle of PBS.
  - 15% sucrose in PBS
    - Take 100 mL of 30% sucrose and add to 100 mL of PBS.
  - 30% sucrose in O.C.T.
    - Add all O.C.T. to a beaker, add 35.4 g of sucrose, parafilm, and shake in the oven at 37 °C for 2-3 days.
    - Return O.C.T. to the original bottle then shake in oven at 37 °C for 1-2 days.
- Sign up to use the microtome (Shikanov lab) and cryostat (Baker lab) using the Google Calendars.
- Paraffin suctions as thin as 5 μm and cryosections as thin as 10 μm have been successfully produced.

Sample Dehydration (Paraffin):
1. Once sample is collected, transfer to formalin fixative (Z-Fix) overnight.
2. Transfer sample to 70% EtOH and keep in fridge for long term storage.
3. Label cassettes for your samples using pencil.
   a. Pink cassettes can be used for most samples, however, if the samples are larger than they may need to be placed in a white cassette.
   b. Do not try to squish your sample into a pink cassette, just use a white one if needed.
4. Trim samples, placing extra tissue back into the vial in case needed later, and place into designated cassettes.
   a. As you place samples into cassettes, place the cassettes in a beaker of 70% EtOH so they do not dry out while you trim the remaining samples.
5. Once all samples are ready to be dehydrated, prepare the Leica Tissue Processor.
   a. Wear a respirator when working with the tissue processor.
6. Check solution levels by raising the plastic cover/top portion of the machine by pressing the up arrow ↑ button.
7. Move grey arm (that will hold the basket) to position 4 by pressing the rotate button, which is a dashed circular arrow.
   a. Note: this can only be done when the top component is raised.
8. Put samples in the metal basket and place the basket on the grey arm connect.
9. Lower the top component and basket into the cylinder by pressing the down arrow ↓ button.
10. Press "Start"

276

11. Check that the setting is program #1, P1, and if not then adjust using the + or – buttons.
    a. Make sure this program is correct, i.e., it should start at position 4 and spend one hour in each position (4-12).
12. Adjust the time so the machine runs overnight (due to noise and chemical release).
    a. This is done by first hitting the right arrow → first to show start time
    b. Timing can be adjusted using the left and right arrows to select position and the + and – buttons to adjust the numbers.
    c. START # - ## : ##
        i. The first # is the day (so set it to 1), the second ## is the hour, the third ## is the minutes.
    d. The program should take 9 hours or so to finish.
13. Press "Start" again once desired time is set.
14. Turn on oscillations with the button that has three up and down arrows with a top and bottom boarder.
15. Close plastic cover.
16. Leave overnight and sign the log.

<u>Paraffin Embedding (Paraffin):</u>
1. Samples should now be in position 12 of the tissue processor, which is hot paraffin wax, and are ready to be transferred to the paraffin bath on the Tissue Embedding Station.
2. Before removing samples, prepare an ice bucket with foil atop the ice.
3. Turn on the cooling block of the embedding station by pressing the "Cool" button.
    a. The red indicator light should turn on.
4. Clean the station of excess wax.
5. Wearing a respirator, raise the top of the machine with the up arrow ↑ button and remove the basket containing your samples placing it on the counter next to the embedding station.
    a. Be careful as the basket may be hot if held for a long time.
6. Lower the top portion of the machine using the down arrow ↓ button, stop the oscillations with the button that has three up and down arrows with a top and bottom boarder, and close the plastic cover.
7. Transfer cassettes with samples in them to the paraffin bath on the right-hand side of the station.
8. Select a sample to embed and move it from the bath to the hot block under the paraffin dispenser.
    a. If the sample is in a pink cassette already, remove and discard the top of the cassette.
    b. If the sample is in a white cassette, label a pink cassette with the sample information and discard the top of the pink cassette.
    c. Note: you must use a pink cassette as the base of your paraffin embedded sample as this is the only size of cassette that will mount onto the microtome.
9. Select a metal tray from the bath on the left-hand side of the station that will fit your sample within the inset and move it onto the hot block.
10. Transfer the sample from the cassette to the metal tray.
11. Using forceps to push the lever located behind the hot block, dispense enough wax to cover the sample.
12. Adjust sample orientation to the center of the metal tray.

13. Place the labelled pink cassette on top of the sample, being careful not to move the sample.
    a. The handwritten label on the pink cassette should be facing upward.
14. Add more wax to fill the cassette, doing so by adding the wax adjacent to the sample and not directly on it to preserve its location.
    a. Wax should be added until there is a convex (bubble) surface of wax.
15. Move sample to cooling block.
    a. While one sample is cooling you can move on to embedding the next one.
16. Once the sample has mostly solidified, move sample from cooling block to foil on ice.
17. Once all samples are on ice, cover the bucket with a lid and leave samples to finish solidifying for at least four hours, but recommended for overnight.
18. Add paraffin wax chips to the paraffin bath or paraffin reservoir at the top of the station if either is low.
19. Turn off cooling block.
20. Clean any extra wax on the station using the scraper.

Sample Preparation for Microtome Sectioning (Paraffin):
1. Prepare a bucket with ice and a little bit of water.
2. Using a razor blade, remove the wax around the cassette and the metal tray until you can pop the cassette with wax and sample out of the tray.
3. Place the samples in the prepared ice bath and put the metal trays back into the bath on the left-hand side of the embedding station.
4. Trim extra wax to make a square around the edges of the implant, leaving a layer of wax on top the surface of the cassette to hold the wax/sample adhered to the cassette.
    a. Leave about 2-3 mm of wax from the edges of the sample.
    b. It is always better to leave more wax around the sample than less,
5. Sharpen edges of the wax square.
6. Cut two corners of the square to make it more of a house shape.
    a. This will help you remember orientation of your sample if you do not finish sectioning an entire lock and need to go back to it, or if orientation is important for later histological analysis.

Sectioning on Microtome (Paraffin):
Materials you will need to bring downstairs: Pencil, paper towels, slides, statistic gun, razor, spray bottle with 70% EtOH, 10% EtOH (if needed), MilliQ water (if needed), extra gloves, and prepared samples in ice bath.

1. Turn on hot block(s).
    a. They should be set anywhere from 39-45°C.
2. Plug in and turn on hot water bath.
    a. The temperature nob should be set to the marked lined.
    b. You can replace the glass lid to speed up heating but be careful as this may result in a bath that is too hot and may disintegrate your samples (test with an empty section of wax).
3. Refill 10% EtOH bath or hot water bath if needed.

4. If not done prior, label slides with pencil, then place labelled slides on the plastic slide holder block.
5. Retrieve a microtome blade from the drawer under the hot blocks and place into the slot on the microtome.
    a. To do this, unlock the blade holder by using the lever on the right side of the stage and slide the blade into the opening.
    b. Adjust the blade and stage so that the sample will be cut with the left most portion of the blade, so as the blade dulls or chips you can progressively slide the blade to the left for a fresh blade surface.
    c. Lock the blade into place using the same lever and cover using the gold safety cover so you do not cut yourself, the blade is VERY sharp.
6. Move the head of the microtome all the way backward by turning the big, lower knob on the left side clockwise.
7. Move the stage away from the head by unlocking it using the lever on the left of the stage and pulling the stage toward you.
8. Dry the sample with a paper towel and place it into the slot on the head.
    a. This is done by pulling the silver lever on the head toward you, inserting the sample (with labelled side down), and releasing the lever which will secure the sample in place.
9. Unlock the large lever on the right side of the microtome by flipping the small, black switch below it.
10. Move the stage close to the sample surface, roughly 0.5 mm or so, and lock into place.
11. Line up sample surface so that it is parallel with the blade at all points.
    a. To do this, unlock the head positioning using the lever on the right side of the head, then use the nobs on the left side of the head.
        i. Lock back into place once finished.
    b. You may need to remove the blade cover to make visualizing the blade easier so be careful.
    c. You will also likely need to move the sample up and down using the large lever on the right side to evaluate all points on the surface of the sample.
12. Set slice thickness to 5 (or whatever you need) using the small, textured knobs on either side of the top of the microtome.
13. Move the stage as close to the sample as possible without the surface touching the blade and lock into place.
14. Again, using the large lever on the right, start moving the sample toward the blade one rotation at a time.
    a. Note: it doesn't matter what direction you turn the large lever in to make the sample move forward.
15. Once the sample contacts the blade it will begin to slice off sections of the sample in a ribbon like fashion, so as this happens you want to hold the ribbon of sample sections up off the stage with a pair of forceps.
16. Once the ribbon is too long to hold or tears, place the ribbon on the counter to the left of the microtome.
    a. I personally like to generate multiple ribbons of sample sections before moving on to the next step of transferring them to slides.

b. If you are going to do this, make sure you place them on the counter in a manner that helps you remember what order you sectioned them in, and BE CAREFUL not to accidentally touch the ribbons with your elbow or anything else as you continue to section.
17. Find where the sample starts in your sections, i.e., when there is a different texture in the center of the section, and remove/discard the extra non-sample containing section
    a. Note: you should keep at least one portion of these non-sample containing sections to test that the temperature of the water bath is not too hot, which will lead to disintegration of the wax/sample.
18. Using a razor blade, cut ribbons into strips of 4-5 sections (or 2-3 if you are being conservative with your sample).
19. Using forceps, transfer one strip of sections to the 10% EtOH bath and **gently** try to flatten out sections and remove bubbles from under them.
    a. Note: you will not be able to get them perfectly flat, the hot bath will help with that, but you should try to remove as many bubbles as possible by lifting the sections with the forceps.
20. Using a labelled slide, transfer the section to the hot water bath.
    a. You want to do this sort of fast, so the slide doesn't heat up causing the sample to stick to it.
    b. You also want to do this at ~45° angle so the sections float off BUT be careful not to touch the bottom of the bath as this will release bubbles that will float under your sample.
21. Once the sample has flattened out, collect it on the slide by positioning the slide underneath the sample and pulling it up at an angle, again be careful not to touch the bottom of the bath.
    a. Don't do this too quickly as you may accidentally touch an unintended part of the slide to the sample and then it is game over as a heated sample will stick to whatever touches it and will tear if you try to remove it,
22. Place slide on hot block and leave overnight for sample to dry and fully adhere to slide.
23. Repeat with remaining sections.
24. If you return to sectioning that same attached block, remove wax fragments on the stage/blade with paintbrushes, cool the sample surface using ice again, and continue.
25. At the conclusion of sectioning, clean up all of the wax, cover the microtome, and turn off and unplug the water bath.

Tips and Tricks
- It will save you time to pre-label your slides before you start sectioning.
- Sectioning is one of those things where "getting in the rhythm" makes it go more smoothly, so I find it easier to plan to section for 3-4 hours at a time.
    o Note: sign up to use the microtome on the Google calendar. Sunny, in the Coleman Lab, is in charge of managing who has access.
- I**f your sample is being particularly difficult** (tearing, rolling, not cutting evenly, really bunching up, etc.) then you should stop sectioning, spray the sample surface with 70% EtOH, gently hold a piece of ice against the surface to cool the wax for 15-30 seconds, and then dry sample before continuing. You may need to do this more often for some samples than others. This should help, but if it doesn't you can also try using a new portion of the blade by shifting it to the left.

- You always want to place sample sections either on the counter or in solutions with the shiny side down. Placing the sample into the EtOH bath with the shiny side up will make it nearly impossible to flatten the sections of remove bubbles below the section.
- If the weather is particularly dry (like in winter months) you may want to use the static gun to try to reduce the likelihood of the sections sticking to the razor, counter, forceps, your hands, etc.
- You can use a blank slide to occasionally clean the hot water bath of left-over wax from samples.
- You should occasionally check to ensure the microtome is still sectioning at the desire section thickness, sometimes the constant movement of the microtome during section causes the knobs used to set the with the wiggle and adjust a little.

Sample Preparation (O.C.T.):
1. Once sample is collected, transfer to formalin fixative (Z-Fix) overnight.
2. Transfer samples to 15% sucrose in PBS for 6 hours.
3. Transfer samples to 30% sucrose in PBS overnight.

Flash Frozen O.C.T. Embedding:
1. Place a dry ice in a Styrofoam container
2. In the fume hood, prepare bath of dry ice pellets in 2-methyl butane in a small glass Pyrex bowl.
   a. Fill the bowl about halfway with 2-methyl butane and add 5-6 dry ice pellets.
   b. This will result in the bath bubbling as it cools.
3. Remove the sample from the sucrose solution and place at the bottom (implant side down) of a peel away mold.
4. Cover sample with O.C.T. plus 30% sucrose solution until there is about 0.5 inch above the sample.
   a. Try to avoid getting bubbles in the sample by adding the solution in one try without releasing pressure on the bottle and causing bubbles.
   b. You can adjust the sample orientation with tweezers if needed.
5. Using the tongs, lower the mold with the sample into the dry ice bath so the bath level is just above the O.C.T. level.
   a. Note: you are not submerging the sample.
6. Hold mold there until it has fully frozen.
7. Move mold to dry ice in Styrofoam and repeat with remaining samples.
8. Store samples in box in – 80 °C freezer until sectioning.

Sectioning on Cryostat (O.C.T.):
Materials you will need to bring downstairs: O.C.T. (normal, without sucrose), cryostat blades, razor, pencil, slides, extra gloves, slide holders (big ones), slide boxes, and samples on dry ice.

1. Turn on light in cryostat chamber.
2. Check cryostat settings (temp) are to your requirements and adjust if needed.
   a. Camber temp should be between -25 to -30 °C.
   b. Hold the key button to lock the settings after changing.
3. Bring sample blocks and slide holders into the chamber.

4. In chamber, remove sample from peel away mold (keep mold to put remainder of block when finished).
5. Mount sample on pedestal with O.C.T.
    a. In chamber, add small layer of O.C.T. to pedestal then when it is about halfway frozen add additional O.C.T. and place sample onto pedestal.
    b. Use the weight to make sure the sample stays flat and wait for the O.C.T. to be fully frozen.
6. Move the head all the way back using the button with two up arrows.
7. Attached the pedestal to head.
8. Set the desire section thickness with the dial in the back right corner of the chamber.
9. Attached the low profile blade to the stage using by adjust the lever on the right side of the stage.
10. You will want to use the "trim" ability to get the sample closer to the blade since the stage cannot be moved forward.
    a. Unlock the lever on the right side of the cryostat by moving the metal lever the cryostat.
        i. Note: the level is ONLY locked when the metal lever is lined up with the dot.
    b. Select the desired trim thickness and turn the lever to start sectioning.
        i. Note: trim only works if the lever is unlocked before setting it.
    c. You can decrease the trim thickness as the block gets closer to avoid accidentally cutting into your sample.
11. Once you have reached you sample, decrease the trim setting to 30 μm and trim the block until you start to see sample.
12. Turn trim setting off and lock the lever into place.
13. Prepare your slides so they are easy to grab.
    a. Note: slides should be stored outside of the chamber, so they are not cooled down. Sections stick to the slides because it is a cold material meting a warm material. I like to line up the slides on the glass chamber window so I can easily grab them.
14. Start sectioning your sample.
    a. As you cut the section from the block, use the small paint brush in your left hand to try to prevent the sample from rolling.
    b. Once the section is cut and on the stage, continue to use the brush to flatten out the sample.
15. Grab the slide and tap it to your sample to adhere it to the slide.
    a. You will cut and collect on section at a time. Slides can hold 3-4 sections.
16. Pull the slide out of the chamber then repeat for remaining sections.
17. Store the complete slides in the chamber in slide holders until the end of your sectioning session.
18. Remove the block from the pedestal using a razor blade and put back in peel away mold.
    a. I like to add tape to the top of the mold to keep the sample inside.
19. At the end of the session, transfer slides to slide box, transfer blocks to dry ice in Styrofoam container, clean up the residual O.C.T. in the chamber, clean off the O.C.T. from the pedestal using pure EtOH, turn off the light in the chamber, and close the chamber.
20. Store slide boxes in – 80 °C freezer until staining.

Tips and Tricks
- It will save you time to pre-label your slides before you start sectioning.
- If the chamber is too cold, your samples may not section properly (more like shaved ice). In this case, decrease the chamber temperature and let the block equilibrate for a while (maybe 20 mins).
- Try to orient the blocks so that the samples are on the top of the block as this region is likely to roll up during sectioning.
- I have never really gotten the glass slab attachment on the stage to effectively work for my sections. This attachment is intended to prevent section rolling if it is placed flat on the stage during sectioning. If you want to give it a try, I recommend doing so on empty sections before you get to your sample.

- Cryosectioning requires a lot of patience. Ideally you will slowly cut the block and use the small paint brush to prevent the sample from rolling while cutting.

Appendix N – Immunohistochemistry, Immunofluorescent Staining, and Imaging of Paraffin and O.C.T. Tissue Sections
Adapted from Ana Rioja

Materials:
- 0.1% Tween-20 in 1x TBS (TBS-T)
- 0.5% Triton-X in 1x TBS
- 1x TBS
- Clear nail polish
- Coverslips
- DAPI
- DI water
- Dual Endogenous Enzyme Block (Dako #S2003 or Agilent # S200380-2) – stored in fridge
- EnVision+ System- HRP Labelled Polymer Anti-mouse (Dako #K4001or Agilent #K400111-2)
- Eosin Y (Sigma HT110132)
- Ethanol
- Kimwipes
- Liquid DAB+Substrate Chromagen System (Dako #K3467 or Agilent # K346811-2) – stored in fridge
- Mayer's Hematoxylin (Electron Microscopy Sciences 26252)
- Monoclonal Mouse Anti-Human CD31, Endothelial Cell Clone (Dako #JC70A or Agilent # M082301-2) – stored in fridge
- PAP pen
- Paper towels
- Permount
- Phalloidin (Alexa Fluor 488 Phalloidin; Fisher/Invitrogen #A12379)
- SlowFade Gold Antifade Mountant (Fisher/Invitrogen # S36937)
- Smooth muscle actin monoclonal antibody (1A4 (asm-1)) [Invitrogen: Thermo Fisher Scientific]
- Target Retrieval Solution 10x Concentrate (Dako #S1699 or Agilent #S169984-2) – stored in fridge
- UEA (Vector # RL-1062-2)
- Xylene

Equipment:
- Fume Hood
- Food steamer
- Olympus IX81 with Hamamatsu Camera

- Slide box
- Slide staining rack
- Slide staining jars

Overview:
This protocol describes the process of staining paraffin sections with H&E, hCD31, and α-SMA as well as cryosections with UEA/DAPI/Phalloidin.

Notes:
- Solutions should be prepared with absolute ethanol and can be used for 4-5 cassettes.
- Label slides with type of stain (in pencil) and place slides in the slide rack.
- I recommend laying out the coverslips before starting the mounting process so they are easy to grab in case your gloves get sticky.
- At the conclusion of staining, empty staining jars back into their respective storage containers or waste container and leave open to dry in fume hood overnight. Be sure to let all materials with xylenes on them dry overnight as well. Leave second pair of gloves that touched xylenes in fume hood overnight.
- Before hCD31/α-SMA staining:
  - Prepare TBS-T solution(s) if needed.
    - Make 10x TBS – 44 g sodium chloride, 15.75 g tris base, 500 mL DI water (first add 400 mL of DI water, adjust pH to 7.4, then bring up to 500 mL total with more DI water)
    - Make 1x TBS-T – 100 mL 10x TBS, 1mL Tween-20, ~900 mL DI water
  - Dilute 10x Target Retrieval Solution (1 part solution to 9 parts water) in DI water.
    - Note: this solution can be re-used up to three times if stored in the fridge.

Hematoxylin and eosin – Paraffin sections (1 h 15 min per cassette):
15. Place slides in a **xylene** bath and incubate for 5 min. Transfer to a new xylene bath and leave for 5 min.
16. Tap off excess liquid and place slides in **100% ethanol** for 3 min. Transfer to a new 100% ethanol bath and leave for 3 min.
17. Tap off excess liquid and place slides in **95% ethanol** for 3 min. Transfer to a new bath and leave for 3 min.
18. Tap off excess liquid and place slides in **distilled water** for 3 min.
19. Place slides in **hematoxylin** and incubate for 15 min.
    a. If you want to do more than one cassette, wait to start the next cassette until the first one is in the hematoxylin.
20. Wash gently with **tap water** for 15 min (water container, water should be clear)
21. Wash with **95% ethanol** for 30 s.
22. Wash with **eosin** for 1 min.
23. Wash with **95% ethanol** for 1 min.
24. Two washes with **100% ethanol** (1 min per wash)
25. Two washes with **xylenes** (3 min per wash)
26. Mount slides with mounting medium and coverslips. Let them dry overnight.
    a. Double glove when mounting slides so second pair of gloves can air out in the hood overnight.

    b. Use a cotton applicator to drip 2-3 drops of Permount onto the coverslip before laying the coverslip onto the slide.

    c. If bubbles are present on top of the tissues, you can gently press down on coverslip to move the bubbles to the edge of the slide but be careful not to press too hard and smudge the tissue.

    d. Using a Kimwipe to carefully remove xylenes/paramount from the <u>bottom</u> of the slide will prevent the slide from sticking to the surface you place them on to dry.

    e. Note: If excess Permount has accumulated on the bottom of the slide or on top of the coverslip it can make imaging the samples difficult (blurry). Once the cover slipped slides have completely dried, you can dip a cotton applicator in xylenes and rub off the excess Permount. Then, dry the slide with a Kimwipe. Do this ASAP after mounting coverslips so the slides can air put overnight before imaging.

Human CD31 (hCD31) – Paraffin sections (Day 1: 2 h 30 min; Day 2: 1 h 30 min per cassette):

1. Place tap water in the food steamer and turn on while slides are being deparaffinized and rehydrated (steps below).
2. Add enough 1x Target Retrieval Solution to cover the slide rack with slides (~200 mL) to a 250 mL beaker and leave on bench to come to room temp.
3. Place slides in a **xylene** jar for 5 min. Transfer to a **new xylene** jar for 5 min.
4. Tap off excess liquid and place slides in a **100% ethanol** jar for 3 min. Transfer to a **new 100% ethanol** jar for 3 min.
5. Tap off excess liquid and place slides in a **95% ethanol** jar for 3 min. Transfer to a **new 95% ethanol** jar for 3 min.
6. Tap off excess liquid and place slides in a **DI water** jar for 30 s.
7. Place slides in the previously prepared beaker containing the **1x Target Retrieval Solution**. Use hot gloves to place the beaker in the food steamer.
8. Leave the beaker in the steamer for 35 min (it takes about 13 min for the temperature in the beaker to turn 90°C).
9. While your slides are in the steamer, prepare the slide chamber for the staining protocol.
    a. Cover the bottom of the slide chamber with tissues.
    b. Completely wet tissues with water, making sure some of the water remains in the chamber.
    c. Close the chamber and leave it on the counter until needed.
10. Using hot gloves, take out the beaker and let it cool at room temp for 30 min.
11. Wash slides with **TBS-T** (2 min, 3x). Change baths for every TBS-T wash.
12. Very carefully remove moisture from slides with Kimwipe.
    a. Let solution drip down to bottom of slides onto a paper towel, then use a Kimwipe to remove moisture still remaining on the slide around the tissue samples.
    b. BE VERY CAREFUL not to touch the tissue as this alter the structure or remove the tissue completely.
13. Use PAP pen to mark around the tissue. Make sure not to touch the tissue with the pen.
14. Using dropper, add enough **Dual Endogenous Enzyme Block** (one drop per tissue section) to cover the tissues completely and incubate for 5 min at room temp in slide chamber.

15. Wash slides with **TBS-T** (2 min, 3x). Change baths for every TBS-T wash.
16. Remove moisture around tissues carefully by touching a Kimwipe to the most inner edge of the PAP pen ring.
17. Using a P-200 pipette, add enough **primary antibody** to cover tissue and incubate in slide chamber <u>overnight at 4°C</u>.
    a. The **monoclonal mouse anti-human CD31** primary antibody should be used at a 1:50 dilution in TBS-T.
    b. Add 20 µL of primary antibody to 980 µL of TBS-T.

----

18. The next day, remove antibody carefully one slide at a time (1st dip each slide in TBS-T and gently swirl to remove primary antibody). Then rinse gently with **TBS-T** (2 min, 3x). Change baths for every TBS-T wash.
19. Tap off excess buffer onto paper towel, remove moisture from slides and tissues carefully, and place slides in slide chamber.
20. Using dropper, add enough **HRP-labelled polymer** to cover tissues and incubate for 30 min in slide chamber at room temp.
    a. When there is 5 min remaining for the HRP-labelled polymer, prepare the **Liquid DAB+ substrate-chromogen solution** (see below)
       To make 1 mL of the solution (for up to 10 tissue sections)
    b. Transfer 1 mL of buffer substrate into provided calibrated test tube (~40 µL/drop) [approximately ~33-35 drops]
    c. For each 1 mL of buffer, add one drop (~20 µL) of liquid DAB+ Chromogen
    d. Mix immediately via vortex and apply to tissue section with P-200 pipette.
    e. Note - Prepared solution is stable for 5 days when stored at 4 degrees C. Make sure solution is well mixed prior to adding to tissues.
21. Remove HRP-labelled polymer carefully (1st dip each slide in TBS-T and gently swirl to remove secondary antibody). Then rinse gently with **TBS-T** (2 min, 3x). Change baths for every TBS-T wash.
22. Remove moisture from slides and tissues carefully with a Kimwipe.
23. Place slides in slide chamber and add prepared **Liquid DAB+ substrate-chromogen solution** to slides using P-200 pipetter. Incubate for 5 min in slide chamber at room temp.
24. Rinse gently in **DI water**. Collect waste in hazardous waste container.
25. Immerse slides in **hematoxylin** and incubate for 15 min.
26. Wash gently with **tap water** for 15 min (first dip slides in jar with tap water and gently swirl, dump tap water and repeat until water is clear, then let slides sit for 15 min)
27. Two washes with **95% ethanol** (1 min per wash)
28. Two washes with **100% ethanol** (1 min per wash)
29. Two washes with **xylene** (3 min per wash)
30. Mount coverslips to slide with Permount. Let them dry overnight.
    a. Double glove when mounting slides so second pair of gloves can air out in the hood overnight.
    b. Use a cotton applicator to drip 2-3 drops of Permount onto the coverslip before laying the coverslip onto the slide.
    c. Press down on coverslip to remove bubbles if any are located on top of tissues.
    d. Using a Kimwipe to carefully remove xylenes/paramount from the <u>bottom</u> of the slide will prevent the slide from sticking to the surface you place them on to dry.

e. Note: If excess Permount has accumulated on the bottom of the slide or on top of the coverslip it can make imaging the samples difficult (blurry). Once the cover slipped slides have completely dried, you can dip a cotton applicator in xylenes and rub off the excess Permount. Then, dry the slide with a Kimwipe. Do this ASAP after mounting coverslips so the slides can air put overnight before imaging.

Alpha smooth muscle actin (α-SMA) – Paraffin sections (4 h 30 min per cassette):
1. This procedure is identical to the hCD31 procedure above with the following adjustments:
2. Incubate tissue with the **primary antibody** in slide chamber for <u>2 h at RT</u>.
    a. The α-SMA primary antibody should be used at a 1:800 dilution in TBS-T.
    b. Add 1.25 µL of primary antibody to 998.75 µL of TBS-T.

Imaging IHC sections:
1. Clean slide with ethanol to remove any residue.
2. Place slide on microscope using the slide holder stage attachment.
3. Turn on microscope and all control boxes (besides the fluorescent bulb).
4. Change the light filter ring on the microscope to position 3 for BF (brightfield).
5. Open the Metamorph software.
6. Set light source to brightfield through binoculars.
7. On the microscope itself, switch the light source from binoculars to camera.
8. Open the Cellsense software.
9. Turn on live, focus, and adjust brightness as needed.
    a. Increased magnification needs increased brightness.
    b. Note: Imaging through the coverslip will be clearer as it is thinner than the slide glass. If imaging through the coverslip, 20x should be set to 0.17 on the objective collar.
10. Adjust white balance using the dropper icon, do this for each new section.
11. You can adjust the magnification on Metamorph, but I prefer to do it manually using the control board.
    a. If you change the magnification, you will want to click the correct magnification on the Cellsens side panel so the scale bar is accurate.
    b. You can burn the scale bar onto the image so it is permanently there, but this must be done for each individual image.
        i. Image → Burn info
12. Click Snap to acquire an image.
    a. Each image must be save individually (after you burn in scale bar, if desired).

UEA/DAPI/Phalloidin – Cryosections:
1. Permeabilize slides in 0.5% Triton-X in 1x TBS twice for 10 min.
    a. Prepare staining solution during second rinse, you need ~ 300 µL per slide.
    b. UEA 1:200
    c. Phalloidin 1:200
    d. DAPI 1:100
2. Rinse slides with 1x TBS three times for 1 min.

3. Very carefully remove moisture from slides with Kimwipe.
    a. Let solution drip down to bottom of slides onto a paper towel, then use a Kimwipe to remove moisture still remaining on the slide around the tissue samples.
    b. BE VERY CAREFUL not to touch the tissue as this alter the structure or remove the tissue completely.
4. Use PAP pen to mark around the tissue. Make sure not to touch the tissue with the pen.
5. Place slides in slide chamber with wet paper towels on the bottom.
6. Using a P-200 pipette, add enough stain solution to cover tissue and incubate in slide chamber <u>overnight at 4°C</u>.

----

7. Rinse slides with 1x TBS three times for 1 min, then <u>overnight at 4°C</u>.

----

8. Tap off excess rinse.
9. Using a P-200 pipette, add a few drops of SlowFade to the tissues.
10. Add coverslip to the slide and use clear nail polish to seal the edges.
11. Let dry for 30 min before imaging.
12. Image using Metamorph, similar to bulk hydrogels.
    a. Clean slide with ethanol to remove any residue.
    b. Place slide on microscope (coverslip side down) using the slide holder stage attachment.
    c. Acquire single plane 4x and 10x images, acquire 20x images using small stacks (5-10 µm, 1 µm/slice).
13. Store slides in fridge after imaging.

Appendix O – Fluorescent and Immunofluorescent Staining and Imaging
Adapted from Jonathan Bezenah and Emily Margolis

Materials:
- 0.1% Tween-20 in 1x TBS (TBS-T)
- 0.5% Triton-X in 1x TBS
- 1x TBS
- Antibody dilution buffer (Abdil): 2% (2g/100 mL) of bovine serum albumin (BSA) in TBS-Tween solution – make fresh each day
- Appropriate primary and secondary antibodies
- DAPI
- Phalloidin (Alexa Fluor 488 Phalloidin; Fisher/Invitrogen #A12379)
- Razor
- Scalpel
- UEA (Vector # RL-1062-2)
- Z-fix

Equipment:
- Fume hood
- Olympus IX81 with Hamamatsu Camera

Overview:
This protocol is for fixing hydrogels and staining with standard non-immunofluorescent stains. UEA is commonly used for identifying endothelial cells, DAPI stains all cell nuclei, and phalloidin stains filamentous actin in all cell bodies. Phalloidin is useful for identifying cell bodies and tends to stain stromal cells more strongly than endothelial cells. Additional steps are required for antibody staining and are detailed in the immunofluorescent staining protocol (further below). Red phalloidin and green UEA are also available but not typically used.

Notes:
- Before starting procedure, check the online data sheets for your primary and secondary antibodies by checking their catalog numbers. Take note of their species specific reactivity, host/reactivity, suggested secondary antibody, and recommended dilution.
- If samples are recommended to be stored at -20 °C, it is best to aliquot into microcentrifuge tubes to avoid multiple freeze thaws. I tended to aliquot 5-10 µL of antibody stock per tube.
- Some procedures recommend performing all steps with TBS-TritonX100, however, TritonX is a very strong detergent and I have found that prolonged periods of time in TBS-TritonX100 solutions caused gel degradation, hence the use of TBS-Tween20 for most steps: Tween20 is a milder detergent.

- Although most immuno-fluorescent staining procedures for cells in 2D culture only require ~1 hour per staining/washing steps, the large size of antibodies restricts diffusion into hydrogels, as such, all steps are performed overnight to allow complete diffusion in/out of hydrogels for optimal staining.
- Unlike DAPI, UEA, or Phalloidin staining, which are good for many weeks, antibody staining tends to fade in under a week, make sure your schedule is permissive for imaging right after staining for best results.

Fixation Protocol:
1. Aspirate off culture media in cell culture hood.
2. Add 1 mL Z-fix to each well in fume hood
   a. Make sure PEG hydrogels are fully submerged.
3. Let fix for 10 min at room temp in hood.
4. Remove z-fix with pipette and dispose of in appropriate waste container.
5. Add at least 1 mL TBS to each well, more is better for more thorough washing.
6. Allow to rinse for 3-5 min at room temp.
7. Remove TBS with serological pipet and dispose of in z-fix waste container for the first wash.
8. Repeat washes for a total of 3 washes, the 2nd and 3rd wash can be aspirated with the vacuum pump in the common lab space if you are comfortable (i.e., not worried about sucking up your gels).
9. Gels are ready for storage, staining, or immunofluorescent staining.
10. *If storing, fill well with TBS wrap with parafilm around the edges, and store in the 4 □C fridge. Samples can be stored up to ~ 1 month before staining without noticeable detriment.

Standard staining procedure for UEA, DAPI, and phalloidin:
1. Fibrin hydrogels will be stained directly in the wells and PEG hydrogels should be cut in half using a razor blade and scalpel then transferred to 48-well plates for staining.
   a. Fill a petri dish with enough PBS that it barely covers the bottom of the dish.
   b. Put a single PEG hydrogel into the dish with one its flat sides down.
   c. Push down with a razor blade precisely bisecting the gel and then use a scalpel while holding the razorblade down to finish bisecting the gel cleanly.
   d. PEG hydrogels can be further cut into quarters if needed for multiple different stains on the same gel, but halves are easier to orient for imaging.
2. Prepare solution with desired stains.
3. UEA and phalloidin are best at 1:200 dilutions and DAPI at 1:100 dilution.
   a. 24-well plate fibrin hydrogels require 500 µl of staining solution.
   b. A single half of PEG hydrogel can be stained in a 48-well plate in 300 µl of solution, so each gel would need 600 µl of staining solution.
4. Make sure all remaining TBS is removed from hydrogel wells.
5. Add staining solution to hydrogels.
   a. Make sure PEG hydrogels are fully submerged.
6. Cover well plates in foil to protect from light.
   a. Samples should always be protected from light from here on to reduce photo-bleaching.

b. For best signal to noise, I typically stain overnight in the 4 °C fridge, but 4-6 h is sufficient.
    7. After staining, wash 3x with fresh TBS.
        a. For best signal to noise, I usually allow another rinse overnight, and then another wash the next day before imaging.
    8. Samples are ready for imaging.
    9. Samples should be imaged within 2 weeks for best results.

<u>Immunofluorescent staining of hydrogels</u>
    1. Make enough Abdil solution as needed for the day.
        a. It is best to make Abdil solution fresh as needed (1 mL per well for blocking in 48-well plates).
    2. Permeabilize your samples by incubating gel in TBS-TritonX100 solution at room temp for 1 hour.
        a. Use 1 mL for 24-well plate, 0.5 mL for 48 well plate. Make sure free-floating PEG hydrogels are fully submerged.
    3. Rinse samples 4 times with TBS-Tween20 solution, waiting 3-5 min between rinses.
    4. Block samples overnight in Abdil solution
----
    5. Prepare primary antibody staining solution in Abdil using the recommended dilution.
        a. For PEG gels, to save on expensive antibodies, I have combined both halves into one well of a 48 well-plate and stain with 300-400 µL solution. You may have to use 400 µL if the gels are not cut evenly and one side is larger than the other.
    6. Aspirate off Abdil solution.
        a. For PEG hydrogels I tend to hold gels out of the well with a micro lab spoon while aspirating.
    7. Stain with primary antibody overnight in Abdil solution.
----
    8. Rinse 3x with TBS-T, 5 min each, then rinse overnight.
----
    9. The following day rinse 1x with TBS-T for 5 min.
    10. Prepare secondary antibody staining solution (including counterstains) in Abdil using the recommended dilution.
        a. Make sure to choose your secondary antibody to match the host/isotype of the primary, and that the fluorophore is the appropriate wavelength, so it doesn't overlap with any intended counter stains (e.g., DAPI, UEA, Phalloidin).
        b. For PEG gels, to save on expensive antibodies, I combine both halves into one well of a 48 well-plate and stain with 300-400 µL solution.
    11. Stain with appropriate secondary antibody at recommended dilution and other counter stains (UEA, DAPI, phalloidin, etc.) overnight.
    12. Protect from light as much as possible moving forward.
----
    13. Aspirate off secondary antibody solution.
    14. Rinse 4x with TBS-T.
    15. Rinse overnight with TBS-T before imaging.
    16. Samples can be stored in either TBS-T or TBS at 4 °C.

17. Image samples as soon as possible.
18. If you are making qualitative comparisons between samples, make sure to image them on the same day with the same imaging settings to avoid signal deterioration.

Imaging on the Olympus IX81 with Hamamatsu Camera:
1. Remove microscope cover.
2. Turn on the microscope.
    a. Turn on the UCB (main microscope).
    b. Turn on the Hamamatsu camera.
    c. Turn on the Prior automated stage.
    d. Turn on the mercury bulb if doing fluorescent staining.
        i. Mark the date, bulb h, time, and initials on the sheet.
3. Open Metamorph Premiere software.
4. Wipe down top and bottom of the well plate with 70% ethanol to make sure the surfaces are clean.
5. If imaging PEG gels, make sure the gels are positioned flat, cut side down with only just enough TBS to cover the top of the sample so it does not float.
6. Place samples on stage.
7. The microscope has three view option: binoculars, camera, and DSU.
    a. Binoculars: view through the microscope eye pieces. If you click "show live" the window that pops up will show static in the color channel you are on and only have a clear view through the binoculars.
    b. Camera: view through the Hamamatsu camera.
    c. DSU: uses the DSU to enter confocal mode and view a single z plane.
8. The microscope has four fluorescent filter cubes and brightfield/phase options. *Red, green, blue, and brightfield are in the left-hand panel, far red must be accessed through the camera/filter drop down menu.
    a. Red: mCherry filter (binoculars, camera, and DSU)
    b. Green: GFP filter (binoculars, camera, and DSU)
    c. Blue: DAPI filter (binoculars, camera, and DSU)
    d. Far red: Cy5 filter (camera and DSU only)
    e. Gray: brightfield and phase.
        i. Brightfield and phase are both within the gray color selection that uses the standard lamp not the mercury lamp
        ii. To change between brightfield and phase, the filter ring must be switched.
9. The microscope has five magnifications: 4x, 10x, 20x, 40x, and 60x.
    a. 20x and above magnification objectives have collars that should be adjusted to match the thickness of the materials (well plate, glass slide, coverslip) that you are imaging through.
    b. 4x images should be acquired with the filter wheel set to position 2 or PhL
    c. 10x images and above should be acquired with the filter wheel set to position 1 or Ph1.
    d. Bright field images, regardless of magnification, should be acquired with the filter wheel set to position 3 or BF.
10. The microscope has four different imaging modes:
    a. Brightfield (BF) imaging using the standard halogen lamp on the microscope illuminating the same from above and imaging from below the sample. Features

within the sample will diffract light causing optical disparity and contrast within the image.

  b. Phase contrast imaging also uses the halogen lamp illuminating the same from above and imaging from below the sample. However, phase contrast imaging provides better contrast to view the sample through the use of annular phase rings. On our microscope, the phase rings must be changed for 4x and 10x imaging or BF imaging.

  c. Widefield (WF) imaging uses the epifluorescent mode of the microscope. In this mode, the sample is illuminated with light exposing the entire field of view with unfocused light. The sample is illuminated and imaged from below the sample. WF imaging is good for a single plane image, but not for z-stacks.

  d. Confocal microscopy increases the optical resolution of images by focusing light through a pinhole to eliminate out of focus light and thus yields a better signal-to-noise ratio than WF imaging. Laser scanning confocal microscopes use a single pinhole, while disc spinning units (DSU) employ a disc that is covered with pinholes. The pinholes block out of focus light and therefore requires longer exposure times than WF imaging. Confocal imaging should be used for all z-stacks. All vessel quantifications should be done using Z-stacks obtained using the DSU.

11. To take images and use the automated stage, two key windows are needed – acquire window and move stage to absolute position.

  a. Open acquire window: in the tool bar select acquire and then in the drop-down menu select acquire.

    i. Acquire: captures the current field of view.

    ii. Auto scaling: automatically determines the minimum and maximum exposure limits for the field of view.

    iii. Show live: this opens a window showing the live view of the sample. To close this window you must click stop live (the show live buttons turns to stop live when live is on), it will not close by clicking the x in the right corner.

    iv. You can adjust the exposure time in this window or pre-selected a saved exposure time.

  b. Open stage window: in the tool bar select devices then in the drop down select stage → move stage to absolute position.

    i. Set origin: this creates a new 0, 0, 0 origin at the current location.

12. To acquire stacks, journals are needed to automate the process.

  a. Open the journal editor. a. Select journal in the tool bar and then select edit journal from the dropdown menu to bring up an existing journal.

  b. In the journal editor window, select file, then save as and rename the journal with your initials for your own needs (typically the colors used and size of Z-stack/slice depth).

  c. Required journal elements to capture Z-stacks:

    i. Select magnification: this allows you to select the magnification to run the journal on. *If the microscope is not set to this magnification when you run the journal, the journal will prompt the microscope to switch it.*

      ii.   Run journal, acquire – Load Setting, acquire Z series. These three elements are required for each color channel you want a stack of.
          1.   Run journal loads journals that have already been established on the computer for loading the appropriate view and color options. a. i.e., "GFP_DSU" journal sets the microscope up to image using the GFP filter cube using the DSU and "mCherry_camera" journal sets the microscope up to image using the mCherry filter using the camera without DSU in the widefield settings.
          2.   Acquire – load setting will load the settings in the acquire window (i.e., exposure time, auto scaling, etc.).
          3.   Acquire Z series instructs the microscope to image a Z-stack with specified total depth, slice depth, and number of slices. This information is input by the user and must be identical for all color channels used. In this window, you will also select where you want the stack to start at. I use origin so I can set the origin at the plane I am interested in imaging. If it is set to something else, be sure it is consistent for all stacks and use the stage window accordingly.
     iii.   Run journal, acquire – Load Setting, acquire – start live.
          1.   These three are for showing the live window after all Z-stacks have been acquired.
          2.   Typically, this is set to the mCherry widefield setting to view UEA stained vessels and find a new imaging position.
     iv.   After editing the journal, save it. The microscope will not run an unsaved journal.

13. Image using your journal.
    a.   There are two options to use the journal.
    b.   If you are only taking one set of Z-stacks, choose the run journal option.
       i.   From the toolbar select journal, then in the drop-down menu select run journal.
      ii.   This command runs the journal once without opening the journal window.
    c.   If you are taking multiple sets of Z-stacks, choose the edit journal option.
       i.   From the toolbar select journal, then in the drop-down menu select run journal.
      ii.   *This command opens the journal editor window. From here you can select the run journal button. After running, the editor window will remain open, and you can easily press the button again once you have moved to a new imaging position.*
    d.   If you want to image only some stains within your journal, choose the edit journal option.
       i.   From the toolbar select journal, then in the drop-down menu select run journal.
      ii.   *In the journal editor window, you can disable commands. So, if your journal is for red, green, and blue but you only want to image red and blue, use the same journal and just disable the green commands and save the journal. You can reenable them at any time.*

e. When used in this way, the journal will image through the entire Z-stack for one color channel, then change filters and image the next color, and so on. You will then have separate Z-stacks for each color at the same position.

Scan Slides:

Scan slide is used when a sample is larger than the field of view and you are trying to assess an entire hydrogel. The app will stitch multiple images together to capture the entire sample.

- Scan slide can only be single plane images, not Z-stacks for a stitched together images, but you can set the scanslide to acquire a z-stack at each location by setting "run journal after" to your desired journal.
- If the objects in a stitched image are not properly aligned, then the calibration needs to be redone. Use the calibrate from live mode option.
- Each scanslide will have its own unique scale if the sample sizes are different. To find this, open up the whole scan image and select the calibrate distances option to see the scale for that image.
- If you are just doing a scanslide for qualitative purposed, I would recommend taking WF images to save on time, but if you want a scanslide for quantification or publication I would recommend acquiring DSU images.

1. Go to Apps → Scanslide
2. On the main page, select the location and filename you want the images to be saved as. The program generates individual images at each location and then a stitched together image which will be the last file in the series.
   a. I like to make a folder for each gel since so many images are generated
3. Acquisition
   a. Camera binning → 1 (this can be adjusted to higher numbers to reduce size of image/save memory, i.e., 2)
   b. # wavelengths → 1-4 depending on number of channels being acquired
      i. I personally like to run one wavelength at a time so I can have each stain in the file name, if you do multiple wavelengths at a time it saves the images as "W1" or "W2"
      ii. If you do multiple wavelengths, it will complete the entire process for one wavelength before moving on the next.
4. Select channels (1 and/or 2)
   a. W1: m-Cherry W
      i. Set exposure → determined by using show live on the acquire panel
   b. W2: DAPI W
      i. Set exposure → determined by using show live on the acquire panel
5. Slide Area
   a. Select top left and bottom right corner of your samples
      i. This can be done by finding the top center of well → going to Devices → Stage → Move stage to absolute position → set origin
      ii. Then find center left of well and note that number for the x-coordinate
         1. Top left corner would be positive x-coordinate, zero for y-coordinate

     2. Bottom right corner would be negative x-coordinate, negative double x-coordinate for y-coordinate
  b. Once you set the corners, the program will determine the number of images to take and stitch together.
 6. Select Scan to start the acquisition.

Image Analysis in ImageJ:
 1. Making Max Intensity Projections of z-stacks
  a. Copy and paste Max Projection script into your main folder that contains folders of specific experiments.
  b. Open ImageJ.
  c. Plugins → Macros → Run
  d. Select the script in finder window
  e. A new finder window will open
  f. Find and select the folder of images you want to compress into max intensity projections
  g. The script will make another folder named "Recon" within the main folder containing the images that has all the max intensity projections
    i. Note: the Max Projection scripts also containing image modification commands, like enhancing the contrast and subtracting the background. Make sure you understand what is going on in the script and modify it if needed.
 2. Merging Images (Adding Color)
  a. Open all max projections from the Recon folder that you plan to merge into one image (e.g., UEA/DAPI/Phalloidin or Phase/Live/Dead) by dragging them from the folder onto the ImageJ control panel
  b. Image → Color → Merge Channels
    i. Select the appropriate channels for each image (e.g., phase = grey, UEA/Dead = red, DAPI = blue, Phalloidin/Live = green)
    ii. Check "Create composite"
    iii. Click OK
 3. Adding Scale Bar
  a. First, you will want to convert your merged (or single color) image into an RGB color image. This saves your color selections merged into one image and allows you to add a white scale bar. Otherwise, the scale bar will show up in one of the colors you selected for the stacks you merged. Once you do this, you cannot go back and edit the stacks individually, so make sure you did all the desired modifications before this step.
    i. Image → Type → RGB Color
  b. Next, you need to set the scale before you can add a scale bar
    i. Analyze → Set Scale
    ii. Distance pixels = 1
    iii. Pixel aspect ratio = 1
    iv. Unit of length = um
    v. Known distance is objective specific
      1. 4x: 1.6122

2. 10x: 0.6483
3. 20x: 0.3260
4. Check "Global" if you want to apply this scale bar to all images you will be processing
    a. I would recommend processing all images of the same magnification at once because then the "Global" option will keep the scale constant for all images. Otherwise, you will need to set scale for each image.
c. To add the scale bar to the image
    i. Analyze → Tools → Scale Bar
    ii. Set the desired parameters for your scale bar then select OK
    iii. I try to keep the parameters the same for all images for consistency

Maximum Intensity Projection Script for ImageJ:

```
//This macro creates maximum intensity projections of all z stacks in the user-specified folder.
//Each maximum intensity projection is processed and saved to a folder created within the user-specified folder.

dir = getDirectory("Choose a Directory");
newdir = dir + "/Recon/"
File.makeDirectory(newdir);
list = getFileList(dir);

for(i=0; i<list.length; i++) {
        if (endsWith(list[i], ".tif")){
                open(dir+list[i]);
                imgName=getTitle();
                run("Z Project...", "Max Intensity");
                run("Enhance Contrast", "saturated=0.1 normalize process_all use");
                run("Subtract Background...","rolling=50");
                saveAs("Tiff", newdir + "Recon " + imgName);
                while (nImages>0) {
                        selectImage(nImages);
                        close();
                }
        }
}
```

Vessel Quantification in Metamorph:
1. Open a new excel file.
2. Log → open summary log → DDE, ok (CANNOT have another excel file open)
3. Open images you want to quantify.
    a. These should be the max intensity projection images created above of the UEA channels (BEFORE any additional image modification, like color or scale bar)
4. Measure → calibrate distances → 4x → apply to all open images

298

      a. If you open more images later you need to repeat this process
5. Apps → Angiogenesis tube assay → mid width #, max width #, background ####
      a. Set this for each experiment, but keep the same between replicates
6. The outputs will automatically be loaded into the excel file.

Appendix P – Fabricating Fibrin Hydrogels with Endothelialized Channels
Adapted from Emily Margolis

Materials:
- 12 mm biopsy punch
- 15 mL and 50 mL conical tubes
- 100 mm petri dishes
- 2 mL microcentrifuge tubes
- 22G needles
- 33 mm 0.22 μm filter
- 5 mL syringe
- 8 mm biopsy punch
- Acupuncture needles
- ddH2O
- Epredia Peel-A-Way Mold
- Ethanol (EtOH. 100%)
- Fibrinogen, thrombin, FBS, SF media
- Gelatin (2% solution)
- Glass coverslips (22x40 mm)
- Ice bucket with crushed ice
- Isopropanol (IPA, 70% and 100%)
- Kimwipes
- PDMS kit (Sylgard 184 Kit – base & curing agent)
- Pipette tips
- Plastic cup
- Plastic stir stick (or 2 mL serological pipette)
- Plastic transfer pipettes
- Serological pipets
- Trypsin, PBS, culture media
- Vacuum grease

Equipment:
- Desiccation chamber
- Forceps
- Fume hood
- Oven
- Pipettes
- Plasma etcher
- UV Ozone

Overview:
The protocol describes the process of fabricating PDMS devices for generating bulk fibrin hydrogels containing endothelialized channels. This protocol references portions of Appendices A, C, and H.

Notes:
- I would recommend calculating the necessary masses and volumes needed for the following procedure based on the number of conditions and gels you will be making.
  - Determine the amount of fibrinogen, cell density, and total cell number required, and calculate volumes of each component in the gel precursor solution.
- If encapsulating microbeads instead of cells, be sure to always coat the pipette tip with FBS before manipulating the microbeads as they will stick to the sides of the pipette tip if not properly coated and you will lose the majority of the beads.

PDMS Devices:
1. Turn on the oven to 70 °C.
2. Prepare 5g of PDMS per mold according to Appendix H.
   a. While PDMS is degassing, prepare peel-a-way molds
   b. Insert two 22G needles into the 22 mm edge of the plastic mold close to the bottom.
3. Cut off the tip of a transfer pipette to increase the area and use this to transfer PDMS from the cup to the molds.
4. Transfer PDMS into the molds on the scale to get 5 g in each mold.
   a. Pop any bubbles by pocking them with a pipette tip.
5. Move molds into a 70 °C oven to cure for a minimum of 4 hours and up to overnight.
6. Place extra PDMS in the deli fridge to use for day 2.
   a. PDMS can remain liquid at cool temperatures (typically only for an additional day) but will solidify if left overnight at RT.
----
7. Remove molds from the oven.
8. Remove needles from the PDMS.
9. Peel the plastic mold apart from the PDMS.
10. Cut the 22 mm edges off the PDMS to remove the curved edge features.
11. Over the needle tracks, use an 8 mm biopsy punch to create seeding/media reservoirs.
12. Use a 12 mm biopsy punch and punch two overlapping circles to create the hydrogel chamber.
13. Clean the glass coverslips and PDMS molds with IPA and ethanol rinses.
    a. Rinse a coverslip with IPA on both sides.
    b. Rinse the coverslip with ethanol on both sides.
    c. Use the air gas line with tubing attached to dry the coverslip.
    d. Place the cleaned coverslip rested against the lid of a petri dish.
14. Repeat step 13 for all coverslips and PDMS molds.
15. Place an equal number of coverslips and PDMS molds in the plasma treating cage (three of each fit).
16. Plasma treat the devices and slides for 1min at 10% O_2 (O_2 should be preset).

a. Select Commands → Plasma
b. If you need to change the time, first select Commands → Plasma time then Commands → Plasma
c. If the plasma etcher has not run for the day, it can take a few minutes to reach the vacuum set point.
17. After the treatment is done, remove the molds and coverslips from the chamber.
a. The chamber needs to repressurize first, so I often unlatch the door then wait for it to pop open.
18. Place one coverslip and one PDMS mold together.
a. Adhere the two surfaces that were upward facing during the plasma cycle.
b. Use your fingers to *gently* press the two together.
c. Place the bonded mold down on the bench and use your palm to press into the PDMS side of the mold (not the glass side) multiple times to ensure it is well adhered.
19. Put the devices (glass directly on metal rack) in the 80 °C oven for at least 1 min.
20. Remove the molds from the oven and place them on the bench.
21. Remove devices from oven and cool to RT with light pressure on the glass back (again on a Kimwipe).
22. Repeat steps 18-21 for all remaining molds.
23. Retrieve PDMS from the deli fridge.
a. The glass is a near exact fit in width for the molds so they must be further sealed with PDMS to ensure the edges are well sealed.
24. Use a pipette tip to seal the long edges of the mold with PDMS.
25. Cure PDMS in the oven at 70 °C for least 2 hours and up to overnight.
----
26. Ensure needles are cleaned.
27. Warm 2% gelatin solution in the water bath.
28. Dip each needle in the gelatin solution and then place in a petri dish.
29. Allow gelatin to solidify for 5 minutes at 4 °C.
30. Place a single needle in each needle track (2 per mold).
31. Bring the molds and a sterile 100 mm petri dishes (one per device) to the Baker lab.
32. Place the molds in the UV ozone and sterilize for 5 min.
33. After the cycle has completed, place the sterilized molds in the sterile petri dishes. They are now ready for cell culture.

Endothelialized Bulk Fibrin Gel:
1. Bring PDMS devices into the BSC.
2. Prepare cells (ECs for channels + other cells/beads needed) according to Appendix A.
3. Prepare fibrinogen solution according to Appendix C.
a. Each device can hold 500-750 µL of gel.
4. Prepare one precursor aliquot (microcentrifuge tube) per device.
a. Centrifuge cells in microcentrifuge tube (or add beads).
b. Add SF EGM2 then FBS.
c. Add thrombin.
5. One device at a time, add fibrinogen to the gel aliquot and mix thoroughly (5-7 times).
6. Inject gel solution into center chamber of the PDMS device.

7. Allow fibrin to solidify for 5 minutes at RT in the hood.
8. Incubate devices for 35 minutes at 37 °C.
9. While gels are polymerizing, prepare the EC for cell seeding.
    a. Suspend the remaining EC at 2M/mL in EGM2.
    b. Place on ice.
10. After gelation, add 1 mL of EGM2 to each device (fill the wells and gently place the remaining volume over the gel being careful not to overflow the PDMS) to allow the gel to swell.
11. Incubate devices for 30 minutes at 37 °C.
12. Using forceps, remove the acupuncture needles from each device.
13. Seal the needle tracks with vacuum grease.
14. Remove all media.
15. Inject a suspension of 2M/mL EC into the channels through the circular reservoirs.
    a. Start with 20 µL per channel.
    b. Visualize under microscope to ensure cells are flowing into the channel.
    c. Add more cells if needed.
    d. Balance the hydrostatic pressure gradient with EGM2 in the other well if cells are flowing too fast.
16. Culture molds for 30 minutes to allow cells to adhere.
17. Repeat steps 15 and 16 but flip the mold upside down to allow cells to adhere to the top surface of the channel.
18. Remove cell suspension from the devices.
19. Add EGM2 to media reservoirs.
20. Add PBS to the top of the gel.
21. Change gel media the next day, then every other day following.